Engineered Bone
Matrices, cells and bioactive molecules

Engineered Bone
Matrices, cells and bioactive molecules

Een wetenschappelijke proeve op het gebied van de Medische Wetenschappen

Proefschrift

ter verkrijging van de graad van doctor
aan de Katholieke Universiteit Nijmegen,
volgens besluit van het College van Decanen
in het openbaar te verdedigen op
vrijdag 19 oktober 2001
des namiddags om 1.30 uur precies

door

Johannes Wilhelmus Maria Vehof

geboren op 18 maart 1970 te Ambt-Delden

Aan mijn ouders

Contents

Abbreviation list

AAA bone	*Autolyzed antigen-extracted allogenic bone*	**HA**	*Hydroxyapatite*
AP	*Alkaline phosphatase*	**HD**	*High cell density*
bBMP	*Bovine BMP*	**IBM**	*Insoluble bone matrix*
BGS	*Bone graft substitute*	**IGF**	*Insulin-like Growth Factor*
BMP	*Bone Morphogenetic Protein*	**IM nail**	*Intramedullary nail*
BMSC	*Bone marrow stromal cell*	**LD**	*Low cell density*
BMPR	*Bone Morphogenetic Protein receptor*	**LM**	*Light microscopy*
Ca	*Calcium*	**α-MEM**	*α-Minimal essential medium*
Ca-P	*Calcium phosphate*	**MIH**	*Müllerian Inhibiting Substance*
CDGF	*Cartilage-Derived Growth Factor*	**MSC**	*Mesenchymal stem cell*
CFU-F	*Colony-forming-unit fibroblast*	**NCP**	*Non-collagenous protein*
CHO cells	*Chinese hamster ovary cells*	**OP-1**	*Osteogenic Protein-1 (rhBMP-7)*
CMV	*Cytomegalo virus*	**OP-2**	*Osteogenic Protein-2 (rhBMP-8)*
Co-Smad	*Common Smad*	**PBS**	*Phosphate buffered saline*
(i)DBM	*(inactivated) Demineralized bone matrix*	**PDGF**	*Platelet-Derived Growth Factor*
		PGA	*Poly(glycolic acid)*
Dex	*Dexamethasone*	**PGE**	*Prostaglandin E*
ECM	*Extra-cellular matrix*	**PLA**	*Poly(lactic acid)*
EDS	*Energy dispersive spectroscopy*	**PLGA**	*Poly(lactic-co-glycolic acid)*
EDTA	*Ethylene diamine tetra-acetic acid*	**PMMA**	*Poly methylene methacrylate*
FBS	*Fetal bovine serum*	**PPF**	*Poly(propylene fumarate)*
FCM	*Fibrous collagen membrane*	**PPHAP**	*Porous Particles of Hydroxyapatite*
FCS	*Fetal calf serum*	**Pw**	*Prewetting*
FGM	*Fibrous glass membrane*	**RBM**	*Rat bone marrow*
Fn	*Fibronectin*	**RF**	*Radio-frequent*
FTIR	*Fourrier transform infrared spectroscopy*	**rhBMP**	*Recombinant human BMP*
		R-Smad	*Receptor-regulated Smad*
Gd	*Glow-discharge*	**S-300**	*S-300 BMP fraction*
β-GP	*Na-β-glycerophosphate*	**SEM**	*Scanning electron microscopy*
GuDBM	*Guanidine-treated DBM*	**TCP**	*Tricalcium phosphate*
hBMP	*Human BMP*	**TGF-β**	*Transforming Growth Factor beta*
I-Smad	*Inhibitory Smad*	**Ti**	*Titanium*
GDF	*Growth and Differentiation Factor*	**VEGF**	*Vascular Endothelial Growth Factor*
GDNF	*Glial Derived Neurotrophic Factor*	**WB cells**	*Westen-Bainton cells*
(b)FGF	*(basic) Fibroblast Growth Factor*	**XRD**	*X-ray diffraction*

Chapter 1

General introduction

1.1   The problem

It is estimated that annually more than one million patients need treatment for skeletal problems worldwide.[1] These problems occur in the field of plastic and reconstructive surgery, orthopaedic surgery, craniofacial surgery and dental implantology and include the treatment of bone defects created during tumor surgery or caused by trauma, the reconstruction of congenital skeletal abnormalities, the promotion of fracture healing, spinal arthrodesis and joint and tooth replacement. Treatment does not always result in a solution of the problem because of inadequate local bone conditions and impaired bone healing.[2] Complicated fractures may fail to heal, resulting in so-called delayed unions or non-unions.[3,4] The treatment of bone tumors or congenital syndromes are frequently associated with a large bone defect, which requires the grafting of a large amount of autogenic or allogenic bone.

Autografting, the transplantation of bone from one site to another site in the same individual, is the current golden clinical standard. An advantage of autografts is that they are osteogenic. However, the use of autografts is associated with significant morbidity at the site of harvest, *i.e.* the donorsite. For instance, harvesting bone from the iliac crest has been reported to result in 6-20 % of the patients developing minor complications, such as pain, hypersensitivity, anesthesia, superficial infection, seroma and haematoma, and 3-8 % developing major complications, such as herniation, meralgia paresthetica or pelvic instability.[5-7] In addition, autografting requires a second surgical procedure, which adds operating time. The use of autogenous bone can also be hampered by a lack of the availability of sufficient bone tissue.

Allografting is the transplantation of bone from a donor to a recipient of the same species. Allografts are less osteogenic, more immunogenic and show a greater rate of resorption.[6] In addition, disease transmission (*e.g.* HIV) from donor to recipient is possible and has been reported.[8-11] Xenografting is the transplantation of bone between species. Xenografts are also prone to immune rejection and are generally not considered an option for clinical use.[6] Some of the problems encountered with auto- and allografts can be omitted by using synthetic materials. Materials that have been used are ceramics –*for example, calcium phosphates and glass ceramics*– and polymers –*for example, polymethylene methacrylate (PMMA)*. The advantages of these materials are non-immunogenicity and availability. In addition, some are partly or completely biodegradable. Although some of these materials improve the bone repair process, they do not possess bone-inductive activity.

1.2   Tissue engineering

Tissue engineering is a new interdisciplinary field of research that is formally defined by: "*The application of the principles and methods of engineering and the life sciences toward the fundamental understanding of structure-function relationships in normal and pathological mammalian tissues and the development of biological substitutes that restore, maintain, or improve tissue function.*"[12,13] and "*....tissue engineering applies the principles of biology and engineering to the development of functional substitutes for damaged tissue.*"[1]

10

Tissue engineering strategies can be used to create organs like the liver, kidney, heart, pancreas, intestine and skin, and tissues such as adipose tissue, tendon, muscle, nerves, cartilage and bone.[14] Tissue engineering requires the use of three key elements: (1) a matrix –*also termed scaffold or carrier material*– combined with (2) cells and/or (3) bioactive molecules (*e.g.* growth factors). The matrix provides mechanical support and serves as a substrate upon which the cells attach, proliferate and undergo differentiation. Further, the matrix can serve as a delivery vehicle for cells or growth factors.

If tissue engineering is applied for the regeneration of bone by creating so-called bone graft substitutes (BGS), three strategies can be pursued: a matrix-based, a cell-based and growth factor-based strategy or a combination of growth factors and cells.

In view of this, bone (graft) substitutes can be divided in three classes: (1) **osteo-conductive**, (2) **directly osteogenic** and (3) **osteoinductive**.[15] Additionally, a combination of (2) and (3) is possible. To date, mainly osteoconductive bone graft substitutes, like allograft bone and ceramic materials (*for example hydroxyapatite or tricalcium phosphate*), have been used clinically.

For directly osteogenic bone graft substitutes, cells from the osteogenic lineage –*osteo-progenitor cells or osteoblast-like cells*– are added to a porous scaffold. In post-natal life, osteoprogenitor cells or Mesenchymal Stem Cells (MSCs) can be derived from bone marrow. For osteoinductive bone graft substitutes, osteoinductive growth factors especially members of the Transforming Growth Factor beta superfamily [Bone Morphogenetic Proteins (BMPs) or Transforming Growth Factor betas (TGF-βs)], are combined with the carrier. Upon implantation, cells are recruited by chemotaxis and induced to form bone by these bioactive molecules.

A combination of osteoinductive and directly osteogenic BGS can be created by simply combining cells with growth factors or with genetically transfected cells that overexpress growth factors.[16]

1.3 Osteoinductive bone graft substitutes

While several growth factors, like Insulin-like Growth Factor (IGF), basic Fibroblast Growth Factor (bFGF) and Platelet-Derived Growth Factor (PDGF), have been shown to stimulate bone formation, two members of the Transforming Growth Factor beta super-family –*Bone Morphogenetic Proteins and Transforming Growth Factor betas*– have been most extensively studied.

1.3.1 Transforming Growth Factor beta superfamily

Bone Morphogenetic Proteins and Transforming Growth Factor betas are members of the TGF-β superfamily, which is a large family of secreted signalling molecules that are related to each other by sequence similarities but possess a wide ranging number of biological functions. The TGF-β superfamily comprises the TGF-βs, BMPs (except BMP-1, which is a metalloprotease),[17,18] Growth and Differentiation Factors (GDFs), inhibins/activins,

Müllerian Inhibiting Substance (MIH), Vg-related genes, nodal-related genes, *Drosophila* genes [*e.g. Drosophila decapentaplegic* (dpp) and 60A] and glial-derived neurotrophic factor (GDNF)[19,20] (**Figure 1**).

1.3.2 Bone Morphogenetic Protein

In the early 1960s demineralized bone matrix (DBM) was discovered to induce ossification in intramuscular sites in rabbits.[21] The responsible molecule was found to be a protein called Bone Morphogenetic Protein.[22] Morphogenesis is defined as the generation of form, the process of tissue and organ construction and assembly. A morphogen is a molecule that initiates the formation of a morphogenetic field by means of a single or complex stimulus to the genome.[23] BMPs function as signalling molecules in embryonal morphogenesis, *e.g.* limb development, and are also involved in fracture repair.[4,24-29]

To date 15 BMPs are known (BMP1–15).[30] BMP-2 to -9 are members of the TGF-β superfamily on the basis of their similar amino acid sequences. Other BMPs have been identified by low-stringency hybridization and consensus polymerase chain reaction.[19,20,31] Based upon sequence similarities, three separate subgroups of BMPs exist within the BMP family: (**1**) BMP-3 by itself, (**2**) BMP-5, -6, -7 [Osteogenic Protein-1 (OP-1)] and -8 (OP-2) and (**3**) BMP-2 and BMP-4.[31] BMP-2, BMP-4, BMP-5, BMP-6 and BMP-7 have been shown to be osteoinductive *in vivo*, while BMP-13 and -14 have been shown to induce tendon and ligament in ectopic implantation.[30,31]

BMP is a low-molecular-weight glycoprotein with a primary structure 40–50 % similar to that of TGF-β.[23] BMPs are synthesized as larger precursor molecules consisting of a signal peptide, a prodomain and a carboxy-terminal region of 100–125 amino acids. This carboxy-terminal region contains a pattern of seven highly conserved cysteine residues. When the carboxy-terminal region is cleaved from the precursor, the molecule becomes a dimer bound by a cysteine-disulfide bridge. In this way, active homodimeric and hetero-dimeric BMPs are secreted.[20] Heteromeric BMPs of BMP-2/7 and BMP-4/7 have been shown to be more active than homodimeric BMPs, both *in vitro* and *in vivo*.[32,33]

BMPs are present in bone matrix, dentin matrix, osteosarcoma and many other tissues. In cortical bone, BMPs are present in low quantities: 1–2 µg BMP/kg bone.[34] BMPs can be isolated from demineralized bone matrix (DBM) – *for example, by guanidine extraction*; these BMPs are termed purified or native BMPs. Following extraction, they are purified using chromatographic techniques. These BMPs can either be highly purified or partially purified, depending on the number of chromatographic steps. Highly purified BMPs possess a higher osteogenic activity than partially purified BMPs and have also been shown to be more potent than recombinant human BMP-2.[35]

Since 1988, BMPs have been produced using molecular cloning techniques, the so-called recombinant BMPs.[36] These recombinant BMPs can be produced by transfected cells; mammalian Chinese hamster ovary cells[37] or bacteria like *E. coli* are two examples.[38-40] Recombinant BMPs have been produced from humans and other species (*e.g.* bovines).

Members of the TGF-β superfamily exert their effect through transmembrane receptor complexes.[19] These receptors are members of a family of serine/threonine kinase receptors that includes receptors for BMPs, TGF-βs, activins and inhibins. There are two types of
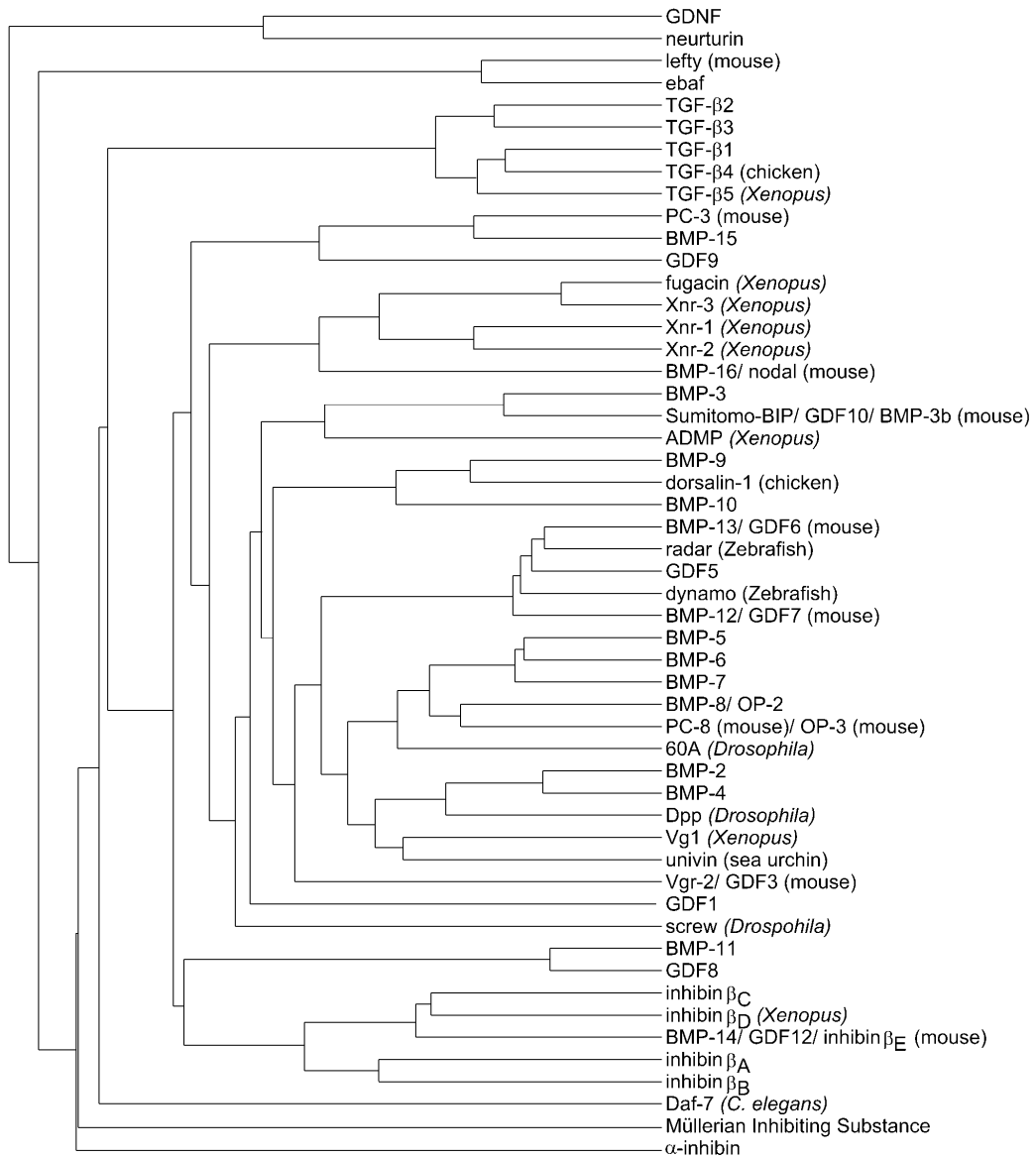
Figure 1.

Dendrogram of the TGF-β superfamily.

BMP receptors: Type-I (BMPR-1A or BMPR-1B) and type-II (BMPR-II) receptors. These BMP receptors have been shown to bind BMP-2, BMP-4 and BMP-7. While individual receptors show a low affinity for BMPs, binding affinity is high when receptors form a heterotetramer. To initiate cell signals, both types of receptors are required. Upon the binding of BMPs, the type-II receptor activates the type-I receptor which initiates an intracellular response through the so-called Smad pathway. The type-I receptor primarily determines the specificity in signalling. Three types of Smads can be distinguished: receptor-regulated Smads (R-Smads), common Smads (Co-Smads) and the inhibitory smads (I-Smads).[41] Smads play a critical role in transmitting signals to the nucleus. TGF-β and inhibin type-I receptors activate Smad 2 and 3, while BMP type-I receptors activate Smad 1, 5 and 8. Once phosphorylated, these R-Smads dissociate from the receptor and enter the nucleus. In the nucleus heteromeric complexes of Smads regulate gene transcription.

1.3.3   Transforming Growth Factor beta

TGF-β was discovered as a product of murine sarcoma virus transformed cells.[42] It was first defined by, and named after, its ability to induce the formation of colonies in normal rat kidney fibroblasts in anchorage-independent culture. As tumor-derived cells or induced tumor cells were known to form similar colonies, TGF-β was therefore thought to "transform" normal cells into neoplastic cells.[43] Transforming Growth Factor alpha is an unrelated peptide that shares a high degree of homology with Epidermal Growth Factor (EGF).

Active TGF-β is a 25-kDa polypeptide consisting of 112 amino acids. Similar to BMP, TGF-β consists of two polypeptide chains; these chains can either be identical (homodimers) or different (heterodimers). TGF-β homodimers consist of five subtypes: TGF-β_{1-5}. There are three main types in mammals: TGF-β_{1-3}, while TGF-β_4 and TGF-β_5 have been found in chicken and amphibians, respectively. TGF-β_4 in chicken is homologous to mammalian TGF-β_1. Structural homology between isomers is 64–82 %.[44] Heteromers TGF-$\beta_{1.2}$ and TGF-$\beta_{2.3}$ also occur in mammals but in lower amounts.[45]

TGF-β is present mostly in platelets[10] and bone[2] from which it has been isolated. Alternatively, TGF-β can be produced by transfected cells using molecular cloning techniques; for example Chinese Hamster ovary cells.[46,47] In many tissues, TGF-β is secreted in a latent form, which consists of a TGF-β dimer, a precursor and a TGF-β binding protein. Bone cells also produce a latent form without the binding protein. TGF-β must be dissociated from the latent complex to become biologically active.[48]

Almost all cells have surface receptors for TGF-β,[49] with osteoblasts bearing the highest number of TGF-β receptors.[50,51] TGF-β receptors are trans-membrane receptors and members of the serine/threonine kinase receptor family. Three types of TGF-β receptors can be distinguished: type-I, type-II and betaglycan (previously termed type-III) receptors. Heteromeric complexes of type-I and -II receptors appear to be a general requirement for signalling in the TGF-β superfamily. Following binding of the TGF-βs to the receptor complex, signalling occurs through the Smad pathway as described for BMPs. TGF-β type-I receptors activate Smad 2 and 3, while BMP type-I receptors activate Smad 1, 5 and 8.[41,52]

1.4 Biological effects of BMP

1.4.1 BMP *in vitro*

BMPs have been described to have both stimulating and inhibiting effects on cellular differentiation and proliferation of various cell types. Their effects are dependent on cell type, differentiation stage, dose and exposure time. Different BMPs can also show varying levels of activity. The cells that respond to BMP include mesenchymal-type cells, cartilage, bone and muscle cells.

For undifferentiated cells and cells within the osteogenic lineage, BMPs (rhBMP-2 and rhBMP-7) have been described to enhance proliferation *in vitro*. This has been shown for cell lines C3H10T1/2 (murine multipotential mesenchymal cells), ROB-C26 (a potential rat osteoblast precursor cell line) and fetal rat calvarial cells.[53-58] However, with respect to the latter cells, it has also been reported that proliferation is not increased by rhBMP-2.[59] Cell growth has been reported to be unaffected by rhBMP-2 in W20-17 cells (a bone marrow stromal cell line) and rat bone marrow stromal cells.[55,56,60] In contrast, MC3T3-E1 (mouse osteoblastic cells) and ROB-C20 (a more differentiated rat osteoblast cell line than ROB-C26) have been reported to be growth-inhibited by BMPs.[57,61]

The most striking ability of BMPs is to stimulate the differentiation of undifferentiated cells towards the chondroblastic and osteoblastic phenotype and to inhibit it towards the myogenic and adipocytic phenotype. In C3H10T1/2 cells, rhBMP-2 inhibits adipocytic differentiation and stimulates development of the chondroblastic and osteoblastic phenotype.[54,62] In addition, when these cells are transfected with the BMP-2 or BMP-4 gene, they also show ostegenic expression.[63,64] In another cell line BMS2 (murine multipotent bone marrow stromal cells), rhBMP-2, rhBMP-4 and rhBMP-6 inhibit the differentiation of adipocytes and stimulate the development of the osteoblastic phenotype.[65] In ROB-C26 cells (a cell line capable of differentiating into muscle cells and adipocytes) and myoblastic cells, rhBMP-2 has been shown to inhibit myogenic differentiation and stimulate development of the osteoblastic phenotype.[57,66] The osteoblastic phenotype was stimulated by BMP-2 in MC3T3-E1 and W-20-17 cell-lines[60,65,67] and in more heterogenous cell cultures like rat and human bone marrow stromal cell cultures.[55,68,69] In fetal rat calvarial osteoblast cell cultures, BMP-2, -4, -6 and -7 have also been shown to enhance osteogenic expression.[53,70-74]

The various BMPs have different activities. BMP-6 has been shown to have a higher activity in rat calvarial osteoblast cultures than BMP-2 and BMP-4,[75] while BMP-2 seems to have a higher activity than BMP-4 and -6 in ST2 and MC3T3 bone marrow stromal cell lines.[76]

BMPs exert their effects *in vitro* in a dose-dependent manner.[54,56,57,60,72] In C3H10T1/2 cells, rhBMP-2 at low concentrations (10 ng/ml) stimulates development of the adipocyte phenotype, while the chondroblastic and osteoblastic phenotype is stimulated at higher concentrations (100 ng/ml and 1,000 ng/ml).[54] Not only the concentration but also the duration of BMP stimulation affects differentiation. An exposure to 100 ng/ml rhBMP-2, for as short a period as 1 hour stimulates adipocytic differentiation in C3H10T1/2 cells.[54] On the other hand, Katagiri *et al*.[62] found that 100 ng/ml rhBMP-2 for 3 days stimulated alkaline phosphatase (AP) expression in C3H10T1/2 cells. In C26 cells (a potential rat osteoblast

precursor cell) also a 3-day exposure to 1,000 ng/ml and a 6-day exposure to doses of 10, 100 and 1,000 ng/ml significantly stimulated AP expression.[57] Thies *et al.* found an effect in W-20-17 cells, a bone marrow stromal cell line, on AP activity 12 h after rhBMP-2 stimulation.[60] In bone marrow stromal cells, a maximum effect was found after 2 weeks of stimulation with 1,000 ng/ml rhBMP-2, while C3H10T1/2 cells exhibited higher osteogenic expression with increasing duration up to 4 weeks.[55]

Effects of BMPs on osteoblast differentiation can be synergistically enhanced by glucocorticoids like dexamathasone and triamcinolone.[68,77] In view of this, glucocorticoid co-treatment potentiates BMP effects up to tenfold.[77] In addition, BMP-2 is also expressed by rat bone marrow stromal cells and enhanced by exposure to dexamethasone.[78]

In very low concentrations (1 ng/ml), rhBMP-2, but not rhBMP-4 and rhBMP-6, exerts a chemotatic effect on the migration of human stromal osteoblasts, human osteoblasts and U2-OS cells.[79] In addition, rhBMP-4 and native BMPs in the femto-molar range have been shown to be chemo-attractive for monocytes.[80]

1.4.2 BMP *in vivo*

1.4.2.1 BMP in heterotopic locations
BMPs combined with a suitable carrier material induce new bone in heterotopic implantation. The rodent ectopic assay model is frequently used to assess osteogenic activity. Sampath *et al.*[81] studied different substances in a rat subcutaneous assay model. These substances included BMP, TGF-β, Platelet-Derived Growth Factor (PDGF), Epidermal Growth Factor (EGF), Fibroblast Growth Factor (FGF), Cartilage-Derived Growth Factor (CDGF), insulin and growth hormone. Only BMP was shown to be capable of inducing bone formation in a rat ectopic assay model.[81,82] On the other hand, another group reported that in baboons rhTGF-β_1 and rhTGF-β_2 can induce bone formation in a heterotopic location when combined with inactivated DBM (iDBM).[83-85] However, it should be stated that iDBM might still contain trace amounts of other substances, like BMPs.

1.4.2.2 Endochondral ossification
The classical description of BMP- or DBM-induced osteogenesis in heterotopic locations suggests that BMPs induce enchondral osteogenesis in which cartilage formation precedes the formation of bone.[86] When DBM or BMPs are implanted in an extraskeletal site in rodents a sequence of events is activated that is quite similar to embryonic bone formation and fracture healing.[87] Initially, the chemotaxis of undifferentiated mesenchymal cells occurs, following which the cells proliferate (**Figure 2**). Subsequently, these cells differentiate into chondroblasts and chondrocytes that produce cartilaginous extracellular matrix including type-II collagen and proteoglycans. The chondrocytes mature and become hypertrophic, and cartilage begins to mineralize. Following the period of chondrogenesis, blood vessels appear at the implantation site. Bone-forming cells are then observed, which produce bone matrix while the calcified cartilage is being removed by osteoclasts. Mineralized bone matrix is observed, which contains osteocalcin. Once bone has been formed, hemopoietic bone marrow appears within the bone. Eventually, the newly formed bone undergoes remodelling. In **Figure 2**, the time sequence of the events as proposed by

Wozney is also depicted. The speed of the bone formation process is dependent upon the concentration of BMP used.[88]

1.4.2.3 Influence of vascularization

Caplan *et al.* also described the ectopic ossification process upon implantation of DBM or BMPs.[89] He hypothesized that in endochondral ossification a sequence of events takes place similar to embryonic endochondral ossification in which two waves of Mesenchymal Stem Cells (MSCs) are recruited to the implantation site, and osteogenesis occurs though a vascular driven process completely independent of the prior presence of cartilagenous matrix. The formation of cartilage and bone is dependent on two distinct waves of MSCs in which vascularization plays an important role. Cartilage is thought to be replaced by marrow and not to be a template on which bone is formed.

The initial inflammatory response brings in and provides factors that attract MSCs. MSCs are recruited by BMPs and other factors in the DBM by chemotactic effects. MSCs subsequently proliferate. These MSCs and the inflammatory response are encysted in a relatively a-vascular environment by a surrounding cell layer of flattened fibroblasts (MSCs) designated the "stacked cell layer"; which causes the a-vascular environment. Capillaries can be observed outside this cell layer. The next phase is a cartilage differentiation phase in which the MSCs inside the stacked cell layer differentiate towards chondrocytes. This is followed by cartilage hypertrophy and first bone formation in which chondrocytes in the core of the implant differentiate into hypertrophic cartilage cells, produce cartilaginous matrix and start to mineralize. Cells on the outside close to the "stacked cell layer" differentiate into osteoblasts, which produce osteoid. The next phase is the vasculature invasion stage, which is believed to be initiated by angiogenic factors produced by hypertrophic cartilage cells; the result is that vasculature and resorptive cells are brought in. The outer bony collar is resorbed and vascularization takes place. Caplan hypothesized that in this phase a new wave of MSCs is attracted. These synthesize osteoid directly on the surface of the carrier which subsequently becomes mineralized and forms bone while the calcified cartilage is resorbed. The final phase is the marrowization phase in which it is thought that MSCs differentiate into marrow stroma. In addition, hemopoietic cells and osteoclasts can be seen in the newly formed bone.

1.4.2.4 Direct ossification and the role of vascularization

As stated above, BMP-induced bone formation was believed to follow the sequence of endochondral ossification.[86] More recently, direct ossification without pre-existing cartilage has been reported to occur on implanted BMP carriers: initially on fibrous collagen membrane (FCM) and subsequently on hydroxyapatite.[90,91] On the other hand, fibrous glass membrane (FGM) and insoluble bone matrix (IBM) have been shown to induce an endochondral ossification-like process.[92,91]

Although the exact mechanism by which vascularization influences the differentiation between chondroblasts and osteoblasts has not been fully elucidated, a strong connection exists between vascularization and bone formation. Consequently, vascularization is considered to be a crucial step in ectopic bone formation.[93] For example, anti-angiogenic agents like TNP-470 have been shown to inhibit rhBMP-2-induced ectopic osteogenesis.[94] Some researchers attribute the effect of vascularization to the supply of osteoblasts.[95] Vascular
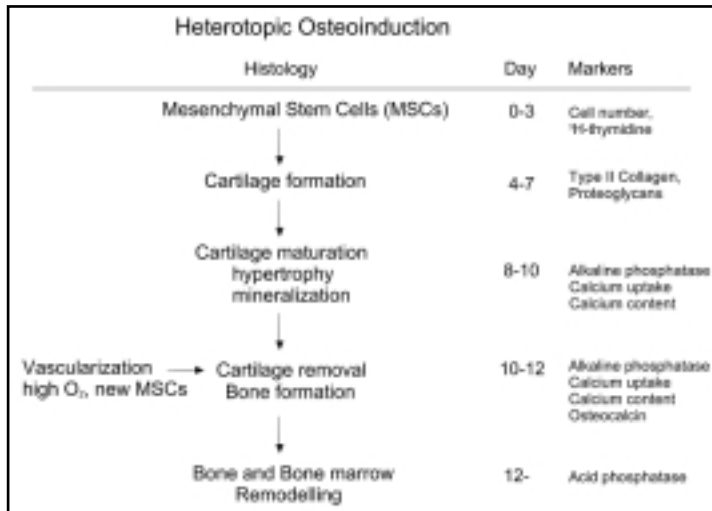
Figure 2.

The sequence of events in the heterotopic ossification process upon implantation of DBM or BMPs.

pericytes, which are undifferentiated cells, have been shown to be able to differ-entiate into chondrocytes and osteoblasts *in vitro* and can form cartilage and bone *in vivo*.[96] Other studies have shown that a low oxygen concentration favors chondrogenesis, while a higher oxygen concentration supports bone formation.[97-100] This is thought to be related to the higher oxygen and nutrient requirement of osteoblasts.[97]

It is also well known that carrier geometry influences the bone formation process,[101-103] which is supposed to be related to the influence of carrier geometry on vascularization and thereby on oxygen supply.[101] Consequently, carriers which induce bone formation independent of cartilage have been hypothesized to provide a higher oxygen supply due to geometry.[90] Direct bone formation was first shown for fibrous collagen membrane (FCM).[90] In addition, comparison of porous particles of hydroxyapatite (PPHAP) and fibrous glass membrane (FGM) revealed that the latter exhibited chondrogenesis while the former showed membranous ossification.[91] For FGM, rhBMP-2 induced osteogenesis was enhanced by the addition of bFGF, while the amount of cartilage decreased. This was attributed to the stimulating effect of bFGF on vascularization.[104] A comparsion between BMP-induced osteogenesis in hydroxyapatite carriers with different shapes –*porous particles (PPHAP), porous block and non-porous particles*– in an ectopic assay model revealed that the first two carriers effectively induced ectopic osteogenesis while the latter did not.[105] The solid particles were hypothesized to prevent vascularization through close contact between the particles and the absence of an interconnected porosity. A similar observation was made in a carrier of hydroxyapatite particles having a honey-comb shape. Here, bone formation occurred between the particles, while cartilage formation occurred in the small pores which were thought to inhibit vascularization.[106] For BMP induced osteogenesis, the optimal pore size for block-shaped hydroxyapatite carriers has been reported to be between 300 and 400 µm.

Recently, an observation which supports the relationship between neovascularization and osteogenesis has been made for a scaffold composed of bioglass fibers [composed of

CaO, P_2O_5, and SiO_2 (CPSA)].[107] Bone formation was observed completely around a porous ball-shaped CPSA implant, whereas scant bone formation was observed in a less porous bundle-shaped implant. Further research revealed that Vascular Endothelial Growth Factor (VEGF) receptors (Flt-1 and KDR) were expressed in the porous ball-shaped implant but not in the bundle-shaped implant.

In light of the above-mentioned, carriers have been identified that have a vascular inducing geometry –*for example FCM and PPHAP*– and a vascular-inhibiting geometry –*for example FGM*.[106,107]

1.4.2.5 Heterotopic implantation

In rodents, implant locations are either subcutaneous, mostly at the back or ventral thorax, or intra-muscular (for example the thigh muscles, calf muscles or abdominal muscles). In a comparative study in which osteoinduction by native bovine BMP in different tissues was observed, it was demonstrated that muscle was the best responding tissue.[108] Recent studies using rhBMP-2 also found that intra-muscular implantation was superior to subcutaneous,[109] inter-muscular and intra-fatty implantation.[110]

Only a few reports describe ectopic bone formation in higher animals, *i.e.* non-human primates. The first publication of ectopic induction of bone and cartilage is of subcutaneously implanted DBM in rhesus monkeys.[111] Native and recombinant human BMPs have also been shown to induce heterotopic bone formation in non-human primates. In the squirrel monkey, rhBMP-2 with DBM as a carrier has been shown to induce bone when implanted intramuscularly.[112] In baboon, native BMP together with baboon inactivated DBM or hydroxyapatite induced bone and cartilage in the rectus abdomis muscle.[113,114] In the same animal, OP-1 (rhBMP-7) also induced bone and cartilage formation in an intra-muscular site.[85]

1.4.2.6 Concentration

In vivo, BMPs show a dose-response relationship and, generally, higher doses are needed in higher animals. In the rat ectopic assay model, a concentration study was performed using rhBMP-2 (50 % pure) with rat insoluble bone matrix (IBM or inactivated DBM) as a carrier.[88] Bone and cartilage formation were studied from day 5 to 21. When subcutaneously implanted in rats, 0.5 to 115 µg BMP induced cartilage formation by day 7 and bone formation by day 14. Higher doses induced more reproducible bone formation. A dose of 600 ng rhBMP-2 consistently induced the formation of cartilage and bone.[88] In addition, high doses induced bone formation earlier – *by day 5*; at day 7 the amount of cartilage formed reached a plateau at doses higher than 6.2–12.0 µg. The amount of bone increased with increasing dosage. This was confirmed by Volek-Smith *et al.*, who showed a linear dose-response relationship between 0.2 and 150 µg rhBMP-2 with inactivated rat matrix as a carrier.[115]

If BMPs are injected without a carrier material in an ectopical implantation site they may quickly diffuse without inducing bone formation. At high concentrations, however – *100–200 µg rhBMP-2* – this procedure has been shown to be osteoinductive[88] in the rat ectopic assay model. The presence of a carrier material allows BMPs to be present locally at a high concentration.

It has been recently demonstrated that *in vivo* BMP effects can be synergistically

enhanced by other factors such as TGF-β_1,[82,85] TGF-β_2,[116] Prostaglandin E$_1$ (PGE$_1$)[117,118] and bFGF.[104]

A comparison regarding osteoinductive effectiveness between the BMPs is hard to make because of the great difference in animal models. However, it has been demonstrated that BMP-5 is less osteoinductive than BMP-7 or BMP-2.[34] It has also been reported that highly purified native BMPs are more effective in heterotopical osteoinduction than recombinant human BMPs.[35] A comparative study showed that rhBMP-2 was less osteoinductive than equivalent amounts (50 µg) of native bovine BMP (bBMP) in a rat ectopic assay model using atelopeptide collagen type-I as a carrier. Calcium content produced by rhBMP-2 was 1/10 of that produced by bBMP. A possible explanation for this difference is that native BMP is a mixture, which allows the substances present to act synergistically in bone formation.

1.4.2.7 BMPs in orthotopic locations

BMPs have been shown to be effective in bone healing in a number of locations and animal models. These include spinal fusion (*rabbits, dogs, sheep, goats and non-human primates*), long bone defects (*mice, rats, rabbits, dogs, sheep and non-human primates*), mandibular and cranial bone defects (*mice, rats, rabbits, dogs, pigs, sheep and goats*), fracture healing (*rabbits, goats and dogs*) and dental situations, such as periodontal regeneration (*rats, cats, dogs and non-human primates*), alveolar ridge augmentation, maxillary sinus floor augmentation (*goats and non-human primates*) and osseo-integration of dental implants (*dogs and non-human primates*).[119]

1.5 Biological effects of TGF-β

1.5.1 TGF-β *in vitro*

Although the three mammalian isoforms of TGF-β may have different effects *in vivo*, they have similar activities *in vitro* while showing quantitative differences.[44,120,121] The effect of TGF-β is dependent on cell type, differentiation stage, growth conditions and the presence of other growth factors.[122]

Three major biological activities exist for TGF-β:[44,120] (**1**) TGF-β inhibits cell growth in most cell types, but stimulates cell growth in mesenchymal cell types, including os-teoblasts and chondroblasts; (**2**) TGF-β also exerts an immunosuppressive effect that is partly related to the inhibiting effect on the proliferation of T-and B-lymphocytes; (**3**) TGF-β stimulates extracellular matrix deposition (*e.g.* collagen, fibronectin, glycosaminoglycans and proteoglycans).

TGF-β acts on osteoblasts, chondrocytes and cells of the osteoclastic lineage as well as on other cells.[123-125] With respect to bone cells, both stimulating and inhibiting effects have been described for cellular differentiation and proliferation. *In vitro* osteoblasts synthesize and respond to TGF-β.[50] Not fully differentiated cells within the osteoblast lineage are sensitive to the mitogenic effect of TGF-β.[123,124] For example, TGF-β has been found to stimulate proliferation in fetal bovine bone cells.[50] This stimulating effect on proliferation has been shown to be biphasic: low concentrations stimulate proliferation and high concen-

trations inhibit it.[50,126,127] In more differentiated cell cultures, TGF-β stimulates the synthesis of type-I collagen and suppresses alkaline phosphatase activity.[123] This has been shown for osteoblast-enriched cultures from fetal rat calvaria and MC3T3-E1 cells.[126,128] The concentration of TGF-β that stimulated collagen synthesis was higher (15 ng/ml) than those which stimulated proliferation (0.15–15 ng/ml).[126] Both effects have recently been reported for human bone marrow stromal cells: TGF-β_2 increased collagen synthesis and proliferation while it decreased alkaline phosphatase activity.[69]

TGF-β inhibits the formation of osteoclast-like cells *in vitro* and decreases bone resorption in bone organ cultures.[123] In calvaria and long bone cultures, the mineral resorbing effect of TGF-β has been reported to be biphasic: low concentrations (0.01–0.2 ng/ml) stimulate while higher concentrations (1–4 ng/ml) inhibit.[129]

In addition, TGF-β is a potent chemotactic factor for a number of different cell types, including fibroblasts[130] and osteoblast-like cells (*e.g.* fetal rat calvarial cells and rat osteosarcoma cells).[131] For osteoblast-like cells, concentrations between 5 and 15 pg/ml are the most chemotactic.

1.5.2   TGF-β *in vivo*

TGF-β plays a significant role in wound healing[132] by enhancing the repair of injured tissue like skin and bone.[120,121] TGF-β_1 and TGF-β_2 have also been shown to stimulate osteogenesis in orthotopic sites in rats and mice.[133,134] However, TGF-β does not induce bone formation in a rodent ectopic assay model.[81,82] Despite this, the group of Ripamonti *et al.* did report the induction of heterotopic ossification by TGF-β_1 and TGF-β_2 in baboons.[83-85]

In bone defect healing studies, TGF-β_1 with different carriers has been shown to be beneficial in bone defect healing in different animals and at various locations: cranial defects (*rats, rabbits and baboons*), mandibular defects (*rats and dogs*), radial (*rabbits*) and tibial defects (*sheep*).[135-145] TGF-β_1 has also been shown to enhance the osseointegration of metal implants in the humerus and femoral chondyle (*dogs*).[146-148]

For bone induction *in vivo*, a dose-responsive effect exists for TGF-β_1 within a certain range; there is, however, an optimum dose. Therefore, higher doses do not necessarily generate more bone formation. For example, Beck *et al.* found that 2 µg of TGF-β_1 applied in a 3 % methyl cellulose gel was able to regenerate a critical size defect in a rabbit skull within 28 days;[136,137] the 0.1- and 0.4-µg doses showed less bone formation. On the other hand, in the same model they found no difference between an 1-µg and 5-µg rhTGF-β_1 dose. Also in a rabbit critical size cranial defect model,[141] a 40-µg dose was found to be superior to a 0.4- and 4-µg dose with a DBM carrier. Using the same model, Zellin *et al.* found that 5 or 10 µg rhTGF-β_1 with porous $CaCO_3$ particles (Coral) was able to close a critical size cranial defect by 28 days.[145] In a rat mandibular defect model, dose-dependent bone bridging with concentrations ranging from 0.5 µg to 20 µg, has been described to be independent of the carrier used (methyl cellulose gel, porous $CaCO_3$ particles or poly (lactide-co-glycolide) beads).[145] However, when very low doses of 10 ng and 25 ng in a calcium phosphate cement were implanted into rat cranial defects, only minimal bone formation was observed. The low dose stimulated the resorption of the bone cement, which might be explained by the stimulation of osteoclastic activity.[149]

1.6 Directly osteogenic bone graft substitutes

1.6.1 Mesenchymal stem cells

1.6.1.1 The mesengenic process

In embryogenesis the mesoderm differentiates into bone, cartilage, muscle, dermis and other (connective) tissues.[150] The genesis of mesodermal tissues is termed the mesengenic process.[151] Pluripotential progenitor cells are thought to exist that have the ability to differentiate into different mesenchymal tissues. These cells, designated osteogenic (stromal) or mesenchymal stem cells (MSCs),[152-154] are hypothesized to enter separate multi-stepped lineages that will eventually give rise to different tissues: bone, cartilage, tendon/ligament, muscle, marrow and other connective tissues (**Figure 3A**).

In post-natal life, the process of tissue repair is thought to be analogous to the mesengenic process in embryological development. In tissue repair, mesenchyal stem cells are first recruited by chemotaxis and then proliferate and commit to a pathway under the influence of bioactive molecules. Thereafter, the cells progress through a lineage in which they proliferate and eventually differentiate with matrix production. Finally, the cells undergo a maturation stage.[151]

1.6.1.2 The osteoblast lineage

One definition of a stem cell is "*a cell that in the adult organism can maintain its own numbers in spite of physiological or artificial removal of cells from the population*".[155] The differentiation stages of the osteoblast lineage have been designed analogous to the hematopoietic lineage. Based upon histological and morphological studies, osteoblastic cells have been categorized in a presumed linear sequence progressing from osteoprogenitor to pre-osteoblasts, osteoblasts and then lining cells or osteocytes (**Figure 3B**). At least two distinctive populations of osteoprogenitor cells exist: one type determined to differentiate into the mature osteoblastic phenotype [in medium with FCS, Na-β-Glycerophosphate (β-GP) and ascorbic acid] and the other type that only differentiates in the presence of inductive factors (dexamethasone (dex) and BMPs). The process of progression from progenitor cells to osteoblasts was initially subdivided in three developmental time stages: (**1**) proliferation, (**2**) extracellular matrix development and (**3**) mineralization with characteristic changes in gene expression.[156] Osteoblast-associated genes show time-dependent expression when progenitors differentiate.[157] Recent analysis of cell- and tissue-specific macromolecules, including bone matrix molecules (*e.g.* type-I collagen, osteocalcin, osteopontin, bone sialoprotein) and multiple other markers[156,157] led to the further categorization of osteoblast differentiation into a minimum of seven different stages[157,158] (**Figure 3B**). According to Aubin, these stages include multipotential stem cell, immature osteoprogenitor, mature osteoprogenitor, pre-osteoblast, mature osteoblast, osteocytes and lining cells. For the osteoblast lineage, a reciprocal relationship exists between proliferation and differentiation.[159]

1.6.1.3. Bone marrow stroma

For tissue engineering purposes, undifferentiated cells can be isolated from fetal tissue and autologous tissue. Autologous stem cells can be isolated from bone marrow. Although the

presence of a true stem cell in bone marrow has not been proven, these cells are termed mesenchymal stem cells.[157] Recently, it has been reported that these cells can also be harvested from adipose tissue.[64] The focus here is on bone marrow-derived cells.

In Greek, stroma means "*the physical substrate, or something upon which one rests or lies*".[160] *In vivo*, the bone marrow stroma supports the function and physiology of hematopoetic cells. Within the bone marrow space, the stroma includes all cell types between the marrow blood vessels and the surrounding bone that are not of the hemopoietic lineage. These cells include marrow adipocytes, stromal fibroblasts [which have also been termed Westen-Bainton (WB) cells or (adventitial) reticular cells], bone-lining cells and osteoblastic cells. In post-natal marrow, WB cells are specialized hemopoiesis supporting cells that express alkaline phosphatase.[161,162] These cells are located along the outer wall of the sinusoids and are considered to be fibroblastic in nature. In post-natal human marrow, WB cells demonstrate the characteristics of pre-adipocytes,[163] which lose their AP activity and are converted to adipose cells.[164] WB cells are multipotential cells in post-natal marrow and have therefore stem cell characteristics.

1.6.2   Bone marrow stromal cells *in vitro*

When bone marrow is plated in plastic tissue culture flasks *in vitro*, non-hematopoietic cells adhere to the plastic material of the culture flask and can be cultured.[153,160,165,166] When single-cell suspensions are used, colonies are formed, each derived from a single colony-forming-unit fibroblast (CFU-F).[167,168] The cells share some characteristics with fibroblasts but lack the characteristics of macrophages and endothelial cells. The cells that are grown from CFU-Fs are termed bone marrow stromal cells (BMSCs).[160] Whether these cells are the same as the earlier described WB cells that occur *in vivo* is not entirely clear.[160] CFU-F are heterogenous in size and morphology and in their potential for differentiation. Some of the cells are believed to be multipotential while others are more restricted.[157] It is hypothesized that two types of osteoprogenitor cells exist, "inducible" and "determined" osteoprogenitor cells[153] (**see figure 3B**). When these cells are plated at adequate densities they proliferate and form monolayers. BMSCs can be isolated by marrow aspiration (*e.g. dogs, goats, sheep and humans*), by removal from trabecular bone (*e.g. humans*) or by removal of bone marrow from long bones (*e.g. rats, mice, rabbits and guinea pigs*).[15,166,169-172] Bone marrow cells have been cultured from various species including humans, rodents, dogs, sheep and goats.[166,170,169,172,173]

The stromal compartment is heterogeneous in composition and contains undifferentiated cells that can differentiate into several phenotypes *in vitro* and maintain the ability to form bone, cartilage, fibrous tissue and hematopoiesis-supporting stroma with adipocytes *in vivo*.[157,160,174] MSCs represent only a small fraction of the total number of bone marrow cells: between 0.01 and 0.0001% of the total number of nucleated cells in humans[174] or approximately 1 MSC per 10^5 adherent stromal cells.[64] The number of progenitor cells has even been shown to decrease with ageing.[175-179] In view of this, methods have been developed to culture-expand and select the osteoprogenitor cell fraction from bone marrow.[15,173,174,180] These methods include density gradient selection of the cell fraction from the bone marrow, preferential adherance to tissue culture polystyrene and subsequent serial
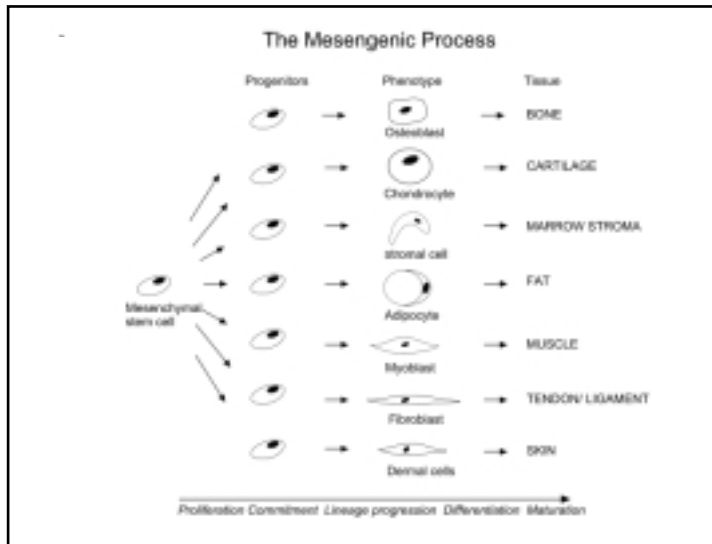
Figure 3A.

The mesengenic process.

passage to expand the cells. In addition, the identification of matrix and soluble markers and the use of monoclonal antibodies to cell surface antigens [for example STRO-1, SB-10 (antibody recognizing ALCAM) and HOP-26] can be used to select certain immature cell types.[174,181-185] However, no markers are currently available to identify true osteogenic stem cells.

In addition to proliferation, the differentiation of osteoprogenitor cells can be directed during culture. In view of this, several factors, like dexamethasone and BMPs, are known to direct the differentiation of undifferentiated cells into the osteoblast lineage *in vitro*.[62,68,186] The addition of proliferation (bFGF) and differentiation (rhBMP-2) stimulating agents during culture has been shown to enhance the *in vivo* osteogenic potential.[187,188] Prolonged culturing on a carrier after cell loading has also been shown to be more effective with respect to final *in vivo* bone formation,[189] especially when the medium is supplemented with dexamethasone during this period.[190,191]

The osteogenic potential of cell-loaded scaffolds can further be enhanced by modifying the conditions during seeding (by optimizing the number of loaded cells)[188,192,193] and conditions during culturing (*e.g.* static vs. dynamic culturing).[194,195]

1.6.3   Bone marrow stromal cells *in vivo*

While fresh marrow can form bone upon implantation *in vivo*,[196,197] the culturing of cells from bone marrow has several advantages. Due to their high proliferation potential, cells can be culture-expanded by a billion-fold or 30 population doublings.[198] This limits the amount of harvested cells and can increase the number of loaded cells or specimens. In addition, it has been shown that cultured bone marrow-derived MSCs result in earlier bone formation[199-201] and are more effective than fresh total bone marrow.[15]
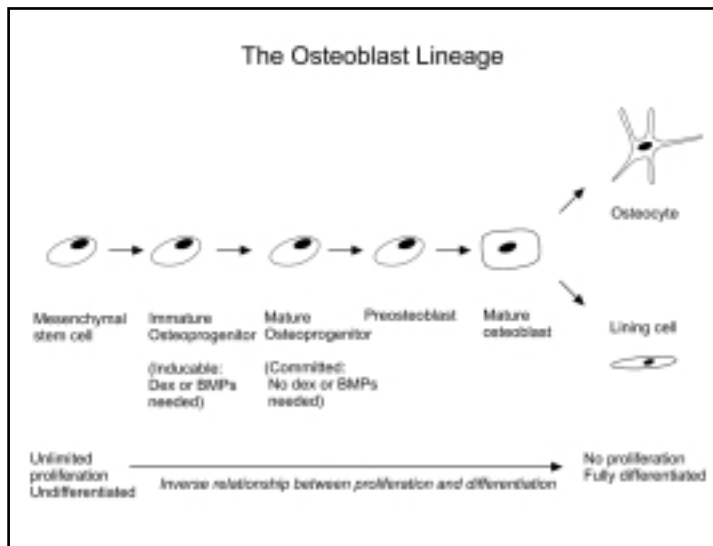
Figure 3B.

The osteoblast lineage.

Bone formation upon the implantation of cell-loaded scaffolds has been shown in heterotopic (subcutaneous, intramuscular, under the kidney capsule and intra-abdominal) and orthotopic sites.[15,180,196,199,202,203]

Heterotopic bone formation *in vivo* has been studied in closed and open systems. In closed systems, bone marrow stromal cells are placed into a diffusion chamber. In this system, there is no direct contact between host and recipient cells. In open systems, bone marrow stromal cells are implanted with a scaffold material. In this system, direct contact between host cells and recipient cells is possible, and vascular ingrowth can occur.

In closed systems, dependent on the size of the chamber, bone or bone and cartilage are formed.[200,204-206] In the heterotopic implantation of fresh or cultured bone marrow cells loaded on a scaffold, bone is formed with bone marrow-like tissue, without significant amounts of cartilage, and is therefore similar to intra-membranous bone formation. [190,196,199,193,207,208] However, occasionally minimal amounts of cartilage occur that is thought to be related to the geometry of the porous scaffold.[193,199,207]

Heterotopic bone formation by fresh and cultured bone marrow cells from different animals loaded onto scaffolds has been shown in nude mice, rats, rabbits and canine.[160,173] In addition, cultured human cells have been shown effective in ectopic bone formation in nude mice. Following heterotopic implantation in rodents with fresh or cultured bone marrow cells, hematopoietic cells originate from the recipient, while bone originates from the donor. However, when quail marrow cells were implanted in nude mice, bone was of donor origin for up to 4 weeks, and of recipient origin after 12 weeks.[160]

In orthotopic implantation, fresh and cultured bone marrow cells from different animals loaded onto scaffolds have been successful in the regeneration of cranial defects (*mice*) and long bone defects in the radius (*dogs*), femur (*rats and dogs*) and tibia (*sheep*).[15,160,169,180,209] In addition, human cells have also been shown to be effective in bone formation in long bone defects in athymic rats.[210]

1.6.4   Dynamic culture methods

To overcome the problems associated with static culture methods (*e.g.* limited diffusion of nutrients), dynamic methods have recently been developed. These dynamic methods have been applied to the engineering of bone, cartilage, endothelium, liver and other tissues. [194,195,211-217] The application of dynamic culture methods such as spinner flasks, micro-carriers, perfusion culture and rotating wall bioreactors has been reviewed recently by Temenoff *et al.* with respect to cartilage engineering. [218] The methods that have been applied to the engineering of bone tissue are perfusion flow and rotating wall vessels. [194,195,219,217]

In rotating wall vessels, microcarriers are used for anchorage-dependent cells, and a zero-gravity environment is created in which the forces of gravity are neutralized by rotation. The use of rotating wall vessels has been shown to sustain osteogenic expression for rat bone marrow stromal cells and osteoblast-like cells (SaOS cells and ROS17/2.8 cells) on different microcarriers. [217] In addition, it has been shown to enhance osteogenic expression *in vitro* for the latter cells (SaOS cells and ROS17/2.8 cells) when compared with static culture methods. [195,219]

The same has been proven for perfusion flow *–a three-dimensional medium-rotating configuration system–* on the osteogenic expression of rat bone marrow stromal cells cultured on calcium phosphate samples. The dynamic culture method was found to sustain a viable cell population, and more bone matrix was formed in the dynamic than in the static culture environment. [194]

Although these results hold some promise for the future, the beneficial effect of rotating wall vessels has been proven for immortalized and osteosarcoma cell lines only; a rat bone marrow stromal cell culture was used, but no comparison was made between static and dynamic culturing. For perfusion flow, only preliminary data are available. Nevertheless, this method has been shown to enhance osteogenic expression for bone marrow stromal cells over static culture. No data are currently available on the *in vivo* osteogenic activity of these constructs.

1.7   Combination of cells and growth factors

1.7.1   Direct combination

The combination of cells and growth factors has been shown to enhance the osteogenic response. For example, fresh bone marrow combined with rhBMP-2 or TGF-β_1 has been shown to be more effective in bone defect healing *in vivo* than marrow alone.[220-222] In these studies, the combination of rhBMP-2 and marrow was even more effective than the carrier with BMP alone.[222,220] These results hold some promise for future applications.

1.7.2   Gene therapy

In gene therapy, genetic information is transferred to cells. When the gene is transfected into the cells, the targeted cells produce the encoded protein. In this way, both short- and long-term expression are possible. Gene therapy can either be systemic or regional. The vector can be introduced directly into a certain location *in vivo*, or specific cells can be harvested, which are then transfected *ex vivo*. This latter approach offers a better control over which cells receive the vector. The vector that is used can either be viral [*e.g.* retro-viruses, adeno-virsuses, cytomegalo viruses (CMV), herpes simplex viruses and adeno-associated viruses] or non-viral (*e.g.* liposomes or DNA ligand complexes).[223] While the non-viral vectors are easier to produce, raise less safety concern and are less immunogenic, they are also less effective.

Various types of cells that have been *ex vivo* transfected have been proven to be osteinductive *in vivo*. For example, *ex vivo* transfected cells with the BMP-2 gene induce ectopic bone formation *in vivo*. In mice or rats, these cells include bone marrow stromal cells, muscle derived cells, articular chondrocytes, fibroblasts and W-20-17 cells.[224,225] Bone marrow stromal cells, transfected with the BMP-2 gene, combined with a DBM carrier were effective in the healing of femoral defects in rats.[226] In addition, fibroblasts transfected with the BMP-7 gene, combined with gelatin sponges, could induce ectopic bone formation and regenerate calvarial defects in rats.[227]

Alternatively, BMP genes can be introduced *in vivo*. An adenoviral vector containing the BMP-2 gene induced ectopic bone formation after injection in mice.[228] A CMV vector containing the BMP-2 gene induced ectopic bone formation when injected in rats,[229] while, an adenoviral vector containg the BMP-2 gene promoted spinal fusion in rats.[230] A CMV vector containing the BMP-7 gene, mixed with a collagen carrier, induced ectopic bone formation when implanted in mice.[231]

DNA plasmids encoding for BMP-4 together with a collagen carrier have been shown to regenerate femoral defects in rats.[232] Moreover, an adenovirus with BMP-2 or TGF-β genes could heal a rabbit femoral defect, although BMP-2 was more effective than TGF-β.[233]

These observations hold some promise for the future though the fate of transfected cells and the safety of viral vectors need further investigation.

1.8   Carrier materials

1.8.1   Carrier materials for BMP

Numerous carrier materials in combination with native BMPs from different species or recombinant human BMPs have been used in heterotopic and orthotopic implantation [119,234] (**Table 1**). These carrier materials include both organic and inorganic materials. Organic materials can be divided into biological materials and synthetic materials. The former include demineralized bone matrix (DBM), inactivated DBM [iDBM or insoluble bone matrix (IBM)], non-collagenous proteins, collagen (type-I and type-IV, absorbable collagen sponge, collagen membrane, gel and others), fibrin and AAA (Autolyzed Antigen - extracted Allogenic) bone. Synthetic organic carriers consist mainly of the poly(α-hydroxyl acids) such as poly(lactic acid) (PLA), poly(glycolic acid) (PGA) or poly(lactic-co-glycolic acid) (PLGA).[235] Inorganic carriers that have been used include calcium phosphate (CaP) ceramics –*like hydroxyapatite (HA) and tricalcium phosphate (TCP) or HA/TCP composites, coral and natural bone mineral*–, bioglass and metals, for example titanium. In addition, composite carriers have been created that are a combination of different materials, examples of these are poly(glycolic acid) with poly-ethylene glycol and hydroxyapatite with collagen.

A large number of prerequisites have been postulated for the ideal scaffold material with regard to biocompatibility and biodegradability, absence of allergic reactions and disease transmission, gross architectural qualities, osteoconductivity, chemotaxis, delivery/control of osteoinductive protein, angiogenesis and vascularization and administrative issues.[236] The carriers that are mainly used are CaP ceramics, poly(α-hydroxyl acids) and collagen.[237] However, it has to be emphasized that none of the currently used carrier materials meet all of the properties postulated. Some of the materials –*synthetic polymers for example*– can elicit an undesirable inflammatory response or foreign body reaction. These reactions are associated with a reduced osteoinductive response.[238,239] Other drawbacks include the lack of structural support and good mechanical characteristics.[240,241]

1.8.2   BMP release

Few reports exist on the release of BMPs from carrier materials. The release of different BMPs from frequently used carriers, including collagen, synthetic and natural ceramics, DBM and PGA, was studied in the rat ectopic assay model by the Genetics Institute.[242,243] The release of rhBMP-2 was found to occur in two phases – an initial phase, characterized by a rapid release in the first hours, and a secondary phase, characterized by a slower more gradual release. Collagen was found to retain the highest fraction of BMPs during the initial period (70 %), gradually releasing BMP over the next 2 weeks. The other materials retained 30-50 % of their load in this initial period. Synthetic hydroxyapatite particles seemed to retain the lowest amount during the initial phase (10 %). In general, mineral and mineral-based carriers (except synthetic hydroxyapatite) retained a high fraction of the BMPs in the secondary phase, which reflects a high affinity for BMPs. The release rate of BMP shown by DBM was similar to collagen, though the latter retained higher amounts.

Table 1.

Table showing the carrier/scaffold materials that have been described for BMP, TGF-β and osteogenic cells.

Carriers / scaffolds	BMP	TGF-β	Osteogenic cells
1 Inorganic materials			
Ceramic materials:			
Calcium phosphate ceramics:			
Hydroxapatite (HA) (synthetic and coral-derived)	∗		∗
Tricalcium phosphate (TCP)	∗	∗	∗
Hydroxyapatite / tricalcium phosphate (HA/TCP)	∗		∗
Calcium sulphate paste	∗	∗	
Coral (calcium carbonate)	∗	∗	∗
Natural bone mineral	∗		
Other ceramics:			
Bioglass	∗		
Apatite-wollastonite containing glass ceramic	∗		
Alumina ceramic (with or without a CaP coating)			∗
Metals:			
Titanium	∗		∗
Tinium alloy (Ti-6Al-4V) (with a CaP coating)	∗	∗	
2 Organic materials			
A. Biological materials			
Demineralized bone matrix / inactivated demineralized bone matrix	∗	∗	∗
Collagen	∗		∗
Non-collagenous protein (NCP)	∗		
Fibrin	∗		
Others:			
Lyophilized cartilage	∗		
Autolyzed Antigen - extracted Allogenic (AAA) bone	∗		
Inactivated dentin matrix	∗		

Table 1. *continued*

Table showing the carrier/scaffold materials that have been described for BMP, TGF-β and osteogenic cells.

Carriers / scaffolds	BMP	TGF-β	Osteogenic cells
2 Organic materials			
B. Synthetic materials			
Polymers:			
Poly(α-hydroxyl acids):			
Poly(lactic acid) (PLA)	*		
Poly(glycolic acid) (PGA)	*		
Poly(lactic-co-glycolic acid) (PLGA)	*	*	*
Poly(lactic acid) -polyethylene glycol	*		
Hydrogels	*		
Methyl cellulose gel		*	
3 Composites			
PLGA / DBM		*	
PLGA / polyethylene glycol	*		
PLGA / gelatin sponge	*		
TCP / collagen	*		
HA / collagen	*		*
HA / TCP / Collagen (*e.g.* Collagraft)	*		*
Coral / Collagen	*		

In addition to carrier properties, the release of BMPs is influenced by intrinsic protein properties like solubility.[243] BMP-carrier affinity has been found to vary for different recombinant human BMPs (rhBMP-2, chemically modified rhBMP-2, rhBMP-4 and rhBMP-6). RhBMP-2 and rhBMP-6 showed the highest affinity for the carriers, while rhBMP-4 showed a lower affinity, and the chemically modified rhBMP-2 even less. Further, a higher retention of BMP within the implant was positively correlated with a higher osteo-inductive response.

1.8.3   Carrier materials for TGF-β

The literature available on *in vivo* bone induction by TGF-βs is substantially less than for BMPs. TGF-β has been shown to be beneficial in bone defect healing *–cranial defects,*

mandibular defects and long bone defects–, and in the osseointegration of implants (see earlier).

The carrier materials include organic and inorganic materials (**Table 1**). Organic materials comprise DBM[140-142] or inactivated DBM (iDBM)[143,244] and methyl cellulose gel.[245,246] A polymer that has been investigated is poly(lactic-co-glycolic acid) (PLPG).[247] In addition, a composite of PLPG and DBM[144] has been studied. Inorganic materials used include calcium phosphate ceramics, for example tricalcium phosphate granules,[221,248] coral[249] and calcium phosphate cement.[250] Calcium sulphate paste has also been used.[144]

While most of these formulations have been shown to be effective in bone defect healing when combined with various doses of TGF-β_1, negative results have also been reported. For example, despite relatively high TGF-β_1 doses, Gombotz *et al.* only found an inflammatory response with the PLPG/DBM carrier in critical size defects in rat calvaria with little bone formation.[251] This reaction might be attributable to the PLPG but also to the xenogenic DBM. Although a TGF-β_1-loaded iDBM carrier could regenerate a critical size defect in sheep tibia,[139] this carier was not able to close critical sized defects in baboons but only stimulated bone formation at the edges.[143] Blom *et al.*[250] only found limited bone formation when calcium phosphate cement was used with a very low concentration of rhTGF-β_1. Similarly, in a dog radial defect model a 10-ng dose combined with a PLPG carrier did not show any response.[252]

In osteointegration studies, rhTGF-β_1 stimulated bone ingrowth up to threefold in hydroxyapatite/tricalcium phosphate (HA/TCP)-coated titanium-fiber-metal-coated titanium alloy rods.[148] In a similar manner, rhTGF-β_1 has been shown to enhance mechanical fixation and bone ongrowth for TCP-coated solid titanium alloy implants.[146,147]

1.8.4   Carrier materials for osteogenic cells

The carriers that have been used for osteogenic cells are mainly ceramic materials (**Table 1**). These materials are either coral-derived or synthetic hydroxyapatite (HA), tricalcium-phosphate (TCP), composites of HA and TCP (60/40 and 65/35), coral and alumina ceramic. Other materials that have occasionally been studied are biological materials like collagen and demineralized bone matrix, porous titanium felt and polymers, like PLGA. In addition, composites such as HA and collagen have been investigated.[160,253]

1.9   Clinical research

The clinical use of BMPs has been described in orthopedic and oral-maxillo-craniofacial applications. In the first investigations carried out, native BMP was used in a non-controlled manner. Johnson *et al.* treated segmental defects of the tibia and resistant non-unions of the tibia, femur and humerus.[254-260] In these studies, native human BMP (hBMP) with non-collagenous protein (NCP) was used. This BMP was either suspended in gelatin capsules, in a strip of poly(lactic-co-glycolic acid) or absorbed to autogenic or allogenic autolyzed antigen-extracted bone. The concentration of BMP used in these studies

was 50–100 mg per implant. In segmental defects, the healing periods varied between 4 and 9 months; in non-unions, healing varied between 3 and 7 months. In most patients successful healing could be obtained without an immunological response or any other adverse effects. Although many patients were treated with human BMP/NCP, no control group was included and, as a result, no final conclusions could be drawn as to whether BMP was effective in this treatment.

Sailer et al.[261] used native bovine BMP (bBMP) for the treatment of craniofacial defects including maxillofacial reconstructions, pseudarthroses (mandible and maxilla), cranial reconstructions (contour augmentation) and compromised situations in implantology. In the majority of cases, BMP was combined with bone matrix granules at a bBMP concentration of 1 mg purified BMP/cm^3; in other cases bBMP was combined with lyophilized cartilage or bone. In this way, 482 patients were treated in which 381 craniomaxillofacial operations were performed (Le Fort osteotomies, saggital splitting of the skull, mandibular reconstruction, genioplasty etc.), and 725 implants were placed. Sailer also concluded that no adverse reactions were observed towards bBMP and found bBMP to be effective in these cases. However, the patient groups were not homogeneous and no controls were included.

More recently, pilot studies have been published in which rhBMP-2 and rhBMP-7 (OP-1) have been used clinically in orthopaedic and dental and cranio-maxillofacial applications.[30,262-267]

Maxillary sinus floor augmentation has been performed with absorbable collagen sponge together with rhBMP-2 (1.77–3.40 mg) in 12 patients. The average height increase of the maxillary sinus floor was 8.51 mm, but this varied between 2.3 and 15.7 mm.[262] No immunological or adverse effects were noted. In another clinical study, absorbable collagen sponge with rhBMP-2 was unable to stimulate bone formation in alveolar ridge augmentation but it did stimulate bone formation in extraction pockets.[263] Maxillary sinus floor augmentation with OP-1 and a collagen carrier only demonstrated bone formation in one of the three patients.[265]

In 12 patients with open tibial fractures, rhBMP-2 (3.4–6.8 mg) with an absorbable collagen sponge carrier was used.[267] Fractures were fixed with an external fixator or intramedullary (IM) nail. In 9 patients the fracture healed without further surgical intervention. The remaining 3 patients, all treated with external fixator, needed further treatment. No second intervention was needed in the group treated with IM nail fixation. In a feasibility study, the same authors found a 40 % second intervention rate for current treatment methods. In addition, no adverse effects occurred, but 2 patients showed a transient occurrence of antibodies against rhBMP-2 at 2 weeks.

Two controlled studies have been performed with rhBMP-7. In 30 patients with non-union tibial fractures, 14 patients were treated with rhBMP-7 and a type-I collagen carrier, and a control group of 16 patients were treated with autogenous iliac crest bone. After 9 months, healing of non-unions could be confirmed radiographically in 27 patients; 1 autograft and 2 rhBMP-7-treated non-unions failed to heal. In addition, 2 patients were not fully weight-bearing. Of the remaining patients, 18 patients were pain-free, while the others had mild to moderate pain upon weight-bearing.

Another controlled study by Geesink et al.[264] demonstrated that 2.5 mg rhBMP-7 with a collagen type-I carrier could regenerate a 15-mm tibial defect in patients undergoing a

tibial osteotomy. RhBMP-7 significantly stimulated bone defect healing compared to collagen alone. However, with DBM, 6/6 patients demonstrated healing, while in 5/6 patients healing was observed with rhBMP-7. No adverse reaction from or immunological reaction towards the rhBMP-7 was observed; however, only in the OP-1 group had 3 patients pain 1 year post-operative, which could be related to excessive bone formation.

No clinical data are available for TGF-β in bone defect healing. However, when systemically administered in patients with progressive multiple sclerosis, TGF-β_2 has been shown to result in a reversible decline in renal function.[268]

Conolly *et al.* developed a method in which a percutaneous injection of autologous marrow aspirate was effective in 80 % of the cases in stimulating bone healing, including delayed unions and fracture non-unions, arthrodeses and bone defects.[269,270]

Limited clinical studies are available in which marrow stromal cells have been *ex vivo* expanded for clinical use. In a non-controlled study, cultured human bone marrow stromal cells have been loaded into DBM and transplanted into non-unions, pseudarthrosis and bone defects. A 2-year follow-up in 15 patients revealed that healing occurred in all patients.[271] In another study, allogenic lyophilyzed bone fragments combined with either fresh autogenous marrow (30 patients) or cultured autogenous bone marrow stromal cells with autogenous marrow (10 patients) were evaluated for the healing of mandibular defects (cyst excision or correction of mandibular deformation). While both strategies were able to regenerate the defect, the cultured bone marrow stromal cells with autogenous marrow resulted in faster bone healing.[201]

Taken together, these studies show that BMPs and osteogenic cells can be used to stimulate bone healing.[160] Nevertheless, the response shows inter-individual differences.

1.10 Titanium and calcium phosphate coatings

1.10.1 Titanium

In addition to polymers and ceramics, metals like titanium can also be used to create BGS. Porous and non-porous titanium implants with varying geometrical properties have been investigated. In a preliminary study, a titanium fiber mesh (similar to the one we propose) with a thickness of 2 mm, a fiber diameter of 50 μm and a pore range of 100- 600 μm has been used as a scaffold for osteogenic cells. When loaded with fresh autogenous bone marrow cells, this fiber mesh could generate bone formation in heterotopic implantation.[272] Another porous sintered titanium fiber metal implant loaded with syngeneic marrow cells has been found to generate bone formation in a rat femoral defect model. However, this titanium implant was less effective in healing the defect than a hydroxy-apatite/tricalcium phosphate ceramic.[273] Other titanium wire metals or fiber meshes have also been shown to allow bone ingrowth[274,275] which is enhanced by TGF-β_1.[148]

Porous and non-porous titanium implants have also been studied as carriers for Bone Morphogenetic Proteins both in heterotopic and orthotopic locations. Cylindrical porous titanium implants loaded with rhBMP-2 induced heterotopic bone formation.[276] The same was found for non-porous titanium alloy substates loaded with native BMP[277] in which the

application of a titanium or hydroxyapatite coating increased the amount of newly formed bone.[278] In an orthotopic location, rhBMP-7 was observed to enhance osseointegration of non-porous titanium implants.[279]

1.10.2   Calcium phosphate coatings

Titanium fiber mesh can be provided with a calcium phosphate (Ca-P)-coating. It is generally supposed that Ca-P coatings enhance the bone formation process. Calcium phosphate coatings can be applied using various methods such as plasma spraying, high velocity oxygen-fuel spraying, electrophoretic deposition, sol-gel deposition, hot isostatic pressing, frit enamelling, ion-assisted deposition, pulsed laser deposition, electrochemical deposition, biomimetic deposition and sputter coating.[280] We propose the use of a sputter coating since the coating is very thin and suitable for coating substrates with difficult geometrical shapes. Sputter coating is a process in which the atoms or molecules of a material are ejected by bombardment of high-energy ions. The freed particles deposit on a substrate placed in the vacuum chamber. Several sputter techniques exist: diode sputtering, direct current or ion-beam, and radio-frequent (RF) sputtering. We use a magnetically enhanced variant of the diode sputtering – the so-called RF magnetron sputter technique, which is suitable for sputtering metals, alloys and ceramics as well as other materials.

The use of such a thin RF magnetron-sputtered ceramic coating on metal implants has already been proven to enhance osteogenic expression *in vitro* and osteoconduction *in vivo*.[281-283] A thicker plasma spray coating has been shown to enhance bone formation in fresh marrow cell-loaded alumina ceramic,[284] but it has not been proven that it stimulates BMP-induced bone formation.[276,278,279]

1.11 Objective and hypothesis

Because of the associated disadvantages of currently used carrier materials in the creation of BGSs, titanium fiber mesh might be a potential scaffold material for loaded applications. This titanium mesh has excellent mechanical properties in terms of stiffness and elasticity. Further, it is biocompatible both for soft tissue and bone, and easy to handle during surgery. Although titanium is not degradable, for a large number of reconstructive procedures, this is no drawback. An additional advantage is that the titanium fiber mesh can be provided with a calcium phosphate coating.

On the basis of available literature, we hypothesize that a Ca-P ceramic coating will also have a beneficial effect on the effectiveness of a titanium scaffold in the creation of BGS.[235] Therefore, the objective of this thesis was to examine the use of a titanium fiber mesh scaffold with or without a thin calcium phosphate coating in the creation of BGS.

In order to evaluate the feasibility of a titanium fiber mesh scaffold in the creation of BGS the following questions have to be answered:

1. *What is the osteogenic expression in porous titanium fiber mesh loaded with rat bone marrow cells in vitro, and how is it influenced by cell seeding density and rhBMP-2 concentration?*

2. *What is the efficacy of a titanium fiber mesh loaded with cultured osteogenic cells on bone formation in an ectopic location, and what is the additional influence of the application of a thin Ca-P coating?*

3. *What is the effect of the cell seeding method in combination with prolonged in situ culturing on bone formation in titanium fiber mesh scaffolds in an ectopic location?*

4. *Can titanium fiber mesh loaded with Bone Morphogenetic Proteins (BMPs) induce bone formation in an ectopic location, and can the osteoinductive effect of recombinant human BMP synergistically be enhanced by native bovine BMPs?*

5. *What is the nature of the bone induction process in various BMP-loaded carrier materials?*

6. *What is the bone formation-supporting efficacy of titanium fiber mesh as-received, provided with a thin calcium phosphate coating, or loaded with $rhTGF\text{-}\beta_1$ in an orthotopic site?*

7. *What is the efficacy of porous PPF provided with $rhTGF\text{-}\beta_1$ on bone induction in an orthotopic site, and what is the effect of a fibronectin coating on the bone response to porous PPF?*

References

1. **Langer R, Vacanti JP.** Tissue engineering. Science 1993; 260:920.
2. **Lind M.** Growth factors: possible new clinical tools. A review. Acta Orthop Scand 1996; 67:407.
3. **Mendicino SS, Rockett A, Wilber MR.** The use of bone grafts in the management of nonunions.
    J Foot Ankle Surg 1996; 35:452.
4. **Bostrom MP, Camacho NP.** Potential role of bone morphogenetic proteins in fracture healing.
    Clin Orthop 1998; 355 Suppl: S274.
5. **Younger EM, Chapman MW.** Morbidity at bone graft donor sites. J Orthop Trauma 1989; 3:192.
6. **Damien CJ, Parsons JR.** Bone graft and bone graft substitutes: a review of current technology and applications.
    J Appl Biomater 1991; 2:187.
7. **Arrington ED, Smith WJ, Chambers HG, Bucknell AL, Davino NA.** Complications of iliac crest bone graft harvesting.
    Clin Orthop 1996; 329:300.
8. Leads from the MMWR. Transmission of HIV trough bone transplantation: Case report and public health
    recommendations. JAMA 1988; 260:2487.
9. **Simonds RJ.** HIV transmission by organ and tissue transplantation. AIDS 1993; 7 Suppl 2:S35.
10. **Buck BE, Resnick L, Shah SM, Malinin TI.** Human immunodeficiency virus cultured from bone. Implications for
    transplantation. Clin Orthop 1990; 251:249.
11. **Buck BE, Malinin TI, Brown MD.** Bone transplantation and human immunodeficiency virus. An estimate of risk
    of acquired immunodeficiency syndrome (AIDS). Clin Orthop 1989; 240:129.
12. **Skalak R, Fox CF.** Tissue Engineering, Editor: Alan R. Liss, New York, 1988, preface.
13. **Nerem RM, Sambanis A.** Tissue engineering: from biology to biological substitutes.
    Tissue Eng 1995; 1:3-12.
14. **Patrick CP, Mikos AG, Mc Intire LV.** Frontiers in tissue engineering. Elsevier Science, Ltd., Oxford, UK, 1998.
15. **Kadiyala S, Neelam J, Bruder SP.** Culture-expanded, bone marrow-derived mesenchymal stem cells can regenerate
    a critical-sized segmental bone defect. Tissue Eng 1997; 3:173.
16. **Winn SR, Hu Y, Sfeir C, Hollinger JO.** Gene therapy approaches for modulating bone regeneration.
    Adv Drug Deliv Rev 2000; 42:121.
17. **Kessler E, Takahara K, Biniaminov L, Brusel M, Greenspan DS.** Bone morphogenetic protein-1: the type I
    procollagen C-proteinase. Science 1996; 271:360.
18. **Hofbauer LC, Heufelder AE.** Updating the metalloprotease nomenclature: bone morphogenetic protein 1
    identified as procollagen C proteinase. Eur J Endocrinol 1996; 135:35.
19. **Schmitt JM, Hwang K, Winn SR, Hollinger JO.** Bone morphogenetic proteins: an update on basic biology and
    clinical relevance. J Orthop Res 1999; 17:269.
20. **Wozney JM, Rosen V.** Bone morphogenetic protein and bone morphogenetic protein gene family in bone
    formation and repair. Clin Orthop 1998; 346:26.
21. **Urist MR.** Bone: formation by autoinduction. Science 1965; 150:893.
22. **Urist MR.** Strates BS. Bone morphogenetic protein. J Dent Res 1971; 50:1392.
23. **Urist MR.** Bone morphogenetic protein in biology and medicine. In: Bone Morphogenetic Proteins: biology,
    biochemistry and reconstructive surgery. Editor: Lindolm TS, Academic Press, London UK, 1996, 7.
24. **Hogan BL.** Morphogenesis. Cell 1999; 96:225.
25. **Bostrom MP, Lane JM, Berberian WS, Missri AA, Tomin E, Weiland A, Doty SB, Glaser D, Rosen VM.**
    Immunolocalization and expression of Bone Morphogenetic Proteins 2 and 4 in fracture healing.
    J Orthop Res 1995; 13:357.
26. **Bostrom MP.** Expression of Bone Morphogenetic Proteins in fracture healing. Clin Orthop 1998; 355 Suppl:S116.
27. **Bostrom MP, Asnis P.** Transforming Growth Factor β in fracture repair. Clin Orthop 1998; 355 Suppl: S124.
28. **Jin Y, Yang L, White FH.** An immunocytochemical study of bone morphogenetic protein in experimental fracture
    healing of the rabbit mandible. Chin Med Sci J 1994; 9:91.
29. **Nakase T, Nomura S, Yoshikawa H, Hashimoto J, Hirota S, Kitamura Y, Oikawa S, Ono K, Takaoka K**.
    Transient and localized expression of bone morphogenetic protein 4 messenger RNA during fracture healing.
    J Bone Miner Res 1994; 9:651.
30. **Groeneveld EH, Burger EH.** Bone Morphogenetic Proteins in human bone regeneration.
    Eur J Endocrinol 2000; 142:9.
31. **Wozney JM.** The bone morphogenetic protein family: multifunctional cellular regulators in the embryo and adult.
    Eur J Oral Sci 1998; 106 Suppl 1:160.

32. **Suzuki A, Kaneko E, Maeda J, Ueno N.** Mesoderm induction by BMP-4 and -7 heterodimers. Biochem Biophys Res Commun 1997; 232:153.
33. **Israel DI, Nove J, Kerns KM, Kaufman RJ, Rosen V, Cox KA, Wozney JM.** Heterodimeric bone morphogenetic proteins show enhanced activity *in vitro* and *in vivo*. Growth Factors 1996; 13:291.
34. **Riley EH, Lane JM, Urist MR, Lyons KM, Lieberman JR.** Bone morphogenetic protein-2: biology and applications. Clin Orthop 1996; 324:39.
35. **Bessho K, Kusumoto K, Fujimura K, Konishi Y, Ogawa Y, Tani Y, Iizuka T.** Comparison of recombinant and purified human bone morphogenetic protein. Br J Oral Maxillofac Surg 1999; 37:2.
36. **Wozney JM, Rosen V, Celeste AJ, Mitsock LM, Whitters MJ, Kriz RW, Hewick RM, Wang EA.** Novel regulators of bone formation: molecular clones and activities. Science 1988; 242:1528.
37. **Israel DI, Nove J, Kerns KM, Moutsatsos IK, Kaufman RJ.** Expression and characterization of bone morphogenetic protein-2 in Chinese hamster ovary cells. Growth Factors 1992; 7:139.
38. **Bessho K, Konishi Y, Kaihara S, Fujimura K, Okubo Y, Iizuka T.** Bone induction by Escherichia coli-derived recombinant human bone morphogenetic protein-2 compared with Chinese hamster ovary cell-derived recombinant human bone morphogenetic protein-2. Br J Oral Maxillofac Surg 2000; 38:645.
39. **Kubler NR, Reuther JF, Faller G, Kirchner T, Ruppert R, Sebald W.** Inductive properties of recombinant human BMP-2 produced in a bacterial expression system. Int J Oral Maxillofac Surg 1998;27:305.
40. **Kubler NR, Moser M, Berr K, Faller G, Kirchner T, Sebald W, Reuther JF.** Biological activity of E. coli expressed BMP-4. Mund Kiefer Gesichtschir 1998; 2 Suppl 1:S149.
41. **Wrana JL.** Regulation of Smad activity. Cell 2000; 100:189.
42. **de Larco JE, Todaro GJ.** Growth factors from murine sarcoma virus-transformed cells. Proc Natl Acad Sci USA 1978; 75:4001.
43. **Roberts AB, Anzano MA, Lamb LC, Smith JM, Sporn MB.** New class of Transforming Growth Factors potentiated by epidermal growth factor: isolation from non-neoplastic tissues. Proc Natl Acad Sci USA 1981; 78:5339.
44. **Roberts AB, Sporn MB.** The Transforming Growth Factor betas. In: Handbook of experimental pharmacology: Peptide growth factors and their receptors. Editors: Sporn MB and Roberts AB. Springer Verlag, New York, USA, 1990, 419.
45. **Ogawa Y, Schmidt DK, Dasch JR, Chang RJ, Glaser CB.** Purification and characterization of Transforming Growth Factor beta-2.3 and -beta-1.2 heterodimers from bovine bone. J Biol Chem 1992; 267:2325.
46. **Gentry LE, Webb NR, Lim GJ, Brunner AM, Ranchalis JE, Twardzik DR, Lioubin MN, Marquardt H, Purchio AF.** Type 1 Transforming Growth Factor beta: amplified expression and secretion of mature and precursor polypeptides in Chinese hamster ovary cells. Mol Cell Biol 1987; 7:3418.
47. **Lioubin MN, Madisen L, Marquardt H, Roth R, Kovacina KS, Purchio AF.** Characterization of latent recombinant TGF-beta2 produced by Chinese hamster ovary cells. J Cell Biochem 1991; 45:112.
48. **Bonewald LF, Dallas SL.** Role of active and latent Transforming Growth Factor beta in bone formation. J Cell Biochem 1994; 55:350.
49. **Wakefield LM, Smith DM, Masui T, Harris CC, Sporn MB.** Distribution and modulation of the cellular receptor for Transforming Growth Factor beta. J Cell Biol 1987; 105:965.
50. **Robey PG, Young MF, Flanders KC, Roche NS, Kondaiah P, Reddi AH, Termine JD, Sporn MB, Roberts AB.** Osteoblasts synthesize and respond to Transforming Growth Factor-type beta (TGF-beta) *in vitro*. J Cell Biol 1987; 105:457.
51. **Sporn MB, Roberts AB.** The multifunctional nature of growth factors. In: Handbook of experimental pharmacology: Peptide growth factors and their receptors. Editors: Sporn MB and Roberts AB. Springer Verlag, New York, USA, 1990, 3.
52. **Wrana JL, Attisano L.** The Smad pathway. Cytokine Growth Factor Rev 2000; 11:5.
53. **Sampath TK, Maliakal JC, Hauschka PV, Jones WK, Sasak H, Tucker RF, White KH, Coughlin JE, Tucker MM, Pang RH *et al*.** Recombinant human osteogenic protein-1 (hOP-1) induces new bone formation *in vivo* with a specific activity comparable with natural bovine osteogenic protein and stimulates osteoblast proliferation and differentiation *in vitro*. J Biol Chem 1992; 267:20352.
54. **Wang EA, Israel DI, Kelly S, Luxenberg DP.** Bone morphogenetic protein-2 causes commitment and differentiation in C3H10T1/2 and 3T3 cells. Growth Factors 1993; 9:57.
55. **Puleo DA.** Dependence of mesenchymal cell responses on duration of exposure to bone morphogenetic protein-2 *in vitro*. J Cell Physiol 1997; 173:93.
56. **Puleo DA, Huh WW, Duggirala SS, DeLuca PP.** *In vitro* cellular responses to bioerodible particles loaded with recombinant human bone morphogenetic protein-2. J Biomed Mater Res 1998;41:104.
57. **Yamaguchi A, Katagiri T, Ikeda T, Wozney JM, Rosen V, Wang EA, Kahn AJ, Suda T, Yoshiki S.** Recombinant human bone morphogenetic protein-2 stimulates osteoblastic maturation and inhibits myogenic differentiation *in vitro*. J Cell Biol 1991; 113:681.
58. **Chen TL, Bates RL, Dudley A, Hammonds RG Jr, Amento EP.** Bone morphogenetic protein-2b stimulation of growth and osteogenic phenotypes in rat osteoblast-like cells: comparison with TGF-beta1. J Bone Miner Res 1991; 6:1387.

59. **Zerath E, Holy X, Noel B, Malouvier A, Hott M, Marie PJ.** Effects of BMP-2 on osteoblastic cells and on skeletal growth and bone formation in unloaded rats. Growth Horm IGF Res 1998; 8:141.

60. **Thies RS, Bauduy M, Ashton BA, Kurtzberg L, Wozney JM, Rosen V.** Recombinant human bone morphogenetic protein-2 induces osteoblastic differentiation in W-20-17 stromal cells. Endocrinology 1992; 130:1318.

61. **Paralkar VM, Hammonds RG, Reddi AH.** Identification and characterization of cellular binding proteins (receptors) for recombinant human bone morphogenetic protein 2B, an initiator of bone differentiation cascade. Proc Natl Acad Sci USA 1991; 88:3397.

62. **Katagiri T, Yamaguchi A, Ikeda T, Yoshiki S, Wozney JM, Rosen V, Wang EA, Tanaka H, Omura S, Suda T.** The non-osteogenic mouse pluripotent cell line, C3H10T1/2, is induced to differentiate into osteoblastic cells by recombinant human bone morphogenetic protein-2. Biochem Biophys Res Commun 1990; 172:295.

63. **Mie M, Ohgushi H, Yanagida Y, Haruyama T, Kobatake E, Aizawa M.** Osteogenesis coordinated in C3H10T1/2 cells by adipogenesis-dependent BMP-2 expression system. Tissue Eng 2000; 6:9.

64. **Zuk PA, Zhu M, Mizuno H, Huang J, Futrell W, Katz AJ, Benhaim P, Lorenz HP, Hedrick MH**. Multilineage Cells from Human Adipose Tissue: Implications for Cell-Based Therapies. Tissue Eng 2001; 7:211.

65. **Gimble JM, Morgan C, Kelly K, Wu X, Dandapani V, Wang CS, Rosen V.** Bone Morphogenetic Proteins inhibit adipocyte differentiation by bone marrow stromal cells. J Cell Biochem 1995; 58:393.

66. **Katagiri T, Yamaguchi A, Komaki M, Abe E, Takahashi N, Ikeda T, Rosen V, Wozney JM, Fujisawa-Sehara A, Suda T.** Bone morphogenetic protein-2 converts the differentiation pathway of C2C12 myoblasts into the osteoblast lineage. J Cell Biol 1994; 127:1755.

67. **Takuwa Y, Ohse C, Wang EA, Wozney JM, Yamashita K.** Bone morphogenetic protein-2 stimulates alkaline phosphatase activity and collagen synthesis in cultured osteoblastic cells, MC3T3-E1. Biochem Biophys Res Commun 1991; 174:96.

68. **Rickard DJ, Sullivan TA, Shenker BJ, Leboy PS, Kazhdan I.** Induction of rapid osteoblast differentiation in rat bone marrow stromal cell cultures by dexamethasone and BMP-2. Dev Biol 1994; 61:218.

69. **Fromigue O, Marie PJ, Lomri A.** Bone morphogenetic protein-2 and Transforming Growth Factor beta-2 interact to modulate human bone marrow stromal cell proliferation and differentiation. J Cell Biochem 1998; 68:411.

70. **Asahina I, Sampath TK, Nishimura I, Hauschka PV.** Human osteogenic protein-1 induces both chondroblastic and osteoblastic differentiation of osteoprogenitor cells derived from newborn rat calvaria. J Cell Biol 1993; 123:921.

71. **Chen D, Harris MA, Rossini G, Dunstan CR, Dallas SL, Feng JQ, Mundy GR, Harris SE.** Bone morphogenetic protein-2 (BMP-2) enhances BMP-3, BMP-4, and bone cell differentiation marker gene expression during the induction of mineralized bone matrix formation in cultures of fetal rat calvarial osteoblasts. Calcif Tissue Int 1997; 60:283.

72. **Chen TL, Bates RL, Dudley A, Hammonds RG Jr, Amento EP.** Bone morphogenetic protein-2b stimulation of growth and osteogenic phenotypes in rat osteoblast-like cells: comparison with TGF-beta1. J Bone Miner Res 1991; 6:1387.

73. **Chaudhari A, Ron E, Rethman MP.** Recombinant human bone morphogenetic protein-2 stimulates differentiation in primary cultures of fetal rat calvarial osteoblasts. Mol Cell Biochem 1997; 167:31.

74. **Boden SD, Hair G, Titus L, Racine M, McCuaig K, Wozney JM, Nanes MS.** Glucocorticoid-induced differentiation of fetal rat calvarial osteoblasts is mediated by bone morphogenetic protein-6. Endocrinology 1997; 138:2820.

75. **Hughes FJ, Collyer J, Stanfield M, Goodman S.** The effects of bone morphogenetic Protein-2, -4, and -6 on differentiation of rat osteoblast cells *in vitro*. Endocrinology 1995; 136:2671.

76. **Yamaguchi A, Ishizuya T, Kintou N, Wada Y, Katagiri T, Wozney JM, Rosen V, Yoshiki, S.** Effects of BMP-2, BMP-4, and BMP-6 on osteoblastic differentiation of bone marrow-derived stromal cell lines, ST2 and MC3T3-G2/PA6. Biochem Biophys Res Commun 1996; 220:366.

77. **Boden SD, McCuaig K, Hair G, Racine M, Titus L, Wozney JM, Nanes MS.** Differential effects and glucocorticoid potentiation of bone morphogenetic protein action during rat osteoblast differentiation *in vitro*. Endocrinology 1996; 137:3401.

78. **Bi LX, Simmons DJ, Mainous E.** Expression of BMP-2 by rat bone marrow stromal cells in culture. Calcif Tissue Int 1999; 64:63.

79. **Lind M, Eriksen EF, Bunger C.** Bone morphogenetic protein-2 but not bone morphogenetic protein-4 and - 6 stimulates chemotactic migration of human osteoblasts, human marrow osteoblasts, and U2-OS cells. Bone 1996; 18:53.

80. **Cunningham NS, Paralkar V, Reddi AH.** Osteogenin and recombinant bone morphogenetic protein 2B are chemotactic for human monocytes and stimulate Transforming Growth Factor beta-1 mRNA expression. Proc Natl Acad Sci USA 1992; 89:11740.

81. **Sampath TK, Muthukumaran N, Reddi AH.** Isolation of osteogenin, an extracellular matrix-associated, bone- inductive protein, by heparin affinity chromatography. Proc Natl Acad Sci USA 1987;84:7109.

82. **Si X, Jin Y, Yang L.** Induction of new bone by ceramic bovine bone with recombinant human bone morphogenetic protein 2 and Transforming Growth Factor beta. Int J Oral Maxillofac Surg 1998;27:310.

83. **Duneas N, Crooks J, Ripamonti U.** Transforming Growth Factor beta-1: induction of bone morphogenetic protein genes expression during endochondral bone formation in the baboon, and synergistic interaction with osteogenic

protein-1 (BMP-7). Growth Factors 1998; 15:259.

84. **Ripamonti U, Crooks J, Matsaba T, Tasker J.** Induction of endochondral bone formation by recombinant human Transforming Growth Factor beta-2 in the baboon (Papio ursinus). Growth Factors 2000; 17:269.

85. **Ripamonti U, Duneas N, Van Den Heever B, Bosch C, Crooks J.** Recombinant Transforming Growth Factor beta-1 induces endochondral bone in the baboon and synergizes with recombinant osteogenic protein-1 (bone morphogenetic protein-7) to initiate rapid bone formation. J Bone Miner Res 1997; 12:1584.

86. **Reddi AH.** Cell biology and biochemistry of endochondral bone development. Coll Relat Res 1981; 1:209.

87. **Wozney JM.** Molecular bioloy of the Bone Morphogenetic Proteins. In: Bone grafts, Derivatives and Substitutes. Editors: Urist MR, O' Connor BT, Burwell RG. Butterworth-Heinemann Ltd., Oxford, UK, 1994, 397.

88. **Wang EA, Rosen V, D'Alessandro JS, Bauduy M, Cordes P, Harada T, Israel DI, Hewick RM, Kerns KM, LaPan P et al.** Recombinant human bone morphogenetic protein induces bone formation. Proc Natl Acad Sci USA 1990; 87:2220.

89. **Caplan AI, Boyan BD.** Enchondral bone formation the lineage cascade. In: Bone volume 8: Mechanisms of bone development. Hall BK editor. CRC press Inc., Boca Raton, Florida, USA, 1994, 1.

90. **Sasano Y, Ohtani E, Narita K, Kagayama M, Murata M, Saito T, Shigenobu K, Takita H, Mizuno M, Kuboki Y.** BMPs induce direct bone formation in ectopic sites independent of the endochondral ossification *in vivo*. Anat Rec 1993; 236:373.

91. **Kuboki Y, Saito T, Murata M, Takita H, Mizuno M, Inoue M, Nagai N, Poole AR.** Two distinctive BMP-carriers induce zonal chondrogenesis and membranous ossification, respectively; geometrical factors of matrices for cell- differentiation. Connect Tissue Res 1995; 32:219.

92. **Sasano Y, Mizoguchi I, Takahashi I, Kagayama M, Saito T, Kuboki Y.** BMPs induce endochondral ossification in rats when implanted ectopically within a carrier made of fibrous glass membrane. Anat Rec 1997; 247:472.

93. **Caplan AI** Cartilage begets bone versus endochondral myelopoiesis. Clin Orthop 1990; 261:257.

94. **Mori S, Yoshikawa H, Hashimoto J, Ueda T, Funai H, Kato M, Takaoka K.** Antiangiogenic agent (TNP-470) inhibition of ectopic bone formation induced by bone morphogenetic protein-2. Bone 1998; 22:99.

95. **Trueta J.** The role of the vessels in osteogenesis. J Bone Joint Surg1963; 45B:402.

96. **Doherty MJ, Ashton BA, Walsh S, Beresford JN, Grant ME, Canfield AE.** Vascular pericytes express osteogenic potential *in vitro* and *in vivo*. J Bone Miner Res 1998; 13:828.

97. **Basset CAL, Hermann I.** Influence of oxygen concentration and mechanical factors on differentiation of connective tissues *in vitro*. Nature 1962; 190:460.

98. **Hall BK.** Hypoxia and differentiation of cartilage and bone from common germinal cells *in vitro*. Life Sci 1969; 8:533.

99. **Caplan AI, Pechak DG.** The cellular and molecular embryology of bone formation. J Bone Miner Res1987; 5:117.

100. **Caplan AI.** Cartilage begets bone versus endochondral myelopoiesis. Clin Orthop 1990; 261:257.

101. **Reddi AH, Huggins CB.** Influence of geometry of transplanted tooth and bone on transformation of fibroblasts. Proc Soc Exp Biol Med 1973; 143:634.

102. **Sampath TK, Reddi AH.** Importance of geometry of the extracellular matrix in endochondral bone differentiation. J Cell Biol 1984; 98:2192.

103. **Ripamonti U, Ma S, Reddi AH.** The critical role of geometry of porous hydroxyapatite delivery system in induction of bone by osteogenin, a bone morphogenetic protein. Matrix 1992; 12:202.

104. **Takita H, Tsuruga E, Ono I, Kuboki Y.** Enhancement by bFGF of osteogenesis induced by rhBMP-2 in rats. Eur J Oral Sci 1997; 105:588.

105. **Kuboki Y, Takita H, Kobayashi D, Tsuruga E, Inoue M, Murata M, Nagai N, Dohi Y, Ohgushi H.** BMP-induced osteogenesis on the surface of hydroxyapatite with geometrically feasible and nonfeasible structures: topology of osteogenesis. J Biomed Mater Res 1998; 39:190.

106. **Jin QM, Takita H, Kohgo T, Atsumi K, Itoh H, Kuboki Y.** Effects of geometry of hydroxyapatite as a cell substratum in BMP- induced ectopic bone formation. J Biomed Mater Res 2000; 52:491.

107. **Mahmood J, Takita H, Ojima Y, Kobayashi M, Kohgo T, Kuboki Y.** Geometric effect of matrix upon cell differentiation: BMP-induced osteogenesis using a new Bioglass with a feasible structure. J Biochem (Tokyo) 2001; 129:163.

108. **Khouri RK, Brown DM, Koudsi B, Deune EG, Gilula LA, Cooley BC, Reddi AH.** Repair of calvarial defects with flap tissue: role of Bone Morphogenetic Proteins and competent responding tissues. Plast Reconstr Surg 1996; 98:103.

109. **Yoshida K, Bessho K, Fujimura K, Kusumoto K, Ogawa Y, Tani Y, Iizuka T**. Osteoinduction capability of recombinant human bone morphogenetic protein-2 in intramuscular and subcutaneous sites: an experimental study. J Craniomaxillofac Surg 1998;26:112.

110. **Okubo Y, Bessho K, Fujimura K, Konishi Y, Kusumoto K, Ogawa Y, Iizuka T.** Osteoinduction by recombinant human bone morphogenetic protein-2 at intramuscular, intermuscular, subcutaneous and intrafatty sites. Int J Oral Maxillofac Surg 2000; 29:62.

111. **Hosny M, Sharawy M.** Osteoinduction in rhesus monkeys using demineralized bone powder allografts. J Oral Maxillofac Surg 1985; 43:837.

112. **Aspenberg P, Wang E, Thorngren KG.** Bone morphogenetic protein induces bone in the squirrel monkey, but bone matrix does not. Acta Orthop Scand 1992; 63:619.
113. **Ripamonti U, Magan A, Ma S, van den Heever B, Moehl T, Reddi AH.** Xenogeneic osteogenin, a bone morphogenetic protein, and demineralized bone matrices, including human, induce bone differentiation in athymic rats and baboons. Matrix 1991; 11:404.
114. **Ripamonti U.** The induction of bone in osteogenic composites of bone matrix and porous hydroxyapatite replicas: an experimental study on the baboon (Papio ursinus). J Oral Maxillofac Surg 1991; 49:817.
115. **Volek-Smith H, Urist MR.** Recombinant human bone morphogenetic protein (rhBMP) induced heterotopic bone development *in vivo* and *in vitro*. Proc Soc Exp Biol Med 1996; 211:265.
116. **Bentz H, Thompson AY, Armstrong R, Chang RJ, Piez KA, Rosen DM.** Transforming Growth Factor beta-2 enhances the osteoinductive activity of a bovine bone-derived fraction containing bone morphogenetic protein- 2 and 3. Matrix 1991; 11:269.
117. **Ono I, Inoue M, Kuboki Y.** Promotion of the osteogenetic activity of recombinant human bone morphogenetic protein by prostaglandin E1. Bone 1996; 19:581.
118. **Ono I, Tateshita T, Kuboki Y.** Prostaglandin E1 and recombinant bone morphogenetic protein effect on strength of hydroxyapatite implants. J Biomed Mater Res 1999; 45:337.
119. **Kirker-Head CA.** Potential applications and delivery strategies for Bone Morphogenetic Proteins. Adv Drug Deliv Rev 2000; 43:65.
120. **Lawrence DA.** Transforming Growth Factor beta: a general review. Eur Cytokine Netw 1996; 7:363.
121. **Roberts AB, Sporn MB.** Physiological actions and clinical applications of Transforming Growth Factor beta (TGF-beta). Growth Factors 1993; 8:1.
122. **Sporn MB, Roberts AB, Wakefield LM, de Crombrugghe B.** Some recent advances in the chemistry and biology of Transforming Growth Factor beta. J Cell Biol 1987; 105:1039.
123. **Centrella M, McCarthy TL, Canalis E.** Effects of Transforming Growth Factors on bone cells. Connect Tissue Res 1989; 20:267.
124. **Centrella M, McCarthy TL, Canalis E.** Transforming Growth Factor beta and remodeling of bone. J Bone Joint Surg Am 1991; 73:1418.
125. **Centrella M, Horowitz MC, Wozney JM, McCarthy TL.** Transforming Growth Factor beta gene family members and bone. Endocr Rev 1994; 15:27.
126. **Centrella M, McCarthy TL, Canalis E.** Transforming Growth Factor beta is a bifunctional regulator of replication and collagen synthesis in osteoblast-enriched cell cultures from fetal rat bone. J Biol Chem 1987; 262:2869.
127. **ten Dijke P, Iwata KK, Goddard C, Pieler C, Canalis E, McCarthy TL, Centrella M.** Recombinant Transforming Growth Factor type beta-3: biological activities and receptor-binding properties in isolated bone cells. Mol Cell Biol 1990; 10:4473.
128. **Noda M, Rodan GA.** Type-beta Transforming Growth Factor inhibits proliferation and expression of alkaline phosphatase in murine osteoblast-like cells. Biochem Biophys Res Commun 1986; 140:56.
129. **Dieudonne SC, Foo P, van Zoelen EJ, Burger EH.** Inhibiting and stimulating effects of TGF-beta1 on osteoclastic bone resorption in fetal mouse bone organ cultures. J Bone Miner Res 1991; 6:479.
130. **Postlethwaite AE, Keski-Oja J, Moses HL, Kang AH.** Stimulation of the chemotactic migration of human fibroblasts by Transforming Growth Factor beta. J Exp Med 1987; 165:251.
131. **Pfeilschifter J, Wolf O, Naumann A, Minne HW, Mundy GR, Ziegler R.** Chemotactic response of osteoblastlike cells to Transforming Growth Factor beta. J Bone Miner Res 1990; 5:825.
132. **Lawrence WT, Diegelmann RF.** Growth factors in wound healing. Clin Dermatol 1994; 12:157.
133. **Noda M, Camilliere JJ.** *In vivo* stimulation of bone formation by Transforming Growth Factor beta. Endocrinology 1989; 124:2991.
134. **Joyce ME, Roberts AB, Sporn MB, Bolander ME.** Transforming Growth Factor beta and the initiation of chondrogenesis and osteogenesis in the rat femur. J Cell Biol 1990; 110:2195.
135. **Arnaud E, Morieux C, Wybier M, de Vernejoul MC.** Potentiation of Transforming Growth Factor (TGF-beta1) by natural coral and fibrin in a rabbit cranioplasty model. Calcif Tissue Int 1994; 54:493.
136. **Beck LS, Amento EP, Xu Y, Deguzman L, Lee WP, Nguyen T, Gillett NA.** TGF-beta1 induces bone closure of skull defects: temporal dynamics of bone formation in defects exposed to rhTGF-beta1. J Bone Miner Res 1993; 8:753.
137. **Beck LS, Deguzman L, Lee WP, Xu Y, McFatridge LA, Gillett NA, Amento EP.** Rapid publication. TGF-beta1 induces bone closure of skull defects. J Bone Miner Res 1991; 6:1257.
138. **Beck LS, Wong RL, DeGuzman L, Lee WP, Ongpipattanakul B, Nguyen TH.** Combination of bone marrow and TGF-beta1 augment the healing of critical-sized bone defects. J Pharm Sci 1998; 87:1379.
139. **Moxham JP, Kibblewhite DJ, Dvorak M, Perey B, Tencer AF, Bruce AG, Strong DM.** TGF-beta1 forms functionally normal bone in a segmental sheep tibial diaphyseal defect. J Otolaryngol 1996; 25:388.
140. **Sun Y, Zhang W, Lu Y, Hu Y, Ma F, Cheng W.** Role of Transforming Growth Factor beta (TGF-beta) in repairing of bone defects. Chin Med Sci J 1996; 11:209.

141. **McKinney L, Hollinger JO.** A bone regeneration study: Transforming Growth Factor beta-1 and its delivery. J Craniofac Surg 1996; 7:36.
142. **Sherris DA, Murakami CS, Larrabee WF Jr, Bruce AG.** Mandibular reconstruction with Transforming Growth Factor beta-1. Laryngoscope 1998; 108:368.
143. **Ripamonti U, Bosch C, van den Heever B, Duneas N, Melsen B, Ebner R.** Limited chondro-osteogenesis by recombinant human Transforming Growth Factor beta-1 in calvarial defects of adult baboons (Papio ursinus). J Bone Miner Res 1996; 11:938.
144. **Gombotz WR, Pankey SC, Bouchard LS, Phan DH, Puolakkainen PA.** Stimulation of bone healing by transforming growth factor-beta 1 released from polymeric or ceramic implants. J Appl Biomater 1994; 5:141.
145. **Zellin G, Beck S, Hardwick R, Linde A.** Opposite effects of recombinant human transforming growth factor-beta 1 on bone regeneration *in vivo*: effects of exclusion of periosteal cells by microporous membrane. Bone 1998; 22:613.
146. **Lind M, Overgaard S, Nguyen T, Ongpipattanakul B, Bunger C, Soballe K.** Transforming Growth Factor beta stimulates bone ongrowth. Hydroxyapatite-coated implants studied in dogs. Acta Orthop Scand 1996; 67:611.
147. **Lind M, Overgaard S, Ongpipattanakul B, Nguyen T, Bunger C, Soballe K.** Transforming Growth Factor beta-1 stimulates bone ongrowth to weight- loaded tricalcium phosphate coated implants: an experimental study in dogs. J Bone Joint Surg Br 1996; 78:377.
148. **Sumner DR, Turner TM, Purchio AF, Gombotz WR, Urban RM, Galante JO.** Enhancement of bone ingrowth by Transforming Growth Factor beta. J Bone Joint Surg Am 1995; 77:1135.
149. **Blom EJ, KleinNulend J, Yin L, Wenz R, Van Waas MAJ, Burger EH.** Transforming Growth Factor beta-1 in Calcium Phosphate Cement Stimulates Osteotransductivity. In: Proceedings of the 6th World Congress Biomaterials, Kamuela, Hawaii, USA, 2000, abstract no 338.
150. **Langman's Medische Embryologie.** Editor: Sadler TW. Bohn, Scheltema and Holkema. Utrecht, The Netherlands, 1988.
151. **Caplan AI.** The mesengenic process. Clin Plast Surg 1994; 21:429.
152. **Beresford JN.** Osteogenic stem cells and the stromal system of bone and marrow. Clin Orthop 1989; 240:270.
153. **Owen M.** Marrow stromal stem cells. J Cell Sci Suppl 1988; 10:63.
154. **Owen M, Friedenstein AJ.** Stromal stem cells: marrow-derived osteogenic precursors. Ciba Found Symp 1988; 136:42.
155. **Lajtha LG.** Tissues and stem cells. Biomed Pharmacother 1982; 36:231.
156. **Stein GS, Lian JB, Stein JL, Wijnen AJ, Frenkel B, Montecino M.** Mechanisms regulating osteoblast proliferation and differentiation. In: Principles of bone biology. Editors: Bilezikian JP, Raisz LG, Rodan GA. Academic Press, San Diego, CA, USA, 1996, 69.
157. **Aubin JE.** Bone stem cells. J Cell Biochem Suppl 1998; 30-31:73.
158. **Aubin JE, Liu F.** The osteoblast lineage. In: Principles of bone biology. Editors: Bilezikian JP,Raisz LG, Rodan GA. Academic Press, San Diego, CA, USA, 1996, 51.
159. **Owen TA, Aronow M, Shalhoub V, Barone LM, Wilming L, Tassinari MS, Kennedy MB, Pockwinse S,Lian JB, Stein GS.** Progressive development of the rat osteoblast phenotype *in vitro*: reciprocal relationships in expression of genes associated with osteoblast proliferation and differentiation during formation of the bone extracellular matrix. J Cell Physiol 1990; 143:420.
160. **Krebsbach PH, Kuznetsov SA, Bianco P, Robey PG.** Bone marrow stromal cells: characterization and clinical application. Crit Rev Oral Biol Med 1999; 10:165.
161. **Bianco P, Boyde A.** Confocal images of marrow stromal (Westen-Bainton) cells. Histochemistry 1993; 100:93.
162. **Westen H, Bainton DF.** Association of alkaline-phosphatase-positive reticulum cells in bone marrow with granulocytic precursors. J Exp Med 1979; 150:919.
163. **Bianco P, Costantini M, Dearden LC, Bonucci E.** Alkaline phosphatase positive precursors of adipocytes in the human bone marrow. Br J Haematol 1988; 68:401.
164. **Bianco P, Bradbeer JN, Riminucci M, Boyde A.** Marrow stromal (Westen-Bainton) cells: identification, morphometry, confocal imaging and changes in disease. Bone 1993; 14:315.
165. **Ashton BA, Abdullah F, Cave J, Williamson M, Sykes BC, Couch M, Poser JW.** Characterization of cells with high alkaline phosphatase activity derived from human bone and marrow: preliminary assessment of their osteogenicity. Bone 1985; 6:313.
166. **Maniatopoulos C, Sodek J, Melcher AH.** Bone formation *in vitro* by stromal cells obtained from bone marrow of young adult rats. Cell Tissue Res 1988; 254:317.
167. **Friedenstein AJ, Chailakhjan RK, Lalykina KS.** The development of fibroblast colonies in monolayer cultures of guinea- pig bone marrow and spleen cells. Cell Tissue Kinet 1970; 3:393.
168. **Castro-Malaspina H, Gay RE, Resnick G, Kapoor N, Meyers P, Chiarieri D, McKenzie S, Broxmeyer HE, Moore MA.** Characterization of human bone marrow fibroblast colony-forming cells (CFU-F) and their progeny. Blood 1980; 56:289.

169. **Kon E, Muraglia A, Corsi A, Bianco P, Marcacci M, Martin I, Boyde A, Ruspantini I, Chistolini P, Rocca M, Giardino R, Cancedda R, Quarto R.** Autologous bone marrow stromal cells loaded onto porous hydroxyapatite ceramic accelerate bone repair in critical-size defects of sheep long bones. J Biomed Mater Res 2000; 49:328.

170. **Haynesworth SE, Goshima J, Goldberg VM, Caplan AI.** Characterization of cells with osteogenic potential from human marrow. Bone 1992; 13:81.

171. **Friedenstein AJ.** Stromal mechanisms of bone marrow: cloning *in vitro* and retransplantation *in vivo*. Hamatol Bluttransfus 1980; 25:19.

172. **Bruijn JD, Yuan H, Dekker R, Layrolle P, de Groot K, van Blitterswijk CA.** Osteoinductive biomimetic calcium phosphate coatings and their potential use as tissue engineering scaffolds. In: Bone Engineering. Editor: Davies JE. EM squared incorporated, Toronto, Canada, 2000.

173. **Kadiyala S, Young RG, Thiede MA, Bruder SP.** Culture expanded canine mesenchymal stem cells possess osteochondrogenic potential *in vivo* and *in vitro*. Cell Transplant 1997; 6:125.

174. **Haynesworth SE, Reuben D, Caplan AI.** Cell-based tissue engineering therapies: the influence of whole body physiology. Adv Drug Deliv Rev 1998; 33:3.

175. **Bergman RJ, Gazit D, Kahn AJ, Gruber H, McDougall S, Hahn TJ.** Age-related changes in osteogenic stem cells in mice. J Bone Miner Res 1996; 11:568.

176. **Egrise D, Martin D, Vienne A, Neve P, Schoutens A.** The number of fibroblastic colonies formed from bone marrow is decreased and the *in vitro* proliferation rate of trabecular bone cells increased in aged rats. Bone 1992; 13:355.

177. **Kahn A, Gibbons R, Perkins S, Gazit D.** Age-related bone loss. A hypothesis and initial assessment in mice. Clin Orthop 1995; 313: 69.

178. **Liang CT, Barnes J, Seedor JG, Quartuccio HA, Bolander M, Jeffrey JJ, Rodan GA.** Impaired bone activity in aged rats: alterations at the cellular and molecular levels. Bone 1992; 13:435.

179. **Quarto R, Thomas D, Liang CT.** Bone progenitor cell deficits and the age-associated decline in bone repair capacity. Calcif Tissue Int 1995; 56:123.

180. **Bruder SP, Kraus KH, Goldberg VM, Kadiyala S.** The effect of implants loaded with autologous mesenchymal stem cells on the healing of canine segmental bone defects. J Bone Joint Surg Am 1998; 80:985.

181. **Barry FP, Boynton RE, Haynesworth S, Murphy JM, Zaia J.** The monoclonal antibody SH-2, raised against human mesenchymal stem cells, recognizes an epitope on endoglin (CD105). Biochem Biophys Res Commun 1999; 265:134.

182. **Bruder SP, Horowitz MC, Mosca JD, Haynesworth SE.** Monoclonal antibodies reactive with human osteogenic cell surface antigens. Bone 1997; 21:225.

183. **Bruder SP, Ricalton NS, Boynton RE, Connolly TJ, Jaiswal N, Zaia J, Barry FP.** Mesenchymal stem cell surface antigen SB-10 corresponds to activated leukocyte cell adhesion molecule and is involved in osteogenic differentiation. J Bone Miner Res 1998; 13:655.

184. **Haynesworth SE, Baber MA, Caplan AI.** Cell surface antigens on human marrow-derived mesenchymal cells are detected by monoclonal antibodies. Bone 1992; 13:69.

185. **Joyner CJ, Bennett A, Triffitt JT.** Identification and enrichment of human osteoprogenitor cells by using differentiation stage-specific monoclonal antibodies. Bone 1997; 21:1.

186. **Leboy PS, Beresford JN, Devlin C, Owen ME.** Dexamethasone induction of osteoblast mRNAs in rat marrow stromal cell cultures. J Cell Physiol 1991; 146:370.

187. **Hanada K, Dennis JE, Caplan AI.** Stimulatory effects of basic fibroblast growth factor and bone morphogenetic protein-2 on osteogenic differentiation of rat bone marrow-derived mesenchymal stem cells. J Bone Miner Res 1997; 12:1606.

188. **Mendes SC, Van den Brink I, de Bruijn JD, van Blitterswijk CA.** *In vivo* bone formation by human bone marrow cells: Effect of osteogenic culture supplements and cell densities. J Mater Sci Mater in Med 1998; 9:855.

189. **Mizuno M, Shindo M, Kobayashi D, Tsuruga E, Amemiya A, Kuboki Y.** Osteogenesis by bone marrow stromal cells maintained on type I collagen matrix gels *in vivo*. Bone 1997; 20:101.

190. **Yoshikawa T, Ohgushi H, Tamai S.** Immediate bone forming capability of prefabricated osteogenic hydroxyapatite. J Biomed Mater Res 1996; 32:481.

191. **Yoshikawa T, Ohgushi H, Nakajima H, Yamada E, Ichijima K, Tamai S, Ohta T.** *In vivo* osteogenic durability of cultured bone in porous ceramics: a novel method for autogenous bone graft substitution. Transplantation 2000; 69:128.

192. **Holy CE, Shoichet MS, Davies JE.** Engineering three-dimensional bone tissue *in vitro* using biodegradable scaffolds: investigating initial cell-seeding density and culture period. J Biomed Mater Res 2000; 51:376.

193. **Dennis JE, Caplan AI.** Porous ceramic vehicles for rat-marrow-derived (Rattus norvegicus) osteogenic cell delivery: effects of pre-treatment with fibronectin or laminin. J Oral Implantol 1993;19:106.

194. **Baksh D, Davies JE.** Three dimensional fluid flow enhances bone matrix elaboration *in vitro*. In: Transactions of the Sixth World Biomaterials Congress, Kamuela, Hawaii, USA, 2000.

195. **Granet C, Laroche N, Vico L, Alexandre C, Lafage-Proust MH.** Rotating-wall vessels, promising bioreactors for

osteoblastic cell culture: comparison with other 3D conditions. Med Biol Eng Comput 1998; 36:513.

196. **Ohgushi H, Goldberg VM, Caplan AI.** Heterotopic osteogenesis in porous ceramics induced by marrow cells. J Orthop Res 1989; 7:568.

197. **Goshima J, Goldberg VM, Caplan AI.** The origin of bone formed in composite grafts of porous calcium phosphate ceramic loaded with marrow cells. Clin Orthop 1991; 269:274.

198. **Jaiswal N, Haynesworth SE, Caplan AI, Bruder SP.** Osteogenic differentiation of purified, culture-expanded human mesenchymal stem cells *in vitro*. J Cell Biochem 1997; 64:295.

199. **Goshima J, Goldberg VM, Caplan AI.** Osteogenic potential of culture-expanded rat marrow cells as assayed *in vivo* with porous calcium phosphate ceramic. Biomaterials 1991; 12:253.

200. **Gundle R, Joyner CJ, Triffitt JT.** Human bone tissue formation in diffusion chamber culture *in vivo* by bone-derived cells and marrow stromal fibroblastic cells. Bone 1995; 16:597.

201. **Krzymanski G, Wiktor-Jedrzejczak W.** Autologous bone marrow-derived stromal fibroblastoid cells grown *in vitro* for the treatment of defects of mandibular bones. Transplant Proc 1996; 28:3528.

202. **Friedenstein AJ, Latzinik NW, Grosheva AG, Gorskaya UF.** Marrow microenvironment transfer by heterotopic transplantation of freshly isolated and cultured cells in porous sponges. Exp Hematol 1982; 10:217.

203. **Ishaug-Riley SL, Crane GM, Gurlek A, Miller MJ, Yasko AW, Yaszemski MJ, Mikos AG.** Ectopic bone formation by marrow stromal osteoblast transplantation using poly(DL-lactic-co-glycolic acid) foams implanted into the rat mesentery. J Biomed Mater Res 1997; 36:1.

204. **Friedenstein AJ, Chailakhyan RK, Gerasimov UV.** Bone marrow osteogenic stem cells: *in vitro* cultivation and transplantation in diffusion chambers. Cell Tissue Kinet 1987; 20:263.

205. **Ashton BA, Allen TD, Howlett CR, Eaglesom CC, Hattori A, Owen M.** Formation of bone and cartilage by marrow stromal cells in diffusion chambers *in vivo*. Clin Orthop 1980; 151:294.

206. **Ashton BA, Eaglesom CC, Bab I, Owen ME.** Distribution of fibroblastic colony-forming cells in rabbit bone marrow and assay of their osteogenic potential by an *in vivo* diffusion chamber method. Calcif Tissue Int 1984; 36:83.

207. **Dennis JE, Haynesworth SE, Young RG, Caplan AI.** Osteogenesis in marrow-derived mesenchymal cell porous ceramic composites transplanted subcutaneously: effect of fibronectin and laminin on cell retention and rate of osteogenic expression. Cell Transplant 1992; 1:23.

208. **Yoshikawa T, Ohgushi H, Okumura M, Tamai S, Dohi Y, Moriyama T.** Biochemical and histological sequences of membranous ossification in ectopic site. Calcif Tissue Int 1992; 50:184.

209. **Johnson KD, Frierson KE, Keller TS, Cook C, Scheinberg R, Zerwekh J, Meyers L, Sciadini MF.** Porous ceramics as bone graft substitutes in long bone defects: a biomechanical, histological, and radiographic analysis. J Orthop Res 1996; 14:351.

210. **Bruder SP, Kurth AA, Shea M, Hayes WC, Jaiswal N, Kadiyala S.** Bone regeneration by implantation of purified, culture-expanded human mesenchymal stem cells. J Orthop Res 1998; 16:155.

211. **Freed LE, Hollander AP, Martin I, Barry JR, Langer R, Vunjak-Novakovic G.** Chondrogenesis in a cell-polymer-bioreactor system. Exp Cell Res 1998; 240:58.

212. **Freed LE, Langer R, Martin I, Pellis NR, Vunjak-Novakovic G**. Tissue engineering of cartilage in space. Proc Natl Acad Sci USA 1997; 94:13885.

213. **Freed LE, Martin I, Vunjak-Novakovic G.** Frontiers in tissue engineering. *In vitro* modulation of chondrogenesis. Clin Orthop 1999; 367 Suppl:S46.

214. **Freed LE, Vunjak-Novakovic G, Langer R.** Cultivation of cell-polymer cartilage implants in bioreactors. J Cell Biochem 1993; 51:257.

215. **Kim SS, Sundback CA, Kaihara S, Benvenuto MS, Kim BS, Mooney DJ, Vacanti JP.** Dynamic seeding and *in vitro* culture of hepatocytes in a flow perfusion system. Tissue Eng 2000; 6:39.

216. **Burg KJ, Holder WD Jr, Culberson CR, Beiler RJ, Greene KG, Loebsack AB, Roland WD, Eiselt P, Mooney DJ, Halberstadt CR.** Comparative study of seeding methods for three-dimensional polymeric scaffolds. J Biomed Mater Res 2000; 51:642.

217. **Qiu QQ, Ducheyne P, Ayyaswamy PS.** Fabrication, characterization and evaluation of bioceramic hollow microspheres used as microcarriers for 3-D bone tissue formation in rotating bioreactors. Biomaterials 1999; 20:989.

218. **Temenoff JS, Mikos AG.** Review: tissue engineering for regeneration of articular cartilage. Biomaterials 2000; 21:431.

219. **Botchwey EA, Pollack SR, Levine EM, Laurencin CT.** Bone tissue engineering in a rotating bioreactor using a microcarrier matrix system. J Biomed Mater Res 2001; 55:242.

220. **Lane JM, Yasko AW, Tomin E, Cole BJ, Waller S, Browne M, Turek T, Gross J.** Bone marrow and recombinant human bone morphogenetic protein-2 in osseous repair. Clin Orthop 1999; 361:216.

221. **Beck LS, Wong RL, DeGuzman L, Lee WP, Ongpipattanakul B, Nguyen TH.** Combination of bone marrow and TGF-beta1 augment the healing of critical-sized bone defects. J Pharm Sci 1998; 87:1379.

222. **Arnaud E, De Pollak C, Meunier A, Sedel L, Damien C, Petite H.** Osteogenesis with coral is increased by BMP and BMC in a rat cranioplasty. Biomaterials 1999; 20:1909.

223. **Scaduto AA, Lieberman JR.** Gene therapy for osteoinduction. Orthop Clin North Am 1999; 30:625.
224. **Musgrave DS, Bosch P, Lee JY, Pelinkovic D, Ghivizzani SC, Whalen J, Niyibizi C, Huard J.** *Ex vivo* gene therapy to produce bone using different cell types. Clin Orthop 2000; 378:290.
225. **Lou J, Xu F, Merkel K, Manske P.** Gene therapy: adenovirus-mediated human bone morphogenetic protein-2 gene transfer induces mesenchymal progenitor cell proliferation and differentiation *in vitro* and bone formation *in vivo*. J Orthop Res 1999; 17:43.
226. **Lieberman JR, Daluiski A, Stevenson S, Wu L, McAllister P, Lee YP, Kabo JM, Finerman GA,Berk AJ, Witte ON.** The effect of regional gene therapy with bone morphogenetic protein-2- producing bone-marrow cells on the repair of segmental femoral defects in rats. J Bone Joint Surg Am 1999; 81:905.
227. **Krebsbach PH, Gu K, Franceschi RT, Rutherford RB.** Gene therapy-directed osteogenesis: BMP-7-transduced human fibroblasts form bone *in vivo*. Hum Gene Ther 2000; 11:1201.
228. **Musgrave DS, Bosch P, Ghivizzani S, Robbins PD, Evans CH, Huard J.** Adenovirus-mediated direct gene therapy with bone morphogenetic protein- 2 produces bone. Bone 1999; 24:541.
229. **Alden TD, Pittman DD, Hankins GR, Beres EJ, Engh JA, Das S, Hudson SB, Kerns KM, Kallmes DF, Helm GA.** *In vivo* endochondral bone formation using a bone morphogenetic protein 2 adenoviral vector. Hum Gene Ther 1999; 10:2245.
230. **Alden TD, Pittman DD, Beres EJ, Hankins GR, Kallmes DF, Wisotsky BM, Kerns KM, Helm GA.** Percutaneous spinal fusion using bone morphogenetic protein-2 gene therapy. J Neurosurg 1999; 90:109.
231. **Franceschi RT, Wang D, Krebsbach PH, Rutherford RB.** Gene therapy for bone formation: *in vitro* and *in vivo* osteogenic activity of an adenovirus expressing BMP7. J Cell Biochem 2000; 78:476.
232. **Fang J, Zhu YY, Smiley E, Bonadio J, Rouleau JP, Goldstein SA, McCauley LK, Davidson BL, Roessler BJ.** Stimulation of new bone formation by direct transfer of osteogenic plasmid genes. Proc Natl Acad Sci USA 1996; 93:5753.
233. **Baltzer AW, Lattermann C, Whalen JD, Ghivizzani S, Wooley P, Krauspe R, Robbins PD, Evans CH.** Potential role of direct adenoviral gene transfer in enhancing fracture repair. Clin Orthop 2000; 379 Suppl: S120.
234. **Lindholm TS, Gao TJ.** Functional carriers for Bone Morphogenetic Proteins. Ann Chir Gynaecol 1993; 207 Suppl:3.
235. **Hollinger JO, Leong K.** Poly(alpha-hydroxy acids): carriers for Bone Morphogenetic Proteins. Biomaterials 1996; 17:187.
236. **Brekke JH.** A rationale for the delivery of osteoinductive proteins. Tissue Eng 1996; 2:97.
237. **Hollinger JO, Uludag H, Winn SR.** Sustained release emphasizing recombinant human bone morphogenetic protein-2. Adv Drug Deliv Rev 1998; 31:303.
238. **Sela J.** Osteogenesis induced by bone matrix is inhibited by inflammation. Biomater Med Devices Artif Organs1988; 14:227.
239. **Miyamoto S, Takaoka K, Okada T, Yoshikawa H, Hashimoto J, Suzuki S, Ono K.** Evaluation of polylactic acid homopolymers as carriers for bone morphogenetic protein. Clin Orthop 1992; 278: 274.
240. **Girton TS, Oegema TR, Tranquillo RT.** Exploiting glycation to stiffen and strengthen tissue equivalents for tissue engineering. J Biomed Mater Res 1999; 46:87.
241. **Zhang R, Ma PX.** Poly(alpha-hydroxyl acids)/hydroxyapatite porous composites for bone- tissue engineering. I. Preparation and morphology. J Biomed Mater Res 1999; 44:446.
242. **Uludag H, D'Augusta D, Palmer R, Timony G, Wozney J.** Characterization of rhBMP-2 pharmacokinetics implanted with biomaterial carriers in the rat ectopic model. J Biomed Mater Res 1999; 46:193.
243. **Uludag H, D'Augusta D, Golden J, Li J, Timony G, Riedel R, Wozney JM.** Implantation of recombinant human bone morphogenetic proteins with biomaterial carriers: A correlation between protein pharmacokinetics and osteoinduction in the rat ectopic model. J Biomed Mater Res 2000; 50:227.
244. **Moxham JP, Kibblewhite DJ, Bruce AG, Rigley T, Gillespy T 3rd, Lane J.** Transforming Growth Factor beta-1 in a guanidine-extracted demineralized bone matrix carrier rapidly closes a rabbit critical calvarial defect. J Otolaryngol 1996; 25:82.
245. **Beck LS, Deguzman L, Lee WP, Xu Y, McFatridge LA, Gillett NA, Amento EP.** Rapid publication. TGF-beta1 induces bone closure of skull defects. J Bone Miner Res 1991; 6:1257.
246. **Beck LS, Amento EP, Xu Y, Deguzman L, Lee WP, Nguyen T, Gillett NA.** TGF-beta1 induces bone closure of skull defects: temporal dynamics of bone formation in defects exposed to rhTGF-beta1. J Bone Miner Res 1993; 8:753.
247. **Meikle MC, Papaioannou S, Ratledge TJ, Speight PM, Watt-Smith SR, Hill PA, Reynolds JJ.** Effect of poly DL-lactide--co-glycolide implants and xenogeneic bone matrix-derived growth factors on calvarial bone repair in the rabbit. Biomaterials 1994; 15:513.
248. **Ongpipattanakul B, Nguyen T, Zioncheck TF, Wong R, Osaka G, DeGuzman L, Lee WP, Beck LS.** Development of tricalcium phosphate/amylopectin paste combined with recombinant human Transforming Growth Factor beta as a bone defect filler. J Biomed Mater Res 1997; 36:295.
249. **Arnaud E, Morieux C, Wybier M, de Vernejoul MC.** Potentiation of Transforming Growth Factor (TGF-beta1) by natural coral and fibrin in a rabbit cranioplasty model. Calcif Tissue Int 1994; 54:493.

250. **Blom EJ, KleinNulend J, Yin L, Wenz R, Van Waas MAJ, Burger EH.** Transforming Growth Factor beta-1 in Calcium Phosphate Cement Stimulates Osteotransductivity. In: Proceedings of the 6th World Congress Biomaterials, Kamuela, Hawaii, USA, 2000, abstract no 338.

251. **Gombotz WR, Pankey SC, Bouchard LS, Phan DH, Puolakkainen PA.** Stimulation of bone healing by transforming growth factor-beta 1 released from polymeric or ceramic implants. J Appl Biomater 1994; 5:141.

252. **Heckman JD, Ehler W, Brooks BP, Aufdemorte TB, Lohmann CH, Morgan T, Boyan BD.** Bone morphogenetic protein but not Transforming Growth Factor beta enhances bone formation in canine diaphyseal nonunions implanted with a biodegradable composite polymer. J Bone Joint Surg Am 1999; 81:1717.

253. **Ohgushi H, Caplan AI.** Stem cell technology and bioceramics: from cell to gene engineering. J Biomed Mater Res 1999; 48:913.

254. **Johnson EE, Urist MR, Finerman GA.** Repair of segmental defects of the tibia with cancellous bone grafts augmented with human bone morphogenetic protein. A preliminary report. Clin Orthop 1988; 236: 249.

255. **Johnson EE, Urist MR, Finerman GA.** Bone morphogenetic protein augmentation grafting of resistant femoral nonunions. A preliminary report. Clin Orthop 1988; 230:257.

256. **Johnson EE, Urist MR, Finerman GA.** Distal metaphyseal tibial nonunion. Deformity and bone loss treated by open reduction, internal fixation, and human bone morphogenetic protein (hBMP). Clin Orthop 1990; 250:234.

257. **Johnson EE, Urist MR, Finerman GA.** Resistant nonunions and partial or complete segmental defects of long bones. Treatment with implants of a composite of human bone morphogenetic protein (BMP) and autolyzed, antigen-extracted, allogeneic (AAA) bone. Clin Orthop 1992; 277:229.

258. **Johnson EE, Urist MR.** One-stage lengthening of femoral nonunion augmented with human bone morphogenetic protein. Clin Orthop 1998; 347:105.

259. **Croteau S, Rauch F, Silvestri A, Hamdy RC.** Bone Morphogenetic Proteins in orthopedics: from basic science to clinical practice. Orthopedics 1999; 22: 686.

260. **Johnson EE, Urist MR.** Human bone morphogenetic protein allografting for reconstruction of femoral nonunion. Clin Orthop 2000; 371: 61.

261. **Sailer HF, Kolb E.** Purified bone morphogenetic protein for clinical use in difficult conditions of cranio-maxillofacial surgery. In: Bone Morphogenetic Proteins: biology, biochemistry and reconstructive surgery. Editor: Lindolm TS. Academic Press, London, UK, 1996, 207.

262. **Boyne PJ, Marx RE, Nevins M, Triplett G, Lazaro E, Lilly LC, Alder M, Nummikoski P**. A feasibility study evaluating rhBMP-2/absorbable collagen sponge for maxillary sinus floor augmentation. Int J Periodontics Restorative Dent 1997; 17:11.

263. **Howell TH, Fiorellini J, Jones A, Alder M, Nummikoski P, Lazaro M, Lilly L, Cochran D.** A feasibility study evaluating rhBMP-2/absorbable collagen sponge device for local alveolar ridge preservation or augmentation. Int J Periodontics Restorative Dent 1997; 17:124.

264. **Geesink RG, Hoefnagels NH, Bulstra SK.** Osteogenic activity of OP-1 bone morphogenetic protein (BMP-7) in a human fibular defect. J Bone Joint Surg Br 1999; 81:710.

265. **Groeneveld EH, van den Bergh JP, Holzmann P, ten Bruggenkate CM, Tuinzing DB, Burger EH.** Histomorphometrical analysis of bone formed in human maxillary sinus floor elevations grafted with OP-1 device, demineralized bone matrix or autogenous bone. Comparison with non-grafted sites in a series of case reports. Clin Oral Implants Res 1999; 10:499.

266. **Cook SD.** Preclinical and clinical evaluation of osteogenic protein-1 (BMP-7) in bony sites. Orthopedics 1999; 22:669.

267. **Riedel GE, Valentin-Opran A.** Clinical evaluation of rhBMP-2/ACS in orthopedic trauma: a progress report. Orthopedics 1999; 22:663.

268. **Calabresi PA, Fields NS, Maloni HW, Hanham A, Carlino J, Moore J, Levin MC, Dhib-Jalbut S, Tranquill LR, Austin H, McFarland HF, Racke MK.** Phase 1 trial of Transforming Growth Factor beta 2 in chronic progressive MS. Neurology 1998; 51:289.

269. **Connolly JF.** Injectable bone marrow preparations to stimulate osteogenic repair. Clin Orthop 1995; 313:8.

270. **Connolly JF.** Clinical use of marrow osteoprogenitor cells to stimulate osteogenesis. Clin Orthop 1998; 355 Suppl: S257.

271. **Osepjan IA, Chailakhjan RK, Garibjan RK, Aivaizjan VP.** Treatment of nonunions, pseudarthrosis, and long bone defects by transplantation of autologous bone marrow fibroblasts grown *in vitro* and embedded into a spongeous bone matrix. Orthop Traumatol 1987; 9:59.

272. **Okumura M, Ohgushi H, Ducheyne P.** Porous titanium felt as a carrier of osteogenic cells. In: Bioceramics. Editors: Ducheyne P, Christiansen D. Butterworth-Heinemann Ltd., Linnacre House, Jordan Hill, Oxford, England, 1993, vol. 6, 305.

273. **Wolff D, Goldberg VM, Stevenson S.** Histomorphometric analysis of the repair of a segmental diaphyseal defect with ceramic and titanium fibermetal implants: effects of bone marrow. J Orthop Res 1994; 12:439.

45

274. **Chang YS, Oka M, Kobayashi M, Gu HO, Li ZL, Nakamura T, Ikada Y.** Significance of interstitial bone ingrowth under load-bearing conditions: a comparison between solid and porous implant materials. Biomaterials 1996; 17:1141.
275. **Evaskus DS, Rostoker W, Laskin DM.** Evaluation of sintered titanium fiber composite as a subperiosteal implant. J Oral Surg 1980; 38:490.
276. **Cole BJ, Bostrom MP, Pritchard TL, Sumner DR, Tomin E, Lane JM, Weiland AJ.** Use of bone morphogenetic protein 2 on ectopic porous coated implants in the rat. Clin Orthop 1997; 345:219.
277. **Kawai T, Mieki A, Ohno Y, Umemura M, Kataoka H, Kurita S, Koie M, Jinde T, Hasegawa J, Urist MR.** Osteo-inductive activity of composites of bone morphogenetic protein and pure titanium. Clin Orthop 1993; 290:296.
278. **Herr G, Hartwig CH, Boll C, Kusswetter W.** Ectopic bone formation by composites of BMP and metal implants in rats. Acta Orthop Scand 1996; 67:606.
279. **Lind M, Overgaard S, Song Y, Goodman SB, Bunger C, Soballe K.** Osteogenic protein 1 device stimulates bone healing to hydroxyapaptite- coated and titanium implants. J Arthroplasty 2000;15:339.
280. **Wolke JGC.** Sprayed and sputtered calcium phosphate coatings for medical implants. Thesis, University of Nijmegen, Nijmegen, The Netherlands, 1997.
281. **Hulshoff JE, van Dijk K, van der Waerden JP, Wolke JG, Kalk W, Jansen JA.** Evaluation of plasma-spray and magnetron-sputter Ca-P-coated implants: an *in vivo* experiment using rabbits. J Biomed Mater Res 1996; 31:329.
282. **Vercaigne S, Wolke JG, Naert I, Jansen JA.** A mechanical evaluation of TiO2-gritblasted and Ca-P magnetron sputter coated implants placed into the trabecular bone of the goat: Part 1. Clin Oral Implants Res 2000; 11:305.
283. **Vercaigne S, Wolke JG, Naert I, Jansen JA.** A histological evaluation of TiO2-gritblasted and Ca-P magnetron sputter coated implants placed into the trabecular bone of the goat: Part 2. Clin Oral Implants Res 2000; 11:314.
284. **Takaoka T, Okumura M, Ohgushi H, Inoue K, Takakura Y, Tamai S.** Histological and biochemical evaluation of osteogenic response in porous hydroxyapatite coated alumina ceramics. Biomaterials 1996; 17:1499.

Chapter 2

Influence of rhBMP-2 on rat bone marrow stromal cells cultured on titanium fiber mesh

J.W.M. Vehof, J.E. de Ruijter, P.H.M. Spauwen and J.A. Jansen.

2.1 Introduction

Bone Graft Substitutes (BGSs) can be fabricated using a porous carrier material together with osteogenic cells or osteoinductive factors like Bone Morphogenetic Proteins (BMPs). One disadvantage of most of the currently used carrier materials is that they are not very strong and can easily transform. Another candidate carrier material for the creation of BGS is sintered titanium (Ti) fiber mesh material. Ti-mesh loaded with BMPs has been shown to adequately induce ectopic bone formation *in vivo*.[1-3] We also know that a porous scaffold material loaded with bone marrow stromal cells can generate ectopic bone formation. If this technique is also to be applied for Ti-fiber mesh, we first have to demonstrate that bone marrow stromal cells will show osteogenic expression in Ti-fiber mesh. An additional factor is that the level of *in vitro* and *in vivo* osteogenic expression in a porous scaffold material is dependent on the number of loaded osteogenic cells and culture conditions.[4-6]

Some investigators have attempted to improve culture conditions (for other cell types) by optimizing nutrient supply using dynamic culture methods, *i.e.* perfusion culture, spinner flasks and rotating wall bioreactors.[7] Others have experimented with various growth factors, for example, bFGF to promote cell growth and rhBMP-2 to stimulate cell differentiation.[8]

The objective of the study reported here was to investigate: (**1**) the osteogenic expression in porous titanium mesh loaded with rat bone marrow cells *in vitro*; (**2**) the influence of cell seeding density on the osteogenic expression in porous titanium mesh *in vitro* and (**3**) the rhBMP-2 concentration dependency of the osteogenic expression in titanium mesh *in vitro*.

2.2 Materials and methods

2.2.1 Substrates

Porous Ti-fiber mesh (Bekaert, Zwevegem, Belgium) with a volumetric porosity of 86 % and a fiber diameter of 50 µm was used as-received. The average pore size of Ti-fiber mesh is approximately 250 µm. Discs were fabricated from 0.8-mm-thick titanium fiber mesh sheets to a diameter of 6 mm and a weight of approximately 15 mg. Larger discs were used for DNA measurements: 10 mm in diameter and a weight of approximately 40 mg.

2.2.2 Bone Morphogenetic Protein

The BMP used in the present study was recombinant human BMP-2 (rhBMP-2). RhBMP-2 was produced by Chinese hamster ovary (CHO) cells[9] and was a kind gift from Genetics Institute, Cambridge, Mass., USA. RhBMP-2 was used in various concentrations: 10 ng/ml, 100 ng/ml and 1,000 ng/ml. Controls without BMP were used as well. In appropriate samples, BMP was present in the media from day 0 up to day 7 postseeding. During this period rhBMP-2-containing medium was changed 3 times. Thereafter, medium without BMP was used.

2.2.3   Cell isolation and culture

In order to test the effect of the Ti-mesh and rhBMP-2 dose on bone induction, we used a rat bone marrow stromal (RBM) cell culture technique.[10] Briefly, bone marrow cells were obtained from femora of young male Wistar rats (weight: 120–150 g, age: 40–43 days). The femurs were excised, epiphyses were cut off and both diaphyses were washed 3 times in α-Minimal Essential Medium (α-MEM, Gibco BRL, Life Technologies B.V., Breda, The Netherlands) with gentamycin (10 times culture concentration). The femurs were then flushed out, using complete medium: α-MEM supplemented with 10 % fetal calf serum (FCS, heat induced at 56°C for 35 min, Gibco), 50 µg/ml freshly prepared ascorbic acid (Sigma, Chemical Co., St. Louis, Mo., USA), 10 mM Na-β-glycerophosphate (Sigma), 10^{-8} M dexamethasone (Sigma) and antibiotics [gentamycin and amphotericine B (Fungizone®)]. Per two femurs 15 ml of this medium was used. The cells were suspended and cultured in three 80-cm² tissue culture flasks (Nunc Products, by Gibco) maintained in a humidified atmosphere of 95 % air, 5 % CO_2 at 37°C.

After 7 days of primary culture, cells were detached using trypsin/EDTA (0.25 % w/v trypsin/0.02 % ethylene diamine tetra acetic acid), concentrated by centrifugation at 1,500 rpm for 5 min and resuspended in a known amount of media. A Coulter® counter was used to count the cells. The cell suspension was diluted to 3.33 x 10^5 cells/ml [low cell density (LD)] and 3.33 x 10^6 cells/ml [high cell density (HD)] in complete media.

The Ti-meshes were placed in 24-well plates. Thirty-microliter aliquots (85-µl aliquots for the larger substrates for DNA analysis) of the cell suspensions were seeded onto the top of the meshes, resulting in a seeding density of 3,54 x 10^4 cells/cm² (LD) and 3,54 x 10^5 cells/ cm² (HD) when normalized to the top surface area of the meshes. In this way a total of 10,000 and 100,000 cells (28,000 and 280,000 cells for the larger substrates for DNA analysis) were added to the LD and HD meshes, respectively.

After seeding, the meshes were left undisturbed in an incubator for 3 h to allow for cellular attachment to the substrates. Thereafter, an additional 1 ml of media was added to each well. Appropriate meshes received medium with rhBMP-2. The medium was changed every 2-3 days.

In this way eight experimental groups were created (**Table 1**). The cells were kept in culture for different time periods up to 16 days. Each experiment was performed twofold, and in each experiment four replicate samples were used (in total, $n = 8$ for each material and time period).

2.2.4   Scanning electron microscopy, energy dispersive spectroscopy and X-ray diffraction

The influence of material properties on cell morphology and extra-cellular matrix (ECM) synthesis of RBM cells was studied using scanning electron microscopy (SEM) and energy dispersive spectroscopy (EDS). After 8 and 16 days of incubation the substrates were rinsed three times with 0.1 M sodium-cacodylate buffer (pH = 7.4, 37°C). Fixation was subsequently carried out for 60 min at 4°C in 2 % glutaraldehyde in the same buffer. The specimens were then dehydrated in a graded series of ethanol and dried by tetramethylsilane

Table 1.
Eight experimental groups were created

Cell seeding density	BMP concentration (ng/ml):			
LD (Low Density)	0	10	100	1,000
HD (High Density)	0	10	100	1,000

and kept dry until SEM evaluation. Just before analysis, the specimens were sputtered with gold and examined and photographed using a Jeol 6310 SEM at an accelerating voltage of 10-15 kV.

Additional samples were sputtered with carbon, and EDS (single spot or line) was performed to identify the elemental composition of the extracellular matrix using the same Jeol 6310 SEM which was equipped with a energy disperse X-ray detector (Voyager).

Other samples were used for X-ray diffraction (XRD) analysis at 16 days of culture. Samples were rinsed twice with phosphate buffered saline (PBS) and dehydrated in a graded series of alcohol. The samples were then dried using tetramethylsilane and kept dry until XRD was performed. The crystallographic structure of the deposited matrix was determined using a Philips PW 3710 based diffractometer. The angle of incidence was kept fixed at $10°\theta$. To analyze the reflected beam, we used a collimator, monochromator and proportional counter. The step was $0.02°$ 2θ, with a counting time per step of 12 s.

2.2.5 Light microscopy

After 8 and 16 days of culture, specimens for light microscopical analysis were rinsed twice with PBS and fixed in 4 % formaldehyde buffer (pH = 7.4) for 1 h, then rinsed twice with PBS and once with water and finally stained with Alizarin Red-S for 60 s before dehydration in a graded series of ethanol. These samples were eventually embedded in methylmethacrylate. After polimerization thin sections were made using a modified sawing microtome technique.[11] The prepared sections were analyzed under a light microscope (Leica®).

2.2.6 DNA analysis

After 4, 8 and 16 days of culture, DNA content was determined in order to obtain indirect information about cellular proliferation. Incubated specimens were rinsed twice using PBS, and the cells were lysed using 0.5 ml 1 M NaOH with subsequent sonication for 15 min. Until the time of analysis, specimens were kept at $-20°C$. After thawing, samples were neutralized with 0.5 ml 1 M $HCl-PO_4$ buffer. Fluorescence was read in a fluorometer using bisbenzimidazole (Hoechst® 33258 reagent).[12]

2.2.7   Calcium content

Calcium (Ca) content was assessed after 4, 8 and 16 days of culture to obtain information about mineralized matrix formation. The samples were rinsed twice with milliQ and kept at –20°C until calcium assessment. After thawing, 1 ml of acetic acid was added to each sam-ple and stored overnight under vigorous constant shaking. The calcium content was deter-mined using the orthocresolphthalein (OCPC) method.[13] Optic density was read with an ELISA reader at a wavelength of 575 nm.

2.3   Results

2.3.1   SEM, EDS and XRD

At low magnification a confluent (multi-) layer of cells was present on top of the meshes. The surface area covered by this cell layer appeared to increase with increasing cell seeding density (**Figures 1A, 1B**) for all time periods. At 8 days, a whitish deposit could be observed for LD 1,000 and all HD specimens, that covered significant parts of the mesh surface (**Figure 1B**). At 16 days this deposit could be observed for all specimens.

At 8 days, examination at high magnification confirmed the presence of cells in the confluent (multi-) layer on top of the meshes. These cells had spread and exhibited filopodia (**Figure 1C**). Collagen bundles and early signs of calcification, as characterized by the presence of calcified globular accretions, were seen in LD 1,000 specimens and all HD specimens (**Figure 1C, 1D**). EDS confirmed the presence of Ca and P in these calcified globular accretions.

At 16 days, abundant calcification associated with collagen bundles was observed in all specimens (**Figure 1D**). The amount of calcification seemed to increase with increasing concentration of rhBMP-2 (**Figure 1E**). The size of the globular accretions increased over time, and appeared to be cell density-and rhBMP-2 dose-dependent (**Figure 1E**). This effect was only seen in the HD specimens.

Further analysis of the samples by XRD revealed that at 16 days the deposited matrix contained a precipitate of a stable calcium phosphate phase (**Figure 2**).

2.3.2   Light microscopy

In general, sections showed a red-stained layer on top of the meshes. This layer penetrated up to approximately 250 µm into the mesh (**Figure 3C**). Due to the staining technique, cell morphology itself could not be observed. Although no quantitative analysis was performed, subjective analysis indicated that the HD specimens appeared to be more densely stained than LD specimens (**Figures 3A, 3B**) for both incubation times and showed higher penetration depth (**Figure 3C**). Further, the staining density appeared to increase with culture time (16 days > 8 days) and presence of rhBMP-2 in the culture medium (**Figures 3B, 3C**).
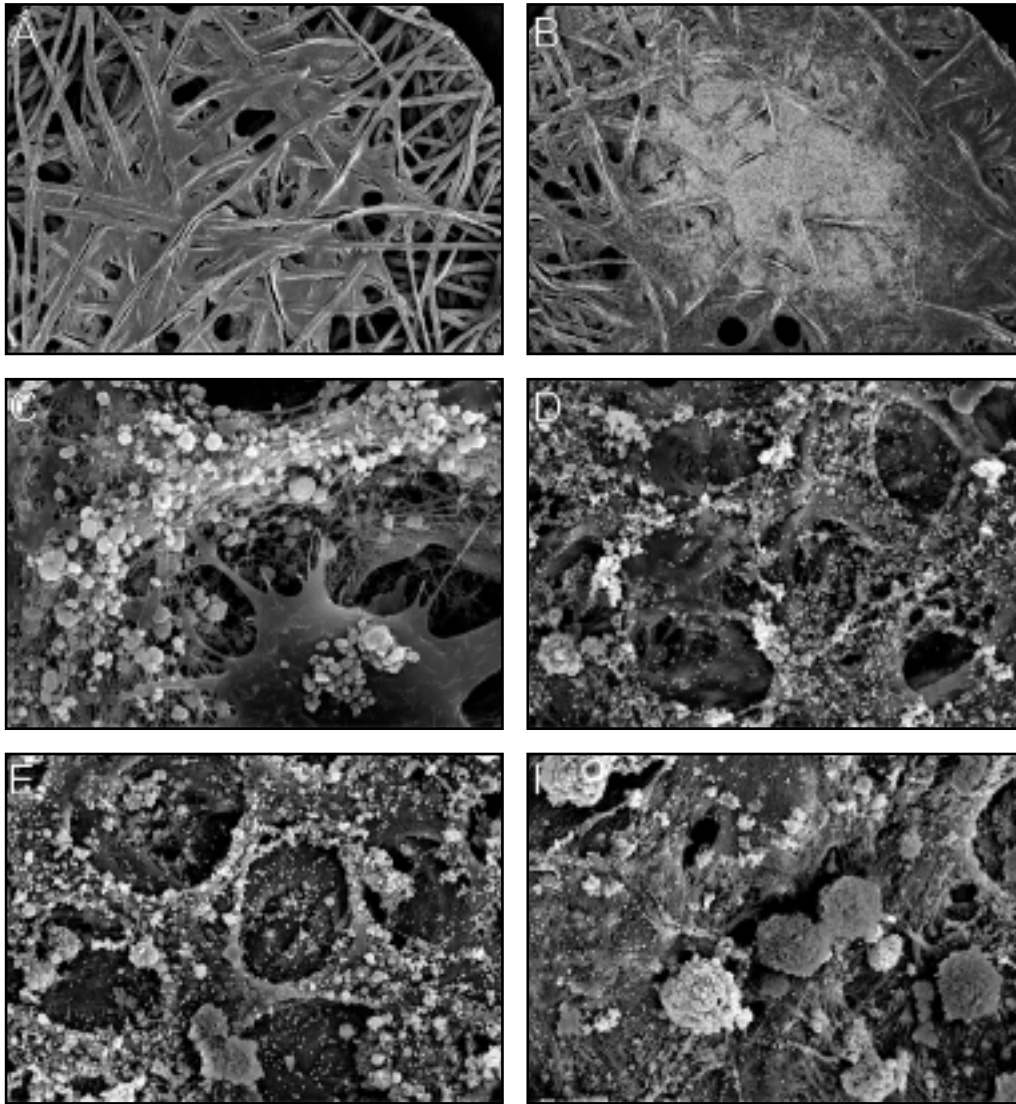
Figure 1.

(A) Scanning electron microscopical image at low magnification of a LD 0 sample at 8 days. The surface is only partially coved by the multilayer of cells (*orig. magn. 25x*).

(B) Scanning electron microscopical image at low magnification of a HD 0 sample at 8 days. Note that a larger surface area is covered by the multilayer of cells than in the LD 0 specimen. A whitish deposit can be observed that covers a part of the mesh surface (*orig. magn. 25x*).

(C) Scanning electron microscopical image at high magnification of a HD 10 sample at 8 days. A bone-like tissue formation can be observed. A spread osteoblast-like cell is present which exhibits philopodia (*orig. magn. 5,000x*).
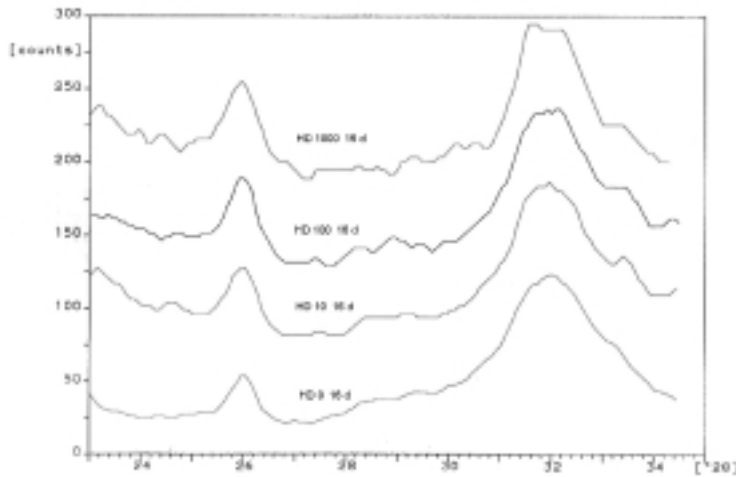
Figure 2.

X-ray diffraction pattern of HD specimens at 16 days treated with different concentrations of rhBMP-2. For all rhBMP-2 concentrations, the X-ray diffraction pattern clearly shows the presence of a precipitate of a stable calcium phosphate phase in the deposited matrix.

2.3.3 DNA

The results of the DNA measurements are depicted in **Figure 4**. ANOVA, and multiple regression analysis were used to analyze the data from the DNA measurements. The data showed a normal distribution and ANOVA subsequently showed an influence of experimental run. At 8 days, the DNA level was generally higher in the second run than in the first run (P < 0.0005, 3-way ANOVA). A significant overall effect of culture time (P < 0.0005, 3-way ANOVA) and cell seeding density (P < 0.0005, 3-way ANOVA) was also present. From 4 to 8 days DNA increased, from 8 to 16 days DNA content decreased to a level below that at 4 days. In addition, the higher cell seeding density resulted in a higher DNA content than that found with the lower cell seeding density. In the first run, a 2-way interaction was noted between culture time and cell seeding density, but such an interaction was not observed in the second run. The interaction in the first run includes lower DNA measurements for the HD specimens at 8 days. In this run, at 4 to 8 days, the DNA content remained at about the same level in the HD group. On the other hand, in the

Figure 1.

(D)   Scanning electron microscopical image at high magnification of a HD 0 specimen at 8 days. Globular accretions together with collagen bundles can be observed (*orig. magn. 1,500x*).

(E)   Scanning electron microscopical image at high magnification of a HD 0 specimen at 16 days. Abundant calcification can be seen together with collagen bundles. The globular accretions become larger (*orig. magn. 1,500x*).

(F)   Scanning electron microscopical image at high magnification of a HD 1,000 specimen at 16 days. The globular accretions become larger (*orig. magn. 1,500x*).

second run an increase in DNA content was found from 4 to 8 days for the HD group. No significant effect was noted with respect to BMP concentration on DNA measurements (3-way ANOVA, multiple regression analysis).

2.3.4   Calcium content

The results of the calcium measurement are shown in **Figure 5**. ANOVA and multiple regression analysis were used to analyze the data from the calcium measurements. The data showed a lognormal distribution and ANOVA subsequently showed an influence of experimental run. Levels of calcification were generally higher in the second experimental run. No calcification was seen at 4 days. Multiple regression analysis revealed a significant overall effect of cell seeding density at 8 days (*run 1*: $P < 0.001$, *run 2*: $P < 0.00005$) and 16 days (*run 1*: $P < 0.0005$, *run 2*: $P < 0.005$). In general, HD specimens showed a higher calcium content than LD specimens. Multiple regression analysis revealed that significant rhBMP-2 concentration effects were found for the HD specimens at 8 days [*run 1*: 1,000 ng/ml ($P < 0.00005$); *run 2*: 10 ng/ml ($P < 0.005$), 100 ng/ml ($P < 0.0005$) en 1,000 ng/ml
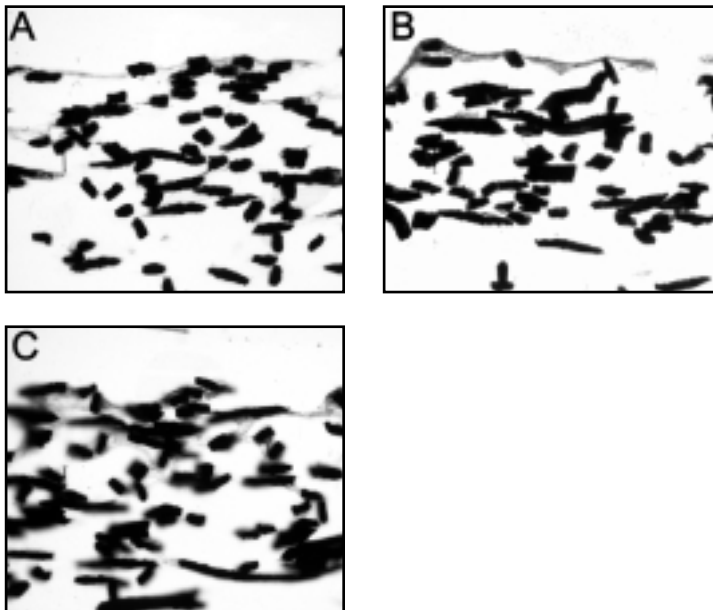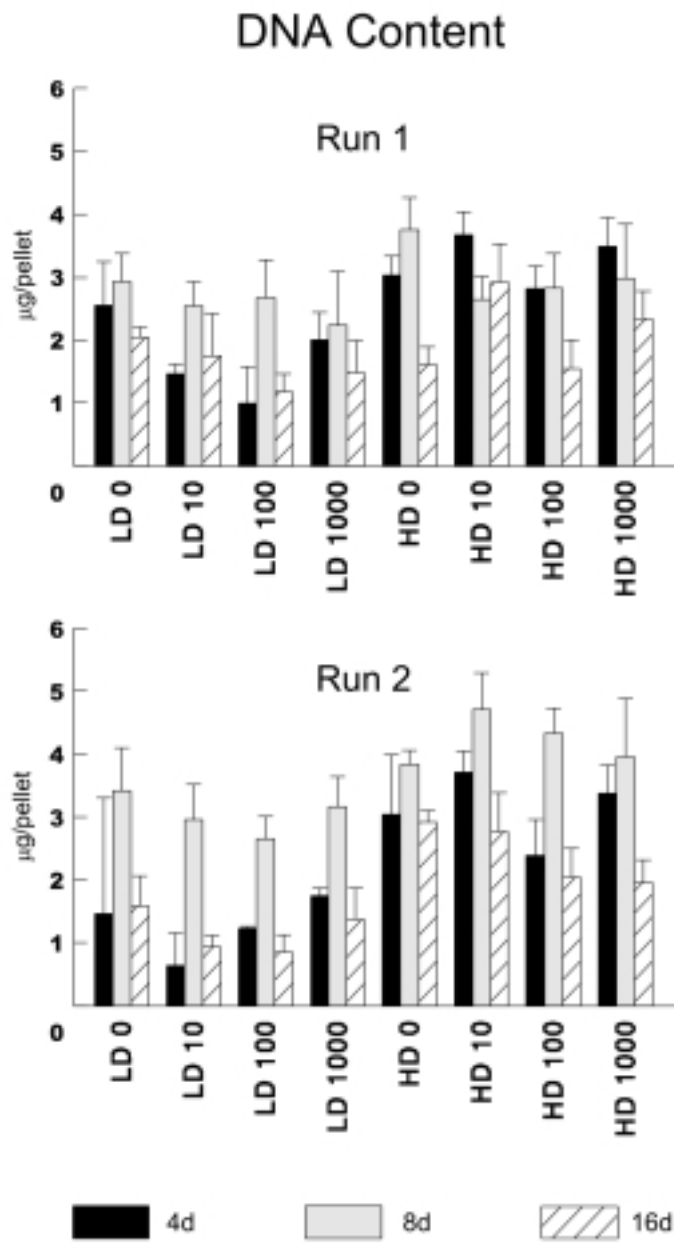

Figure 3.

(A)   Light microscopical image of a LD 0 specimen at 16 days. A red-stained layer with mineralization is present on top of the mesh (*orig. magn. 10x*).

(B)   Light microscopical image of a HD 0 specimen at 16 days. The layer on top of the mesh is more densely stained than in the LD specimen (*orig. magn. 10x*).

(C)   Light microscopical image of a HD 100 specimen at 16 days stained with alizarin red-S. A layer with mineralization is present in the upper part of the mesh, which penetrates up to approximately 250 μm into the mesh (*orig. magn. 10x*).

Figure 4.

This graph shows the results of the DNA measurements for both experimental runs (mean and standard deviation [SD]).
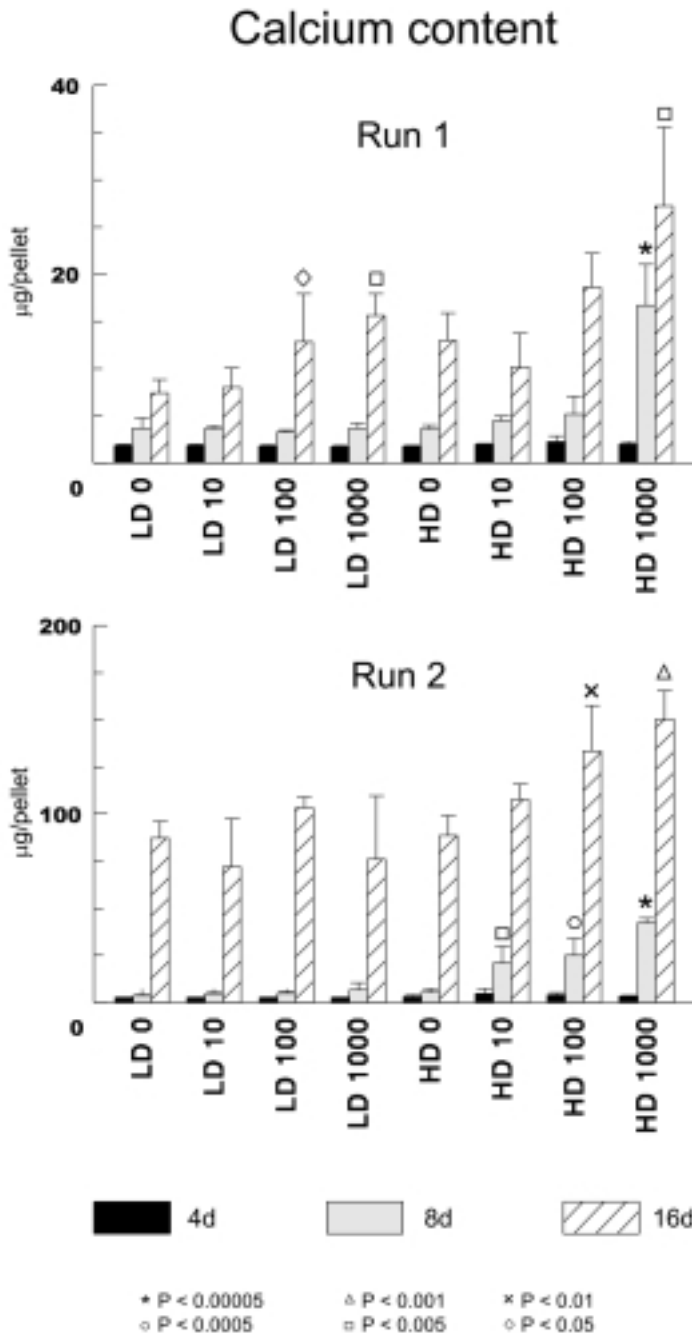
Figure 5.

This graph shows the results of the calcium measurements for both experimental runs (mean and SD). ANOVA and Multiple regression analysis were used to analyze the calcium content data. The influence of rhBMP-2 concentration was evaluated using multiple regression analysis and significant differences are shown. In this evaluation, the effects of different concentrations of rhBMP-2 (10 ng/ml, 100 ng/ml and 1,000 ng/ml) were compared to the control (0 ng/ml) for the same culture period, cell seeding density and experimental run.

(P < 0.00005)] and at 16 days [*run 1*: 1,000 ng/ml (P < 0.005); *run 2*: 100 ng/ml (P < 0.01) en 1,000 ng/ml (P < 0.001)]. In addition, in the first run a significant concentration effect was found for the LD specimens [100 ng/ml (P < 0.05) and 1,000 ng/ml(P < 0.005)] at 16 days. Specimens treated with 100 ng/ml and 1,000 ng/ml showed the highest calcification.

2.4 Discussion and conclusion

Our findings show that cells attach and grow well in Ti-fiber mesh. The Ti-fiber mesh supports differentiation of the bone marrow stromal cells as demonstrated by the presence of calcified globular accretions and collagen bundles. The calcium measurements suggest that increasing cell seeding density and high rhBMP-2 concentrations (100 and 1,000 ng/ml) stimulate calcification, while the DNA measurements indicate that increasing cell seeding density increases the number of loaded cells and that rhBMP-2 does not influence proliferation.

In contrast to our earlier studies using rat bone marrow stromal cells cultured on solid Ti-discs, in the present study we found that titanium clearly supports the formation of a mineralized matrix.[14] This finding might be explained by the difference in total number of cells seeded and number of cells seeded per surface area. In this study, we applied 10,000 or 100,000 cells per Ti-mesh disc (diameter: 6 mm), whereas in the former study only 10,000 cells were applied on larger solid Ti-discs (diameter: 12 mm). Another factor that might explain these observations is the difference in the geometry of the substrates.

Our light microscopical results demonstrated only limited cellular penetration into the fiber mesh material. This has also been observed for other carrier materials, such as poly-(DL-lactic-*co*-glycolic acid) (PLGA)[4,5] and collagen.[15] In the PLGA studies, cells penetrated up to 240 µm. In the collagen study, cell density was higher in the upper region of the substrate at 21 days, while at 56 days a two-layer structure existed: osteocytes with mineralization in the upper region, and osteoblasts with less mineralization in the lower region. Unfortunately, the Alizarin red-S staining used in our experiment is specific for mineralization. Therefore, no cellular morphology could be observed in our mesh material.

Although penetration depth was not quantified because no clear migration front was seen, increasing the cell seeding density seemed to enhance penetration. This finding does not corroborate with other studies. For example, Ishaug *et al*.[4] found that cell seeding density did in fact influence penetration depth; higher cell seeding densities (22.1 x 10^5 cells/cm^2) negatively influenced penetration depth. Nevertheless, we have to emphasize that the low cell seeding density (6.83 x 10^5 cells/cm^2) as used in that study is about twice as high as our high cell seeding density.

We assume that the phenomenon of limited cellular penetration is due to a diffusion effect: lower oxygen tension and nutrient supply in the lower regions of the carrier material inhibit cell growth. This effect will be enhanced when very high cell seeding densities[4] are used. A mechanical obstructive effect due to pore size is not very likely for scaffolds with pore sizes ranging from 150 µm to 710 µm.[4,5] The pore size we used has already been shown adequate for both blood vessel and bone ingrowth in various ectopic assay models *in vivo*.[1,2,3,16]

Our DNA measurements revealed that cellular proliferation increased from 4 to 8 days for all specimens. From 8 to 16 days DNA decreased for all specimens. This decrease in proliferation was accompanied by a simultaneous increase in calcium content. Three explanations can be given for this increase in differentiation and decrease in proliferation: (**1**) the inverse relationship that exists between proliferation and differentiation;[17] (**2**) because of the mineralization the nutrient status deteriorates and causes a decrease in the number of cells; (**3**) because of the increase in calcification at 16 days and the high affinity of DNA for calcium, total DNA could not be retrieved. At this moment no final answer can be given as to which of these three explanations is true. We observed that an increase in rhBMP-2 concentration does not affect cellular proliferation. This corroborates with earlier findings of Puleo *et al.*[18] in which rhBMP-2 did not affect cell growth for rat bone marrow stromal cells but stimulated cell growth in C3H10T1/2 cells .

With respect to mineralized matrix formation, BMP treatment had an increasing effect. In addition, matrix deposition occurred at earlier time periods. The results of the present study indicate that rhBMP-2 stimulates the differentiation of RBM cells cultured on Ti-fiber mesh in a dose-dependent manner. The 1,000 ng/ml concentration stimulated mineralization in both runs at both 8 days and 16 days, for high density specimens. For high density specimens, the 100 ng/ml rhBMP-2 concentration was also able to stimulate differentiation at 8 and 16 days, but only in the second run. The 10 ng/ml rhBMP-2 did not stimulate mineralization in a reproducible manner. Consequently, the highest concentration (1,000 ng /ml) appears to be the most stimulative on differentiation. For titanium, a rhBMP-2 concentration of 40 ng/ml has been reported to stimulate differentiation of the mouse osteoprogenitor cell line 2T9.[19,20] The dose response effect we found, corroborates with a study in which rat bone marrow stromal cells were cultured with rhBMP-2 loaded PLGA microspheres as scaffold material.[18] This dose response effect of BMPs does not occur only with primary cell cultures like bone marrow stromal cells and calvarial cell cultures,[21] it has also been reported for bone cell lines.[22,23] In addition, not only the concentration but also duration of rhBMP-2 stimulation affects differentiation. Puleo *et al.*[24] found that a 1-week exposure of 1,000 ng/ml rhBMP-2 was able to stimulate matrix mineralization of rat bone marrow stromal cells. An exposure time of 2 weeks further enhanced differentiation. Exposure times longer than two weeks did not further enhance osteoblast differentiation. For this reason we decided to supplement our medium only from day 0 till day 7 with rhBMP-2. We also know that rhBMP-2 and glucocorticoids, like dexamathasone and triamcinolone, act synergistically on osteoblast differentiation.[25,26] In view of this Boden *et al.*[26] reported that glucocorticoid co-treatment potentiates BMP effects up to tenfold.

The rat bone marrow stromal cell culture we used is a primary cell culture. The different experimental runs showed different cellular behavior, although overall trends were the same, the level of DNA and calcium differed between the runs. Under the influence of growth and systemic factors, bone marrow stromal cells can differentiate into either adipocytes, chondroblasts, fibroblasts, myoblasts, osteoblasts or reticular cells.[27] However, rat bone marrow stromal cell cultures are inhomogeneous cell cultures. Consequently, not only uncommitted pluripotent but also predetermined cells are present.[24] This causes a certain unpredictability of results between separate cultures. It also emphasizes the problems with primary cell cultures. In view of this, we assume that

different numbers of undifferentiated pluripotent cells were present in both runs because the number of loaded cells and culture conditions were the same for both experimental runs. To prevent these problems cell lines can be used which represent more homogenous cultures. An example of a mesenchymal progenitor cell line is the mouse embryonic fibroblast line C3H10T1/2. These cells are uncommitted and can be induced to differentiate into myoblasts, adipocytes, chondroblasts and osteoblasts depending on the differentiation promoting agent used.[28,29,30,31,32] A serious disadvantage is that C3H10T1/2 cells need the continuous presence of a differentiation-stimulating agent for their osteoblastic phenotype to be maintained.[24]

Based upon our observations we conclude that: (**1**) titanium fiber mesh indeed sustains excellent osteogenic expression *in vitro*; (**2**) increasing the cell seeding density has a positive effect on osteogenic expression in Ti-mesh *in vitro*; (**3**) in high density specimens, rhBMP-2 concentrations of 100 and 1,000 ng/ml stimulate extracellular matrix calcification in a dose-responsive manner.

References

1. **Jansen JA, Takita H, Tsuruga E, Mizuno M, Kuboki Y.** Tissue engineered bone grafts. Abstract presented at the First Smith & Nephew International Symposium, York, UK, 1997. Abstract no. S20.
2. **Kuboki Y, Takita H, Tsuruga E, Ono M, Jansen JA.** Rationale for hydroxyapatite-coated titanium mesh as an effective carrier for BMP. J Dent Res 1998; 77:263 (Abstract no. 1262).
3. **Vehof JWM, Mahmood J, Takita H, van 't Hof MA, Kuboki Y, Spauwen PHM, Jansen JA.** Ectopic bone formation in titanium mesh loaded with Bone Morphogenetic Protein and coated with calcium phosphate. Plast Reconstr Surg 2001; 108:434.
4. **Ishaug SL, Crane GM, Miller MJ, Yasko AW, Yaszemski MJ, Mikos AG.** Bone formation by three-dimensional stromal osteoblast culture in biodegradable polymer scaffolds. J Biomed Mater Res 1997; 36:17.
5. **Ishaug-Riley SL, Crane-Kruger GM, Yaszemski MJ, Mikos AG.** Three-dimensional culture of rat calvarial osteoblasts in porous biodegradable polymers. Biomaterials 1998; 19:1405.
6. **Mendes SC, Van den Brink I, de Bruijn JD, van Blitterswijk CA.** *In vivo* bone formation by human bone marrow cells: Effect of osteogenic culture supplements and cell densities. J Mater Sci Mater in Med 1998; 9:855.
7. **Temenoff JS, Mikos AG.** Review: tissue engineering for regeneration of articular cartilage. Biomaterials 2000; 21:431.
8. **Hanada K, Dennis JE, Caplan AI.** Stimulatory effects of basic fibroblast growth factor and bone morphogenetic protein-2 on osteogenic differentiation of rat bone marrow-derived mesenchymal stem cells. J Bone Miner Res 1997; 12:1606.
9. **Israel DI, Nove J, Kerns KM, Moutsatsos IK, Kaufman RJ.** Expression and characterization of bone morphogenetic protein-2 in Chinese hamster ovary cells. Growth Factors 1992; 7:139.
10. **Maniatopoulos C, Sodek J, Melcher AH.** Bone formation *in vitro* by stromal cells obtained from bone marrow of young adult rats. Cell Tissue Res 1998; 254:317.
11. **van der Lubbe HB, Klein CP, de Groot K.** A simple method for preparing thin (10 microM) histological sections of undecalcified plastic embedded bone with implants. Stain Technol 1988; 63:171.
12. **Labarca C, Paigen K.** A simple, rapid, and sensitive DNA assay procedure. Anal Biochem 1980; 102:344.
13. **Kind PRN, King EJ.** Estimation of plasma phosphatase by determination of hydrolyzed phenol with amino-antipyrine. J Clin Pathol 1954; 7:322.
14. **Hulshoff JE, van Dijk K, van der Waerden JP, Wolke JG, Ginsel LA, Jansen JA.** Biological evaluation of the effect of magnetron sputtered Ca/P coatings on osteoblast-like cells *in vitro*. J Biomed Mater Res 1995; 29:967.
15. **Casser-Bette M, Murray AB, Closs EI, Erfle V, Schmidt J.** Bone formation by osteoblast-like cells in a three-dimensional cell culture. Calcif Tissue Int 1990; 46:46.

16. **Dennis JE, Haynesworth SE, Young RG, Caplan AI.** Osteogenesis in marrow-derived mesenchymal cell porous ceramic composites transplanted subcutaneously: effect of fibronectin and laminin on cell retention and rate of osteogenic expression. Cell Transplant 1992; 1:23.

17. **Owen TA, Aronow M, Shalhoub V, Barone LM, Wilming L, Tassinari MS, Kennedy MB, Pockwinse S, Lian JB, Stein GS.** Progressive development of the rat osteoblast phenotype *in vitro*: reciprocal relationships in expression of genes associated with osteoblast proliferation and differentiation during formation of the bone extracellular matrix. J Cell Physiol 1990; 143:420.

18. **Puleo DA, Huh WW, Duggirala SS, DeLuca PP.** *In vitro* cellular responses to bioerodible particles loaded with recombinant human bone morphogenetic protein-2. J Biomed Mater Res 1998; 41:104.

19. **Ong JL, Cardenas HL, Cavin R, Carnes DL.** Osteoblast responses to BMP-2-treated titanium *in vitro*. Int J Oral Maxillofac Implants 1997; 12:649.

20. **Ong JL, Carnes DL, Cardenas HL, Cavin R.** Surface roughness of titanium on bone morphogenetic protein-2 treated osteoblast cells *in vitro*. Implant Dent 1997; 6:19.

21. **Chen TL, Bates RL, Dudley A, Hammonds, RG, Amento, EP.** Bone morphogenetic protein-2b stimulation of growth and osteogenic phenotypes in rat osteoblast-like cells: comparison with TGF-beta1. J Bone Miner Res 1991; 6:1387.

22. **Thies RS, Bauduy M, Ashton BA, Kurtzberg L, Wozney JM, Rosen V.** Recombinant human bone morphogenetic protein-2 induces osteoblastic differentiation in W-20-17 stromal cells. Endocrinology 1992; 130:1318.

23. **Yamaguchi A, Katagiri T, Ikeda T, Wozney JM, Rosen V, Wang EA, Kahn AJ, Suda T, Yoshiki S.** Recombinant human bone morphogenetic protein-2 stimulates osteoblastic maturation and inhibits myogenic differentiation *in vitro*. J Cell Biol 1991; 113:681.

24. **Puleo DA.** Dependence of mesenchymal cell responses on duration of exposure to bone morphogenetic protein-2 *in vitro*. J Cell Physiol 1997; 173:93.

25. **Rickard DJ, Sullivan TA, Shenker BJ, Leboy PS, Kazhdan I.** Induction of rapid osteoblast differentiation in rat bone marrow stromal cell cultures by dexamethasone and BMP-2. Dev Biol 1994; 161:218.

26. **Boden SD, McCuaig K, Hair G, Racine M, Titus L, Wozney JM, Nanes MS.** Differential effects and glucocorticoid potentiation of bone morphogenetic protein action during rat osteoblast differentiation *in vitro*. Endocrinology 1996; 137:3401.

27. **Owen M.** Marrow stromal stem cells. J Cell Sci Suppl 1988; 10:63.

28. **Taylor SM, Jones PA.** Multiple new phenotypes induced in 10T1/2 and 3T3 cells treated with 5-azacytidine. Cell 1979; 17:771.

29. **Ibric II, Benedict WF, Peterson AR.** Simultaneous determination of ascorbic acid and dehydroascorbic acid in cultures of C3H10T1/2 cells. *In vitro* Cell and Dev Biol 1988; 24:669.

30. **Guernsey DL, Schmidt TJ.** Cortisone effects on differentiation and X-ray induced transformation of C3H10T1/2 mouse cells. Cell Diff 1988; 24:159.

31. **Katagiri T, Yamaguchi A, Ikeda T, Yoshiki S, Wozney JM, Rosen V, Wang EA, Tanaka H, Omura S, Suda T.** The non-osteogenic mouse pluripotent cell line, C3H10T1/2, is induced to differentiate into osteoblastic cells by recombinant human bone morphogenetic protein-2. Biochem Biophys Res Commun 1990; 172:295.

32. **Wang EA, Israel DI, Kelly S, Luxenberg DP.** Bone morphogenetic protein-2 causes commitment and differentiation in C3H10T1/2 and 3T3 cells. Growth Factors 1993; 9:57.

Chapter 3

Bone formation in calcium-phosphate-coated titanium mesh

J.W.M. Vehof, P.H.M. Spauwen and J.A. Jansen.

3.1   Introduction

At the present time, the clinical standard in the treatment of bone defects is still the use of autologous bone tissue. Nevertheless, due to both availability and patient-associated problems, alternative treatment techniques are under development. The rationale of these new strategies is the construction of a so-called bone graft substitute (BGS) consisting of a porous material to which bone growth-promoting factors or bone-forming cells are added. It is this latter technique that especially appears to have great potential in terms of both cost and human ectopical effectiveness.

In post-natal life, precursors of osteogenic cells, the so-called osteoprogenitor cells or mesenchymal stem cells (MSCs), are present in bone marrow. Osteoprogenitor cells represent only a small fraction of the total number of bone marrow cells, in humans this has reported to be 0.01-0.0001%.[1] Whilst some authors have shown decreased progenitor cells with ageing,[2-6] others have not.[7] In view of this, methods have been developed to culture-expand and select the osteoprogenitor cell fraction from bone marrow.[8-10] Preliminary studies of Bruder *et al.* demonstrated that BGSs with culture-expanded bone marrow-derived MSCs are more effective in bone formation in segmental defects than BGSs loaded with fresh syngeneic marrow.[8] On the other hand, not only the proliferation but also the differentiation of osteoprogenitor cells can be directed. Several factors have been shown to direct differentiation of marrow-derived MSCs into the osteoblast lineage *in vitro*: dexamethasone[11,12] BMPs,[12,13] 1,25-dihydroxyvitamin D3,[14] retinoic acid[13] and fluoride.[15]

In addition to osteogenic potential, a BGS requires the use of a suitable carrier or scaffold material. Applied carrier materials include ceramics (*e.g.* hydroxyapatite and/or tricalcium phosphate), and polymers (*e.g.* poly(α-hydroxyl acids): poly(lactic acid), poly (glycolic acid) or co-polymers). The disadvantage of most of these scaffold materials is that they are not very strong and can easily transform.[16] Another candidate scaffold material for loaded applications is titanium (Ti) fiber mesh.[17] This titanium mesh has excellent mechanical properties in terms of stiffness and elasticity.[17] Further, it is bone-compatible and easy to handle during surgery. Although titanium is not degradable, for a large number of reconstructive procedures, this is no drawback. An additional advantage is that the titanium fiber mesh can be provided with a very thin calcium phosphate (Ca-P)-coating. It is generally assumed that calcium phospate coatings enhance the bone formation process.[18]

The current study is part of a series of experiments in which we explore the efficacy of titanium fiber mesh as scaffold material in the creation of BGSs. The objective of the present study was to investigate whether: (**1**) titanium mesh loaded with cultured osteogenic cells can generate bone formation in an ectopic location, and (**2**) the application of a thin Ca-P coating will have an additional effect on bone formation.

3.2 Materials and methods

3.2.1 Scaffold materials

Sintered porous Ti-fiber mesh (Bekaert N.V., Zwevegem, Belgium) with a volumetric porosity of 86%, density of 600 g/m^2 and fiber diameter of 50 µm was used as scaffold material. The average pore size of the mesh was about 250 µm. The prepared implants were disc shaped with a diameter of 6 mm, thickness of 0.8 mm, and weight of about 15 mg. All implants were ultrasonically cleaned with 70% ethanol for 15 min. The mesh was applied as-received (Ti) or provided with a thin (1 µm) Ca-P coating (Ti-CaP) on both sides. The coating procedure was performed using a commercially available RF magnetron sputter unit (Edwards ESM 100).[19] The target material used in the deposition process was a copper disc provided with a plasma-sprayed hydroxyapatite coating (CAMCERAM®). The process pressure was 5 x 10^{-3} mbar and the sputter power was 400 W. The deposition rate of the films was 100–150 nm/min sputtering.

After deposition, all coated specimens were subjected to an additional heat treatment for 2 h at 500°C. X-ray diffraction (XRD) (**Figure 1**), Fourier Transform Infrared spectroscopy (FTIR) and Energy Dispersive Spectroscopical (EDS) analysis showed that this resulted in the coatings having a crystalline apatite structure with a Ca/P ratio of 1.8–2.0. Before use, implants were sterilized by autoclaving for 15 min at 121°C. A total of 120 discs were prepared: 60 Ti and 60 Ti-CaP.

3.2.2 Cell culture technique

The rat bone marrow (RBM) cell culture technique was used as described by Maniatopoulos.[20] Rat bone marrow (RBM) cells were obtained from femora of 5 six-week-old syngeneic Fisher 344 male rats (100–120 g). Epiphyses were cut off, and both diaphyses were flushed out using complete medium consisting of α-Minimal Essential Medium (α-
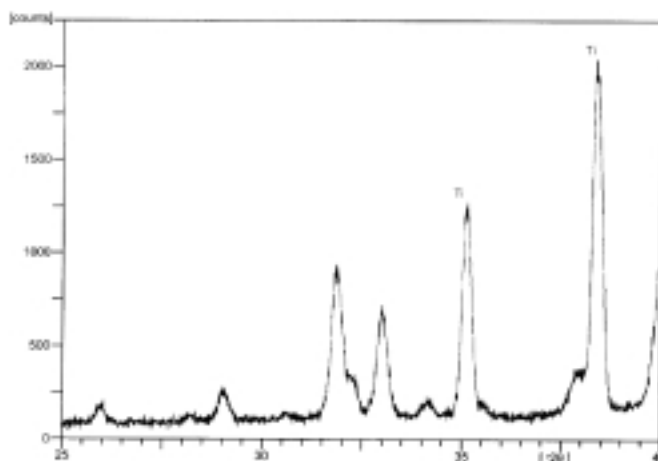

Figure 1.

X-ray diffraction pattern of a crystalline sputter coating deposited on titanium fiber mesh (heat treatment for 2 h at 500ºC) (Ti = titanium substrate).

MEM, Gibco BRL, Life Technologies B.V., Breda, the Netherlands) supplemented with 10% fetal calf serum (FCS, heat induced at 56°C for 35 min., Gibco), 50 µg/ml freshly prepared ascorbic acid (Sigma, Chemical Co., St. Louis, Mo., USA), 10 mM Na-β-glycero-phosphate (Sigma), 10^{-8} M dexamethasone (Sigma), and gentamycin. Per two femurs, 15 ml of this medium was used. Finally, cells were suspended and cultured in complete medium in three 80-cm^2 tissue culture flasks (Nunc. Products, Gibco). Cultures were incubated in a humidified atmosphere of 95% air, 5% CO_2 at 37°C. After seven days of primary culture, cells were detached using trypsin/ EDTA (0.25% w/v trypsin/ 0.02% ethylene diamine tetra acetic acid (EDTA)).

3.2.3   Bone graft substitute preparation

The cells were concentrated by centrifugation at 1,500 rpm for 5 min and resuspended in a known amount of media. Cells were counted by a Coulter counter and diluted to 5.0 x 10^6 cells/ml in serum-free α-MEM. A total of 120 meshes, 60 Ti and 60 Ti-CaP, were placed in 24-well plates. Half of these meshes were loaded with cells and the other half were used as controls. Before loading, all materials were treated with RF glow-discharge (Harrick PDC-3XG, Argon, 0.15 Torr, for 5 min) to enhance wettability. Subsequently, under a sterile laminar flow, 20 µl aliquots of the cell suspensions were seeded onto the top of appropriate meshes, resulting in a seeding density of 3.54 x 10^5 cells/cm^2. After that, the 24-well plates were exposed to a vacuum (5 x 10^4 N/m^2 Vacuum) for 10 min. Subsequently, the meshes were left in an incubator at 37°C for 20 min, at which time the meshes were turned and the other side was loaded in a similar manner. The meshes were then placed in an incubator for an additional 1.5 h to enable the cells to attach. In this way, both sides of the mesh material were loaded, resulting in a total seeding density of 200,000 RBM cells per mesh. Finally, 1 ml of serum free medium was added to each well. All non-loaded control meshes were treated in a similar manner using serum free medium without cells. After incubation all implants were transported in serum free medium to the animal facility.

3.2.4   Experimental design and surgical procedure

For implantation, 30 four-week-old syngeneic Fisher 344 male rats (50-60 g) were used. Surgery was performed under general inhalation anesthesia with a combination of halothane, nitrous oxide and oxygen. The RBM-loaded and non-loaded control meshes were subcutaneously implanted into the back of the animals. To insert the implants, the animals were immobilized and placed in a ventral position. The back of the animals was shaved, washed and disinfected with povidone-iodine. To insert the subcutaneous implants, we made four small longitudinal incisions on both sides of the vertebral column. Lateral to the incisions, a subcutaneous pocket was created using blunt dissection. After placement of the implants, the skin was closed using staples (Agraven®).

Each animal received one subcutaneous implant of each type. To localize the implants a latin square design was used to assure complete statistical randomization. A total of 120 implants were placed: 30 Ca-P-coated Ti-implants loaded with RBM cells (Ti-CaP-RBM);

30 Ca-P-coated Ti-implants without RBM cells (Ti-CaP); 30 non-coated Ti-implants loaded with RBM cells (Ti-RBM); 30 non-coated Ti-implants without RBM cells (Ti). The samples without cells served as controls. Implantation periods were 2, 4 and 8 weeks. At the end of each implantation period, 10 rats were sacrificed ($n = 10$ for each material and time period). Further, six out of the ten rats in the 8-week group received sequential triple fluorochrome labeling. The fluorochrome labels tetracline (yellow), alizarin-complexone (red), and calceine (green) were administered at 2, 4 and 6 weeks post-operatively, respectively. These labels were injected intramuscularly except for alizarin-complexone, which was given subcutaneously. The treatment dose was 25 mg/kg body weight for each label. In this study, national guidelines for the care and use of laboratory animals were respected.

3.2.5 Histological preparation and evaluation

At the end of the experiment, euthanasia was performed using an overdose of ether anesthesia. Following euthanasia, the implants with their surrounding tissue were retrieved and prepared for histological evaluation. The specimens were then fixed in 4% phosphate-buffered formaldehyde solution (pH = 7.4), dehydrated in a graded series of ethanol and embedded in methylmethacrylate. Following polymerization, at least three 10-µm-thick sections were prepared per implant using a modified sawing microtome technique.[21] Before sections were made, the specimens were etched with hydrochloric ethanol for 15 s, stained with methylene blue for 1 min and stained with basic fuchsin for 30 s. Finally, sections were investigated with a light microscope.

Besides thin sections, two additional 30-µm-thick sections were prepared from the 24 samples of the six animals that received fluorochromes, these sections were not stained. They were evaluated with a fluorescence microscope equipped with an excitation filter of 470-490 nm.

The light and fluorescent microscopical assessment consisted of a complete morphological description of the tissue response to the different implants. In addition, quantitative information was obtained on the amount of bone formation into the various mesh implants, *i.e.*:(**1**) the number of specimens which showed bone formation; (**2**) largest horizontal and vertical diameter of the observed bone formation.

3.3 Results

During the experiment, all rats remained in good health and did not show any wound complications. At the end of the experiment, all implants could be retrieved. At retrieval, the implants were surrounded by a thin reaction-free fibrous capsule. There was no indication that the thickness of the capsule varied between the various implantation periods and implantation types. No bone formation could be observed macroscopically.

3.3.1 Light microscopical evaluation

Evaluation of the prepared sections revealed no big differences in overall tissue response with respect to the various implantation periods and fiber mesh materials. All implants were surrounded by a thin fibrous tissue capsule about four to six cell layers thick. The capsule became more dense over time, but the thickness in cell layers remained the same. The capsule was free of inflammatory cells and contained fibrocytes, collagen and blood vessels. Inside the implants, the mesh porosity was filled with fibrous tissue and capillaries. Some implants also showed fatty tissue ingrowth. Hardly any inflammatory cells could be seen (**Figure 2**).

Further analysis revealed that for all implantation periods none of the Ca-P-coated and non-coated control meshes supported bone formation (**Table 1**). On the other hand, the RBM-loaded specimens showed osteogenic capacity: 5 Ti-CaP-RBM and 2 Ti-RBM samples showed bone formation at 2 weeks post-implantation. At 4 weeks, this increased to 6 Ti-CaP-RBM and 3 Ti-RBM specimens. Finally, at 8 weeks, in the Ti-RBM meshes bone formation decreased to zero. On the other hand, in 6 Ti-CaP-RBM specimens bone was still present at 8 weeks (**Table 1**).

Statistical analysis, using the Fisher's exact test, revealed that there was significantly more bone formation in the Ti-CaP-RBM group than in the Ti-RBM group only at 8 weeks (two-tailed Fisher's exact test, $p = 0.01084$) (**Table 1**).

Bone formation was generally characterized by the presence of randomly distrib-uted single or multiple spheres in the pores of the Ti-mesh in close contact to the Ti-fibers without an intervening fibrous tissue layer (**Figure 3**). No preference for the inner or outer mesh area was observed. Quantitative measurements showed that the horizontal diameter of these spheres varied from about 50 µm to 700 µm. Morphologically, the appearance of these spheres was characterized by the presence of osteocyte-like cells embedded in a mineralized matrix. The amount of bone was found to be small. In addition, the morpho-logical examination revealed that in none of the sections either cartilage or bone marrow

---

Table 1.
Scheme showing the number of implants in which bone formation could be observed at different explan-tation periods (*n*=10 for each implant and time period). In addition, results are shown of the statistical evaluation (two-tailed Fisher's exact test), comparing Ti-CaP-RBM and Ti-RBM groups at various im-plantation periods.

Implant:	Implantation period:		
	2 weeks	**4 weeks**	**8 weeks**
Ti-CaP-RBM	5 (*n=10*)	6 (*n=10*)	6 (*n=10*)
Ti-Ca P	0 (*n=10*)	0 (*n=10*)	0 (*n=10*)
Ti-RBM	2 (*n=10*)	3 (*n=10*)	0 (*n=10*)
Ti	0 (*n=10*)	0 (*n=10*)	0 (*n=10*)
P-value*:	0.34985 (**NS**)	0.36985 (**NS**)	0.01084 (**P<0.05**)

* Fisher's exact test (two-tailed)
NS = non-significant

Figure 2.

Undecalcified section of a
control mesh without bone
formation 2 weeks
after implantation.
The implant is surrounded by
a thin fibrous tissue capsule.
No inflammatory cells are
observable. Inside the implant,
the mesh porosity is filled with
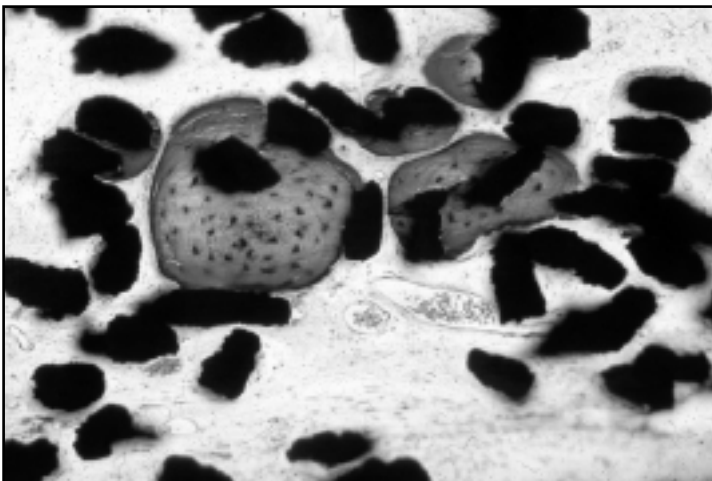fibrous tissue with capillaries
(*orig. magn. 20x*).

Figure 3.

Undecalcified section of a
calcium phosphate-coated
mesh loaded with RBM cells
(Ti-CaP-RBM) 8 weeks after
implantation. Bone formation
is characterized by the
presence of randomly
distributed multiple spheres
in the porosity of the Ti-mesh.
Osteocyte-like cells are
present, embedded in a
mineralized matrix
(*orig. magn. 20x*).

formation was observed. Finally, in only one Ti-CaP-RBM and one Ti-RBM implant was bone formation more pronounced at 4 weeks. In these specimens, bone penetrated almost through the total thickness and extended to about half of the diameter of the mesh material (**Figure 4A** and **Figure 4B**).

3.3.2 Fluorescence microscopical evaluation

Fluorescence microscopical evaluation of the labeled 8-week sections confirmed that mineralized tissue was present in four Ti-CaP-RBM samples. No fluorescence staining could be observed in Ti-RBM or control implants. The accumulation of the fluorescent labels demonstrated that the bone was indeed deposited in spherical foci. The multiple labeling procedure also revealed that the bone formation started from the center of a pore and proceeded in a centrifugal manner (**Figure 5**).

3.4   Discussion and conclusion

The results of this study show that the biocompatibility of titanium mesh is excellent as demonstrated by the thin capsule thickness and absence of inflammatory cells in both loaded and non-loaded meshes. These findings corroborate those of our earlier studies in which the soft tissue reaction to a similar titanium mesh was investigated in rabbits[22] and goats.[23] However, in contrast with the latter experiments, the present study did not indicate any variation in the thickness of the capsule with respect to the length of the implantation period (**Figure 2**). Apparently, this lack of variation is due to the rapid wound healing response in this small animal model and once again emphasizes that the results of the present study cannot be freely extrapolated to the human situation.

The RBM-loaded meshes showed only a very limited amount of bone formation. Consequently, histomorphometrical measurements to quantify the area occupied by bone in relation to the total mesh volume, were not useful. In addition, the number of "positive" implants as well as the amount of bone formation were significantly lower compared with other studies.[8-10,24] We assume that this difference in bone formation is due to our culture
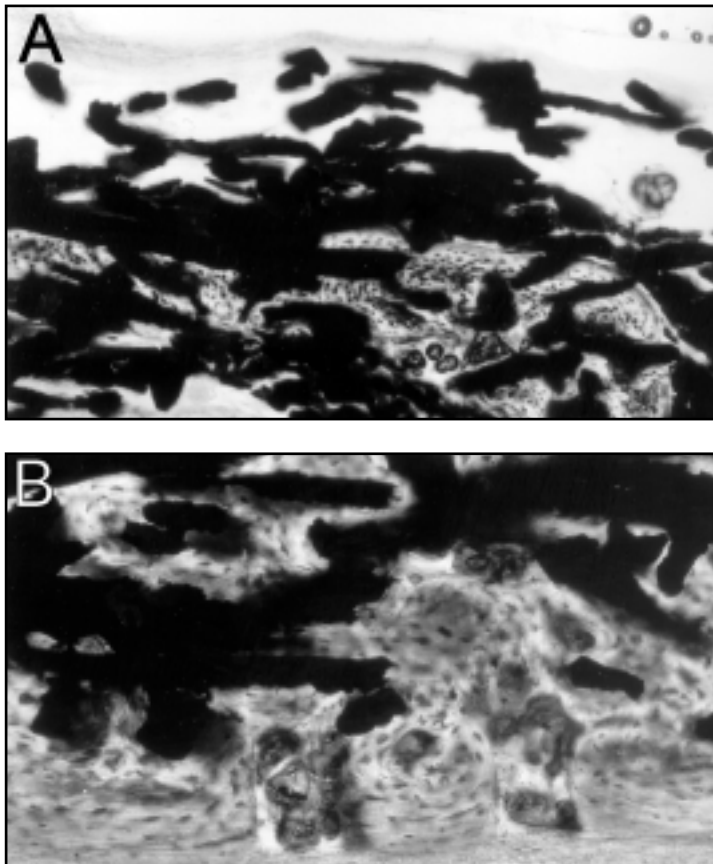

Figure 4.

(A)   Undecalcified section of a non-coated mesh loaded with RBM cells (Ti-RBM) 4 weeks after implantation. Bone formation penetrates through half of the total thickness of the mesh and about half of the diameter of the mesh (*orig. magn. 10x*).

(B)   Undecalcified section of a Ca-P-coated mesh loaded with RBM cells (Ti-CaP-RBM) 4 weeks after implantation. In this section bone formation also penetrates through half of the total thickness of the mesh and about half of the diameter of the mesh (*orig. magn. 20x*).
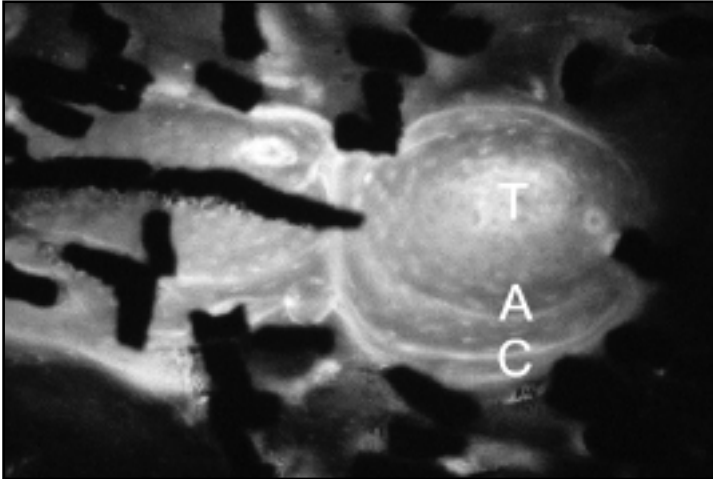
Figure 5.
Fluorescent light micrograph
of a calcium phosphate coated
mesh loaded with RBM cells
(Ti-CaP-RBM) 8 weeks after
implantation. In the center
of the bone sphere the
tetracycline label (T) can be
observed. Followed more
excentrically by the alizarin
complexone label (A) and
the calcein label (C).
The accumulation sequence
of the various labels
demonstrates that the newly
formed bone was deposited in
a centrifugal manner starting
from the center of a pore
(*orig.magn. 20x*).

and loading technique. For example, culture techniques that have been used in previous studies were based on the expansion of undifferentiated cells before their differentiation was directed into the osteogenic lineage. Consequently, the addition of dexamethasone to the culture medium has been shown to be a very relevant parameter in osteogenic expression and differentiation. However, dexamethasone does inhibit the proliferation of mesenchymal stem cells. In the current study, dexamethasone was already present in the primary culture medium during expansion, in most other studies, mesenchymal stem cells are precultured in the absence of dexamethasone. Occasionally, in addition to dexametha-sone, other proliferation and differentiation simulating growth factors, like bFGF and rhBMP-2, have been supplemented to the medium during culture expansion of MSCs.[25] Therefore, the timing of our addition of dexamethasone can be questioned. Perhaps, a later moment is more appropriate. Additional research will have to be conducted to answer this question. The same is true for the addition of other factors used to influence the loading efficiency. For example, the presence of Fetal Bovine Serum (FBS) or Fetal Calf Serum (FCS) in the cell suspension during loading has been shown to increase the loading efficiency more than 2 times.[26] We omitted the use of FCS to avoid an adverse immunological reaction. Fibronectin has also been demonstrated to enhance the loading efficiency of bone cells in porous scaffolds.[27]

In contrast with other studies, we also preferred not to continue culturing after seeding the cells into the scaffolds. Nevertheless, prolonged culturing after loading has been shown to be more effective with respect to final bone formation, especially when the medium is supplemented with dexamethasone during this period. This method can be

considered as *in situ* cell expansion. Our choice is based on the fact that the current study is part of a series of experiments, in which we intend to examine the final potential of our scaffold material in a step-like manner.

The most frequently used loading techniques are the suspension and droplet methods. In suspension methods, scaffolds are incubated in a cell suspension with a known number of cells for a predetermined time.[8-10] An advantage of this technique is that the entire surface of the mesh is surrounded by a highly concentrated cell suspension, thereby allowing for attachment. After that, these scaffolds can either be submitted to further culturing or immediately implanted. Before implantation, the total number of cells attached to such a construct has been reported to be increased up to 15 million cells per milliliter carrier volume.[9] In the droplet methods, droplets of cell suspension with equal volumes and known numbers of cells are placed on top of the scaffold. After a certain incubation period a sufficient amount of medium is added and the scaffolds can either be incubated for prolonged culturing or implanted directly. One advantage of the droplet method is that the number of loaded cells can be standardized. Also, the total number of cells required for loading is less. In the present study, we applied about 9 million cells per milliliter carrier. The final number of cells per surface area, was $3.54 \times 10^5/cm^2$. In contrast, Mikos *et al.*[28] used a similar loading technique, with a seeding density of $6.83 \times 10^5/cm^2$. In this study, significantly more bone formation occurred. Therefore, we cannot exclude that the number of cells we applied per mesh was below a certain required critical threshold.

Loading techniques often include the use of a mild vacuum for a short period of time in order to remove air from the porous scaffolds to enhance the contact between the scaffold material and cell suspension. To our knowledge no detrimental effect of the use of mild vacuum on bone formation has been published to date. For example, the loading technique used by Bruder *et al.* involves the application of a vacuum[9] in 3 bursts of 5 seconds each.[8,10] Still adequate bone formation was found. In our study we exposed the specimens only to a mild vacuum of $5 \times 10^4 N/m^2$ (500 mbar) for a very short time period.

The fluorescent labeling study revealed that the newly formed bone was deposited in a centrifugal manner. This finding agrees with another study in which a comparable titanium scaffold material was used.[24] However, bone formation and consequent fluorochrome labeling only occurred in the Ca-P-coated mesh implants. For so-called bioactive implant materials or implants provided with a bioactive surface coating, bonding osteogenesis has been described.[24,29] We know that the thin RF magnetron sputter coating did not penetrate completely throughout the mesh, despite the fact that we coated the mesh on both sides. As a result, the inside of the mesh still consists of the original titanium surface. This explains the absence of bonding osteogenesis.

On the other hand, the applied coating was evidently able to further enhance bone formation, as in the non-coated specimens less bone was formed and bone formation was even completely absent at 8 weeks. A similar effect on osteogenesis has been described for thick plasma-sprayed hydroxyapatite (HA) coatings.[18] This effect is supposed to be due to the high affinity of calcium phosphate ceramics to bone-growth-stimulating proteins, like Bone Morphogenetic Proteins (BMPs). In addition to plasma-sprayed HA coatings, a similar increased adsorption and efficacy of BMP has also been shown recently for thin Ca-P coatings.[30]

On the basis of our observations we conclude that the combination of Ti-mesh with RBM cells can indeed generate bone formation. Nevertheless, the occurrence as well as the amount of new bone is very limited, using the procedures described in this study. Further, we confirm our earlier observations that a thin Ca-P coating can have an additional positive effect on the bone-generating properties of a scaffold material.

References

1. **Haynesworth SE, Reuben D, Caplan AI.** Cell-based tissue engineering therapies: the influence of whole body physiology. Adv Drug Delivery Rev 1998; 33:3.
2. **Bergman RJ, Gazit D, Kahn AJ, Gruber H, McDougall S, Hahn TJ.** Age-related changes in osteogenic stem cells in mice. J Bone Miner Res 1996; 11:568.
3. **Egrise D, Martin D, Vienne A, Neve P, Schoutens A.** The number of fibroblastic colonies formed from bone marrow is decreased and the *in vitro* proliferation rate of trabecular bone cells increased in aged rats. Bone 1992; 13:355.
4. **Kahn A, Gibbons R, Perkins S, Gazit D.** Age-related bone loss. A hypothesis and initial assessment in mice. Clin Orthop 1995; 313:69.
5. **Liang CT, Barnes J, Seedor JG, Quartuccio HA, Bolander M, Jeffrey JJ, Rodan GA.** Impaired bone activity in aged rats: alterations at the cellular and molecular levels. Bone 1992; 13:435.
6. **Quarto R, Thomas D, Liang CT.** Bone progenitor cell deficits and the age-associated decline in bone repair capacity. Calcif Tissue Int 1995; 56:123.
7. **Oreffo RO, Bord S, Triffitt JT.** Skeletal progenitor cells and ageing human populations. Clin Sci 1998; 94:549.
8. **Kadiyala S, Neelam J, Bruder SP.** Culture-expanded, bone marrow-derived mesenchymal stem cells can regenerate a critical-sized segmental bone defect. Tissue Eng 1997; 3:173.
9. **Kadiyala S, Young RG, Thiede MA, Bruder SP.** Culture expanded canine mesenchymal stem cells possess osteochondrogenic potential *in vivo* and *in vitro*. Cell Transplant 1997; 6:125.
10. **Bruder SP, Kraus KH, Goldberg VM, Kadiyala S.** The effect of implants loaded with autologous mesenchymal stem cells on the healing of canine segmental bone defects. J Bone Joint Surg Am 1998; 80:985.
11. **Leboy PS, Beresford JN, Devlin C, Owen ME.** Dexamethasone induction of osteoblast mRNAs in rat marrow stromal cell cultures. J Cell Physiol 1991; 146:370.
12. **Rickard DJ, Sullivan TA, Shenker BJ, Leboy PS, Kazhdan I.** Induction of rapid osteoblast differentiation in rat bone marrow stromal cell cultures by dexamethasone and BMP-2. Dev Biol 1994; 161:218.
13. **Katagiri T, Yamaguchi A, Ikeda T, Yoshiki S, Wozney JM, Rosen V, Wang EA, Tanaka H, Omura S, Suda T.** The non-osteogenic mouse pluripotent cell line, C3H10T1/2, is induced to differentiate into osteoblastic cells by recombinant human bone morphogenetic protein-2. Biochem Biophys Res Commun 1990; 172:295.
14. **Skjodt H, Gallagher JA, Beresford JN, Couch M, Poser JW, Russell RG.** Vitamin D metabolites regulate osteocalcin synthesis and proliferation of human bone cells *in vitro*. J Endocrinol 1985; 105:391.
15. **Hall BK.** Sodium fluoride as an initiator of osteogenesis from embryonic mesenchyme *in vitro*. Bone 1987; 8:111.
16. **Zhang R, Ma PX.** Poly(α-hydroxyl acids)/hydroxyapatite porous composites for bone-tissue engineering. I. Preparation and morphology. J Biomed Mater Res 1999; 44:446.
17. **Jansen JA, von Recum AF, van der Waerden JP, de Groot K.** Soft tissue response to different types of sintered metal fibre-web materials. Biomaterials 1992; 13:959.
18. **Takaoka T, Okumura M, Ohgushi H, Inoue K, Takakura Y, Tamai S.** Histological and biochemical evaluation of osteogenic response in porous hydroxyapatite coated alumina ceramics. Biomaterials 1996; 17:1499.
19. **Jansen JA, Wolke JG, Swann S, Van der Waerden JP, de Groot K.** Application of magnetron sputtering for producing ceramic coatings on implant materials. Clin Oral Implants Res 1993; 4:28.
20. **Maniatopoulos C, Sodek J, Melcher AH.** Bone formation *in vitro* by stromal cells obtained from bone marrow of young adult rats. Cell Tissue Res 1988; 254:317.
21. **van der Lubbe HB, Klein CP, de Groot K.** A simple method for preparing thin (10 microM) histological sections of undecalcified plastic embedded bone with implants. Stain Technol 1988; 63:171.
22. **Jansen JA, Paquay YG, van der Waerden JP.** Tissue reaction to soft-tissue anchored percutaneous implants in rabbits. J Biomed Mater Res 1994; 28:1047.

23. **Paquay YC, de Ruijter JE, van der Waerden JP, Jansen JA.** Wound healing phenomena in titanium fibre mesh: the influence of the length of implantation. Biomaterials 1997; 18:161.
24. **Okumura M, Ohgushi H, Ducheyne P.** Porous titanium felt as a carrier of osteogenic cells. In: Ducheyne P, Christiansen D, editors. Butterworth-Heinemann Ltd, Linnacre House, Jordan Hill, Oxford, England. Bioceramics 1993, vol. 6, 305.
25. **Hanada K, Dennis JE, Caplan AI.** Stimulatory effects of basic fibroblast growth factor and bone morphogenetic protein-2 on osteogenic differentiation of rat bone marrow-derived mesenchymal stem cells. J Bone Miner Res 1997; 12:1606.
26. **Gao JM, Niklason L, Langer R.** Surface hydrolysis of poly(glycolic acid) meshes increases the seeding density of vascular smooth muscle cells. J Biomed Mater Res 1998; 42:417.
27. **Dennis JE, Caplan AI.** Porous ceramic vehicles for rat-marrow-derived (Rattus norvegicus) osteogenic cell delivery: effects of pre-treatment with fibronectin or laminin. J Oral Implantol 1993; 19:106.
28. **Ishaug Riley SL, Crane GM, Gurlek A *et al*.** Ectopic bone formation by marrow stromal osteoblast transplantation using poly(DL-lactic-co-glycolic acid) foams implanted into the rat mesentery. J Biomed Mater Res 1997; 36:1.
29. **Ohgushi H, Goldberg VM, Caplan AI.** Heterotopic osteogenesis in porous ceramics induced by marrow cells. J Orthop Res 1989; 7:568.
30. **Jansen JA, Takita H, Tsuruga E, Mizuno M, Kuboki Y.** Tissue Engineered Bone Grafts. Proc. 1st Smith & Nephew International Symposium, York, UK, 1997, abstr. no. S20.

....

Chapter 4

....

Bone formation in Ca-P-coated and non-coated titanium fiber mesh

J.W.M. Vehof, J. van den Dolder, J.E. de Ruijter, P.H.M. Spauwen and J.A. Jansen.

....

4.1 Introduction

Mesenchymal stem cells (MSCs) can be used for the functional repair or regeneration of large bone defects. In this approach a three-dimensional (3-D) scaffold material is used to deliver the cells to the bone defect site. The final success of this tissue-engineered strategy is determined by the number of responsive MSCs loaded in the scaffold as well as by the material characteristics of the delivery vehicle.

MSCs, or osteoprogenitor cells, which are precursors of osteogenic cells, are present in bone marrow, where they represent only a small fraction of the total number of bone marrow cells.[1] The number of progenitor cells has even been shown to decrease with ageing.[2-6] In view of this, methods have been developed to culture-expand and select the osteoprogenitor cell fraction from bone marrow.[7-9] In addition, it has been shown that cultured bone marrow-derived MSCs are more effective in bone formation than fresh marrow.[7,10-12]

It is important to note that besides proliferation also the differentiation of osteoprogenitor cells can be directed during culture. In view of this, several factors, like dexamethasone and Bone Morphogenetic Proteins (BMPs), are known to direct the differentiation of these cells into the osteoblast lineage *in vitro*.[13-15] The addition of proliferation (basic Fibroblast Growth Factor, bFGF) and differentiation [recombinant human (rh)BMP-2] stimulating agents during culture has been shown to enhance the *in vivo* osteogenic potential.[16,17] The osteogenic potential of cell-loaded scaffolds can further be increased by modifying the conditions during seeding (by optimizing the number of loaded cells),[17-20] and culturing for example, static versus dynamic culturing.[21-23]

Tissue engineering of bone requires the use of a suitable carrier or scaffold material. The currently applied 3-D scaffold materials include ceramics, polymers and collagen. The disadvantage of most of these scaffold materials is that they are not very strong and can easily transform.[24] Consequently, we have suggested previously the use of porous sintered titanium (Ti) fiber mesh as a scaffold for MSCs.[25] This titanium mesh has excellent mechanical properties[26] and has been proven to be bone-compatible and is easy to handle during surgery. Although titanium is not degradable, this is no drawback for a large number of reconstructive procedures. An additional advantage is that the titanium fiber mesh can be provided with a very thin calcium phosphate (Ca-P) coating which has been described to have a positive effect on bone formation.[25,27] Conversely, we found the occurrence as well as the amount of bone formation to be very limited when osteogenic cells were seeded in Ti-fiber mesh scaffolds.[25] We assumed this latter result to be related to the culture and cell-loading technique, which involved the use of a droplet-loading technique without prolonged culturing *in vitro*. In view of this it should be noted that prolonged culturing after loading has been shown to be more effective with respect to final bone formation,[28] especially when the medium is supplemented with dexamethasone during this period.[29,30]

The objective of the present study was to investigate the effect of a suspension-loading method versus a droplet-loading method in combination with prolonged *in situ* culturing on bone formation in titanium fiber (Ti) mesh scaffolds in a rat ectopic assay model.

4.2 Materials and methods

4.2.1 Scaffold materials

Sintered porous Ti-fiber mesh (Bekaert N.V., Zwevegem, Belgium) with a volumetric porosity of 86 %, a density of 600 g/m^2 and a fiber diameter of 50 µm was used as scaffold material. The average pore size of the mesh was about 250 µm. Ti-fiber mesh discs were punched out of a Ti-fiber mesh sheet. As a result of the fabrication process, the meshes had an easily discernable top and bottom. The prepared implants were disc-shaped with a diameter of 6 mm, a thickness of 0.8 mm, and a weight of about 15 mg.

All implants were ultrasonically cleaned with 70 % ethanol for 15 min. The mesh was applied as-received (Ti) or provided with a thin (2 µm) Ca-P coating (Ti-CaP) on both sides. The coating procedure was performed using a commercially available RF magnetron sputter unit (Edwards ESM 100).[31] The target material used in the deposition process was a copper disc provided with a plasma-sprayed hydroxylapatite coating (CAMCERAM®). The process pressure was 5×10^{-3} mbar, and the sputter power was 400 W. The deposition rate of the films was 100–150 nm/min sputtering.

After deposition, all coated specimens were subjected to an additional heat treatment for 2 h at 500°C. X-ray diffraction (XRD), Fourier Transform Infrared spectroscopy (FTIR) and Energy Dispersive Spectroscopical (EDS) analysis showed that this resulted in coatings having a crystalline apatite structure with a Ca/P ratio of 1.8–2.0.[25] Before use, the implants were sterilized by autoclaving for 15 min at 121°C. A total of 156 discs were prepared: 78 Ti and 78 Ti-CaP.

4.2.2 Cell culture technique

The rat bone marrow (RBM) cell culture technique was used as described by Maniatopoulos.[32] RBM-cells were obtained from femora of 16 six-week-old syngeneic Fisher 344 male rats (110–130 g). Epiphyses were cut off, and both diaphyses were flushed out using complete medium consisting of α-Minimal Essential Medium (α-MEM, Gibco BRL, Life Technologies B.V., Breda, the Netherlands) supplemented with 10 % fetal calf serum (FCS, heat induced at 56°C for 35 min., Gibco), 50 mg/ml freshly prepared ascorbic acid (Sigma, Chemical Co., St. Louis, Mo., USA), 10 mM Na-β-glycerophosphate (Sigma), 10^{-8} M dexamethasone (Sigma), and gentamycin. A 15-ml aliquot of this medium was used per two femurs. The cells were then suspended and cultured in complete medium in three 80-cm^2 tissue culture flasks (Nunc. Products, Gibco) in a humidified atmosphere of 95 % air, 5 % CO_2 at 37°C. After 8 days of primary culture, the cells were detached using trypsin/EDTA [0.25 % (w/v) trypsin/0.02 % ethylene diamine tetra-acetic acid].

4.2.3   Scaffold preparation

After detachment, the cells were concentrated by centrifugation at 1,500 rpm for 5 min, resuspended in a known amount of medium and counted using a Coulter® counter. The cell suspension was diluted to 5 x 10^6 cells/ml in complete medium. Thereafter, the cells were seeded onto the carrier materials.

Cells were seeded on top of the scaffold materials using either a droplet (D) or a suspension (S) loading method. For the droplet method, appropriate meshes were placed, top-side up, in a 24-well plate and loaded by placing 40-µl-aliquots of the cell suspension (200,000 cells/mesh) on top of the meshes. The meshes were exposed to a mild vacuum (5 x 10^4 N/m²) for 10 min and then placed in an incubator (95 % air, 5 % CO_2, at 37°C) for 2 h. With the suspension method, appropriate meshes were loaded by placing them in the cell suspension (5 x 10^6 cells/ml) in an Eppendorf® tube (6 meshes/0.8 ml cell suspension). After a brief exposure to a mild vacuum applied with a 50-ml syringe, the tubes with the cell suspension and meshes were placed in an incubator for 2 h (95 % air, 5 % CO_2 at 37°C). The tubes were shaken manually every 30 min. After 2 h the meshes were removed from the tubes with the suspension and also placed in 24-well plates.

Following the incubation period, all specimens were placed in 24-well plates and 1 ml of complete medium was added to each well. The medium was changed every 2–3 days. All constructs were cultured for 8 days in a humidified atmosphere of 95 % air, 5 % CO_2 at 37°C prior to implantation. After that, the medium was replaced by serum-free medium, and all of the scaffolds were transported to the animal facility.

4.2.4   Experimental design and surgical procedure

For implantation, thirty-nine 4-week-old syngeneic Fisher 344 male rats (50–60 g) were used. Surgery was performed under general inhalation anesthesia with a combination of halothane, nitrous oxide and oxygen. The RBM-loaded meshes were subcutaneously implanted into the back of the animals. To insert the implants, we immobilized the animals in a ventral position. The back of the animals was shaved, washed, and disinfected with povidone-iodine. To insert the subcutaneous implants, we made four small longitudinal incisions on both sides of the vertebral column. Lateral to the incisions, a subcutaneous pocket was created using blunt dissection. Implants were inserted with their top side towards the skin. After placement of the implants, the skin was closed using staples (Agraven®).

Each animal received one subcutaneous implant of each type. A statistical randomization scheme was used to localize the implants. A total of 156 implants were placed: (**1**) 39 droplet-loaded Ca-P-coated Ti implants, (Ti-CaP-RBM-D); (**2**) 39 suspension-loaded Ca-P-coated Ti implants (Ti-CaP-RBM-S); (**3**) 39 droplet-loaded non-coated Ti implants, (Ti-RBM-D); and (**4**) 39 suspension-loaded non-coated Ti implants, (Ti-RBM-S). Implantation periods were 2, 4, and 8 weeks. At the end of each implantation period, 13 rats were euthanized.

Four rats in the 8-week group received sequential triple fluorochrome labeling. The fluorochrome labels tetracycline (yellow), alizarin-complexone (red), and calceine (green) were administered at 2, 4, and 6 weeks post-operatively, respectively. These labels were

injected intramuscularly except for alizarin-complexone, which was given subcutaneously. The treatment dose was 25 mg/kg body weight for each label.

In this study, national guidelines for the care and use of laboratory animals were respected.

4.2.5　Implant retrieval and evaluation

At the end of the experiment, euthanasia was performed using carbon dioxide. Following euthanasia, the implants with their surrounding tissue were retrieved and prepared for histological ($n = 7$ for each material and time period) and calcium content analysis ($n = 6$ for each material and time period).

4.2.6　Histology

The histological samples were fixed in 4% phosphate-buffered formaldehyde solution (pH = 7.4), dehydrated in a graded series of ethanol and embedded in methylmethacrylate. Following polymerization 10-µm-thick sections were prepared per implant using a modified sawing microtome technique.[33] Before sections were made, the specimens were etched with hydrochloric ethanol for 15 s, stained with methylene blue for 1 min and stained with basic fuchsin for 30 s. The prepared sections were examined under a light microscope (Leica®).

In addition to the thin sections described above, two additional 30-µm-thick sections were prepared from the samples of the four animals that received fluorochromes. These sections were not stained but evaluated with a fluorescence microscope equipped with an excitation filter of 470–490 nm.

The light and fluorescent microscopical assessment consisted of a complete morphological description of the tissue response to the different implants. In addition, quantitative information was obtained on the amount of bone formation into the various mesh implants *i.e.*, the number of specimens which showed bone formation.

4.2.7　Calcium content measurement

The specimens for the calcium content analysis were lyophilized and kept at –80°C until the time of measurement. After thawing, 1 ml of acetic acid was added to each sample and stored overnight under constant shaking. The calcium content was determined using the orthocresolphthalein (OCPC) method[34] with an ELISA reader set at a wavelength of 575 nm.

4.2.8   Statistical evaluation

A Fisher's exact test was used to analyze the results of the histological analysis. A Kruskal-Wallis non-parametric test was applied to evaluate the results of the calcium content measurement. Differences between droplet-loaded and suspension-loaded specimens were tested within Ca-P-coated (Ti-CaP-RBM-D *vs.* Ti-CaP-RBM-S) and within non-coated (Ti-RBM-D *vs.* Ti-RBM-S) specimens at each time period. Differences between Ca-P-coated and non-coated specimens were tested within droplet-loaded (Ti-CaP-RBM-D *vs.* Ti-RBM-D) and suspension-loaded (Ti-CaP-RBM-S *vs.* Ti-RBM-S) specimens at each time period.

4.3   Results

During the experiment, all of the rats remained in good health and did not show any wound complications. At the end of the experiment, all of the implants could be retrieved. At retrieval, the implants were surrounded by a thin reaction-free fibrous capsule. No bone formation could be observed macroscopically.

4.3.1   Light microscopical evaluation

Evaluation of the prepared sections revealed no major differences in overall tissue response with respect to the various implantation periods and fiber mesh materials. All of the implants were surrounded by a thin fibrous tissue capsule. Hardly any inflammatory cells could be seen in Ca-P-coated specimens, while some multinucleated cells were present in the non-coated specimens.

Further analysis revealed that in five of the Ti-CaP-RBM-D implants bone-like tissue was present at 2 weeks; this number had increased to six implants at 4 weeks. By 8 weeks

---

Table 1.
The number of specimens which showing bone formation (*n*=7 for each implant and time period) and the results of the two-tailed Fisher's exact test.

Implant:	Implantation period:		
	2 weeks	4 weeks	8 weeks
Ti-CaP-RBM-D	5 (*n=7*) • °	6 (*n=7*) *	4 (*n=7*)
Ti-CaP-RBM-S	0 (*n=7*) •	2 (*n=7*)	2 (*n=7*)
Ti-RBM-D	0 (*n=7*) °	0 (*n=7*) *	0 (*n=7*)
Ti-RBM-S	0 (*n=7*)	0 (*n=7*)	0 (*n=7*)

Fisher's exact test (two-tailed)
(* = $P<0.005$, • = $P<0.05$, ° = $P<0.05$)

there were four implants showing bone-like tissue. In the Ti-CaP-RBM-S implants bone formation was absent in all of the implants at 2 weeks and was present in only two implants at 4 and 8 weeks (**Table 1**).

Bone formation in these Ca-P-coated implants was characterized by the presence of osteocyte-like cells embedded in a bone-like tissue matrix (**Figure 1E**). Bone was present inside the scaffold, although a preference for the upper mesh area was observed. The newly formed bone was always in close contact with the Ti-fibers without an intervening fibrous tissue layer. The suspension-loaded Ca-P-coated implants appeared to support less bone formation than the droplet-loaded Ca-P-coated implants. In none of the sections was cartilagenous tissue observed.

In droplet-loaded specimens the appearance of the bone-like tissue varied from single or multiple spheres (**Figure 1A, B**) to filling a significant part of the mesh porosity (**Figure 1C, D**). The latter was demonstrated by four of the five positive implants at 2 weeks, by two of the six at 4 weeks, and by two of the four at 8 weeks. When bone filled a significant part of the porosity bone marrow-like tissue was observed inside the newly formed bone. For droplet-loaded implants, the amount of bone per implant seemed to be highest at 2 weeks; it had decreased by 4 weeks and had remained at that level at 8 weeks.

In suspension-loaded specimens only single or multiple spheres were observed in the mesh material (**Figure 1A, B**), and in only half of the positive implants was bone present in all three prepared sections of each specimen. In suspension-loaded implants the amount of bone formation seemed to be the same at 4 and 8 weeks.

In none of the Ti-RBM-D and Ti-RBM-S implants was bone-like tissue observed. However, all of these non-coated implants showed irregular deposits of a basic fuchsin-stained layer in close association with the titanium fibers (**Figure 1F, G, H**). Again these deposits showed a preference for the upper mesh area. The deposited layer lacked a typical bone-like organization: no osteocyte-like cells embedded in a mineralized tissue matrix were seen (**Figure 1H**). On the other hand, multi-nucleated cells were observed in close association with the deposits at all evaluation periods.

Table 1 provides quantitative information on the number of specimens showing bone formation. The presence of bone formation was defined as a positive implant. Our statistical analysis, using the Fisher's exact test (two-tailed), revealed a significant difference between Ti-CaP-RBM and Ti-RBM implants for Ti-CaP-RBM-D versus Ti-RBM-D at 2 ($P < 0.05$) and 4 ($P < 0.005$) weeks. In addition, at 2 weeks a significant difference was present between Ti-CaP-RBM-D and Ti-CaP-RBM-S implants ($P < 0.05$) (**Table 1**).

4.3.2 Fluorescence microscopical evaluation

Fluorescence microscopical evaluation of labeled 8-week sections revealed that in only one of the evaluated Ti-CaP-RBM-D and in one of the Ti-CaP-RBM-S bone was present. The newly formed bone was deposited initially at the surface and then grew into the porosity (**Figure 2A, B**). In none of the Ti-RBM implants was organized bone formation with clear ossification fronts observed. In all of the specimens, diffusely stained deposits of tetracycline (and sometimes calcein) were mainly localized in contact with the Ti-fibers (**Figure 2C, D**).
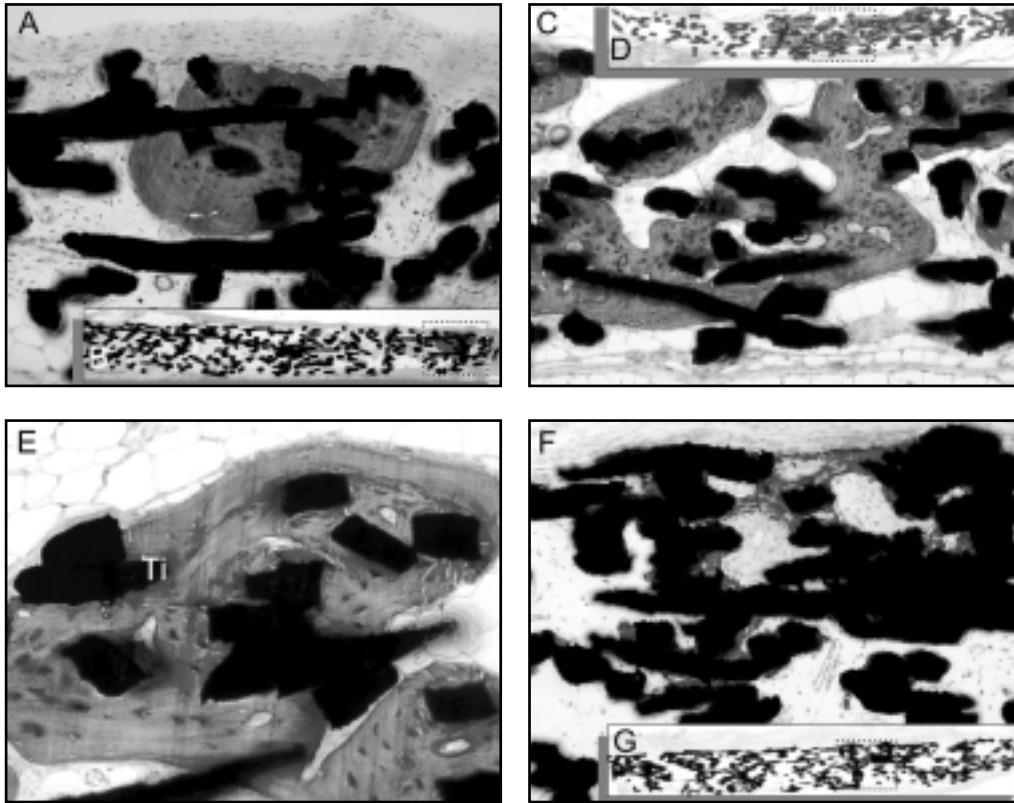
Figure 1.
Undecalcified sections of:

(A,B) A calcium phosphate-coated mesh loaded with RBM cells using a suspension method (Ti-CaP-RBM-S) 8 weeks after implantation. The appearance of spherical-shaped locations of newly formed bone in the porosity of the Ti-mesh was seen for both suspension- and droplet-loaded CaP-coated specimens. Bone was present inside the fiber mesh, althoug a preference for the upper mesh area was observed. Osteocyte-like cells are present, embedded in a mineralized matrix [(A) *orig. magn. 10x*, (B) *orig. magn. 1.6x*].

(C,D) A calcium phosphate-coated mesh loaded with RBM cells using a droplet method (Ti-CaP-RBM-D) 4 weeks after implantation. In some of the droplet-loaded CaP-coated specimens bone filled a significant part of the mesh porosity. In these specimens bone marrow-like tissue can be observed [(C) *orig. magn. 10x*, (D) *orig. magn. 1.4x*].

(E) A calcium phosphate-coated mesh loaded with RBM cells using a droplet method (Ti-CaP-RBM-D) 4 weeks after implantation. Bone formation is present in close contact with the titanium fibers (Ti). In both droplet-and suspension-loaded CaP-coated specimens the morphological appearance of the formed bone was characterized by the presence of osteocyte-like cells embedded in a mineralized matrix (*orig. magn. 20x*).

(F,G) A non-coated mesh loaded with RBM cells using a droplet method (Ti-RBM-D) 4 weeks after implantation. In all droplet-and suspension-loaded non-coated implants irregular deposits were seen throughout the mesh in close association with the titanium fibers. These deposits showed a preference for the upper mesh area [(F) *orig. magn. 10x*, (G) *orig. magn. 1.4x*].
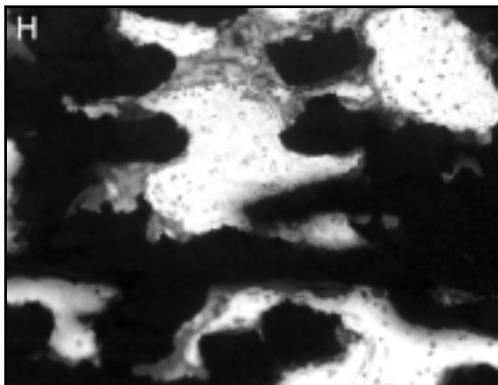
Figure 1. *continued*

Undecalcified section of:
(H) A non-coated mesh loaded with RBM cells using a droplet method (Ti-RBM-D) 4 weeks after implantation. In both droplet-and suspension-loaded non-coated specimens the morphological appearance is characterized by irregular basic fuchsin-stained deposits in close association with the titanium fibers. The deposited layer lacked a typical bone-like organization: No osteocyte-like cells embedded in a mineralized tissue matrix were seen (*orig. magn. 20x*).

4.3.3 Calcium content measurement

The box-whisker plot of **Figure 3** shows the results of the calcium content measurement. Calcification was present in all experimental groups as early as 2 weeks. Nevertheless, a wide variation in the total amount of calcium existed between the various specimens and implantation periods.

Statistical evaluation of the data using a Kruskal-Wallis non-parametric test revealed a significantly lower calcium content in the Ti-CaP-RBM specimens than in Ti-RBM specimens at 2 and 4 weeks for both Ti-CaP-RBM-D versus Ti-RBM-D (2 weeks: $P < 0.01$, 4 weeks: $P < 0.005$) and Ti-CaP-RBM-S versus Ti-RBM-S ($P < 0.005$) specimens, and at 8 weeks for Ti-CaP-RBM-D versus Ti-RBM-D only ($P < 0.01$) (**Figure 3**). In addition, at 2 weeks the Ti-CaP-RBM-D specimens showed a significantly higher calcium content than the Ti-CaP-RBM-S specimens ($P < 0.05$). For non-coated specimens no difference was found with respect to loading method.

4.4 Discussion and conclusion

In a previous rat ectopic assay[25] we evaluated the bone generating properties of Ca-P-coated and non-coated Ti-mesh implants loaded with RBM cells using a droplet-loading technique without prolonged culturing *in vitro*. Bone-like tissue formed in both the Ca-P-coated and non-coated specimens, but disappeared in the non-coated specimens by 8 weeks. In the present study we observed bone-like tissue formation only for Ca-P-coated specimens. No histomorphometrical analysis was performed, instead calcium content was quantified. For non-coated specimens we found only irregular calcified deposits that showed none of the morphological characteristics of bone. The mineralized nature of these deposits was confirmed by the calcium content measurements.

We hypothesize that the beneficial effect of a Ca-P coating is due to a positive effect on cell differentiation.[35-37] Consequently, marrow-derived MSCs are directed into the osteoblast lineage. This corroborates with previous *in vitro* studies of our group in which the
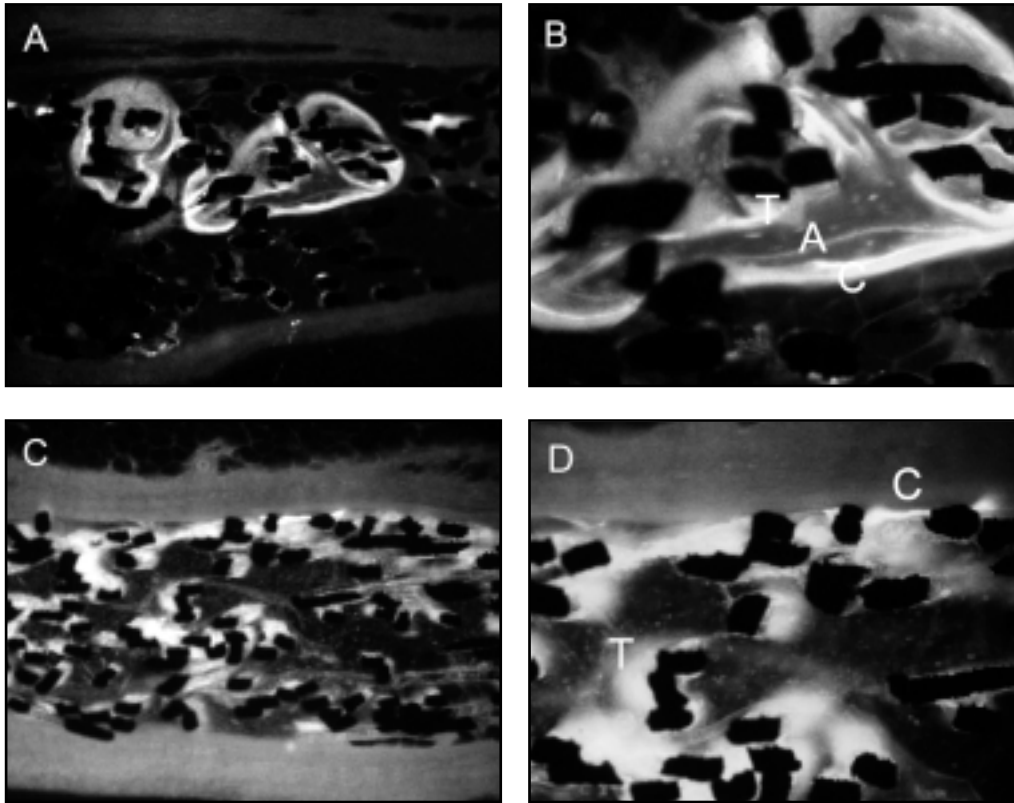
Figure 2.
Fluorescent light micrograph of:

(A) A calcium phosphate-coated mesh loaded with RBM cells using a droplet method (Ti-CaP-RBM-D) 8 weeks after implantation. Clear ossification fronts can be observed in the newly formed bone. The newly formed bone shows a preference for the upper mesh area (*orig. magn. 5x*).

(B) A calcium phosphate-coated mesh loaded with RBM cells using a droplet method (Ti-CaP-RBM-D) 8 weeks after implantation. In the center of the spherical-shaped bone, the tetracycline label (T) can be observed, followed more excentrically by the alizarin complexone label (A) and the calcein label (C). The accumulation sequence of the various labels demonstrates that the newly formed bone was deposited on the fibers proceeding away from the surface (*orig. magn. 20x*).

(C) A non-coated mesh loaded with RBM cells using a droplet method (Ti-RBM-D) 8 weeks after implantation. Fluorochrome stained deposits can be seen throughout the mesh. Suspension-and droplet-loaded implants showed the same image (*orig. magn. 5x*).

(D) A non-coated mesh loaded with RBM cells using a droplet method (Ti-RBM-D) 8 weeks after implantation. No organized bone formation with clear ossification fronts was observed. Diffusely stained deposits of tetracycline (T) [and sometimes calcein (C)] are mainly localized in close contact with the titanium fibers (*orig. magn. 10x*).
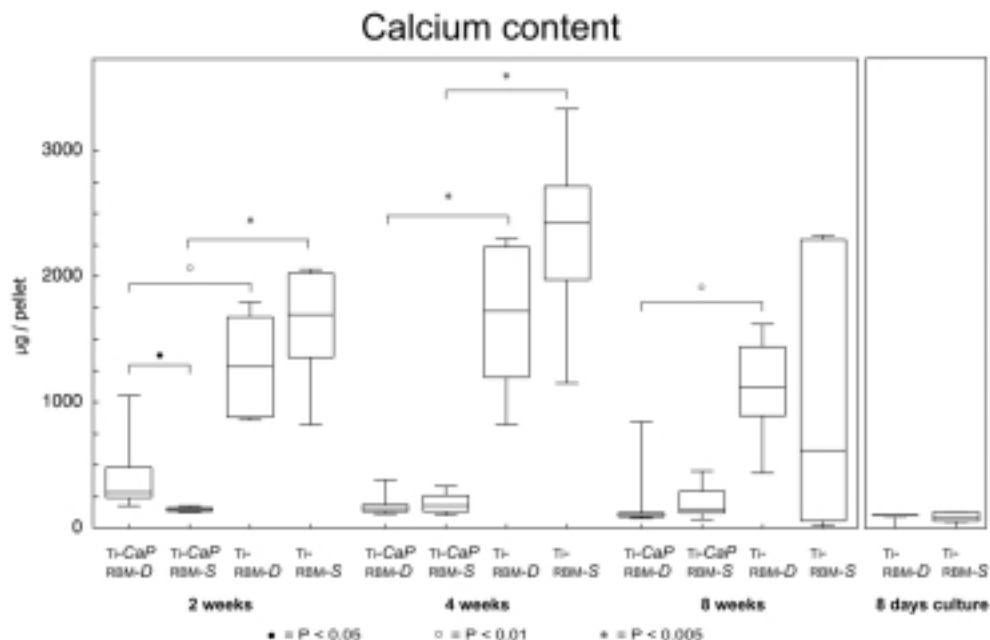
Calcium content

Figure 3.

Figure showing a Box-Whisker plot of the results of the calcium content measurements (n=6 for each implant and time period). The line within the boxes indicates the median. The boxes indicate the 25th to 75th percentile of the data. The error bars indicate the 5th and 95th percentile. Significant differences of the Kruskal-Wallis non-parametric test are also shown.

application of a Ca-P coating on solid titanium discs has been shown to delay the proliferation of rat bone marrow cells by 8 days, while differentiation was stimulated by 16 days.[36, 38] This positive effect of a calcium phosphate coating can be mediated by an increased level of Ca^{2+}-ions that results from the superficial dissolution of the coating. Osteoblast-like cells have been shown to possess calcium receptors on their surface.[39] It is also known that Ca^{2+}-ions can stimulate cells within the osteogenic lineage to express BMP-2 and BMP-4 mRNA, to produce collagen type I and to proliferate.[40,41] An additional effect of a calcium phosphate coating can be achieved due to the high affinity of calcium phosphate ceramics to bone-growth-stimulating proteins, such as BMPs.[42,43] This last suggestion has recently been confirmed for thin Ca-P coatings.[27]

We observed that for all of the implantation periods only a calcified deposit was present in the 8-day cultured non-coated meshes. Earlier scanning electron- and light-microscopical observations of non-coated 3D-Ti-scaffolds revealed that after 8 days of culturing a dense confluent layer of cells with some mineralized matrix is present in the upper part of the mesh.[20] In order to form bone upon implantation, an adequate cell-cell, cell-matrix, and cell-vascular relationship has to be present.[44,45] We suppose that this dense layer prevents the creation of an adequate cell-vascular relationship. Consequently, the cells might not be able to survive.

Nevertheless, calcium measurements revealed an increase in calcium content in these non-coated specimens after implantation (**Figure 3**). This calcification occurred without any morphological evidence of bone formation. This phenomenon has also been described for non-cell loaded solid titanium discs provided with an amorphous calcium-phosphate coating. In that study, a CO_3-AP precipitate was formed on the discs after implantation in rabbits.[46] The formation of such a biological apatite on implant surfaces is probably influenced by dissolution/precipitation-mediated events.[47,48] The partial dissolution of the calcium phosphate surface causes an increase in the levels of local calcium and phosphate ions, thereby increasing the degree of saturation in the micro-environment. This will facilitate the precipitation of a stable calcium phosphate phase which incorporates other ions (carbonate, magnesium etc.) and organic macromolecules from the biological fluids.[49,50] In a similar way, the dissolution of the initial *in vitro* calcification within our Ti-RBM specimens might have initiated a dissolution/precipitation process that resulted in increased mineral deposition. This was confirmed by the fluorescent labeling results. For the non-coated specimens no clear ossification fronts were observed.

The bone formation in our study showed a high inter-implant variability, as illustrated by both the histological and calcium content analyses. The histological analysis demonstrated that not all implants formed bone and that the amount of bone formed varied between implants. Calcium content in the Ti-CaP-RBM meshes was also variable. Some implants revealed high amounts of calcium (up to 1,000 µg per implant), while others showed values not higher than the measured calcium content for the Ca-P coating alone. In the Ca-P-coated meshes a small amount of calcium was present in the Ca-P coating [132 (+/- 11) µg, not shown in **Figure 1**]. We did not subtract the calcium content from the *in vivo* calcium content data since the coating might dissolve *in vivo*.

In light of the above, attention must be given to the fact that apparently optimal culture techniques are scaffold-dependent. Further, our findings emphasize that the use of single bone marker parameters, like calcium content, does not provide sufficient information on the amount and quality of tissue-engineered bone. This underscores the important role of morphological analysis and the assessment of *in vivo* osteogenic activity.

In the histological sections, cartilagenous tissue never was observed. Intramembranous bone formation, without the presence of cartilage, has also been reported for ceramic scaffolds loaded with fresh and cultured bone marrow stromal cells.[29,51,52] Still, in order to fully characterize the bone formation process, shorter implantation periods have to be investigated.

The biochemical and histological analysis of our specimens revealed that the use of two different cell-seeding methods did not affect the final amount of bone formation. Although histological and calcium content measurements showed that at 2 weeks a significant effect was seen with the droplet method, this effect had disappeared by 4 and 8 weeks. With the droplet method, scaffolds are incubated with a cell suspension droplet placed on their upper surface. With the suspension method, scaffolds are in contact with the cell suspension on all sides during incubation. Thereby increasing the potential surface area for attachment. Since our implants are very thin (only 800 µm), this possible advantage of the suspension method may disappear. The initial positive effect of the droplet method can be explained since in our experimental setup with the droplet method the number of loaded cells can be better standardized.

The findings of the fluorescent labeling study showed that in Ca-P-coated meshes bone had been deposited on the titanium fibers, growing away from the surface of the scaffold. This is in concordance with bioactive implant materials or implants provided with a bioactive surface coating, where bonding osteogenesis has been described.[29,51,53-56] In a previous study, we did not observe bonding osteogenesis, but bone formation started in the porosity of the mesh and proceeded towards the titanium surface.[25] We know that the deposited thin RF magnetron sputter coating is present on the outer titanium fibers but does not reach the surface of the inner titanium fibers, despite the fact that we coat the mesh on both sides. As a result, the inside of the mesh still consists of the original titanium surface. In the present study, we found that bone formation showed a preference for the upper mesh area, with the occurence of bonding osteogenesis. In the previous study, bone was present inside the mesh without a preference for the upper mesh area, which could explain the absence of bonding osteogenesis.

We conclude that the combination of Ti-mesh with RBM cells can indeed generate ectopic bone formation after prolonged *in situ* culturing. Prolonged culuring *in vitro* has different effects for Ti and Ti-CaP implants. In Ti-CaP implants bone-like tissue was present, while in Ti-implants only abundant mineralization was present without a bone-like tissue organization. No effect of the loading method, droplet versus suspension, was observed on the final amount of bone. Finally, our results confirm that a thin Ca-P coating can have an additional effect on the bone generating properties of a scaffold material.

References

1. **Haynesworth SE, Reuben D, Caplan AI.** Cell-based tissue engineering therapies: the influence of whole body physiology. Adv Drug Delivery Rev 1998; 33:3.
2. **Bergman RJ, Gazit D, Kahn AJ, Gruber H, McDougall S, Hahn TJ.** Age-related changes in osteogenic stem cells in mice. J Bone Miner Res 1996; 11:568.
3. **Egrise D, Martin D, Vienne A, Neve P, Schoutens A.** The number of fibroblastic colonies formed from bone marrow is decreased and the *in vitro* proliferation rate of trabecular bone cells increased in aged rats. Bone 1992; 13:355.
4. **Kahn A, Gibbons R, Perkins S, Gazit D.** Age-related bone loss. A hypothesis and initial assessment in mice. Clin Orthop 1995; 313:69.
5. **Liang CT, Barnes J, Seedor JG, Quartuccio HA, Bolander M, Jeffrey JJ, Rodan GA.** Impaired bone activity in aged rats: alterations at the cellular and molecular levels. Bone 1992; 13:435.
6. **Quarto R, Thomas D, Liang CT.** Bone progenitor cell deficits and the age-associated decline in bone repair capacity. Calcif Tissue Int 1995; 56:123.
7. **Kadiyala S, Neelam J, Bruder SP.** Culture-expanded, bone marrow-derived mesenchymal stem cells can regenerate a critical-sized segmental bone defect. Tissue Eng 1997; 3:173.
8. **Kadiyala S, Young RG, Thiede MA, Bruder SP.** Culture expanded canine mesenchymal stem cells possess osteochondrogenic potential *in vivo* and *in vitro*. Cell Transplant 1997; 6:125.
9. **Bruder SP, Kraus KH, Goldberg VM, Kadiyala S.** The effect of implants loaded with autologous mesenchymal stem cells on the healing of canine segmental bone defects. J Bone Joint Surg Am 1998; 80:985.
10. **Goshima J, Goldberg, VM, Caplan AI.** Osteogenic potential of culture-expanded rat marrow cells as assayed *in vivo* with porous calcium phosphate ceramic. Biomaterials 1991; 12:253.
11. **Gundle R, Joyner CJ, Triffitt JT.** Human bone tissue formation in diffusion chamber culture *in vivo* by bone-derived cells and marrow stromal fibroblastic cells. Bone 1995; 16:597.
12. **Krzymanski G, Wiktor-Jedrzejczak W.** Autologous bone marrow-derived stromal fibroblastoid cells grown *in vitro* for the treatment of defects of mandibular bones. Transplant Proc 1996; 28:3528.
13. **Leboy PS, Beresford JN, Devlin C, Owen ME.** Dexamethasone induction of osteoblast mRNAs in rat marrow stromal cell cultures. J Cell Physiol 1991; 146:370.
14. **Rickard DJ, Sullivan TA, Shenker BJ, Leboy PS, Kazhdan I.** Induction of rapid osteoblast differentiation in rat bone marrow stromal cell cultures by dexamethasone and BMP-2. Dev Biol 1994; 161:218.
15. **Katagiri T, Yamaguchi A, Ikeda T, Yoshiki S, Wozney JM, Rosen V, Wang EA, Tanaka H, Omura S, Suda T.** The non-osteogenic mouse pluripotent cell line, C3H10T1/2, is induced to differentiate into osteoblastic cells by recombinant human bone morphogenetic protein-2. Biochem Biophys Res Commun 1990; 172:295.
16. **Hanada K, Dennis JE, Caplan AI.** Stimulatory effects of basic fibroblast growth factor and bone morphogenetic protein-2 on osteogenic differentiation of rat bone marrow-derived mesenchymal stem cells. J Bone Miner Res 1997; 12:1606.
17. **Mendes SC, Van den Brink I, de Bruijn JD, van Blitterswijk CA.** *In vivo* bone formation by human bone marrow cells: Effect of osteogenic culture supplements and cell densities. J Mater Sci Mater in Med 1998; 9:855.
18. **Holy CE, Shoichet MS, Davies JE.** Engineering three-dimensional bone tissue *in vitro* using biodegradable scaffolds: investigating initial cell-seeding density and culture period. J Biomed Mater Res 2000; 51:376.
19. **Dennis JE, Caplan AI.** Porous ceramic vehicles for rat-marrow-derived (Rattus norvegicus) osteogenic cell delivery: effects of pre-treatment with fibronectin or laminin. J Oral Implantol. 1993; 19:106.
20. **Vehof JWM, de Ruijter JE, Spauwen PHM, Jansen JA.** Influence of rhBMP-2 on rat bone marrow stromal cells cultured on titanium fiber mesh. Tissue Eng 2001; 7:373.
21. **Baksh D, Davies, JE.** Three dimensional fluid flow enhances bone matrix elaboration *in vitro*. In: Transactions of the Sixth World Biomaterials Congress, Kamuela, Hawaii, USA, May 15-20, 2000, 438.
22. **Granet C, Laroche N, Vico L, Alexandre C, Lafage-Proust MH.** Rotating-wall vessels, promising bioreactors for osteoblastic cell culture: comparison with other 3D conditions. Med Biol Eng Comput 1998; 36:513.
23. **Botchwey, EA, Pollack, SR, Levine, EM, Laurentin, CT.** Bone tissue engineering in a rotating bioreactor using a microcarrier matrix system. J Biomed Mater Res 2001; 55:242.
24. **Zhang R, Ma PX.** Poly(α-hydroxyl acids)/hydroxyapatite porous composites for bone-tissue engineering. I. Preparation and morphology. J Biomed Mater Res 1999; 44:446.
25. **Vehof, JWM, Spauwen, PHM, Jansen, JA.** Bone formation in calcium-phosphate-coated titanium mesh. Biomaterials 2000; 21:2003.

26. **Jansen JA, von Recum AF, van der Waerden JP, de Groot K.** Soft tissue response to different types of sintered metal fibre-web materials. Biomaterials 1992; 13:959.

27. **Vehof JWM, Mahmood J, Takita H, van 't Hof MA, Kuboki Y, Spauwen PHM, Jansen JA.** Ectopic bone formation in titanium mesh loaded with Bone Morphogenetic Protein and coated with calcium phosphate.
Plast Reconstr Surg 2001; 108:434.

28. **Mizuno M, Shindo M, Kobayashi D, Tsuruga E, Amemiya A, Kuboki Y.** Osteogenesis by bone marrow stromal cells maintained on type I collagen matrix gels *in vivo*. Bone 1997; 20:101.

29. **Yoshikawa T, Ohgushi H., Tamai S.** Immediate bone forming capability of prefabricated osteogenic hydroxyapatite. J Biomed Mater Res 1996; 32:481.

30. **Yoshikawa T, Ohgushi H, Nakajima H, Yamada E, Ichijima K, Tamai S, and Ohta T.** *In vivo* osteogenic durability of cultured bone in porous ceramics: a novel method for autogenous bone graft substitution.
Transplantation 2000; 15:1284.

31. **Jansen JA, Wolke JG, Swann S, Van der Waerden JP, de Groot K.** Application of magnetron sputtering for producing ceramic coatings on implant materials. Clin Oral Implants Res 1993; 4:28.

32. **Maniatopoulos C, Sodek J, Melcher AH.** Bone formation *in vitro* by stromal cells obtained from bone marrow of young adult rats. Cell Tissue Res 1988; 254:317.

33. **van der Lubbe HB, Klein CP, de Groot K.** A simple method for preparing thin (10 microM) histological sections of undecalcified plastic embedded bone with implants. Stain Technol 1988; 63:171.

34. **Connerty HV, Briggs AR**. Determination of serum calcium by means of orthocresolphthalein complexone.
Am J Clin Pathol 1966; 45:290.

35. **Kim KJ, Itoh T, Kotake S.** Effects of recombinant human bone morphogenetic protein-2 on human bone marrow cells cultured with various biomaterials. J Biomed Mater Res 1997; 35:279.

36. **Hulshoff JE, van Dijk K, van der Waerden JP, Wolke JG, Kalk W, Jansen JA.** Evaluation of plasma-spray and magnetron-sputter Ca-P-coated implants: an *in vivo* experiment using rabbits. J Biomed Mater Res 1996; 31:329.

37. **Nishio K, Neo M, Akiyama H, Nishiguchi S, Kim HM, Kokubo T, Nakamura T.** The effect of alkali- and heat-treated titanium and apatite-formed titanium on osteoblastic differentiation of bone marrow cells.
J Biomed Mater Res 2000; 52:652.

38. **ter Brugge PJ, Wolke JGC, Jansen JA.** Effect of calcium phosphate coating crystallinity and implant surface roughness on differentiation of rat bone marrow cells. Submitted: J Biomed Mater Res.

39. **Leis H J, Zach D, Huber E, Ziermann L, Gleispach H, Windischhofer W.** Extracellular Ca2+ sensing by the osteoblast like cell line, MC3T3-E1. Cell Calcium 1994; 15:447.

40. **Ariji H, Nakade O, Koyama H, Takada J, Kaku T.** Effects of extacellular calcium on the proliferation and differentiation and gene expressions of Bone Morphogenetic Proteins -2 and -4 in human gingiva derived fibroblasts. Jpn J Oral Biol 2000; 42:49.

41. **Nakade O, Takahashi K, Takuma T, Aoki T, Kaku T.** Effect of extracellular calcium on the gene expression of bone morphogenetic protein-2 and -4 of normal human bone cells. J Bone Miner Metab 2001; 19:13.

42. **Uludag H, D'Augusta D, Palmer R, Timony G, Wozney J.** Characterization of rhBMP-2 pharmacokinetics implanted with biomaterial carriers in the rat ectopic model. J Biomed Mater Res 1999; 46:193.

43. **Uludag, H, D'Augusta D, Golden J, Li J, Timony G, Riedel R, Wozney JM.** Implantation of recombinant human Bone Morphogenetic Proteins with biomaterial carriers: A correlation between protein pharmacokinetics and osteoinduction in the rat ectopic model. J Biomed Mater Res 2000; 50:227.

44. **Caplan AI, Bruder SP.** Cell and molecular engineering of bone regeneration. In: Lanza LP, Langer R, Chick WL, Editors. Principles of Tissue Engineering, New York, Academic Press, 1997, 603.

45. **Lee YM, Seol YJ, Lim YT, Kim S, Han SB, Rhyu IC, Baek SH, Heo SJ, Choi JY, Klokkevold PR, and Chung C P.** Tissue-engineered growth of bone by marrow cell transplantation using porous calcium metaphosphate matrices.
J Biomed Mater Res 2001; 54:216.

46. **Wolke JG, de Groot K, Jansen JA.** *In vivo* dissolution behavior of various RF magnetron sputtered Ca-P coatings.
J Biomed Mater Res 1998; 39:524.

47. **Daculsi G, LeGeros RZ, Nery E, Lynch K, Kerebel B.** Transformation of biphasic calcium phosphate ceramics *in vivo*: ultrastructural and physicochemical characterization. J Biomed Mater Res 1989; 23:883.

48. **Ducheyne P, Cuckler JM.** Bioactive ceramic prosthetic coatings. Clin Orthop 1992; 276:102.

49. **Kokubo T, Ito S, Huang ZT, Hayashi T, Sakka S, Kitsugi T, Yamamuro T.** Ca,P-rich layer formed on high-strength bioactive glass-ceramic A-W. J Biomed Mater Res 1990; 24:331.

50. **LeGeros RZ, Orly I, Gregoire M, Daculsi G.** Substrate surface dissolution and interfacial biological mineralization.
In: Davies JE, editor. The Bone-Biomaterial Interface, Toronto, University of Toronto, 1991, 76.

51. **Ohgushi H, Goldberg VM, Caplan AI.** Heterotopic osteogenesis in porous ceramics induced by marrow cells.
J Orthop Res 1989; 7:568.

52. **Goshima J, Goldberg VM, Caplan AI.** Osteogenic potential of culture-expanded rat marrow cells as assayed *in vivo* with porous calcium phosphate ceramic. Biomaterials 1991; 12:253.

53. **Ohgushi H, Okumura M.** Osteogenic capacity of rat and human marrow cells in porous ceramics. Experiments in athymic (nude) mice. Acta Orthop Scand 1990; 61:431.
54. **Takaoka T, Okumura M, Ohgushi H, Inoue K, Takakura Y, Tamai S.** Histological and biochemical evaluation of osteogenic response in porous hydroxyapatite coated alumina ceramics. Biomaterials 1996; 17:1499.
55. **Okumura M, Ohgushi H, Tamai S.** Bonding osteogenesis in coralline hydroxyapatite combined with bone marrow cells. Biomaterials 1991; 12:411.
56. **Okumura M, Ohgushi H, Takakura Y, van Blitterswijk, CA, Koerten HK.** Analysis of primary bone formation in porous alumina: a fluorescence and scanning electron microscopic study of marrow cell induced osteogenesis. Biomed Mater Eng 1992; 2:191.

Chapter 5

Ectopic bone formation in titanium mesh loaded with Bone Morphogenetic Protein and coated with calcium phosphate

J.W.M. Vehof, J. Mahmood, H. Takita, M.A. van 't Hof, Y. Kuboki, P.H.M. Spauwen and J.A. Jansen.

5.1 Introduction

Bone defects are a significant clinical problem. These defects can be caused by trauma, oncological surgery, or congenital malformations. The clinical standard in the treatment of bone defects is still the use of autologous bone tissue. Unfortunately, in the case of large defects, the use of autografts is hampered by a lack of the availability of sufficient bone tissue. An alternative is the use of so-called bone graft substitutes (BGSs). These substitutes can be fabricated using a porous scaffold or carrier material together with osteogenic cells or osteoinductive factors like Bone Morphogenetic Proteins (BMPs). These BMPs can be isolated and purified from bone of humans or other species (native BMPs). They can also be produced by transfected cells using recombinant DNA techniques, [recombinant (human) BMPs].

Scaffold materials currently used in the creation of osteoinductive BGS are polymers or co-polymers [poly(α-hydroxyl) acids; for example, poly-lactic acid, poly-glycolic acid, and poly(lactic-co-glycolic acid)], calcium phosphate ceramics (*e.g.*, hydroxyapatite and tricalcium phosphate) and collagen. A disadvantage of these materials is that they are not very strong and can easily transform.[1,2] Another candidate carrier material for the creation of BGSs for use in load-bearing situations is sintered titanium (Ti) fiber mesh. Titanium is currently being applied in surgical practice because of its excellent mechanical characteristics in terms of stiffness and elasticity, bone compatibility and ease of use during surgery. On the other hand, it is not degradable. However, this latter property is no drawback for a significant number of reconstructive purposes. An additional advantage of a titanium scaffold material is that functional bone properties can further be enhanced by the deposition of a thin calcium phosphate (Ca-P) coating. In view of this, we know that calcium phosphates have a high affinity for BMPs.[3,4] which allows easier binding.

Recently, it has been demonstrated that BMP effects can be synergistically enhanced by other factors.[5-10] On the other hand, synergistic effects between recombinant BMPs and native BMPs have not yet been investigated.

Consequently, the objective of the study presented here was to investigate: (**1**) the influence of an additional thin Ca-P ceramic coating on the biological activity of a BMP-loaded Ti-mesh; (**2**) synergistic effects between native bovine and recombinant human BMPs.

5.2 Materials and methods

5.2.1 Implant preparation, carrier material

Sintered porous Ti-fiber mesh (Bekaert N.V., Zwevegem, Belgium) with a volumetric porosity of 86%, density of 600 g/m^2 and fiber diameter of 50 µm was used as scaffold material. The average pore size of the mesh was approximately 250 µm. The prepared implants were disc-shaped with a diameter of 6 mm, thickness of 0.8 mm, and weight of approximately 15 mg. All implants were ultrasonically cleaned with 70% ethanol for 15 min. The mesh was applied as-received (Ti) or provided with a thin (1 µm) Ca-P coating

(Ti-CaP) on both sides. The coating procedure was performed using a commercially available RF magnetron sputter unit (Edwards ESM 100).[11] Coating treatment and characteristics have been previously reported in detail.[12] Before use, implants were sterilized by autoclaving for 15 min at 121°C. A total of 224 discs were prepared: 112 Ti and 112 Ti-CaP.

5.2.2 Implant preparation, Bone Morphogenetic Proteins

The BMPs used in the present study were recombinant human BMP-2 (rhBMP-2) and the S-300 BMP cocktail. The rhBMP-2 (a generous gift from Yamanouchi Pharmaceutical co., Tokyo, Japan) was produced by Chinese hamster ovary (CHO) cells,[13] and the S-300 BMP cocktail was isolated from powdered bovine metatarsal bone. Preparation of this partially purified BMP was performed using an earlier described method.[14-17] The S-300 BMP cocktail contains all the fractions that possess bone inductive activity in ectopic implantation, but it does not contain a detectable amount of TGF-β_1 or TGF-β_2.

Before loading with BMPs, all materials were treated with RF glow-discharge (Harrick PDC-3XG, Argon, 0.15 Torr, for 5 min) to enhance wettability. Ca-P-coated and non-coated meshes were loaded with both rhBMP-2 and the S-300 BMP cocktail (BMP2/S300) or with rhBMP-2 (BMP2) alone. The dose of rhBMP-2 and S-300 BMP cocktail that was applied to the Ti-fiber mesh discs was 8.7 µg and 50 µg (as defined by Kuboki *et al*.[15]) in 0.1% TFA (trifluoroacetic acid), respectively. The BMP solutions were applied to the Ti-fiber mesh discs prior to implantation, subsequently lyophilized, and then kept at –80°C until implantation.

5.2.3 Experimental design and surgical procedure

Fifty-six 4-week-old Wistar King rats (80 g) were used for implantation. Surgery was performed following intra-peritoneal injection with 50 mg/ml Nembutal® (10 times diluted, 0.6 ml/100 g body weight). The BMP-loaded Ti-fiber mesh discs were subcutaneously implanted into the back of the animals.[12] Each animal received one subcutaneous implant of each type. The implants were localized using a Latin square design to assure complete statistical randomization.

A total of 224 implants were placed: 56 Ca-P-coated Ti implants loaded with both rhBMP-2 and S-300 (Ti-CaP-BMP2/S300); 56 Ca-P-coated Ti implants loaded with rhBMP-2 only (Ti-CaP-BMP2); 56 non-coated Ti implants loaded with both rhBMP-2 and S-300 (Ti-BMP2/S300); 56 non-coated Ti implants loaded with rhBMP-2 only (Ti-BMP2).

Implantation periods were 5, 10, 20, and 40 days. At the end of each implantation period 14 rats were euthanized ($n = 14$ for each material and time period). In addition, six rats out of the 20-day group received sequential double fluorochrome labeling. Fluorochrome labels, *i.e.* tetracycline (yellow) and calcein (green), were intramuscularly administered at 7 and 14 days post-operatively, respectively. The treatment dose was 25 mg/kg body weight for both labels. After euthanization, the implants with the surrounding tissues were retrieved and prepared for light-microscopical, biochemical, and genetical evaluation.

For each material and time period, 6 implants were used for light-microscopical, 6 for biochemical, and 2 for genetical evaluation.

5.2.4   Light microscopy, subjective and histomorphometry

Implants for histology were fixed in 4 % phosphate-buffered formaldehyde solution (pH = 7.4), dehydrated in a graded series of alcohol, and embedded in methylmethacrylate. After polymerization 10-µm sections were made using a modified microtome technique.[18] Light-microscopical sections were stained with basic fuchsin and methylene blue (3 sections per implant). These sections were evaluated with a light microscope (Leica®).

Slightly thicker sections (30 µm) were made for fluorochrome labeling analysis (2 sections per implant). These sections were left unstained and examined with a fluorescence micoscope (Leica®) equipped with an excitation filter of 470–490 nm.

Light- and fluorescence-microscopical analysis consisted of a full morphological description of the tissue response to the different implants. Further, a semi-quantitative histological grading scale was used to rate the tissue response (**Table 1**).

In addition, image analysis was performed on all sections of the 20-and 40-day samples to evaluate the location of newly formed bone. For this purpose a Leica® Qwin-image analysis system was used. Briefly, the circumferences of both the fiber mesh and bone were marked in an interactive manner. Then, the largest horizontal and vertical diameter of the fiber mesh and newly formed bone were calculated. The value of the difference between the largest vertical diameter of the mesh and the bone was used as a measure of bone outgrowth.

5.2.5   Calcium content and alkaline phosphatase activity

After retrieval, implants were lyophilized and kept at –80°C. Calcium content was assessed using the ortho-cresolphthalein (OCPC) method ($n = 6$ for each material and time period).[19] Alkaline phosphatase (AP) activity was measured using a commercially available alkaline phosphatase kit (Iatron Laboratories, Tokyo, Japan) based upon the Kind and King phenol-phosphate method ($n = 6$ for each material and time period).[20]

5.2.6   Osteocalcin expression

Osteocalcin expression was assessed using a reverse transcriptase polymerase chain reaction method (RT-PCR). Total RNA was isolated and extracted from the implant using Isogen®. A total cDNA library was formed using a commercially available reverse transcriptase (Takara®, Tokyo, Japan). The resulting reverse transcriptase product was then amplified by PCR with Takara Taq (Takara®, Tokyo, Japan) using primers specific for osteocalcin and GADPH, a housekeeping gene. The products were analyzed by electrophoresis on 2 % agarose containing ethidium bromide (50 µg/100 ml in TAE buffer) and then photographed under UV light excitation.

Table 1.
Table showing the semi-quantitative histological grading scale that was used to rate the tissue response.

Score	Response
0	Fibrous tissue
1	Undifferentiated mesenchymal cells
2	Cartilage formation
3	Cartilage maturation, hypertrophy
4	Cartilage maturation, mineralization
5	Mineralized cartilage, bone formation
6	Bone and fully developed bone marrow-like tissue

5.2.7   Statistical methods

A paired t-test was applied to evaluate the CaP-coating and S-300 effects. The CaP-coating effect may be calculated within each rat as the difference between the mean of both CaP-coated implants (Ti-CaP-BMP2/S300 and Ti-CaP-BMP) and non-coated implants (Ti-BMP2/S300 and Ti-BMP2). In the same manner the S-300 effect was calculated as the difference between the mean of both S-300-loaded implants (Ti-CaP-BMP2/S300 and Ti-BMP2/S300) and non-S-300-loaded implants (Ti-CaP-BMP2 and Ti-BMP2). P-values for the effects were calculated. In case of skew distributions, logtransformation to normality was used.

5.3   Results

During the experiment 2 rats died, probably due to the anesthesia. Hence, 8 implants were lost for genetical evaluation, and a total of 216 implants were retrieved. The other rats remained in good health and did not show any wound complications. At explantation, all implants were surrounded by a thin reaction-free fibrous capsule. From 10 days post-operative onwards, bone formation could be observed macroscopically.

5.3.1   Light microscopy, subjective

Light microscopical analysis of the sections revealed that all of the implants showed various stages of the bone formation process; no "negative" implants were observed. Hardly any inflammatory cells were observed in or around all specimens.

At 5 days, dense undifferentiated mesenchymal cells were observed inside the porosity of, and outside the implants. Foci of hypertrophic cartilage cells were present at the margin of, and outside the implant. Only in Ti-CaP-BMP2/S300 and Ti-BMP2/S300 implants the cartilage had started to mineralize (**Figure 1A**).
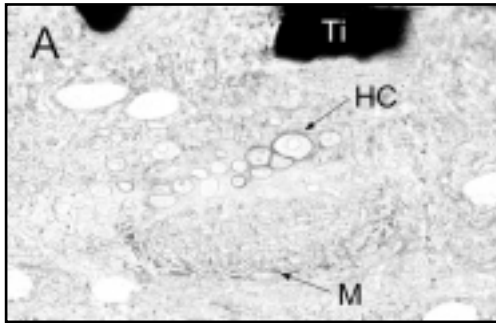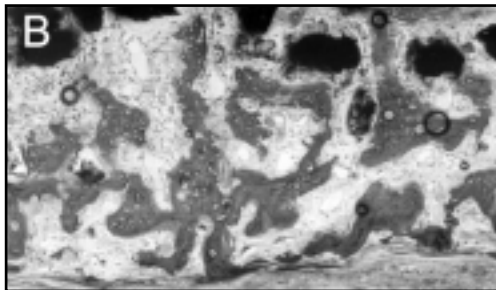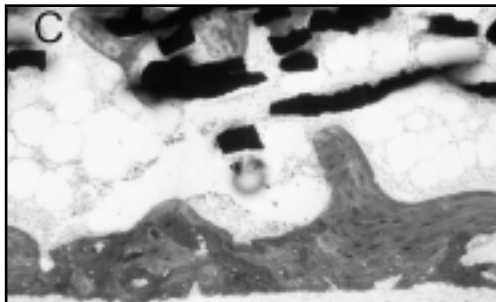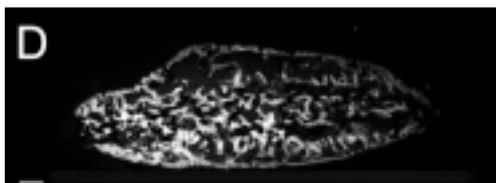
Figure 1.

(A) Undecalcified section of a Ca-P-coated titanum mesh loaded with rhBMP-2 and the S-300 BMP cocktail (Ti-CaP-BMP2/S300) 5 days after implantation. Dense undifferentiated mesenchymal cells are visible inside the porosity of, and outside the titanium (Ti) implant. Foci of hypertrophic cartilage cells (HC) are visible outside the implant. Also in these foci cartilage has started to mineralize (M) (*orig. magn. 40x*).
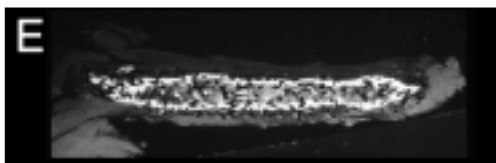
(B) Undecalcified section of a Ca-P-coated Ti-mesh loaded with rhBMP-2 and the S-300 BMP cocktail (Ti-CaP-BMP2/S300) 10 days after implantation. The implant is surrounded by a periosteum-like fibrous layer. Bone formation is seen inside and surrounding the Ti-mesh. Inside the implant cartilage with cartilagenous matrix are present. In the cartilage, areas with mineralization are seen. The bone formation process is more differentiated outside than inside the implant (*orig. magn. 20x*).

(C) Undecalcified section of a Ca-P-coated Ti-mesh loaded with rhBMP-2 and the S-300 BMP cocktail (Ti-CaP-BMP2/S300) 40 days after implantation. A periosteum-like layer with active bone formation surrounds the bone. Bone can be observed surrounding and inside the implant. The bone has a more dense lamellar structure. Some areas with bone remodeling can be observed. Inside the implant there is a large amount of hemopoietic bone marrow-like tissue (*orig. magn. 20x*).

(D) Non-stained undecalcified section of a Ca-P-coated Ti-mesh loaded with rhBMP-2 and the S-300 BMP cocktail (Ti-CaP-BMP2/S300) 20 days after implantation. This section is viewed with a fluorescence microscope. In Ti-CaP-BMP2/S300, Ti-CaP-BMP2 and Ti-BMP2/S300 implants the tetracylin (7 days) label is visible at the margin of and outside the fiber mesh, while the calcein (13 days) label is visible inside the fiber mesh (*orig. magn. 2.5x*).

(E) Non-stained undecalcified section of a non-coated Ti-mesh loaded with rhBMP-2 (Ti-BMP2) 20 days after implantation. This section is viewed with a fluorescence microscope. The tetracylin (7 days) label and the calcein (13 days) label are both visible inside the fiber mesh at some distance from the outer margin (*orig. magn. 2.5x*).

At 10 days, the implants were surrounded by a periosteum-like fibrous layer. Inside the fiber mesh material, cartilage formation with cartilagenous matrix was observed (**Figure 1B**). In these cartilagenous areas mineralization was present. In addition, bone and bone marrow formation were present. Bone was present in the outer layer. For all implant types, large multi-nucleated cells were observed in close contact with the calcified cartilage and bone.

At 20 days trabecular bone was seen throughout the implants in close contact with the titanium fibers. Inside the trabecular bone, in the porosity of the mesh, hemopoietic bone marrow-like tissue was seen. No cartilage was observed in any implant.

At 40 days, a periosteum-like layer with active bone formation was seen surrounding the bone (**Figure 1C**). The bone had a more dense lamellar structure. Some areas with bone remodeling could be observed. A large amount of hemopoietic bone marrow-like tissue was observed inside the implants. In Ti-CaP-BMP2 and Ti-BMP2 implants, there was less hemopoietic bone-marrow-like tissue.

In all S-300-loaded specimens, bone formation was more pronounced and located inside as well as surrounding the Ti-mesh (**Figure 2A,C**). In BMP2-only-loaded specimens bone was mainly localized inside the mesh material (**Figure 2B,D**). In addition, in CaP-coated specimens (**Figure 2A,B**) more bone could be observed in than in non-coated specimens (**Figure 2C,D**).

5.3.2 Fluorochrome labeling

In the 20-day specimens, fluorochrome labels were clearly visible. In the Ti-CaP-BMP2/S300, Ti-CaP-BMP2 and Ti-BMP2/S300 specimens the tetracycline label (*bone formation after 7 days*) was visible at the margin and outside the fiber mesh (**Figure 1D**). In the Ti-BMP2 implants the tetracyclin label was visible only inside the fiber mesh (**Figure 1E**). In the Ti-CaP-BMP2/S300, Ti-CaP-BMP2 and Ti-BMP2/S300 specimens, the calcein label (*bone formation after 14 days*) was seen inside and in a layer at the outer margin of the formed bone. In Ti-BMP2 implants the calcein label was located inside the fiber mesh at some distance form the outer border of the mesh. In all experimental groups bone was formed in a centrifugal manner starting in the porosity of the mesh.

5.3.3 Light microscopy, tissue rating

Although rating indicated that at 5 days the bone formation process had proceeded further in the S-300-loaded specimens (cartilage maturation) than in BMP2-only-loaded specimens (chondrogenesis) (**Figure 3**), statistical analysis using a paired *t*-test revealed that no S-300 effect existed (**Table 2**). In addition, no significant effect was found for the CaP coating (**Table 2**). From 10 days onwards, no differences in stage of bone formation were observed between the different implantation materials. Because all scores were the same at these time periods, no statistical analysis was necessary. At 10 days, bone and cartilage were seen together in all sections. At 20 days and 40 days, bone was observed in all implants without the presence of cartilage.
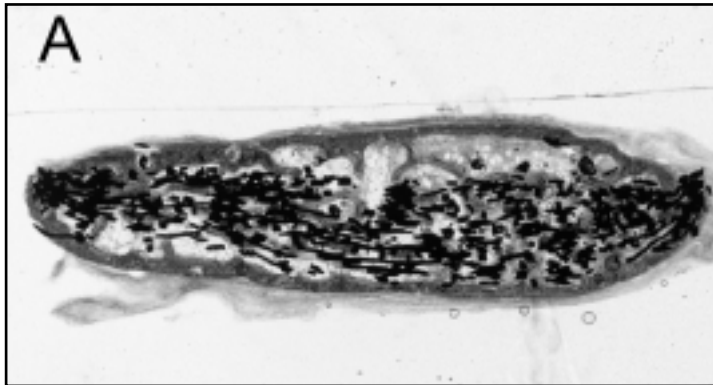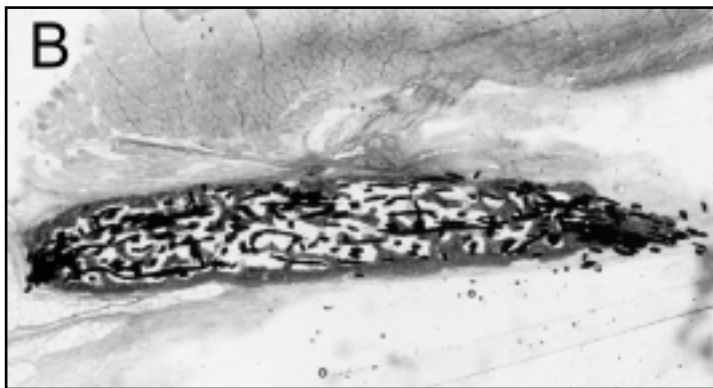
Figure 2.

(A) Undecalcified section of a Ca-P- coated Ti-mesh loaded with rhBMP-2 and the S-300 BMP cocktail (Ti-CaP-BMP2/S300) 40 days after implantation. Bone grows inside and outside the fiber mesh (*orig. magn. 2.5x*).

(B) Undecalcified section of a Ca-P-coated Ti-mesh loaded with rhBMP-2 (Ti-CaP-BMP2) 40 days after implantation. Bone grows just up to the margin of the titanium fiber mesh (*orig. magn. 2.5x*).

5.3.4　Light microscopy, bone location

The results of the histomorphometrical measurements for bone location are depicted in **Figure 4**. In S-300-treated specimens (**Figures 4** and **2A,C**) the bone grew outside the fiber mesh, whereas in BMP2 -only specimens bone grew inside the mesh (**Figures 4** and **2B,D**). In the Ca-P-coated BMP2-only specimens (**Figures 4** and **2B**) bone grew just up to the margin of the mesh and in non-coated BMP2-only specimens bone grew inside the porosity and did not reach the outer margin (**Figures 4** and **2D**).

Statistical evaluation using a paired *t*-test revealed a significant effect of the S-300 BMP cocktail at 20 days ($P < 0.005$) and 40 days ($P < 0.01$) and of the Ca-P coating at 40 days ($P < 0.05$). Both the S-300 and the Ca-P coating showed a positive effect on the difference in bone-titanium diameter (**Table 2**). The S-300 effect was larger than the Ca-P coating effect.
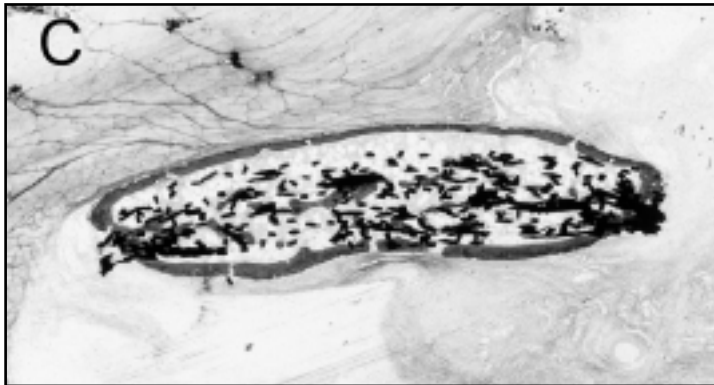
Figure 2.

(C) Undecalcified section of a non-coated Ti-mesh loaded with rhBMP-2 and the S-300 BMP cocktail (Ti-BMP2/S300) 40 days after implantation. Bone grows inside and outside the fiber mesh (*orig. magn. 2.5x*).

(D) Undecalcified section of a non-coated Ti-mesh loaded with rhBMP-2 (Ti-BMP2) 40 days after implantation. Bone grows inside the porosity of the titanium fiber mesh and does not reach the outer margin (*orig. magn. 2.5x*).

5.3.5 Calcium content

The results of the calcium content measurements are depicted in **Figure 5**. No statistical evaluation was performed on the 5-day data because the values approached zero. A paired *t*-test was performed to examine the effects of the Ca-P coating and S-300 factor at each separate time period. At 20 days ($P < 0.0005$) and 40 days ($P < 0.0005$), a positive effect was found with respect to the Ca-P coating (**Table 2**). This test also showed that the S-300 fraction had a significant positive effect ($P < 0.0005$) at 20 days (**Table 2**).

5.3.6 Alkaline phosphatase activity

The results of the alkaline phosphatase activity measurements are depicted in **Figure 6**. Alkaline phosphatase data showed a lognormal distribution; therefore logtransformation was performed. A paired *t*-test was performed to determine the effects of the Ca-P coating and the S-300 BMP cocktail at each separate time period. At 5 days ($P < 0.005$), 20 days ($P < 0.005$) and 40 days ($P < 0.05$) a positive S-300 effect was found (**Table 2**). In addition, at 40 days ($P < 0.05$) a positive Ca-P effect was found. The highest S-300 effect was found at 5 days (**Table 2**).

Table 2.

A paired *t*-test was used to evaluate the CaP-coating effect and the S-300 effect on the tissue rating, bone location, calcium content and alkaline phosphatase data, (*n*=sample size, NS=non-significant P>0.05).

|	Time (days)		Coating versus No Coating				S-300 versus No S-300		
		n	Mean Coating	Mean No Coating	*p*	*n*	Mean S-300	Mean N0 S-300	*p*
Tissue rating	5	6	2.69	2.61	NS	6	3.17	2.14	NS
Bone location (µm)	20	5	197	−57	NS	6	356	−237	<0.005
	40	6	245	−242	<0.05	6	383	−191	<0.01
Calcium content	10	6	2.06	2.13	NS	6	2.84	1.35	NS
(mg/pellet)	20	6	3.6	1.58	<0.0005	6	3.28	1.9	<0.0005
	40	6	3.83	2.11	<0.0005	6	3.31	2.63	NS
Alkaline phosphatase	5	6	486	477	NS	6	561	401	<0.005
(mIU/pellet)	10	6	508	448	NS	6	500	456	NS
	20	6	512	489	NS	6	520	481	<0.005
	40	6	518	462	<0.005	6	515	465	<0.05
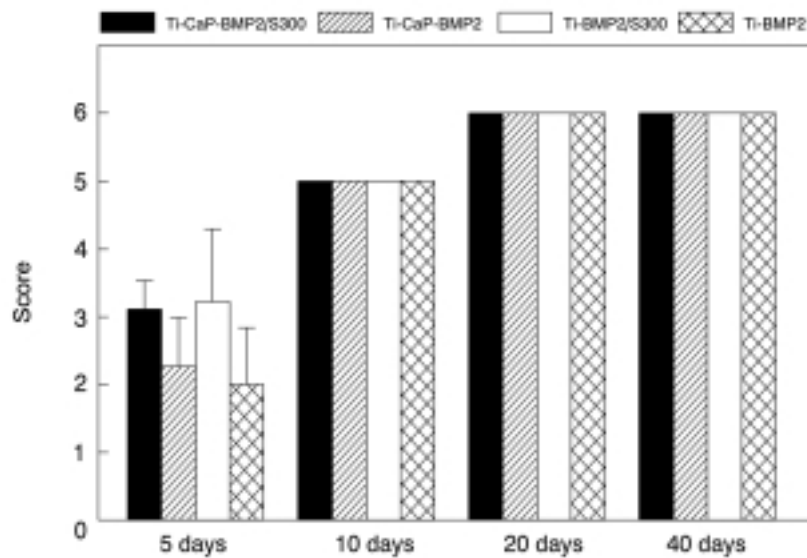
Figure 3.
Results of the semi-quantitative histomorphometrical analysis for tissue rating showing mean and standard deviation (SD) for the different implants.
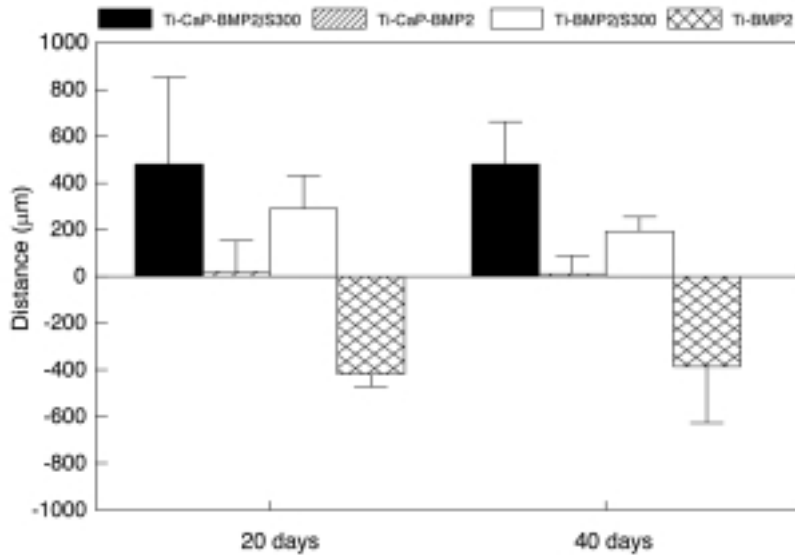
Figure 4.
Figure showing the results of the histomorphometrical analysis for bone location at 20 and 40 days post-implantation (mean and SD). The largest horizontal and vertical diameter of the bone and Ti-mesh were calculated. The difference between the largest vertical diameter of the bone and the Ti-mesh was used as a measure of bone outgrowth.
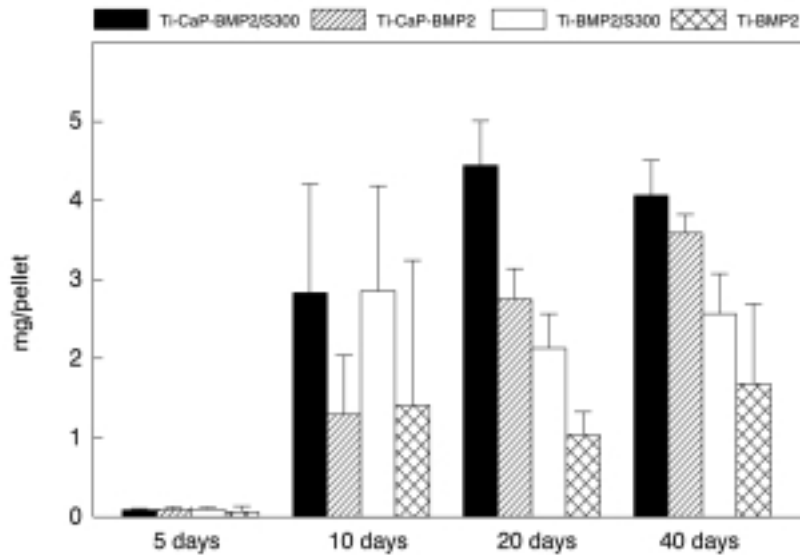

Figure 5.
Figure showing the results of the calcium content measurement at 5, 10, 20, and 40 days post-implantation (mean and SD).
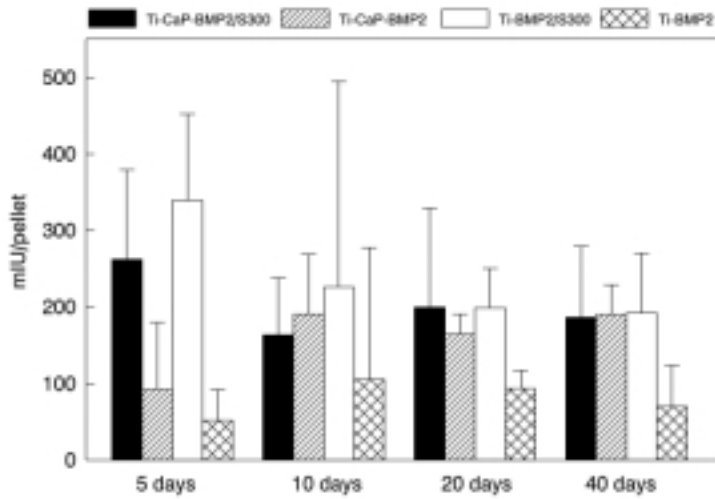
Figure 6.

Figure showing the results of the alkaline phosphatase activity measurement at 5, 10, 20, and 40 days post-implantation (mean and SD).
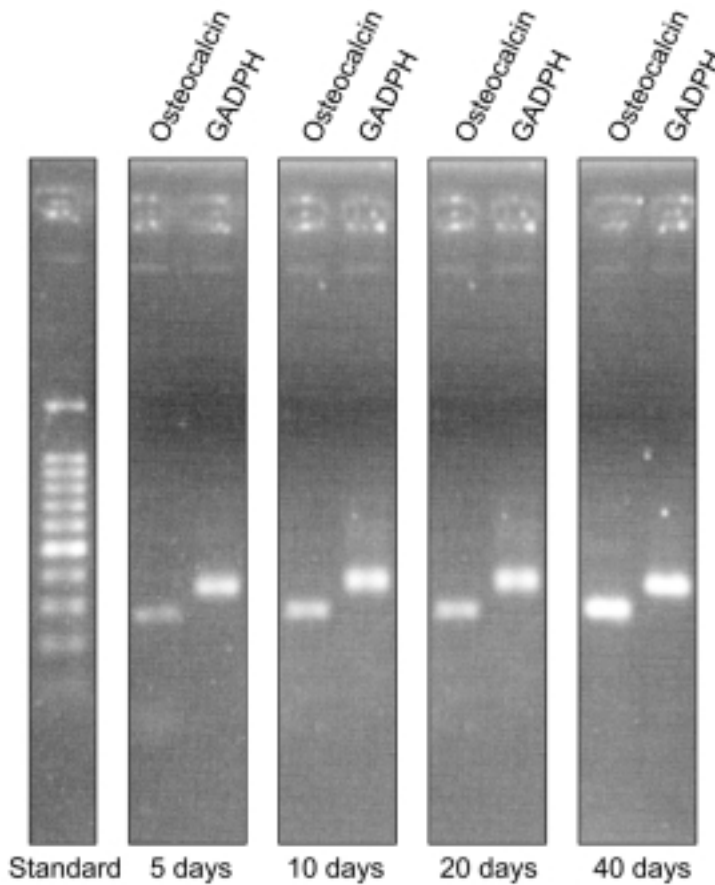

Figure 7.

Figure showing a gel-electrophoresis picture taken under UV light excitation, showing time-dependent osteocalcin expression in (Ti-CaP-BMP2/S300) implants. Electrophoresis pictures were the same for all implantation groups.

5.3.7   RT-PCR for osteocalcin

With RT-PCR osteocalcin expression was detectable as early as 5 days for all specimens (**Figure 7**). Ten days after implantation osteocalcin expression had increased, as demonstrated by the much clearer osteocalcin bands. Thereafter, osteocalcin expression remained at about the same level for all specimens.

5.4   Discussion and conclusion

Our histological findings confirm that Ti-fiber mesh is highly biocompatible as demonstrated by the absence of inflammatory cells in all BMP-loaded implants.[21,22] Further, as indicated by the various evaluations, Ti-mesh loaded with BMP can indeed adequately induce ectopic bone formation.

Although a comparison with other carriers is hard to make, the onset of osteocalcin expression at 5 days seems relatively early, since osteocalcin is a late marker for bone formation. We assume that the early expression of osteocalcin in our study is due to the high compatibility of the Ti-mesh and the Ca-P-coating. The process of bone formation in all our BMP-loaded samples occurred with a cartilagenous phase present. Thus, the bone formation process seems to be similar to "endochondral ossification". Direct ossification without pre-existing cartilage has been reported in implanted BMP carriers: it was first reported for fibrous collagen membrane (FCM) and later for hydroxyapatite.[14,15,23,24] On the other hand, fibrous glass membrane (FGM) and insoluble bone matrix (IBM) have been shown to induce endochondral ossification.[14,25]

Vascularization is considered a crucial step in ectopic bone formation. We also know that the geometry of the carrier influences vascularization and thereby oxygen supply. Various studies have already shown that a low oxygen concentration favors chondrogenesis, while a higher oxygen concentration supports bone formation.[26-28] Carriers that induce bone formation without cartilage have been hypothesized to provide a higher oxygen supply due to geometry.[23]

A precise explanation for the differences in the nature of the bone formation process between various carrier materials is difficult to provide because a clear comparison between the materials is difficult to make due to the variation in material properties. Besides physicochemical properties, materials differ in surface structure, mechanical characteristics, pore size, pore geometry, and pore density.

The fluorescent labeling study revealed that the newly formed bone was deposited in a centrifugal manner, starting in the porosity and growing towards the surface of the carrier. In a previous study,[15] bonding osteogenesis, in which bone formation starts at the surface area and proceeds away from the surface area, was observed for bioactive materials like hydroxyapatite. We know that the thin RF magnetron sputter coating did not completely penetrate throughout the mesh, despite the fact that we coated the mesh on both sides. As a result, the inside of the mesh always consists of the original titanium surface. This probably explains the absence of bonding osteogenesis.

In our current study, we also showed that the additional deposition of a thin calcium phosphate coating on the Ti-mesh had a stimulatory effect on bone formation. We know that Ca-P ceramics combined with BMPs enhance the bone formation process.[14,15,29] This effect is supposed to be due to the high affinity of BMP to Ca-Ps.[3] In a former chromatographic study, we demonstrated that the affinity of BMP for hydroxyapatite is higher than for titanium.[4] Apparently, a similar phenomenon is involved in our Ca-P-coated Ti-mesh. Nevertheless, we were the first to report that a thin Ca-P coating has a stimulatory effect on ectopic bone formation by rhBMP-2.[30,31] This paper confirms these earlier findings using larger experimental numbers, earlier time periods and a combination of all possible factors.

Finally, we observed a synergistic effect between rhBMP-2 and the S-300 BMP cocktail. It has been reported that highly purified native bovine and human BMPs are about 10 times more potent in ectopic osteoinduction than recombinant human BMP-2.[32,33] However, the osteoinductive capacity of the S-300 BMP cocktail, which is a partially purified BMP fraction, is about 50 times less than the osteoinductive capacity of rhBMP-2. An earlier preliminary experiment with Ti-fiber mesh as a carrier reinforces this difference in osteoinductive activity. In that experiment BMP2/S300-loaded as well as BMP2-and S300-only-loaded specimens were included. At 4 weeks the S300-only-implants showed hardly any bone formation, whereas BMP2/S300- and BMP2-only-loaded specimens revealed a level of osteogenesis comparable to that of the current study. Therefore, in the present study, the potentiating effect of the S-300 BMP cocktail is not simply an additive effect but a true synergistic effect. Although potentiating effects *in vivo* between BMP and other factors like TGF-β_1,[5,6] TGF-β_2,[7] Prostaglandin E$_1$ (PGE$_1$)[8,9] and basic Fibroblast Growth Factor (bFGF)[10] have been described, such an effect has never been reported for various types of BMPs.

In summary, we conclude that Ti-mesh loaded with BMPs can indeed induce ectopic bone formation in a rat model during a long time span from 10 to 40 days. Our results confirm our preliminary observations that an additional Ca-P coating can further improve the osteoinductive properties of a BMP-loaded Ti mesh. The bone formation process in Ca-P-coated and non-coated Ti-fiber mesh seems to be similar to "endochondral ossification". Evidently, rhBMP-2 and the S-300 BMP cocktail act synergistically in ectopic bone induction in Ti mesh-based BGSs.

References

1. **Zhang R, Ma PX.** Poly(α-hydroxyl acids)/hydroxyapatite porous composites for bone-tissue engineering. I. Preparation and morphology. J Biomed Mater Res 1999; 44:446.
2. **Girton TS, Oegema TR, TRT.** Exploiting glycation to stiffen and strenghten tissue equivalents for tissue engineering. J Biomed Mater Res 1999; 46:87.
3. **Uludag H, d'Augusta D, Palmer R, Timony G, Wozney J.** Characterization of rhBMP-2 pharmacokinetics implanted with biomaterial carriers in the rat ectopic model. J Biomed Mater Res 1999; 46:193.
4. **Kuboki Y.** Unpublished data, 1999.
5. **Ripamonti U, Duneas N, Van Den Heever B, Bosch C, Crooks J.** Recombinant Transforming Growth Factor beta-1 induces endochondral bone in the baboon and synergizes with recombinant osteogenic protein-1 (bone morphogenetic protein-7) to initiate rapid bone formation. J Bone Miner Res 1997; 12:1584.
6. **Si X, Jin Y, Yang L.** Induction of new bone by ceramic bovine bone with recombinant human bone morphogenetic protein 2 and Transforming Growth Factor beta. Int J Oral Maxillofac Surg 1998; 27:310.
7. **Bentz H, Thompson AY, Armstrong R, Chang RJ, Piez KA, Rosen DM.** Transforming Growth Factor beta 2 enhances the osteoinductive activity of a bovine bone-derived fraction containing bone morphogenetic protein-2 and 3. Matrix 1991; 11:269.
8. **Ono I, Inoue M, Kuboki Y.** Promotion of the osteogenetic activity of recombinant human bone morphogenetic protein by prostaglandin E1. Bone 1996; 19:581.
9. **Ono I, Tateshita T, Kuboki Y.** Prostaglandin E1 and recombinant bone morphogenetic protein effect on strength of hydroxyapatite implants. J Biomed Mater Res 1999; 45:337.
10. **Takita H, Tsuruga E, Ono I, Kuboki Y.** Enhancement by bFGF of osteogenesis induced by rhBMP-2 in rats. Eur J Oral Sci 1997; 105:588.
11. **Jansen JA, Wolke JG, Swann S, Van der Waerden JP, de Groot K.** Application of magnetron sputtering for producing ceramic coatings on implant materials. Clin Oral Implants Res 1993; 4:28.
12. **Vehof JWM, Spauwen PHM, Jansen JA.** Bone formation in calcium-phosphate-coated titanium mesh. Biomaterials 2000; 21:2003.
13. **Israel DI, Nove J, Kerns KM, Moutsatsos IK, Kaufman RJ.** Expression and characterization of bone morphogenetic protein-2 in Chinese hamster ovary cells. Growth Factors 1992; 7:139.
14. **Kuboki Y, Saito T, Murata M et al.** Two distinctive BMP-carriers induce zonal chondrogenesis and membranous ossification, respectively; geometrical factors of matrices for cell-differentiation. Connect Tissue Res 1995; 32:219.
15. **Kuboki Y, Takita H, Kobayashi D et al.** BMP-induced osteogenesis on the surface of hydroxyapatite with geometrically feasible and nonfeasible structures: topology of osteogenesis. J Biomed Mater Res 1998; 39:190.
16. **Iida S, Kawasaki T, Kuboki Y.** Bone formation in osteoporotic rats, reduced effect of bone morphogenetic protein (BMP), ascribed to the suppressed osteoblast differentiation. Jpn J Oral Biol 1994; 36:249.
17. **Kobayashi D, Takita H, Mizuno M, Totsuka Y, Kuboki Y.** Time-dependent expression of bone sialoprotein fragments in osteogenesis induced by bone morphogenetic protein. J Biochem Tokyo 1996; 119:475.
18. **Lubbe, van der HB, Klein CP, de Groot K.** A simple method for preparing thin (10 microM) histological sections of undecalcified plastic embedded bone with implants. Stain Technol 1988; 63:171.
19. **Connerty HV, Briggs AR.** Determination of serum calcium by means of orthocresolphthalein complexone. Am J Clin Pathol 1966; 45:290.
20. **Kind PRN, King EJ.** Estimation of plasma phosphatase by determination of hydrolyzed phenol with amino-antipyrine. J Clin Pathol 1954; 7:322.
21. **Paquay YC, de Ruijter JE, van der Waerden JP, Jansen JA.** Wound healing phenomena in titanium fibre mesh: the influence of the length of implantation. Biomaterials 1997; 18:161.
22. **Jansen JA, Paquay YG, van der Waerden JP.** Tissue reaction to soft-tissue anchored percutaneous implants in rabbits. J Biomed Mater Res 1994; 28:1047.
23. **Sasano Y, Ohtani E, Narita K et al.** BMPs induce direct bone formation in ectopic sites independent of the endochondral ossification in vivo. Anat Rec 1993; 236:373.
24. **Sasano Y, Mizoguchi I, Takahashi I, Kagayama M, Saito T, Kuboki Y.** BMPs induce enchondral ossification in rats when implanted ectopically within a carrier made of fibrous glass membrane. The Anatomical Record 1997; 247:472.
25. **Murata M, Inoue M, Arisue M, Kuboki Y, Nagai N.** Carrier-dependency of cellular differentiation induced by bone morphogenetic protein in ectopic sites. Int J Oral Maxillofac Surg 1998; 27:391.
26. **Basset CAL, Herrmann I.** Influence of oxygen concentration and mechanical factors on differentiation of connective tissues in vitro. Nature 1962; 190:460.

27. **Hall BK.** Hypoxia and differentiation of cartilage and bone from common germ cells *in vitro*. Life Sci 1969; 8:553.
28. **Caplan AI, Pechak DG.** The cellular and molecular embryology of bone formation. Bone Miner Res 1987; 5:117.
29. **Ono I, Ohura T, Murata M, Yamaguchi H, Ohnuma Y, Kuboki Y.** A study on bone induction in hydroxyapatite combined with bone morphogenetic protein. Plast Reconstr Surg 1992; 90:870.
30. **Jansen JA, Takita H, Tsuruga E, Mizuno M, Kuboki Y.** Tissue engineered bone grafts. In proceedings of the 1st Smith & Nephew International Symposium, York, UK, July, 1997, abstract no. S20.
31. **Kuboki Y, Takita H, Tsuruga E, Ono M, Jansen JA**. Rationale for hydroxyapatite-coated titanium mesh as an effective carrier for BMP. J Dent Res 1998; 77:263 (abstract # 1262).
32. **Bessho K.** Ectopic Osteoinductive difference between purified bovine and recombinant human bone morphogenetic protein. In T. S. Lindholm (Ed.), Bone Morphogenetic Proteins: Biology, Biochemistry and Reconstructive Surgery, 1st Ed. Georgetown, Texas, USA, RG Landes Co, 1996.
33. **Bessho K, Kusumoto K, Fujimura K *et al*.** Comparison of recombinant and purified human bone morphogenetic protein. Br J Oral Maxillofac Surg 1999; 37:2.

Chapter 6

Histological characterization of the early stages of Bone Morphogenetic Protein-induced osteogenesis

J.W.M. Vehof, H. Takita, Y. Kuboki, P.H.M. Spauwen and J.A. Jansen.

6.1   Introduction

Bone defects form a significant clinical problem. These defects can be caused by trauma, oncological surgery, or congenital malformations. The golden clinical standard in the treatment of bone defects is still the use of autologous bone tissue, but the clinical use of autografts is hampered by donor-site and availability problems. An alternative is the use of so-called bone graft substitutes (BGSs). These bone graft substitutes can be divided in three classes: (**1**) *osteoconductive*, (**2**) *directly osteogenic*, and (**3**) *osteoinductive*.[1] The main disadvantage of osteoconductive BGS, like allograft bone and ceramic materials (*e.g.*, hydroxyapatite or tricalcium phosphate), is that they do not actively stimulate the bone-forming process. Directly osteogenic and osteoinductive BGS can be fabricated using a porous scaffold (or carrier) material together with osteogenic cells or osteoinductive factors [for example Bone Morphogenetic Proteins (BMPs)], respectively.

Carrier materials currently used in the creation of osteoinductive BGS include polymers, [mainly poly(α-hydroxyl acids)], calcium phosphate ceramics (*e.g.*, hydroxyapatite and tricalcium phosphate), collagen and others. To date our group has tested more than ten different carrier materials. A large number of prerequisites have been postulated for the ideal carrier material,[2] but it must be emphasized that none of the materials used meet all of these demands. For example, a disadvantage of some of these materials is that they are not very strong and can easily transform.[3,4] In view of this, we have suggested the use of titanium fiber mesh as the carrier material.[5,6] An additional advantage of a titanium scaffold material is that bone formation can be significantly enhanced by the deposition of a thin calcium phosphate (Ca-P) coating.[6]

For the final safe and reliable clinical application of BMP-induced BGSs, both a significant amount of and high-quality bone must be formed (in the carrier material) within a reasonable time frame. Consequently, further knowledge about the bone formation process as induced by BMPs has to be obtained. For example, in early studies, BMP-induced bone formation was believed to follow the sequence of endochondral ossification.[7] More recently, however, direct ossification without pre-existing cartilage has been reported on implanted BMP carriers: first for fibrous collagen membrane (FCM) and later for hydroxyapatite.[8,9] On the other hand, fibrous glass membrane (FGM) and insoluble bone matrix (IBM) have been shown to induce endochondral ossification.[9,10] Also, for BMP-loaded titanium (Ti) the process of bone formation seems to occur with a cartilagenous phase present.[6] Nevertheless, a definitive conclusion about the bone formation process, in different scaffold materials, is difficult to draw since bone and cartilage can be independently induced.[8] For the proper characterization of the bone formation process and the elimination of possible observational errors, BMP-loaded scaffolds have to be evaluated at short implantation periods.

Consequently, the objective of the study presented here was to analyze and compare the early stages of the bone formation process in various BMP-loaded "*bone directing*" and "*cartilage directing*" carrier materials.[11]

6.2 Materials and Methods

6.2.1 Implant preparation, carrier materials

6.2.1.1 Ca-P-coated titanium fiber mesh (Ti-CaP)

Sintered porous Ti-fiber mesh (Bekaert N.V., Zwevegem, Belgium) with a volumetric porosity of 86%, density of 600 g/m², and fiber diameter of 50 µm was used as scaffold material. The average pore size of the mesh was approximately 250 µm. The prepared implants were disc-shaped with a diameter of 6 mm, thickness of 0.8 mm, and weight of approximately 15 mg. All implants were ultrasonically cleaned with 70% ethanol for 15 min. The mesh was applied provided with a thin (1 µm) Ca-P coating (Ti-CaP) on both sides. The coating procedure was performed using a commercially available RF magnetron sputter unit (Edwards ESM 100).[12]

After deposition, all coated specimens were subjected to an additional heat treatment for 2 h at 500°C. The coatings had a crystalline apatite structure with a Ca/P ratio of 1.8– 2.0.[5] Before use, implants were sterilized by autoclaving for 15 min at 121°C. Before being loaded with rhBMP-2, the titanium fiber mesh discs were treated with RF glow-discharge (Harrick PDC-3XG, Argon, 0.15 Torr, for 5 min) to enhance wettability. A total of 12 Ti-CaP discs were prepared.

6.2.1.2 Insoluble bone matrix (IBM)

Freshly obtained bovine metatarsal bones were processed to obtain bone powders, which were sieved selectively. After decalcification in diluted HCl at a constant pH of 2.0 at 4°C and defatting with methanol and chloroform (volume ratio 1:1) the powders were extracted four times with 4 M Guanidine HCl, then washed with distilled water and lyophilized. This method has been described previously.[9,13] This preparation is termed insoluble bone matrix (IBM) and was used as the conventional carrier. The average IBM particle size was 500 µm. Twelve IBM implants, each weighing 20 mg, were used.

6.2.1.3 Fibrous glass membrane (FGM)

Fibrous glass membrane, 1-mm thick, was constructed from unwoven glass fibers 1 µm in diameter (Advantec, Tokyo, Japan). The chemical composition has been described previously.[10,14] This FGM was cut into pieces of a uniform size (10 x 5 mm). Twelve FGM sheets, each weighing 6 mg, were used.

6.2.1.4 Porous particles of hydroxyapatite (PPHAP)

Porous particles of hydroxyapatite were developed jointly by the Department of Biochemistry, School of Dentistry, Hokkaido University and Japan Steelworks, Ltd. (Muroran, Japan). The original product consisted of a block of hydroxyapatite with a porosity of 70% and a pore size of 150 µm, which was sintered at 1,200°C for 1h. This product was broken into granules and sieved to obtain a particle size varying from 300 to 500 µm; these granules were used as a carrier material. The PPHAP had an interconnected pore structure.[9] The procedure for preparation of the hydroxyapatite and porous particles has been reported previously in detail.[15, 16] Twelve PPHAP implants, each with a weight of 40 mg, were used.

6.2.2   Implant preparation, Bone Morphogenetic Proteins

The BMP used in the present study was recombinant human (rh)BMP-2. The rhBMP-2 (a generous gift from Yamanouchi Co., Tokyo, Japan) was produced by Chinese hamster ovary (CHO) cells. All materials were loaded with rhBMP-2. A 8.7 µg-dose of rhBMP-2 (diluted in Phosphate Buffered Saline, PBS) was applied to each implant. The BMP solutions were applied to the carrier materials prior to implantation. Ti-CaP and FGM implants were placed in an Eppendorf® tube, and aliquots of rhBMP-2 solution were applied. The IBM particles and PPHAP were placed in a 1-ml tuberculin syringe of which the tip had been cut open,[17] and aliquots of rhBMP-2 solution were applied. Subsequently, all specimens were lyophilized and then kept at –80°C until implantation.

6.2.3   Experimental design and surgical procedure

Sixteen 4-week-old Wistar King rats were used for implantation. The weight of each rat was approximately 60-70 g. Surgery was performed following intra-peritoneal injection with 50 mg/ml Nembutal® (diluted 10 times, 3.6 mg/100 g body weight). The BMP-loaded carriers were subcutaneously implanted into the back of the animals. To insert the implants, we immobilized the animals in a prone position. The backs of the animals were shaved and disinfected with 70% ethanol. To insert the subcutaneous implants, we made three small longitudinal incisions, two on one side and one on the other side of the vertebral column. Lateral to the incisions, we created a subcutaneous pocket using blunt dissection. Just before placement of the IBM and PPHAP implants, 30 µl and 40 µl distilled water was added to each syringe, respectively. After placement of the implants, the skin was closed using 4-0 nylon sutures. In this way, each animal received three subcutaneous implants. The implants were localized using a statistical randomization scheme. A total of 48 implants were placed: 12 Ti-CaP, 12 IBM, 12 FGM and 12 PPHAP implants, all loaded with rhBMP-2. Implantation periods were 3, 5, 7, and 9 days. Four rats were sacrificed at the end of each implantation period. The retrieved implants were used for light-microscopical analysis.

6.2.4   Light microscopy, subjective and tissue rating

For histological preparation, implants were fixed in 4% phosphate-buffered formaldehyde solution (pH = 7.4), dehydrated in a graded series of alcohol, and embedded in methylmethacrylate. After polymerization 10-µm sections were made using a modified microtome technique.[18] Light-microscopical sections were stained with basic fuchsin and methylene blue. At least three sections per implant were made and evaluated with a light microscope (Leica®).

Light microscopical analysis consisted of a full morphological description of the tissue response to the different implants. Further, a semi-quantitative histological grading scale was used to rate the tissue response (**Table 1**).

6.3   Results

All rats survived the experiment in good health and did not show any wound complications. At the end of the experiment, 48 implants were retrieved. At explantation, all implants were surrounded by a thin reaction-free fibrous capsule. Macroscopically, bone formation could be observed only in 9-day IBM implants. In the particulate implants (IBM and PPHAP) seroma formation was occasionally observed macroscopically.

6.3.1   Light microscopy, subjective

6.3.1.1 Ti-CaP
At 3 days of implantation, the porosity of the CaP-coated titanium mesh was almost devoid of cells: only some inflammatory cells could be seen mostly outside but also inside the mesh. This tissue reaction may be associated with the early stage of the wound healing process. Further, a dense layer of cells was seen surrounding the implant (**Figure 1A**).

At 5 days, undifferentiated mesenchymal cells occupied the porosity of the mesh. In addition, foci with cartilage formation and hypertrophic cartilage cells were present, in all specimens. These foci occurred mainly at the margin of the mesh. No signs of calcification were observed (**Figure 1B**), and there were hardly any inflammatory cells present.

At 7 days, cartilage with hypertrophic cartilage cells, had been formed in all implants. The cartilaginous tissue was found inside and at the margin of the mesh. In two implants the cartilage had started to mineralize. At the outer margin of one of these implants the cartilage was already changing to trabecular bone (**Figure 1C**). Scarcely any inflammatory cells were observed.

At 9 days, cartilage with a cartilagenous matrix was formed inside the fiber mesh material. Mineralization was clearly present in these cartilagenous areas. In the outer mesh areas, the cartilage was changing to trabecular bone. This trabecular bone expressed various stages of maturity. Further, some multinucleated cells were present in association with the

Table 1.

Table showing the semi-quantitative histological grading scale that was used to rate the tissue response.

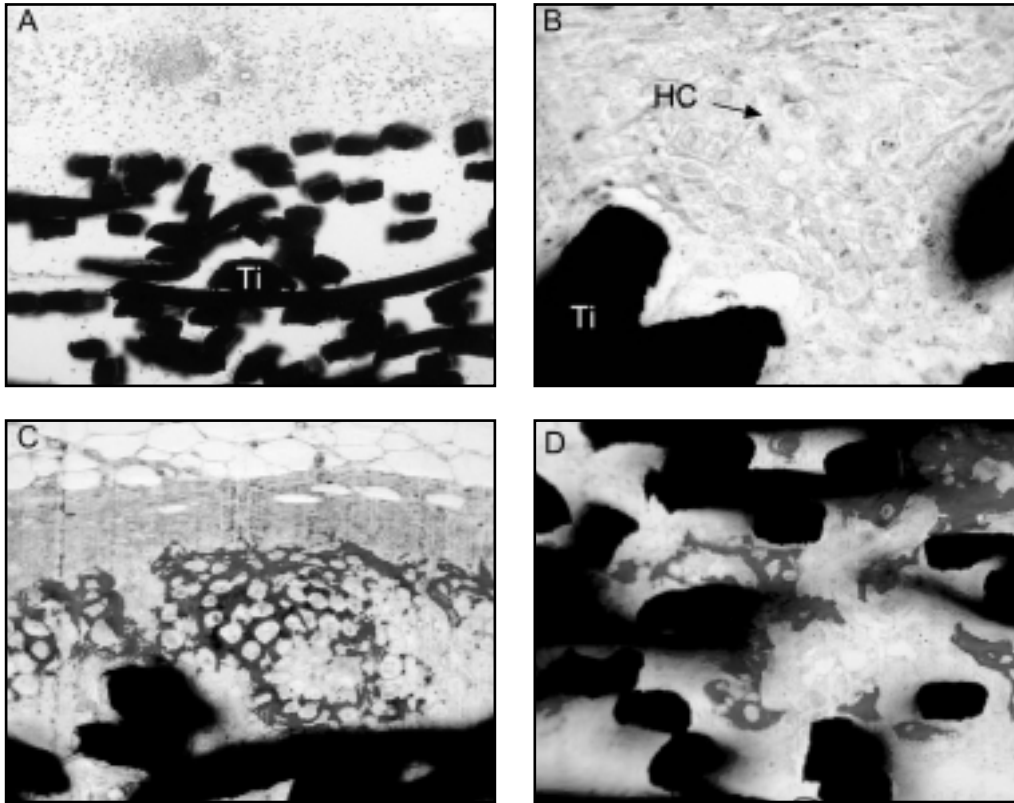| Score	Response
0	Fibrous tissue
1	Undifferentiated mesenchymal cells
2	Cartilage formation
3	Cartilage maturation, hypertrophy
4	Cartilage maturation, mineralization
5	Mineralized cartilage, bone formation
6	Bone and fully developed bone marrow-like tissue

Figure 1.
Undecalcified sections of:

(A) A Ti-CaP implant 3 days after implantation. The porosity of the CaP-coated titanium mesh is almost devoid of cells. Only some inflammatory cells can be seen mostly outside but also inside the titanium mesh (Ti) (*orig. magn.10x*).

(B) A Ti-CaP implant 5 days after implantation. Foci with cartilage formation and hypertrophic cartilage (HC) cells are present mainly at the margin of the mesh while undifferentiated mesenchymal cells are present inside the titanium mesh (Ti) (*orig. magn. 40x*).

(C) A Ti-CaP implant 7 days after implantation. Cartilage, with hypertrophic cartilage cells are found inside and at the margin of the mesh. The cartilage has started to mineralize. At the outer margin, the mineralized cartilage is already changing to trabecular bone (*orig. magn. 20x*).

(D) A Ti-CaP implant 9 days after implantation. In the cartilagenous areas mineralization is clearly present, the cartilage is changing to trabecular bone which expresses various stages of maturity (*orig. magn. 20x*).
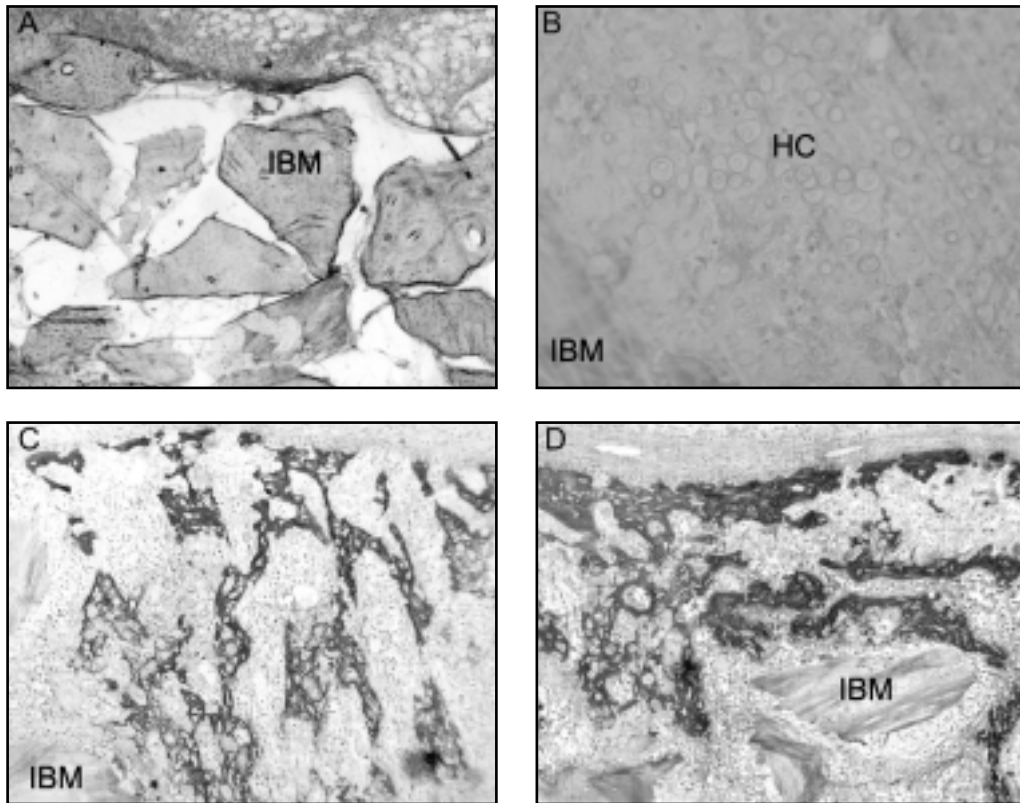
Figure 2.
Undecalcified sections of:

(A)   An IBM implant 3 days after implantation. The porosity between the particles is almost devoid of cells. Only some inflammatory cells are seen in between and covering the surface of the IBM particles. The cell-layer which surrounds the implant seems more dense than in the titanium implants (*orig. magn. 5x*).

(B)   An IBM implant 5 days after implantation. Foci of hypertrofic cartilage (HC) cells can be observed mainly at the outside and in between the outer IBM particles. Undifferentiated mesenchymal cells are present between the inner particles (*not shown*) (*orig. magn. 20x*).

(C)   An IBM implant 7 days after implantation. A significant amount of cartilage was formed surrounding the implant and between the particles. In the cartilage many hypertrophic cells can be seen together with mineralization. At the outside of the IBM implant (*top*) cartilage was already changed in trabecular bone (*orig. magn 10x*).

(D)   An IBM implant 9 days after implantation. Abundant cartilage and trabecular bone is present. Cartilagenous matrix with hypertrophic cartilage cells and mineralization mainly occupy the center of the implants. The bone was observed in the outer implant areas (*top*) and could be associated with the formation of marrow cavities and bone marrow-like tissue (*orig. magn 10x*).

mineralized cartilage. Also, a periosteum-like fibrous layer was formed which surrounded the titanium mesh. In none of the sections was bone marrow-like tissue observed (**Figure 1D**).

6.3.1.2 IBM

Three days after implantation, the porosity between the IBM particles was almost devoid of cells: only some inflammatory cells were seen in between and covering the surface of the IBM particles. This tissue reaction was very similar to the response to the titanium mesh implant, although, the cell layer which surrounded the IBM implant appeared to be more dense (**Figure 2A**).

At 5 days, undifferentiated mesenchymal cells were present between the IBM particles, especially in the outer areas. In addition, in two of the three implants, foci of cartilage, with hypertrophic cartilage cells could already be observed. These foci were mainly at the outside and in between the outer particles. Initial mineralization was seen in the cartilage (**Figure 2B**).

At 7 days, in all implants a significant amount of cartilage was formed surrounding the implant and between the particles. Many hypertrophic cells could be observed, and mineralization had proceeded. At the outside of the IBM implant cartilage had already changed into trabecular bone, and a periosteum-like fibrous tissue layer was being formed. Multinucleated cells, in close contact with the mineralized tissue, were occasionally present (**Figure 2C**).

At 9 days, abundant cartilage and trabecular bone was present in all implants. The cartilage was characterized by the presence of hypertrophic cartilage cells and mineralization and mainly occupied the center of the implants. Bone was observed in the outer implant areas and could be associated with the formation of marrow cavities and bone marrow-like tissue. In addition, cells had grown into the small pores within the IBM particles. Parts of the IBM stained with basic fuchsin, which indicated mineralization (**Figure 2D**).

6.3.1.3 FGM

At 3 days, the initial tissue response to FGM was very similar to the response to titanium implants, including a dense layer of cells which surrounded the implant (**Figure 3A**).

Five days after implantation, an inflammatory reaction was still present: evidently, inside the FGM the number of inflammatory cells had increased. No undifferentiated mesenchymal cells were seen, and in none of the sections was cartilage or bone present (**Figure 3B**).

At 7 days, abundant inflammatory cells (multinucleated cells) were present at the outer region of the FGM. Spindle-shaped undifferentiated cells were observed inside the membrane. At the outer surface of all implants, foci of cartilage with hypertrophic cartilage cells had now formed, which showed some initial mineralization in one implant and initial bone formation in another (**Figure 3C**).

After 9 days, spindle-shaped undifferentiated cells were still present. In two implants foci of cartilage with initial mineralization were located at the outer zone of the FGM implant. In none of the sections bone formation could be observed (**Figure 3D**). Multinucleated cells were still present in abundance.
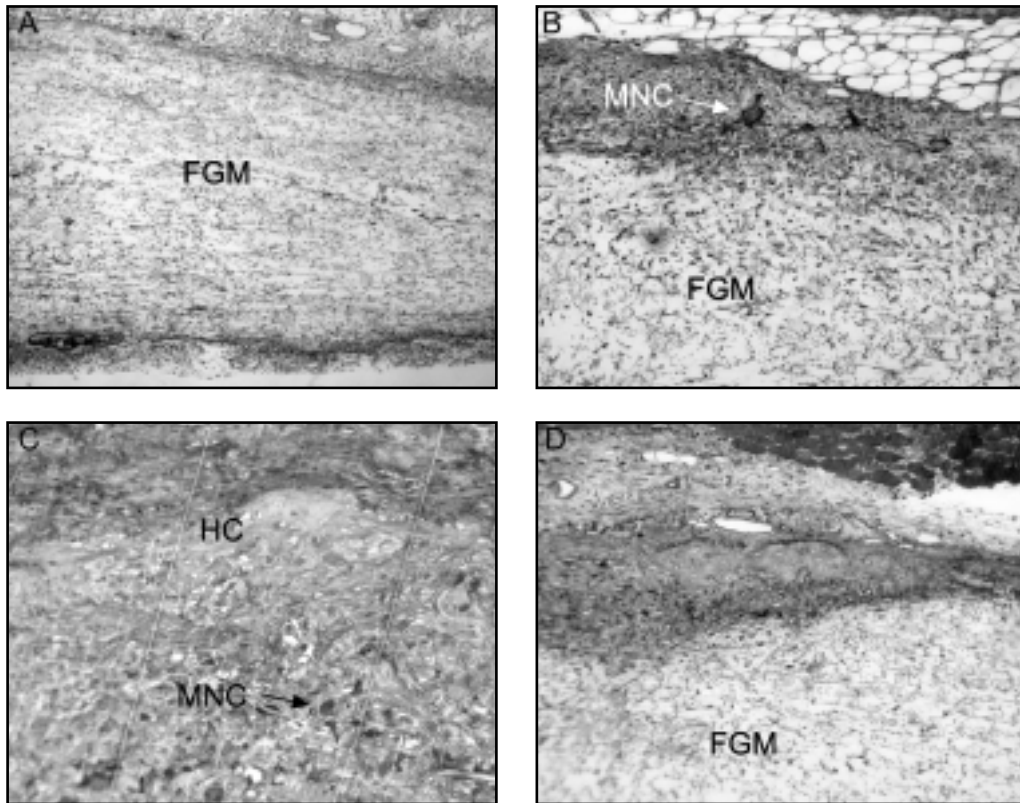
Figure 3.
Undecalcified sections of:

(A)   A FGM implant 3 days after implantation. The initial tissue response to FGM was very similar to other implant types, including an inflammatory reaction and a dense layer of cells which surrounded the implant (*orig. magn. 5x*).

(B)   A FGM implant 5 days after implantation. Still an inflammatory reaction was observed. Inside the FGM the number of inflammatory cells increased compared to 3 days. At the margin multinucleated cells (MNC) can be seen. No undifferentiated mesenchymal cells are present. In addition, neither cartilage, nor bone are present (*orig. magn. 10x*).

(C)   A FGM implant 7 days after implantation. Abundant inflammatory cells [multi-nucleated cells (MNC)] were present at the outer region of the FGM. Spindle-shaped undifferentiated cells can be observed inside the membrane. Now, At the outer surface of the implants, foci of cartilage with hypertrophic cartilage (HC) cells and some initial mineralization can be observed (*orig. magn. 20x*).

(D)   A FGM implant 9 days after implantation. Spindle-shaped undifferentiated cells are still present. Foci of cartilage with initial mineralization are located at the outer zone of the FGM implant. No bone formation can be observed (*orig. magn 10x*).
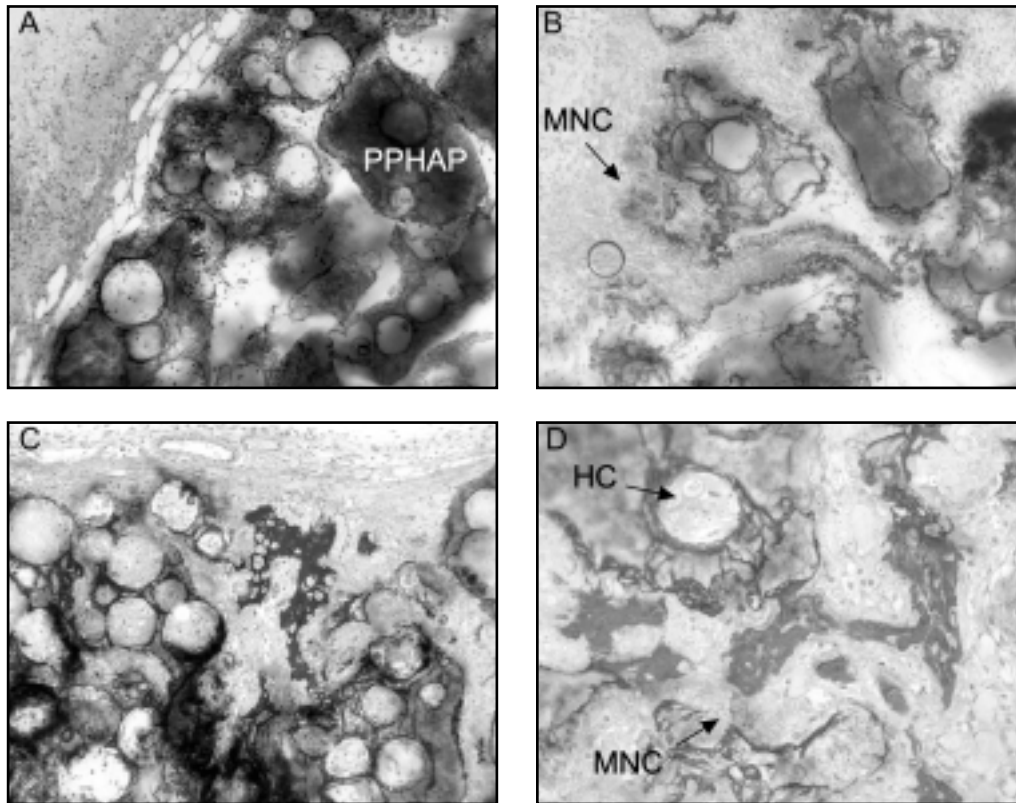
Figure 4.

Undecalcified sections of:

(A) A PPHAP implant implant 3 days after implantation. The tissue response for the PPHAP implant is very much the same as for other implant types. An inflammatory reaction is present and a dense layer of cells which surrounds the implant. In addition, the HA surface within the pores stains with basic fuchsin which indicates mineralization (*orig. magn. 10x*).

(B) A PPHAP implant 5 days after implantation. Inflammatory cells are present inside and between the PPHAP. Also, multinucleated cells (MNC) can be observed in close contact with the particles. Ingrowth of undifferentiated mesenchymal cells had occurred between and inside the porous particles. The surface of the hydroxyapatite stains positive for basic fuchsin, without the presence of osteoblast-like cells or osteocytes. No cartilage or bone is present (*orig. magn 10x*).

(C) A PPHAP implant 7 days after implantation. Calcification without the presence of osteoblast-like cells or osteocytes is clearly visible at the surface of the hydroxyapatite. The pores show the presence of undifferentiated mesenchymal cells with which were also present between porous particles. Inside a part of the pores hypertrophic cartilage cells were observed without mineralization (*not shown*). Between the particles mineralized cartilage with transition to trabecular bone can be seen (*orig. magn 10x*).

(D) A PPHAP implant 9 days after implantation. The presence of calcification at the surface of the hydroxyapatite particles and the presence of multinucleated cells (MNC) surrounding these particles is still unchanged. Inside the pores of the particles hypertrophic cartilage (HC) cells together with mineralization can be observed in close association with the hydroxyapatite surface. Trabecular bone is present between the particles and at the outside of the implants, while some mineralized cartilage remains between the particles (*orig. magn 20x*).
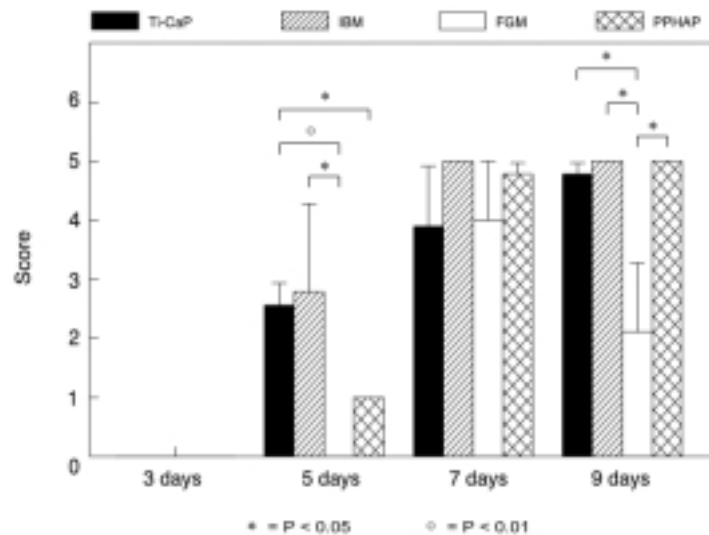
Figure 5.

Results of the semi-quantitative histomorphometrical analysis, showing mean and standard deviation for the different implants (*n*=3 for all materials and time periods). In addition, significant statistical differences are depicted (*t*-test).

6.3.1.4 PPHAP

After 3 days, the tissue response differed only at one point from those to the other implant materials; *i.e.*, the HA surface within the pores was stained with basic fuchsin (**Figure 4A**). Five days after implantation, the number of inflammatory cells had increased inside and between the PPHAP. Also, multinucleated cells were present in close contact with the particles. Ingrowth of undifferentiated mesenchymal cells had occurred between and inside the porous particles. The surface of the hydroxyapatite stained positive for mineralization (basic fuchsin) without the presence of osteoblast-like cells or osteocytes. No cartilage or bone could be observed in any specimen (**Figure 4B**).

At 7 days, calcification without the presence of osteoblast-like cells or osteocytes was clearly visible at the surface of the hydroxyapatite within the pores. Multinucleated cells were present in close contact with the porous particles. Hypertrophic cartilage cells were observed without mineralization inside a portion of the pores; other pores showed the presence of undifferentiated mesenchymal cells, which were also present between porous particles. In all specimens, mineralized cartilage with a transition to trabecular bone was seen between the particles (**Figure 4C**).

Finally, at 9 days, calcification at the surface of the hydroxyapatite particles and the presence of multinucleated cells surrounding these particles were still unchanged. Inside the pores of the particles hypertrophic cartilage cells together with mineralization could be observed in close association with the hydroxyapatite surface. Further, in all implants trabecular bone was present between the particles and at the outside of the implants, while some mineralized cartilage remained between the particles (**Figure 4D**).

6.3.2   Light microscopy, tissue rating

Results of the tissue rating are depicted in **figure 5**. The results show that at 5 days (hypertrophic) cartilage was present in the Ti-CaP and IBM implants. In the PPHAP implants only undifferentiated mesenchymal cells were found, whereas in the FGM implants no mesenchymal cells were seen at all. At this time a significant difference in tissue response existed between the Ti-CaP and PPHAP (P < 0.05, *t*-test), the Ti-CaP and FGM implants (P < 0.01, *t*-test), and the IBM and FGM implants (P < 0.05, *t*-test). At 7 days, cartilage mineralization and bone formation had occurred. Although rating appears to indicate that at 7 days the bone formation process had proceeded further in the IBM and PPHAP specimens (cartilage and bone) than in the Ti-CaP and FGM (cartilage maturation, mineralization), the statistical analysis revealed no differences. At 9 days, the Ti-CaP, IBM and PPHAP rating showed the formation of bone and cartilage; no difference existed between these materials. The FGM implants had a significantly lower score (cartilage) than Ti-CaP (P < 0.05, *t*-test), IBM (P < 0.05, *t*-test) and PPHAP (P < 0.05, *t*-test).

6.4   Discussion and conclusion

The biocompatible response of IBM and Ti-CaP as well as the occurrence of inflammatory cells inside all implants corroborate the results of previous studies.[6,9,10,19,20] Also in agreement with earlier investigations, was our observation that all BMP-carrier combinations initiated an osteoinductive response.[6,7,9,10,21,22,23] On the other hand, we observed a difference in the amount and time-dependent occurrence of cartilage and bone.

Subjectively, by 9 days the IBM implants yielded the largest amount of bone (IBM > PPHAP ~ Ti-CaP > FGM). This corresponds with another study in which IBM, FGM and PPHAP implants were compared.[9] This finding is supported by the observation that collagen, the major constituent of IBM, and calcium phosphates have been proven to have a high affinity for BMPs, although they show different release profiles.[24,25] Unfortunately, no data are currently available on the exact rhBMP-2 release profile of various carrier materials. Nevertheless, the affinity of titanium for BMPs has been shown to be lower than the affinity of calcium phosphates.[26] Further, we know that the *in vivo* osteoinductive activity is positively correlated with the amount of BMP retained at the implantation site.[24,25] In addition to the release profile, other factors like carrier volume and tissue reaction might contribute to the differences in the amount of bone formation.[27,28]

For IBM, PPHAP, and FGM the bone formation process proceeded faster in the present study than in earlier studies.[9,10] We believe that this is due to the concentration and activity of recombinant BMP-2 used. In previous studies 300 μg (0.5 unit) of a partially purified BMP fraction (S-300) was used for IBM, PPHAP, and FGM.[9] In the present study and in a previous titanium study, we used 8.7 μg rhBMP-2 which has a higher activity (2 μg = 1 unit).[29] It is well known that higher concentrations of BMP do not only increase the amount of bone formation but also result in earlier cartilage and bone formation.[30]

The process of bone formation in all our BMP-loaded samples occurred with the presence of chondrogenesis. However, the amount and time-dependent occurrence of

cartilage varied among the carriers, with IBM apparently yielding the largest amount of cartilage. In addition, in IBM and Ca-P-coated Ti-mesh cartilage formation preceded bone formation; this was not seen for PPHAP. For IBM, FGM and Ti-CaP the presence of chondrogenesis agrees with previous studies.[6,9,10] On the other hand, for PPHAP the findings do not correspond with previous studies;[9,29] in the latter no cartilage was observed between 1 and 4 weeks. In addition, the amount of cartilage, as quantified by type II collagen content (*the predominant collagen type present in cartilagenous matrix*), has been reported to be high in IBM and FGM, while PPHAP showed no type II collagen at all (at 3, 5, days and at 1, 2, 3, and 4 weeks).[9] Therefore, the present study supports earlier findings that the bone formation process in IBM and FGM is characterized by an endochondral ossification-like process. Based upon the morphological analysis, the bone formation process in Ti-CaP and PPHAP also seems to be characterized by an endochondral ossification-like process.

Vascularization is considered to be a crucial step in ectopic bone formation.[31] For example, anti-angiogeneic agents like TNP-470 have been shown to inhibit rhBMP-2-induced ectopic osteogenesis.[32] Some researchers ascribe the effect of vasculari-zation to the supply of osteoblasts.[33] Indeed, vascular pericytes, which are undifferentiated cells, have been shown to be able to differentiate into chondrocytes and osteoblasts *in vitro* and can form cartilage and bone *in vivo*.[34] Other studies have shown that a low oxygen concentration favors chondrogenesis, while a higher oxygen concentration supports bone formation.[31,35,36,37] Carrier geometry is known to influence the bone formation process.[38,39,40] The geometry of the carrier influences vascularization and thereby oxygen supply. Consequently, carriers which induce bone formation independent of cartilage have been hypothesized to provide a higher oxygen supply due to geometry.[8] Recently, a similar observation has been made for a scaffold composed of bioglass fibers [composed of CaO, P_2O_5, and SiO_2 (CPSA)].[41] Bone formation was observed all around a porous ball-shaped CPSA implant, whereas scant bone formation was observed in a less porous bundle-shaped implant. Further research revealed that Vascular Endothelial Growth Factor (VEGF) receptors (Flt-1 and KDR) were expressed in the porous ball-shaped implants, but not in the bundle-shaped implant. Again, this finding supports the relationship between neovascularization and osteogenesis.

Consequently, we hypothesize that the differences in the time-dependent occurrence and amount of cartilage between the different carrier materials in our study are caused by differences in vascular-inducing geometry. A greater vascular-inducing geometry leads to early osteogenesis and the early disappearance of cartilage, while a vascular-inhibiting geometry leads to a higher amount of cartilage, which remains for a longer time. Therefore, the terms "*bone-directing*" and "*cartilage-directing*" carrier might be appropriate for the former and the latter, respectively.[11,41] In view of this, PPHAP and Ca-P-coated titanium are bone-directing carriers, while FGM is a cartilage-directing carrier.

It has to be emphasized that, irrespective of the different amounts and different time-dependent occurrence of cartilage for various carriers, the final product of BMP-induced osteogenesis is always bone without cartilage.[6,8,9,10,11,41] The presence of bone and the absence of cartilage has been described to occur at 2 weeks for Ti-CaP and PPHAP and at 3 weeks for IBM;[6,9,42,43,44] for FGM it has been reported to occur at 5 weeks.[10] Again, it has to be emphasized that the BMP concentration also influences the speed of bone formation.[30]

Nevertheless, a carrier which promotes the induction of high-quality bone, in a short time interval, is highly desirable for bone reconstructive procedures.

In summary, we conclude that IBM, CaP-coated Ti mesh, FGM and PPHAP all provided with rhBMP-2, can induce ectopic bone formation with a cartilaginous phase in a rat model at short implantation periods. Considering the different nature of the carrier materials used these findings even suggest that an endochondral ossification-like process is always present in rhBMP-2 induced osteogenesis, although the amount of cartilage differs. These differences are believed to be related to the vascular-inducing geometry: a greater vascular-inducing geometry leads to early osteogenesis and the early disappearance of cartilage, while a vascular-inhibiting geometry will lead to higher amounts of cartilage, which remain for a longer time. Therefore, the terms "*bone-directing*" and "*cartilage-directing*" carrier might be appropriate for the former and the latter, respectively.

References

1. **Kadiyala S, Young RG, Thiede MA, Bruder SP.** Culture expanded canine mesenchymal stem cells possess osteochondrogenic potential *in vivo* and *in vitro*. Cell Transplant 1997; 6:125.
2. **Brekke JH.** A rationale for the delivery of osteoinductive proteins. Tissue Eng 1996; 2:97.
3. **Zhang R, Ma PX.** Poly(α-hydroxyl acids)/hydroxyapatite porous composites for bone-tissue engineering. I. preparation and morphology. J Biomed Mater Res 1999; 44:446.
4. **Girton TS, Oegema TR.** Exploiting glycation to stiffen and strenghten tissue equivalents for tissue engineering J Biomed Mater Res 1999; 46:87.
5. **Vehof, JWM, Spauwen PHM, Jansen JA.** Bone formation in calcium-phosphate-coated titanium mesh. Biomaterials. 2000; 21:2003.
6. **Vehof JWM, Mahmood J, Takita H, van 't Hof MA, Kuboki Y, Spauwen PH, Jansen JA.** Ectopic bone formation in titanium mesh loaded with Bone Morphogenetic Protein and coated with calcium phosphate. Plast Reconstr Surg 2001; 108:434.
7. **Reddi AH.** Cell biology and biochemistry of endochondral bone development. Coll Relat Res 1981; 1:209.
8. **Sasano Y, Ohtani E, Narita K, Kagayama M, Murata M, Saito T, Shigenobu K, Takita H, Mizuno M, Kuboki Y.** BMPs induce direct bone formation in ectopic sites independent of the endochondral ossification *in vivo*. Anat Rec 1993; 236:373.
9. **Kuboki Y, Saito T, Murata M, Takita H, Mizuno M, Inoue M, Nagai N, Poole AR.** Two distinctive BMP-carriers induce zonal chondrogenesis and membranous ossification, respectively; geometrical factors of matrices for cell-differentiation. Connect Tissue Res 1995; 32:219.
10. **Sasano Y, Mizoguchi I, Takahashi I, Kagayama M, Saito T, Kuboki Y.** BMPs induce endochondral ossification in rats when implanted ectopically within a carrier made of fibrous glass membrane. Anat Rec 1997; 247:472.
11. **Jin QM, Takita H, Kohgo T, Atsumi K, Itoh H, Kuboki Y.** Effects of geometry of hydroxyapatite as a cell substratum in BMP- induced ectopic bone formation. J Biomed Mater Res 2000; 51:491.
12. **Jansen JA, Wolke JG, Swann S, Van der Waerden JP, de Groot K.** Application of magnetron sputtering for producing ceramic coatings on implant materials. Clin Oral Implants Res 1993; 4:28.
13. **Kuboki Y, Yamaguchi H, Yokoyama A, Murata M, Takita M, Tazaki M, Mizuno M, Hasegawa T, Iida S, Shigenobu R, Fujisawa R, Kawamura M, Atsuta T, Mutsumoto A, Kato H, Zhou HY, Ono I, Takeshita N, Nagai N.** Osteogenesis induced by BMP-coated Biomaterials: Biochemical principles of bone reconstruction in dentistry. Davies JD, editor. The Bone Biomaterial Interface. Toronto. University Toronto Press, 1992, 127.
14. **Missana L, Nagai N, Kuboki Y.** Comparative histological studies of bone and cartilage formations induced by various carrier composites. Jpn J Oral Biol 1994; 36:9.
15. **Monma H, Kamiya T.** Preparation of hydroxyapatite by the hydrolysis of brushite. J Mater Sci 1987; 22:4247.
16. **Itoh H, Wakisaka Y, Ohnuma Y, Kuboki Y.** A new porous hydroxyapatite ceramic prepared by cold isostatic pressing and sintering synthesized flaky powder. Dent Mater J 1994; 13:25.
17. **Iida S, Kawasaki T, Mizuno M, Kuboki Y.** Bone formation in osteoporotic rats, reduced effect of bone morphogenetic protein ascribed to the suppressed osteoblast differentiation. Jpn J Oral Biol 1994; 36:249.
18. **van der Lubbe HB, Klein CP, de Groot, K.** A simple method for preparing thin (10 microM) histological sections of undecalcified plastic embedded bone with implants. Stain Technol 1988; 63:171.
19. **Jansen JA, Paquay YG, van der Waerden JP.** Tissue reaction to soft-tissue anchored percutaneous implants in rabbits. J Biomed Mater Res 1994; 8:1047.
20. **Paquay YC, de Ruijter JE, van der Waerden JP, Jansen JA.** Wound healing phenomena in titanium fibre mesh: the influence of the length of implantation. Biomaterials 1997; 18:161.
21. **Urist MR, Huo YK, Brownell AG, Hohl WM, Buyske J, Lietze A, Tempst P, Hunkapiller M, DeLange, RJ.** Purification of bovine bone morphogenetic protein by hydroxyapatite chromatography. Proc Natl Acad Sci USA 1984; 81:371.
22. **Luyten FP, Cunningham NS, Ma S, Muthukumaran N, Hammonds RG, Nevins WB, Woods WI, Reddi AH.** Purification and partial amino acid sequence of osteogenin, a protein initiating bone differentiation J Biol Chem 1989; 264:13377.
23. **Reddi AH, Sullivan NE.** Matrix-induced endochondral bone differentiation: influence of hypophysectomy, growth hormone, and thyroid-stimulating hormone. Endocrinology 1980; 107:1291.
24. **Uludag H, D'Augusta D, Palmer R, Timony G, Wozney J.** Characterization of rhBMP-2 pharmacokinetics implanted with biomaterial carriers in the rat ectopic model. J Biomed Mater Res 1999; 46:193.
25. **Uludag H, D'Augusta D, Golden J, Li J, Timony G, Riedel R, Wozney JM.** Implantation of recombinant human bone morphogenetic proteins with biomaterial carriers: A correlation between protein pharmacokinetics and osteoinduction in the rat ectopic model. J Biomed Mater Res 2000; 50:227.

26. **Kuboki Y.** Unpublished data, 1999.
27. **Takaoka K, Nakahara H, Yoshikawa H, Koezuka M, Hashimoto J, Miyamoto S, Suzuki S, Ono K.** Constitution of bone inducing implants by combining bone morphogenetic protein with biomaterials: experimental studies in mice. In: Urist MR, O'Connor BT, Burwell RG, editors. Bone grafts derivatives and substitutes, Oxford, UK, Butterworth-Heinemann, 1994, p377.
28. **Miyamoto S, Takaoka K, Okada T, Yoshikawa H, Hashimoto J, Suzuki S, Ono K**. Evaluation of polylactic acid homopolymers as carriers for bone morphogenetic protein. Clin Orthop 1992; 278:274.
29. **Kuboki Y, Takita H, Kobayashi D, Tsuruga E, Inoue M, Murata M, Nagai N, Dohi Y, Ohgushi H.** BMP-induced osteogenesis on the surface of hydroxyapatite with geometrically feasible and nonfeasible structures: topology of osteogenesis. J Biomed Mater Res 1998; 39:190.
30. **Wang EA, Rosen V, D'Alessandro JS, Bauduy M, Cordes P, Harada T, Israel DI, Hewick RM, Kerns KM, LaPan P**. Recombinant human bone morphogenetic protein induces bone formation. Proc Natl Acad Sci USA 1990; 87:2220.
31. **Caplan AI.** Cartilage begets bone versus endochondral myelopoiesis. Clin Orthop 1990; 261:257.
32. **Mori S, Yoshikawa H, Hashimoto J, Ueda T, Funai H, Kato M, Takaoka K.** Antiangiogenic agent (TNP-470) inhibition of ectopic bone formation induced by bone morphogenetic protein-2. Bone 1998; 22:99.
33. **Trueta J.** The role of the vessels in osteogenesis. J Bone Joint Surg 1963; 45B:402.
34. **Doherty MJ, Ashton BA, Walsh S, Beresford JN, Grant ME, Canfield AE.** Vascular pericytes express osteogenic potential *in vitro* and *in vivo*. J Bone Miner Res 1998; 13:828.
35. **Basset CAL, Herrmann I.** Influence of oxygen concentration and mechanical factors on differentiation of connective tissues *in vitro*. Nature 1962; 190:460.
36. **Hall BK.** Hypoxia and differentiation of cartilage and bone from common germinal cells *in vitro*. Life Sci 1969; 8:533.
37. **Caplan AI, Pechak DG.** The cellular and molecular embryology of bone formation. J Bone Miner Res 1987; 5:117.
38. **Reddi AH, Huggins CB.** Influence of geometry of transplanted tooth and bone on transformation of fibroblasts. Proc Soc Exp Biol Med 1973; 143:634.
39. **Sampath TK, Reddi AH.** Importance of geometry of the extracellular matrix in endochondral bone differentiation. J Cell Biol 1984; 98:2192.
40. **Ripamonti U, Ma S, and Reddi AH.** The critical role of geometry of porous hydroxyapatite delivery system in induction of bone by osteogenin, a bone morphogenetic protein. Matrix 1992; 12:202.
41. **Mahmood J, Takita H, Ojima Y, Kobayashi M, Kohgo T, Kuboki Y.** Geometric Effect of Matrix upon Cell Differentiation: BMP-Induced Osteogenesis Using a New Bioglass with a Feasible Structure. J Biochem (Tokyo) 2001; 129:163.
42. **Kuboki Y, Takita H, Tsuruga E, Ono M, Jansen JA.** Hydroxyapatite-coated titanium mesh as a tissue engineered carrier of BMP induced osteogenesis. Proceedings of the 2nd International Conference of BMP. Sacramento, USA, June, 1997.
43. **Kuboki Y, Takita H, Tsuruga E, Ono M, Jansen JA.** Rationale for hydroxyapatite-coated titanium mesh as an effective carrier for BMP. J Dent Res 1998; 77:263 (abstract # 1262).
44. **Jansen JA, Takita H, Tsuruga E, Mizuno M, Kuboki Y.** Tissue Engineered Bone Grafts. Proceedings of the 1st Smith & Nephew International Symposium, York, UK, July, 1997, abstract no. S20.

Chapter 7

Bone formation in Transforming Growth Factor beta-1-loaded titanium fiber mesh implants

J.W.M. Vehof, M.T.U. Haus, J.E. de Ruijter, P.H.M. Spauwen and J.A. Jansen.

7.1   Introduction

Osteoinductive factors like Bone Morphogenetic Proteins (BMPs) or Transforming Growth Factor-βs (TGF-βs) provided to porous carrier materials have been used to improve healing in bone defects as well as around medical and dental implants. At present more than 14 different BMPs are known (BMP-1 to BMP-15). In mammals 3 isoforms of TGF-β have been described: TGF-β_1, TGF-β_2 and TGF-β_3. BMPs and TGF-βs share a sequence homology of 40 to 50 %. BMPs can be isolated from bone; TGF-βs can be isolated from both bone and platelets. Alternatively, they can be produced by transfected cells using recombinant DNA techniques, the so-called recombinant (human) BMPs or TGF-βs. BMPs are known to induce bone formation in both heterotopic and orthotopic sites. In addition, TGF-β_1 and TGF-β_2 have also been shown to stimulate osteogenesis in orthotopic sites.[1,2] However, TGF-β does not induce bone formation in a rodent ectopic assay model as shown by Sampath *et al.*,[3] although, Ripamonti *et al.*[4] did report the induction of heterotopic ossification by TGF-β_1 in babboons. Considering the final application of dental and medical implants we decided to focus on the effect of TGF-β on implant related bone healing.

A prerequisite to the use of osteoinductive growth factors is a suitable carrier or scaffold material. Carrier materials currently used to support bone healing are polymers or co-polymers, mainly poly(α-hydroxyl) acids) and collagen. For TGF-β_1, mainly demineralized bone matrix (DBM), or Guanidine-treated DBM (GuDBM) has been used as a carrier material. Another candidate material for bone stimulating-factors is sintered titanium (Ti) fiber mesh material. The advantages of this material are that it can be applied directly on, for example titanium implants. This allows its use even in load-bearing situations. Titanium is currently being applied in surgical practice because of its excellent mechanical characteristics in terms of stiffness and elasticity, bone compatibility and ease of use during surgery.

Ti-mesh has been shown to be an effective carrier for both osteogenic cells and BMPs in ectopic bone formation *in vivo*.[5,6] In addition, the osteogenic and osteoinductive properties of a titanium fiber mesh scaffold can be further enhanced by the application of an additional thin calcium phosphate (Ca-P) coating.[5,6] Thin RF magnetron sputtered calcium phosphate coatings have also been shown to enhance the osteoconductive properties of titanium implants.[7-9]

The objective of the study reported here was to investigate: (1) whether Ti-fiber mesh loaded with rhTGF-β_1 can induce bone formation in an orthotopic site; (2) the osteoconductive properties of Ti-fiber mesh; (3) the influence of a Ca-P coating on the osteoconductive properties of Ti-fiber mesh.

7.2   Materials and Methods

7.2.1   Implant preparation, carrier material

Bekaert N.V. (Zwevegem, Belgium) provided the Ti-fiber mesh implants. The mesh implants were fabricated by interengaging and intertwining a multiplicity of commercially

pure titanium fibers with a fiber diameter of 50 μm. After compression against a solid Al_2O_3 rod, the fiber structures were sintered to bond the fibers at their points of contact. In this way, a hollow, cylindrically shaped structure was obtained. The volumetric porosity of the titanium mesh was 86%. One-cm-long tubes, with an outer diameter of 8 mm and an inner diameter of 4 mm, were cut to 2-mm-high discs. The implants had a weight of approximately 40 mg. The central space in each implant was filled with a solid titanium rod with a diameter of 4 mm and a height of 2 mm.

All implants were ultrasonically cleaned with 70% ethanol for 15 min. The mesh was applied as-received (Ti) or provided with a thin (2 μm) Ca-P coating (Ti-CaP) at the outer surface. The coating procedure was performed using a commercially available RF magnetron sputter unit (Edwards ESM 100).[10] The target material used in the deposition process was a copper disc provided with a plasma-sprayed hydroxyapatite coating (CAMCERAM®). The process pressure was 5 x 10^{-3} mbar and the sputter power was 400 W. The deposition rate of the films was 100–150 nm/min sputtering.

After deposition, all coated specimens were subjected to an additional heat treatment for 2 h at 500°C. X-ray diffraction (XRD), Fourier Transform Infrared spectroscopy (FTIR) and Energy Dispersive Spectroscopical (EDS) analysis showed that this resulted in the coatings having a crystalline apatite structure with a Ca/P ratio of 1.8–2.0. Before use, implants were sterilized by autoclaving for 15 min at 121°C. A total of 28 implants were prepared: 19 Ti and 9 Ti-CaP.

7.2.2   Implant preparation, Transforming Growth Factor beta-1

The growth factor used in the present study was recombinant human Transforming Growth Factor beta-1 (rhTGF-β_1) (R&D Systems Inc. Minneapolis, Minn., USA). RhTGF-β_1 was produced by Chinese hamster ovary (CHO) cells.

Before being loaded with rhTGF-β_1, all materials were treated for 5 min with RF glow-discharge (Harrick PDC-3XG, Argon, 0.15 Torr) to enhance wettability. Ten of the non-coated meshes were loaded with rhTGF-β_1. The rhTGF-β_1 was dissolved in sterile 4 mM HCl containing 1 mg/ml bovine serum albumin (BSA). A dose of 2 μg rhTGF-β_1 was applied to each of the 10 Ti-fiber mesh implants. Prior to implantation, 40-μl-aliquots of the rhTGF-β_1 solution were added to each Ti-fiber mesh implant, which was placed in an Eppendorf® tube. The constructs were then lyophilized and kept at 4°C until implantation.

7.2.3   *In vitro* rhTGF-β_1 release

In vitro rhTGF-β_1 release of the loaded implants was measured using an Enzyme-Linked Immunosorbent Assay (ELISA) using a commercially available test kit (Promega® Benelux b.v., Leiden, the Netherlands). One implant was used loaded with 2 μg rhTGF-β_1. The implant was placed in 1 well of a 24-well plate, and 2 ml minimal essential medium (α-MEM, Gibco BRL, Life Technologies B.V., Breda, The Netherlands) containing 10% FCS and gentamycin was added to the well. After that, the 24-well plate was placed in an incubator (humidified atmosphere of 95% air, 5% CO_2 at 37°C). At 15 min, 30 min, 1 h, 2 h, 4 h,

24 h and 1 week, two 50 μl-samples were taken out of the well. Subsequently, 100 μl α-MEM solution was added to the well. Samples were kept at 4°C until the time of meas-urement. Duplicate samples were prepared and diluted, and the ELISA test was performed according to the Promega® protocol. Finally, the absorption was read using a microplate reader set at a wavelength of 450 nm. All measurements were corrected for the dilution that had occurred during sampling.

7.2.4   Experimental animal study

For implantation, 18 healthy skeletally mature male New Zealand White rabbits with a weight between 2.5 and 3.4 kg were used . The animals were housed separately in cages. Surgery was performed under general inhalation anaesthesia. The anaesthesia was induced by an intravenous injection of Hypnorm® (0.315 mg/ml fentanyl citrate and 10 mg/ml fluanisone) and atropine, and maintained by a mixture of nitrous oxide, isoflurane and oxygen through a constant volume ventilator. The peri-operative infection risk was reduced by giving the rabbits antibiotical prophylaxis [Baytril® 2.5 % (Enrofloxacin), 5–10 mg/kg].

For the insertion of the implants, the animals were placed in a ventral position. The skull was shaved, washed and disinfected with povidone-iodine. A longitudinal incision was placed through the skin in the midline over the parietal skull. The skin and subcuta-neous tissue were separated from the periosteum using blunt dissection. After that, a longitudinal incision was made through the periosteum. Subsequently, the periosteum was elevated from the underlying skull bone. After exposure of the parietal calvarial bone, one full-thickness skull defect was drilled on each side using a 7.3 mm-trephine (Merck®) drill at low rotational speed with continuous cooling with saline (**Figure 1A**, **B**). A cylindrical guide, which was used to avoid damage to the underlying dura, surrounded the trephine. The implants were inserted (**Figure 1C**), and the periosteum was closed over the implant using 3-0 Vicryl® sutures. Subsequently, the skin was closed using a subcuticular Vicryl® 3-0 suture.

In this way, a total of 27 implants were placed: 9 non-coated titanium fiber mesh implants (Ti), 9 Ca-P-coated titanium fiber mesh implants (Ti-CaP), and 9 non-coated titanium fiber mesh implants loaded with rhTGF-β_1 (Ti-TGF-β_1). In addition, 9 defects were left empty and used as controls. Nine rabbits received one Ti and one Ti-CaP implant and 9 rabbits recieved one Ti-TGF-β_1-implant with an unfilled defect at the contralateral side. The rhTGF-β_1-loaded implants were not combined with other implants in the same animal in order to avoid crossover effects from the growth factor.

In addition, in 8 rabbits quadruple fluorochrome labeling was performed. Fluoro-chrome labels, *i.e.* tetracycline (yellow), alizarin-complexone (red), calcein (green), and tetracycline (yellow) were subcutaneously administered at 1, 3, 5, and 7 weeks postopera-tively, respectively. The treatment dose was 25 mg/kg body weight for all labels.

At 8 weeks post-implantation, euthanasia was performed with an overdose of Nem-butal® (pentobarbital). Subsequently, the implants with the surrounding tissues were re-trieved *en bloc* and prepared for light-microscopical evaluation. In this study, national guidelines for the care and use of laboratory animals were observed.
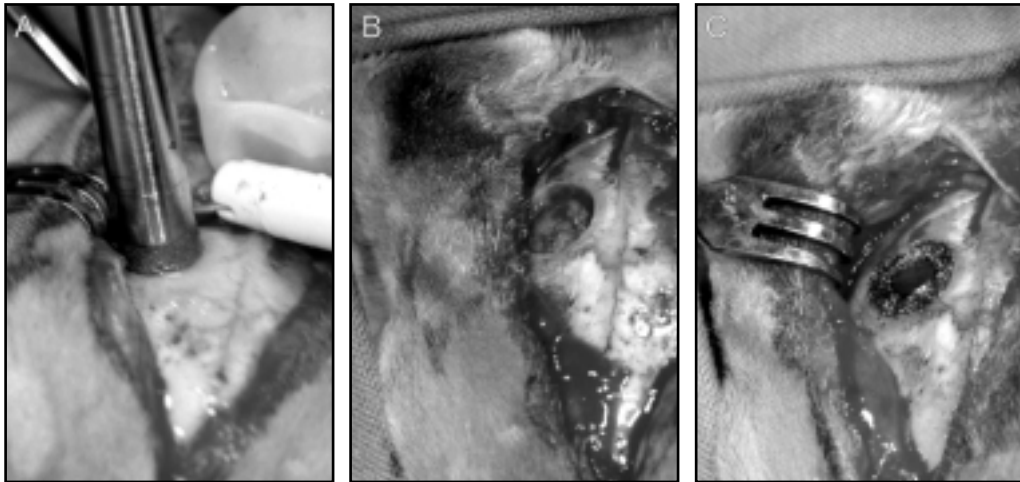
Figure 1.

Figure showing (**A,B**) the drilling of the defect and (**C**) insertion of the Ti-fiber mesh implant.

7.2.5   Light microscopy (subjective and histomorphometry)

Implants for histology were fixed in 4% phosphate-buffered formaldehyde solution (pH = 7.4), dehydrated in a graded series of alcohol and embedded in methylmethacrylate. After polymerization, 10-µm-thick longitudinal sections were made using a modified microtome technique.[11] Light-microscopical sections were stained with basic fuchsin and methylene blue. These sections were evaluated with a light microscope (Leica®).

Two slightly thicker sections (30 µm) were made per implant for fluorochrome labeling analysis. These sections were left unstained and examined with a fluorescence microscope (Leica®) equipped with an excitation filter of 470-490 nm.

Light and fluorescence microscopical analysis consisted of a full morphological description of the tissue response to the different implants. In addition, image analysis was performed on all sections to evaluate the ingrowth of and to quantify the amount of newly formed bone. For this purpose a Leica® Qwin Pro-image analysis system was used.

Therefore, at least 3 histological sections per implant were digitalized at low magnification. For this purpose one digital image was made at both the left and the right side of the solid titanium core (**Figure 2A,B**). In these digital images, the computer detected the bone tissue and titanium. The computer then measured the thickness of the Ti-fiber mesh – *i.e.* the distance from the most peripheral titanium fiber up to the solid titanium core (**Figure 2C**). Subsequently, the absolute bone ingrowth, the distance from the most peripheral titanium fiber up to the front of the newly formed bone in the fiber mesh, and the *bone surface area* were measured by the computer (**Figure 2D**). In addition, the computer calculated the area of this region of interest (ROI) (**Figure 2D**). From these values the *bone ingrowth* percentage (the index of the absolute bone ingrowth and Ti-fiber mesh

thickness) and *bone fill* percentage (the index of the bone surface area and the area of ROI) were calculated. Per section, the average was taken of the values from each side.

7.2.6   Statistical methods

A paired *t*-test was applied to evaluate the differences between the Ti-CaP and Ti implants since the implants were always combined in the same animal. An unpaired *t*-test was used to evaluate differences between Ti-TGF-β_1, and Ti-CaP and Ti implants since the Ti-TGF-β_1 implants were not combined with the other two implant types in the same animal.
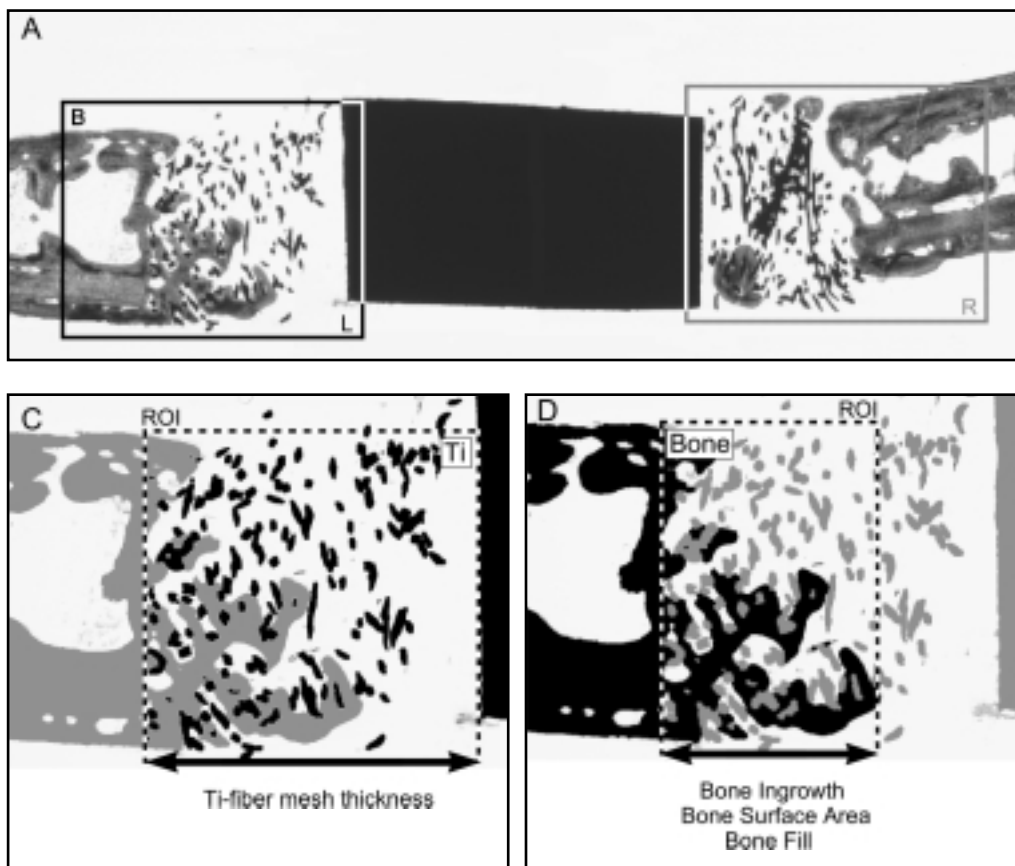
Figure 2.
Figure showing the method of the histomorphometrical analysis. (**A, B**) One digital image was made at both the left and the right side of the solid titanium core. The bone and Ti-fiber mesh were detected. (**C**) The thickness of the Ti-fiber mesh was measured. (**D**) The absolute bone ingrowth and the bone surface area were measured by the computer. In addition, the computer calculated the bone ingrowth percentage and bone fill percentage (*see text*).
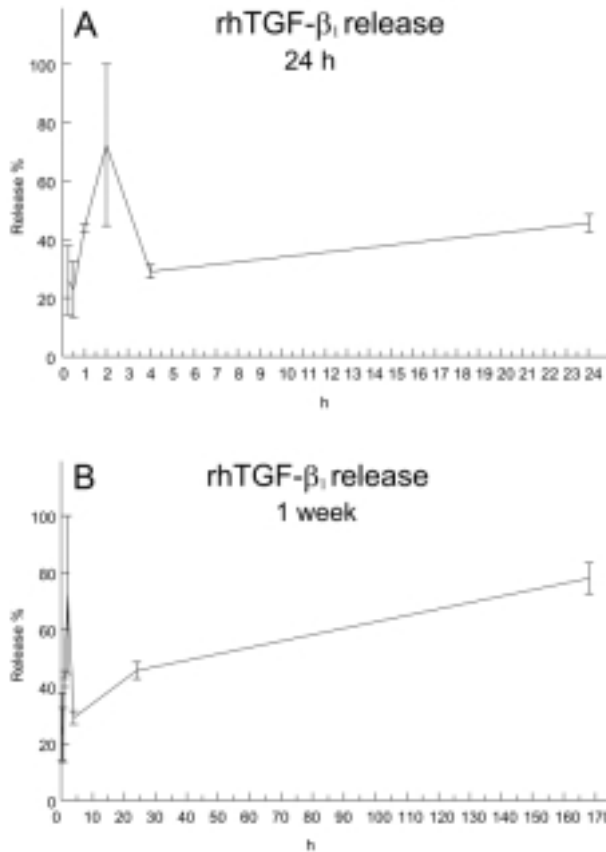
Figure 3.

Graph showing the *in vitro* rhTGF-β_1 release.
(A) A burst release can be seen in which the majority of the rhTGF-β_1 was released by 2 h, **(B)** followed by a slow release up to 1 week.

7.3 Results

7.3.1 In vitro rhTGF-β_1 release

The results of the rhTGF-β_1 release are depicted in **Figure 3**. A rapid release was observed during the first 2 h in which more than 70 % of the total dose of rhTGF-β_1 was released. Following this first peak, a decline in the level of rhTGF-β_1 occurred at 4 h. After 1 week almost 80 % of the theoretical initial 2-µg dose has been released in the medium.

7.3.2 Experimental animal study

During the experiment one rabbit died due to a broken spine. Hence, one Ti-TGF-β_1 implant and one control were lost. The other rabbits remained in good health and did not show any wound complications. At the end, a total of 26 implants (9 Ti, 9 Ti-CaP and 8 Ti-TGF-β_1 implants), and 8 controls were retrieved. At explantation, no inflammatory signs or

Figure 4.
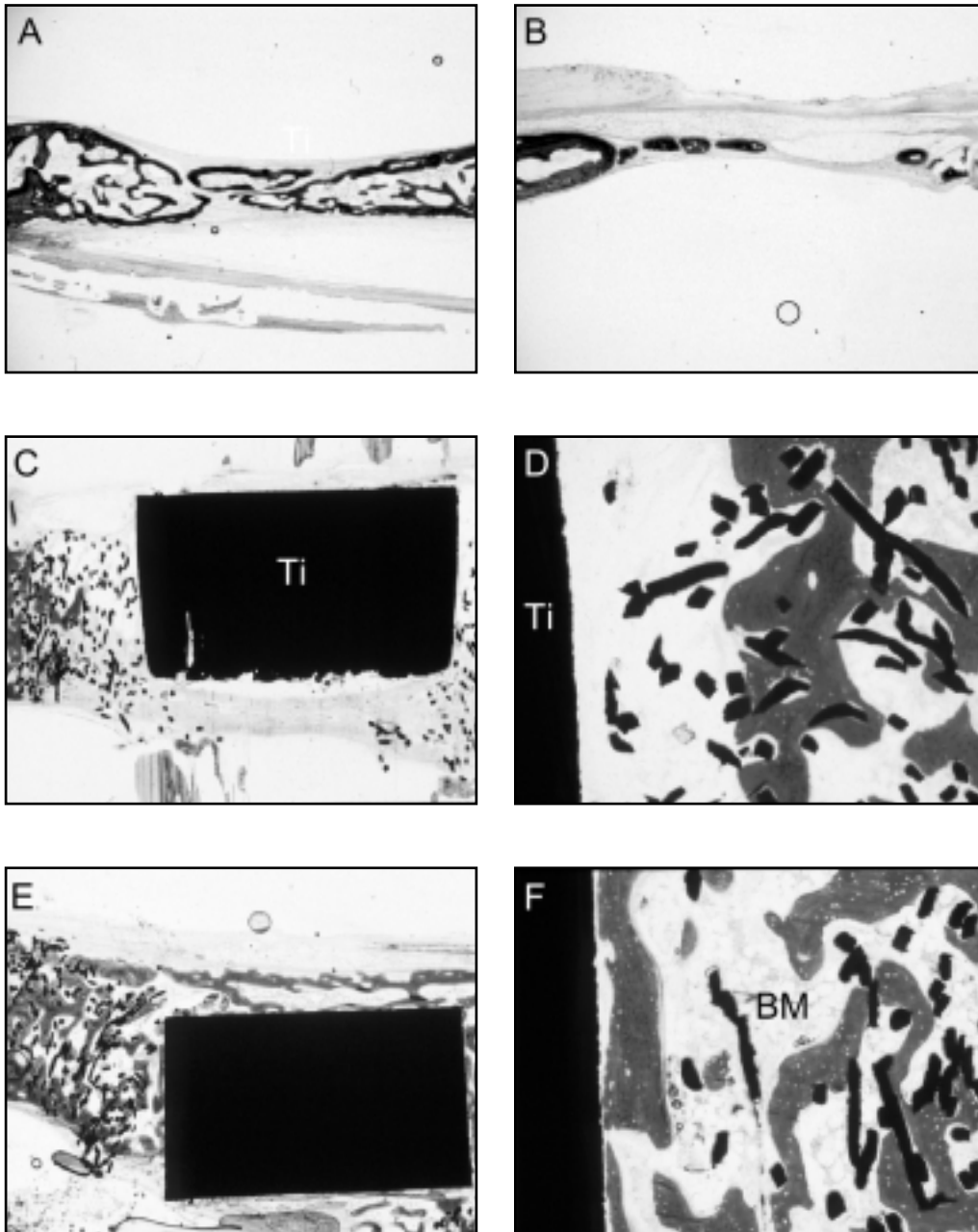
adverse tissue reaction could be seen. For the Ti-TGF-β_1 implants, bone formation could already be observed macroscopically.

7.3.3 Light microscopy, subjective

Light microscopical analysis of the sections revealed that all implants showed various levels of bone formation at 8 weeks post-implantation. The former defect edge was still visible. In and around all specimens, hardly any inflammatory cells were seen.

In two out of the eight control defects complete closure occurred (**Figure 4A**). The newly formed bone had a trabecular appearance with bone marrow lined by periosteum. On the other hand, the newly formed bone was very thin. In the non-closure defects (**Figure 4B**) the center of the defect area was filled with fibrous tissue and capillaries.

In the Ti and Ti-CaP implants bone had grown into the fiber mesh from the edge of the former defect and from the overlying periosteum (**Figure 4C**). However, penetration inside the mesh porosity was limited. Only a part of the porosity was filled with bone. Bone was present in close contact to the titanium fibers. Inside the mesh material, the newly formed bone had a trabecular appearance (**Figure 4D**). Some areas with bone marrow could be observed. The remaining non-bony part of the porosity was filled with fibrous tissue and capillaries. In some specimens bone guidance had occurred from the periosteum and dura over the top and/or bottom part of the solid titanium rod. Hardly any inflamma-

---

Figure 4.

(A) Undecalcified section of a control defect left empty. In 2 defects closure occurred (*orig. magn. 1.6x*).

(B) Undecalcified section of a control defect left empty. In 6 defects no closure occurred (*orig. magn. 1.6x*).

(C) Undecalcified section of a non-coated Ti-mesh implant at 8 weeks post-implantation. Only partial penetration of bone can be observed (Ti = solid titanium rod). Ca-P-coated Ti-mesh implants show the same histological image (*orig. magn. 2.5x*).

(D) Undecalcified section of a non-coated Ti-mesh implant at higher magnification. The Ti-CaP implants have the same morphological appearance. Only a part of the porosity is filled with bone. Bone is present in close contact to the titanium fibers. Inside the mesh material, the newly formed bone has a trabecular appearance; some areas with bone marrow can be observed. The other part of the porosity is filled with fibrous tissue and capillaries without an intervening fibrous capsule around the titanium fibers. Hardly any inflammatory cells could be seen (*orig. magn. 20x*).

(E) Undecalcified section of a non-coated Ti-mesh loaded with TGF-β_1. Bone has grown into the entire mesh up to the solid titanium core (*orig. magn. 2.5x*).

(F) Undecalcified section of a non-coated Ti-mesh loaded with TGF-β_1. The bone has a trabecular appearance and is present in close contact with the Ti-fibers without an intervening fibrous tissue layer. In addition hemopoietic bone marrow-like tissue (BM) can be observed (*orig. magn. 20x*).
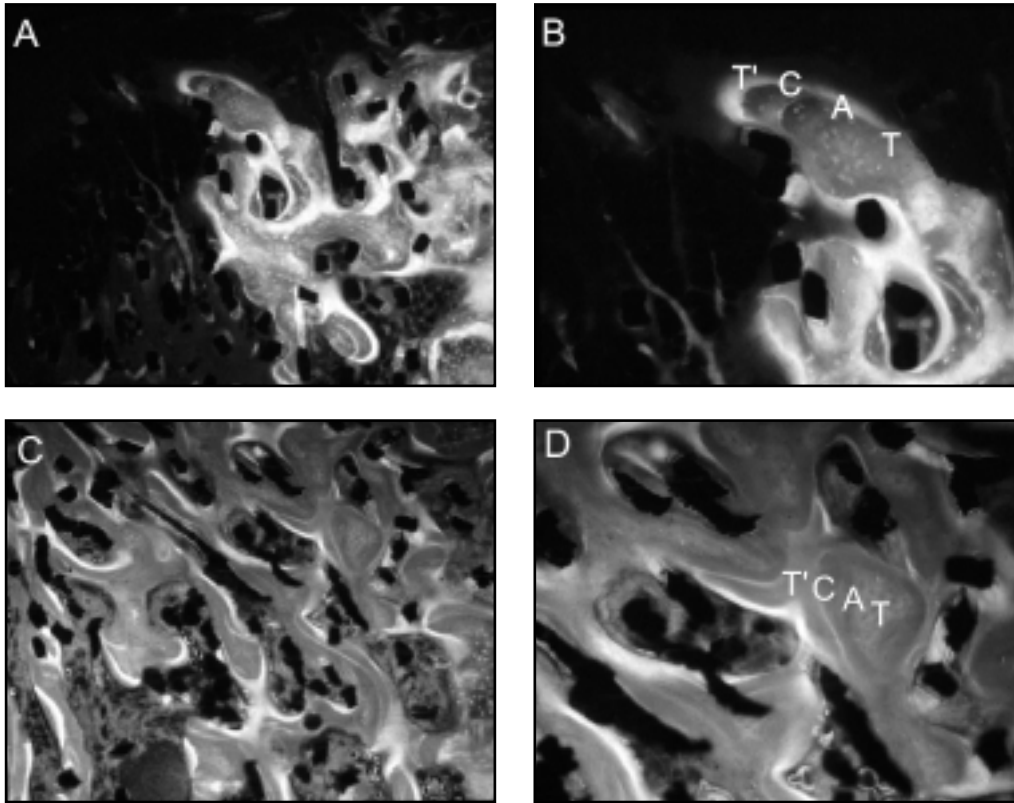
Figure 5.

(A) Non-stained undecalcified section of a non-coated Ti-mesh. This section is viewed with a fluorescence microscope. This section shows that bone formation started from the former defect edge (*orig. magn. 10x*).

(B) Non-stained undecalcified section of a non-coated Ti-mesh. This section is viewed with a fluorescence microscope. In both the Ti-CaP and Ti-implants, the accumulation sequence of the various labels, T = tetracylin (1 week), A = alizarin-complexon (3 weeks), C = calcein (5 weeks) and T' = tetracylin (7 weeks) label, indicates that bone guidance has occurred, starting from the former defect edge (*orig. magn. 20x*).

(C) Non-stained undecalcified section of a non-coated Ti-mesh loaded with rhTGF-β_1. This section is viewed with a fluorescence microscope. Bone formation started in the porosity of the mesh (*orig. magn. 10x*).

(D) Non-stained undecalcified section of a non-coated Ti-mesh loaded with rhTGF-β_1. This section is viewed with a fluorescence microscope. The accumulation sequence of the labels T = tetracylin (1 week), A = alizarin-complexon (3 weeks), C = calcein (5 weeks) and T' = tetracylin (7 weeks) label, (see Figure 5B) indicates that bone formation has started in the center of a pore growing towards the Ti-fibers (*orig. magn. 20x*).

tory cells could be seen. Subjective light microscopical analysis revealed no differences in histological appearance and bone ingrowth between Ti and Ti-CaP implants.

In the Ti-TGF-β_1 implants bone had grown into the fiber mesh up to the solid titanium core (**Figure 4E**) without an intervening fibrous tissue layer (**Figure 4F**). Extensive trabecular bone and hemopoietic bone marrow-like tissue formation was observed. Bone was present throughout and surrounding the implant in close contact with the titanium fibers. At the upper part, the newly formed bone was lined by the periosteum. In the majority of the specimens the bone also covered the top and bottom part of the solid titanium rod. The bone appeared to be more dense than in the Ti-CaP and Ti implants.

7.3.4   Fluorochrome labeling

In all specimens fluorochrome labels were clearly visible. In the Ti-CaP and Ti implants bone formation had mainly started from the wound edges (**Figure 5A**). In these implants, the accumulation sequence of the labels revealed that bone guidance had occurred from the wound edges (**Figure 5B**). In the Ti-TGF-β_1 implants bone formation had mainly started in the in the porosity of the mesh (**Figure 5C**). Fluorochrome labeling also revealed that in these implants bone formation started in the center of a pore and proceeded in a centrifugal manner towards the titanium fibers (**Figure 5D**). In addition, some bone had been formed
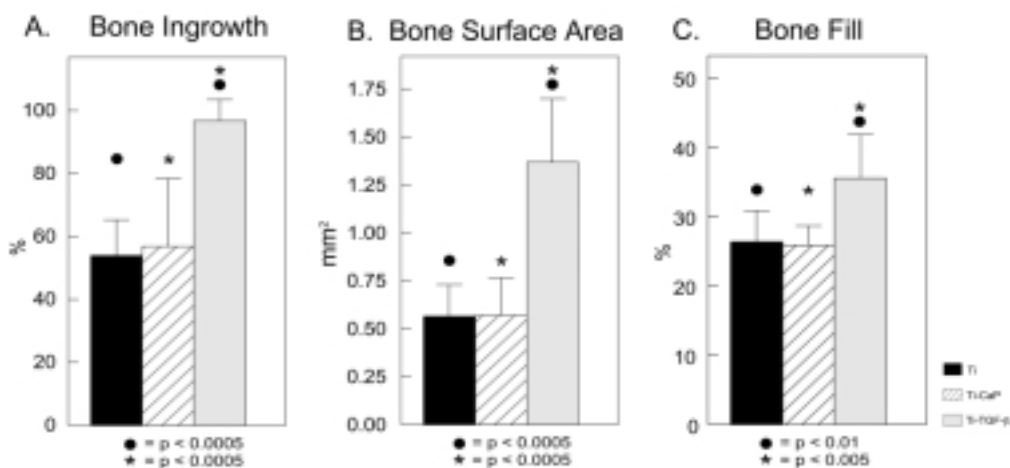

Figure 6.

Figure showing the results of the bone ingrowth (**A**), bone surface area (**B**) and bone fill (**C**). In addition, the results of the paired t-test comparing Ti with Ti-CaP and the t-tests comparing Ti with Ti-TGF-β_1 and Ti-CaP with Ti-TGF-β_1 are shown. Significant differences between Ti and Ti-TGF-β_1 (•) and Ti-CaP and Ti-TGF-β_1 (∗) are marked. No significant difference was found between Ti and Ti-Cap implants for any parameter (P>0.05).

starting from the periosteum and dura. This bone was predominantly observed over the central solid titanium core.

7.3.5 Light microscopy, image analysis

The results of the histomorphometrical measurements are depicted in **Figure 6**. In the TGF-β_1-treated implants average bone ingrowth was 97 %, whereas in the non-TGF-β_1-treated implants the average ingrowth was 57 % for the Ca-P-coated implants and 54 % for the non-coated Ti ones (**Figure 6A**). Total bone surface area was 1.37 mm^2 in the TGF-β_1-treated implants and 0.57 mm^2 in both the Ti-CaP and Ti implants (**Figure 6B**). Bone fill percentage was 36 % in the rhTGF-β_1-treated implants and 26 % in both the non-TGF-β_1-treated Ti-CaP and Ti implants (**Figure 6C**).

Results of the statistical evaluation are also depicted in **Figure 6**. Statistical evaluation revealed significant differences between the Ti-TGF-β_1 implants and the non-loaded (Ti and Ti-CaP, respectively) implants for bone ingrowth percentage, bone surface area and bone fill percentage. No differences were observed between the Ti and Ti-CaP groups for these parameters.

7.4 Discussion and conclusion

In our *in vitro* release study we found a burst release during the first 2 h in which more than 70 % of the TGF-β_1 was released. Other investigators, using different carrier materials, have also observed this kind of burst release for rhTGF-β_1.[12-14] The initial burst release was followed by a slow release, which led to a total release of almost 80 % of the rhTGF-β_1 by 1 week. This indicates that approximately 20 % of the total rhTGF-β_1 was still present on the titanium fiber mesh by that time.

Our histological findings corroborate with our earlier findings[6] and confirm again that Ti-fiber mesh is highly bone compatible as demonstrated by the ingrowth of bone and absence of inflammatory cells in all implants.

With respect to the study design, our purpose was not to create a critical size defect as illustrated by the two control defects that did show complete healing within 8 weeks. Our intent was just to show how titanium fiber mesh can be applied to support bone healing. In addition, in this study we chose not to combine the use of TGF-β_1 with a thin Ca-P-coating. From an earlier study we know that the use of an additional Ca-P-coating enhances BMP-induced bone formation.[6] Similarly, we assume that bone formation in rhTGF-β_1-loaded Ti-mesh implants might be enhanced by the use of an additional Ca-P-coating.

The histological findings also showed that both Ca-P-coated and non-coated implants allowed bone ingrowth of more than 50 % into the mesh porosity. Apparently the additional deposition of a thin calcium phosphate coating on the Ti-mesh did not have a stimulatory effect on its bone conductive properties at 8 weeks. This finding appears to contradict earlier results by our group where a favorable effect of RF magnetron sputtered

Ca-P-coatings on the implant-bone response was observed.[7-9] However, in the previous studies the coatings were deposited on solid titanium implants, whereas in the study presented here the coating was applied on a porous structure. We know that the RF magnetron sputter process does not allow complete coverage of the titanium fibers inside the porous "disc-shaped" mesh. Therefore, the resulting surface coating can be insufficient to improve bone conduction into the implant porosity.

Although the composition and design of our fiber mesh implants differs, the observed beneficial effect of rhTGF-β_1 is in agreement with the results of many other studies.[12,13,15-30]

In vivo within a certain range, a dose-responsive effect exists for TGF-β_1 with respect to bone induction. However, higher doses do not necessarily generate more bone formation as there is an optimum dose. For example, Beck *et al*.[15,16] found that 2 µg of TGF-β_1 applied in a 3 % methyl cellulose gel is able to regenerate a critical size defect in a rabbit skull in 28 days; 0.1- and 0.4-µg dose showed less bone formation. In the same model no difference was found between a 1-µg and 5-µg rhTGF-β_1 dose. In contrast, very low doses, 10 and 25 ng, mixed through a calcium phosphate cement and implanted into rat cranial defects, resulted in minimal bone growth.[31] Similarly, in a dog radial defect model a 10-ng dose combined with a poly(lactic-co-glycolic acid) carrier did not show any response.[32] Considering the available literature and selected experimental animal we decided to apply 2 µg of rhTGF-β_1 in our fiber mesh implants. Future studies have to demonstrate whether a decrease in concentration will result in the same bone response.

Another striking observation was that the Ti and Ti-CaP implants still supported a bone ingrowth of more than 50 % (about 1 mm) at 8 weeks post-implantation. In the study presented here, the thickness of the fiber mesh surrounding the solid central titanium core was 2 mm. Consequently, it can be supposed that in implants provided with a fiber mesh thickness of 1 mm or less, 100 % ingrowth can be obtained. On the other hand, bone fill was higher in the rhTGF-β_1-loaded implants than in the non-rhTGF-β_1-loaded implants. These results can be explained by a more homogenous distribution of bone in the Ti-TGF-β_1 implants. In these implants the entire mesh porosity was filled with bone. This is also illustrated by the more than twofold increase in bone surface area compared to the non-rhTGF-β_1-loaded implants.

Further, the fluorescent labeling study revealed that the process of bone formation was different between TGF-β_1-loaded and non-loaded implants. In TGF-β_1-loaded implants the newly formed bone was deposited in a centrifugal manner, starting in the porosity and growing towards the surface of the carrier. This observation was similar to the one made in previous studies in which we loaded the Ti-fiber mesh with BMPs or osteogenic cells. For bioactive materials, like hydroxyapatite loaded with BMP, so-called bonding osteogenesis, *i.e.* bone formation starting at the surface area and proceeding away from the surface, has been reported.[33] Since titanium is not a bioactive material this explains the absence of bonding osteogenesis.

Despite the favorable effect of TGF-β on bone healing, we have to emphasize that some concern exists about the safety of this growth factor in human administration. Several conditions indicative of fibrosis *a.o.*, renal and hepatic diseases, are associated with increased TGF-β_1 expression.[34,35,36] Studies have shown that transgenic animals with increased plasma levels of TGF-β_1 develop renal[37,38] and liver disease.[38] In animals, systemic injection with high doses of TGF-β_2 can also lead to renal fibrosis and a decline renal

function.[39,40] In humans, one clinical trial has demonstrated that systemic administration of TGF-β_2 can lead to a reversible decline in renal function.[41] However, these observations do not prove a causal connection between local administration of low doses of TGF-β_1 and adverse renal and hepatic effects. Nevertheless, it is important that a therapeutic index is established for TGF-β, allowing a rational approach for safe delivery and dosage of this growth factor in local therapeutic use.

In summary, we conclude that Ti-fiber mesh loaded with TGF-β_1 can indeed stimulate orthotopic bone formation in a rabbit cranial defect model. Titanium fiber mesh has good osteoconductive properties. A thin Ca-P coating, as applied in this study, does not seem to further enhance the bone-conducting properties of a titanium scaffold material at prolonged implantation periods. Although these results hold some promise for clinical application, care has to be taken. More knowledge has to be obtained about the safety of rhTGF-β_1 since systemic as well as crossover effects can occur.

References

1. **Noda M, Camilliere JJ.** *In vivo* stimulation of bone formation by Transforming Growth Factor beta. Endocrinol 1989; 124:2991.
2. **Joyce ME, Roberts AB, Sporn MB, Bolander ME.** Transforming Growth Factor beta and the initiation of chondrogenesis and osteogenesis in the rat femur. J Cell Biol 1990; 110:2195.
3. **Sampath TK, Muthukumaran N, Reddi AH.** Isolation of osteogenin, an extracellular matrix-associated, bone-inductive protein, by heparin affinity chromatography. Proc Ntl Acad Sci USA 1987; 84:7109.
4. **Ripamonti U, Duneas N, Van Den Heever B, Bosch C, Crooks J.** Recombinant Transforming Growth Factor beta-1 induces endochondral bone in the baboon and synergizes with recombinant osteogenic protein-1 (bone morphogenetic protein-7) to initiate rapid bone formation. J Bone Miner Res 1997; 12:1584.
5. **Vehof JWM, Spauwen PHM, Jansen JA.** Bone formation in CaP-coated titanium fiber mesh. Biomaterials 2000; 21:2003.
6. **Vehof JWM, Mahmood J, Takita H, van 't Hof MA, Kuboki Y, Spauwen PHM, Jansen JA.** Ectopic bone formation in titanium mesh loaded with Bone Morphogenetic Protein and coated with calcium phosphate. Plast Reconstr Surg 2001; 108:434.
7. **Hulshoff JE, van Dijk K, van der Waerden JP, Wolke JG, Kalk W, Jansen JA.** Evaluation of plasma-spray and magnetron-sputter Ca-P-coated implants: an *in vivo* experiment using rabbits. J Biomed Mater Res 1996; 31:329.
8. **Vercaigne S, Wolke JGC, Naert I, Jansen JA.** A mechanical evaluation of TiO2 -gritblasted and Ca-P magnetron sputter coated implants placed into the trabecular bone of the goat: part 1. Clin Oral Implants Res 2000; 11:305.
9. **Vercaigne S, Wolke JGC, Naert I, Jansen JA.** A mechanical evaluation of TiO2 -gritblasted and Ca-P magnetron sputter coated implants placed into the trabecular bone of the goat: part 2. Clin Oral Implants Res 2000; 11:314.
10. **Jansen JA, Wolke JG, Swann S, Van der Waerden JP, de Groot K.** Application of magnetron sputtering for producing ceramic coatings on implant materials. Clin Oral Implants Res 1993; 4:28.
11. **van der Lubbe HB, Klein CP, de Groot K.** A simple method for preparing thin (10 microM) histological sections of undecalcified plastic embedded bone with implants. Stain Technol 1988; 63:171.
12. **Lind M, Overgaard S, Nguyen T, Ongpipattanakul B, Bünger C, Soballe K.** Transforming Growth Factor beta stimulates bone ongrowth: Hydroxyapatite-coated implants studied in dogs. Acta Orthop Scand 1996; 67:611.
13. **Ongpipattanakul B, Nguyen T, Zioncheck TF, Wong R, Osaka G, DeGuzman L, Lee WP, Beck LS.** Development of tricalcium phosphate/amylopectin paste combined with recombinant human Transforming Growth Factor beta-1 as a bone defect filler. J Biomed Mater Res 1997; 36:295.
14. **Gombotz WR, Pankey SC, Bouchard LS, Ranchalis J, Puolakkainen P.** Controlled release of TGF-beta1 from a biodegradable matrix for bone regeneration. J Biomater Sci Polymer Ed 1993; 5:49.
15. **Beck LS, Deguzman L, Lee WP, Xu Y, McFatridge LA, Gillett NA, Amento EP.** Rapid publication. TGF-beta induces bone closure of skull defects. J Bone Miner Res 1991; 6:1257.
16. **Beck LS, Amento EP, Xu Y, Deguzman L, Lee WP, Nguyen T, Gillett NA.** TGF-beta1 induces bone closure of skull defects: temporal dynamics of bone formation in defects exposed to rhTGF-beta1. J Bone Miner Res 1993; 8:753.
17. **Beck LS, Wong RL, DeGuzman L, Lee WP, Ongpipattanakul B, Nguyen TH.** Combination of bone marrow and TGF-beta1 augment the healing of critical-sized bone defects. J Pharm Sci 1998; 87:1379.
18. **Arnaud E, Morieux C, Wybier M, de Vernejoul MC.** Potentiation of Transforming Growth Factor (TGF-beta1) by natural coral and fibrin in a rabbit cranioplasty model. Calcif Tissue Int 1994; 54:493.
19. **Meikle MC, Papaioannou S, Ratledge TJ, Speight PM, Watt Smith SR, Hill PA, Reynolds JJ.** Effect of poly DL-lactide--co-glycolide implants and xenogeneic bone matrix-derived growth factors on calvarial bone repair in the rabbit. Biomaterials 1994; 15:513.
20. **Gombotz WR, Pankey SC, Bouchard LS, Phan DH, Puolakkainen PA.** Stimulation of bone healing by transforming growth factor-beta 1 released from polymeric or ceramic materials. J Appl Biomater 1994; 5:141.
21. **Sumner DR, Turner TM, Purchio AF, Gombotz WR, Urban RM, Galante JO.** Enhancement of bone ingrowth by Transforming Growth Factor beta. J Bone Joint Surg Am 1995; 77:1135.
22. **Lind M, Overgaard S, Soballe K, Nguyen T, Ongpipattanakul B, Bünger C.** Transforming Growth Factor beta-1 enhances bone healing to unloaded tricalcium phosphate coated implants: An experimental study in dogs J Orthop Res 1996; 14:343.
23. **Lind M, Overgaard S, Ongpipattanakul B, Nguyen T, Bünger C, Soballe K.** Transforming Growth Factor beta-1 stimulates bone ongrowth to weight-loaded tricalcium phosphate coated implants: An experimental study in dogs. J Bone Joint Surg Br 1996; 78:377.
24. **Moxham JP, Kibblewhite DJ, Bruce AG, Rigley T, Gillespy T, Lane J.** Transforming Growth Factor beta-1 in a guanidine-extracted demineralized bone matrix carrier rapidly closes a rabbit critical calvarial defect. J Otolaryngol 1996; 25:82.

25. **Moxham JP, Kibblewhite DJ, Dvorak M, Perey B, Tencer AF, Bruce AG, Strong DM.** TGF-beta1 forms functionally normal bone in a segmental sheep tibial diaphyseal defect J Otolaryngol 1996; 25:388.

26. **Ripamonti U, Bosch C, van den Heever B, Duneas N, Melsen B, Ebner R.** Limited chondro-osteogenesis by recombinant human Transforming Growth Factor beta-1 in calvarial defects of adult baboons (Papio ursinus). J Bone Miner Res 1996; 11:938.

27. **Mc Kinney L, Hollinger JO.** A bone regeneration study: Transforming Growth Factor beta-1 and its delivery. J Craniofac Surg 1996; 7:37.

28. **Sun Y, Zhang W, Lu Y, Hu Y, Ma F, Cheng W.** Role of Transforming Growth Factor beta (TGF-beta) in repairing of bone defects. Chin Med Sci J 1996; 11:209.

29. **Sherris DA, Murakami CS, Larrabee WF Jr., Bruce AG.** Mandibular reconstruction with transforming growth factor-beta1. Laryngoscope 1998; 108:368.

30. **Zellin G, Beck S, Hardwick R, Linde A.** Opposite effects of recombinant human Transforming Growth Factor beta-1 on bone regeneration *in vivo*: effects of exclusion of periosteal cells by microporous membrane. Bone 1998; 22:613.

31. **Blom EJ, Klein-Nulend J, Yin L, Wenz R, Van Waas MAJ, Burger EH.** Transforming Growth Factor beta-1 in Calcium Phosphate Cement Stimulates Osteotransductivity. In: Proceedings of the 6th World Congress Biomaterials, Kamuela, Hawaii, USA, 2000, abstract no 338.

32. **Heckman JD, Ehler W, Brooks BP, Aufdemorte TB, Lohmann CH, Morgan T, Boyan BD.** Bone morphogenetic protein but not Transforming Growth Factor beta enhances bone formation in canine diaphyseal nonunions implanted with a biodegradable composite polymer. J Bone Joint Surg Am 1999; 81:1717.

33. **Kuboki Y, Takita H, Kobayashi D, Tsuruga E, Inoue M, Murata M, Nagai N, Dohi Y, Ohgushi H.** BMP-induced osteogenesis on the surface of hydroxyapatite with geometrically feasible and nonfeasible structures: topology of osteogenesis. J Biomed Mater Res 1998; 39:190.

34. **Border WA, Noble NA.** Transforming Growth Factor beta in glomerular injury. Exp Nephrol 1994; 2:13.

35. **Border WA, Noble NA.** Transforming Growth Factor beta in tissue fibrosis. N Engl J Med 1994; 331:1286.

36. **Fausto N, Mead JE, Gruppuso PA, Castilla A, Jakowlew SB.** Effects of TGF-betas in the liver: cell proliferation and fibrogenesis. Ciba Found Symp 1991; 157:165.

37. **Kopp JB, Factor VM, Mozes M, Nagy P, Sanderson N, Bottinger EP, Klotman PE., Thorgeirsson SS.** Transgenic mice with increased plasma levels of TGF-beta1 develop progressive renal disease. Lab Invest 1996; 74:991.

38. **Clouthier DE, Comerford SA, Hammer RE.** Hepatic fibrosis, glomerulosclerosis, and a lipodystrophy-like syndrome in PEPCK-TGF-beta1 transgenic mice. J Clin Invest 1997; 100:2697.

39. **Ledbetter S, Kurtzberg L, Doyle S, Pratt BM.** Renal fibrosis in mice treated with human recombinant transforming growth factor-beta2. Kidney Int 2000; 58:2367.

40. **Kelly FJ, Anderson S, Thompson MM, Oyama TT, Kennefick TM, Corless CL, Roman RJ, Kurtzberg L, Pratt BM, Ledbetter SR.** Acute and chronic renal effects of recombinant human TGF-beta2 in the rat J Am Soc Nephrol 1999; 10:1264.

41. **Calabresi PA, Fields NS, Maloni HW, Hanham A, Carlino J, Moore J, Levin MC, Dhib-Jalbut S, Tranquill LR, Austin H, McFarland HF, Racke MK.** Phase 1 trial of Transforming Growth Factor beta 2 in chronic progressive MS. Neurology 1998; 51:289.

Chapter 8

Bone formation in Transforming Growth Factor beta-1-coated porous poly(propylene fumarate) scaffolds

J.W.M. Vehof, J.P. Fisher, D. Dean, J.P.C.M. van der Waerden, P.H.M. Spauwen, A.G. Mikos and J.A. Jansen.

8.1   Introduction

A prerequisite for the use of osteoinductive growth factors or osteogenic cells to regenerate bone tissue is a suitable scaffold. Scaffold materials currently under investigation are polymers or co-polymers, mainly poly(α-hydroxyl acids), ceramic materials (*e.g.* hydroxyapatite and tricalcium phosphate), collagen, and titanium.

A recently developed scaffold material is the polyester poly(propylene fumarate) (PPF). This material has been shown to be biodegradable.[1-3] The degradation products are the non-toxic molecules fumaric acid and propylene glycol as well as excretable molecules related to the crosslinking of the polymer.[4] Another advantage of this viscous polymer is that it can be crosslinked into a solid with relatively low levels of heat release.[5] This allows PPF to be injected into a defect or fabricated into a scaffold prior to implantation.[6] In previous research, a chemical crosslinking method has been used. This crosslinking method uses the monomer N-vinyl pyrrolidone (NVP), the radical initiator benzoyl peroxide (BP), and the accelerator N,N dimethyl-p-toluidine (DMT).[5,7] A drawback of this method is that NVP and DMT may be potentially toxic. A photoinitiated crosslinking method has also been developed. In this method, only the photoinitiator bis(2,4,6-trimethylbenzoyl) phenylphosphine oxide (BAPO) and long wavelength ultraviolet (UV) light are used to cross-link the viscous polymer into a solid. This method eliminates the potential toxicity associated with the use of a crosslinking monomer and accelerator as well as proceeds with low levels of heat release.[8,9]

Porous PPF scaffolds are prepared by photocrosslinking the PPF polymer around a water soluble porogen (NaCl). Afterwards, the composites are placed in water, allowing the soluble NaCl to dissolve and revealing a porous scaffold. Photocrosslinked PPF scaffolds have been shown to generally possess an interconnected pore structure when NaCl porogen content weight exceeds 80 wt% at synthesis. Scanning electron microscopy has shown that pore morphology mostly is related to the porogen shape and content, not the photoinitiated crosslinking process.[9]

Currently, prewetting is the standard treatment of scaffolds before their *in vitro* or *in vivo* use.[10] Physico-chemical techniques, like RF glow-discharge treatment, are also frequently used to enhance biomaterial absorption of moisture. Since PPF is hydrophobic, it is difficult to coat prewetted PPF scaffolds with proteins in a controlled manner. Therefore, RF glow discharge appears to be a more appropriate technique for the coating process for PPF scaffolds.

An approach to improve the tissue response to biomaterials involves the use of organic coatings of proteins (*e.g.*, collagen, laminin, or fibronectin), glycoproteins, and peptides (*e.g.*, RGD peptides). These organic coatings are known for their beneficial effect on cell attachment but have also been applied to modify the *in vivo* biological response.[11-20]

The objectives of the study reported here were to investigate (1) whether PPF coated with rhTGF-β_1 can induce bone formation in an orthotopic site and (2) the effect of a fibronectin coating on the bone response to porous PPF.

8.2   Materials and Methods

8.2.1   Preparation of porous poly(propylene fumarate) scaffolds

PPF with a number average molecular weight (M_n) of 1700 Da and a polydispersity index (PI) of 1.6 (as determined by gel permeation chromatography) was synthesized for this study.[9] Poly(propylene fumarate) scaffolds were photocrosslinked using long wavelength ultraviolet light and the photoinitiator bis(2,4,6-trimethylbensoyl) phenylphosphine oxide (BAPO, Ciba Specialty Chemicals, Tarrytown, NY) in the following manner. One gram of BAPO was dissolved in 10 ml methylene chloride to form the initiator solution. The PPF was first warmed in an oven at 60°C to soften the viscous polymer and then mixed with the initiator solution (0.05 ml/g PPF). The leachable porogen, 80 wt% of 300–500 µm NaCl crystals, was subsequently added to the PPF/BAPO mixture, forming a stiff paste. This paste was packed into a cylindrical polystyrene mold (6.3 mm diameter and 2.0 mm height). The samples were then exposed to ultraviolet light for 30 min at a distance of approximately 15 cm. The UV light source was an Ultralum (Paramount, CA) ultraviolet light box outfitted with four 15W long wavelength UV bulbs. The total light emission covers a range of long UV wavelengths (320–405 nm), with a peak at 365 nm and an intensity of 4 mW/cm^2 at 15 cm. BAPO absorbs wavelengths below 400 nm, with a general increase in absorption as the wavelength decreases to 200 nm (Ciba Specialty Chemicals).

Crosslinked samples were removed from the mold and then soaked in water for three days to remove the NaCl porogen. These samples were dried, first with an absorbent cloth and then with 24 h of vacuum drying. The samples were stored under nitrogen at 4°C until sterilization by ethylene oxide gas exposure (Anprolene Automatic Ventilated Sterilizer, Anderson Products, Chapel Hill, NC). A total of 37 disc shaped implants were prepared, each approximately 6.3 mm in diameter, 2.0 mm in height, 20 mg in weight, and approximately 70% porous with a pore size of 300–500 µm.[9]

8.2.2   Implant preparation

A day before implantation, nine implants were removed from their sterile bags and pre-wetted with 70% ethanol in 2 ml vials under sterile conditions.[10] To remove air from the pores of the samples, a vacuum was pulled above the ethanol using a 50 ml syringe. After 20 min, the ethanol was removed and the samples were washed twice with sterilized distilled, deionized water. These samples were stored in distilled, deionized water and under sterile conditions at 4°C until implantation.

An additional twenty eight PPF scaffolds were removed from their sterile bags and treated for 5 minutes with radio frequency glow discharge (Gd) (Harrick PDC-3XG, Argon, 0.15 Torr) to enhance wettability. Nine of these samples, undergoing no further treatment, were stored in vials under sterile conditions at 4°C until implantation.

Ten of these glow-discharged porous PPF implants were coated with human Transforming Growth Factor beta-1, rhTGF-β_1 (R&D Systems Inc. Minneapolis, Minn., USA), which was produced by Chinese hamster ovary (CHO) cells. The rhTGF-β_1 was dissolved

in sterile 4 mM HCl containing 1 mg/ml bovine serum albumin (BSA). A dose of 30 µl of the HCl solution, containing 2 µg of rhTGF-β_1, was applied to each of the 10 PPF implants. The constructs were subsequently lyophilized and then stored under sterile conditions at 4°C until implantation.

Finally, the last nine glow discharged porous PPF scaffolds were coated with human plasma fibronectin. Lyophilized human plasma fibronectin (Sigma Aldrich Chemie b.v., Zwijndrecht, the Netherlands) was dissolved in PBS at a concentration of 100 µg/ml. A dose of 40 µl of the PBS solution, containing 4 µg of fibronectin, was added to each PPF implant. The constructs were subsequently lyophilized and then stored under sterile conditions at 4°C until implantation.

8.2.3   *In vitro* rhTGF-β_1 release

The *in vitro* release of rhTGF-β_1 from a coated PPF scaffold was measured with a commercially available enzyme-linked, immunosorbent assay (ELISA) kit (Promega® Benelux b.v., Leiden, the Netherlands). One of the rhTGF-β_1 coated implants was placed in a 24-well-plate with 2 ml of minimal essential medium (α-MEM, Gibco BRL, Life Technologies b.v., Breda, the Netherlands) containing 10 % FCS and gentamycin. The 24-well-plate was placed in an incubator (humidified atmosphere of 95 % air and 5 % CO_2 at 37°C). Two 50 µl samples were extracted at 15 min, 30 min, 1 h, 2 h, 4 h, 24 h, and 1 week. Subsequent to each of these extractions, 100 µl α-MEM solution was added to replace the lost volume. Samples were kept at 4°C until the time of measurement. The duplicate samples were prepared and diluted. The ELISA test was then performed according to the Promega® protocol. The absorption was read using a microplate reader set at a wavelength of 450 nm. All measurements were corrected for the dilution that had occurred during sampling.

8.2.4   Experimental animal study

For implantation, nine healthy, skeletally mature, male New Zealand white rabbits with a weight between 2.0 and 2.9 kg were used. The animals were housed separately in cages. Surgery was performed under general inhalation anesthesia. The anesthesia was induced by an intravenous injection of Hypnorm® (0.315 mg/ml fentanyl citrate and 10 mg/ml fluanisone) and atropine, while maintained by a mixture of nitrous oxide, isoflurane, and oxygen through a constant volume ventilator. To reduce the peri-operative infection risk, the rabbits received antibiotic prophylaxis (penicillin).

The animals were placed in a ventral position for the insertion of the implants. The dorsum of the skull was shaved, washed, and disinfected with povidone-iodine. A midsagital incision was made through the skin. The skin and subcutaneous tissue were separated from the periosteum using blunt dissection. A second longitudinal incision was made through the periosteum, which was then elevated and carefully dissected from the underlying skull bone (**Figure 1A**) before retraction. After exposure of the parietal calvarial bone, four full thickness skull defects were drilled (two on each side) using a 6.3 mm trephine (Merck®) drill at low rotational speed with continuous saline cooling (**Figure 1B**).
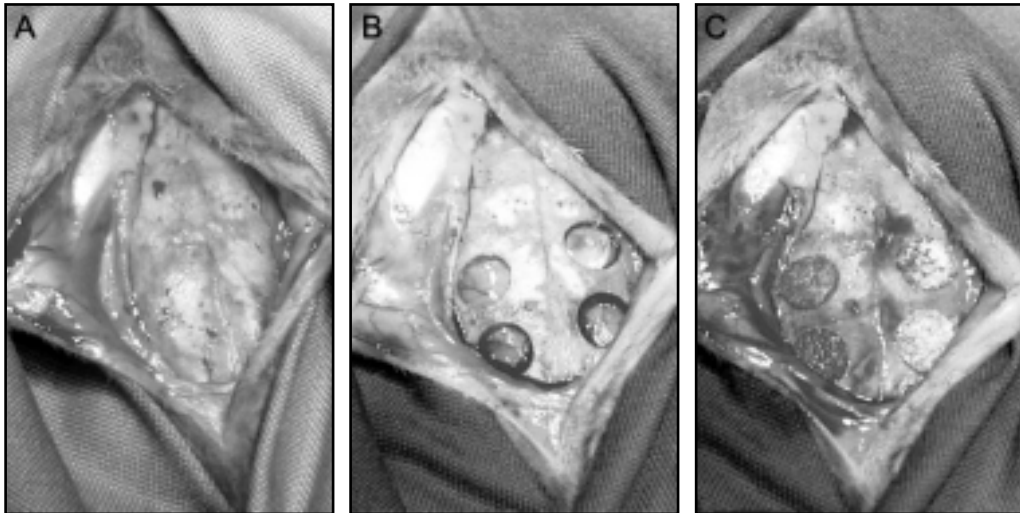
Figure 1.

Figure showing (**A**) the exposure of the skull bone, (**B**) the four cranial defects and (**C**) the inserted porous PPF scaffolds.

A cylindrical guide surrounding the trephine was used to avoid damage to the underlying dura. Subsequently, one of each of the four scaffold types was inserted (**Figure 1C**), the periosteum was closed over the implant using 3-0 Vicryl® sutures, and the skin was closed using a subcuticular Vicryl® suture.

A total of 36 scaffolds were implanted: 9 prewetted PPF scaffolds (PPF-Pw), 9 glow discharge only treated PPF scaffolds (PPF-Gd), 9 glow discharge treated PPF scaffolds coated with rhTGF-β_1 (PPF-TGF-β_1), and 9 glow discharge treated PPF scaffolds coated with fibronectin (PPF-Fn). The PPF-Pw scaffolds were used as a general control since in our group pre-wetting is the standard treatment of PPF scaffolds before experimental use. [39] The PPF-Gd scaffolds were used as a control for the TGF-β_1-coated specimens. All rabbits received one implant of each scaffold type. A statistical randomization scheme was used to locate the scaffolds so that the cranial anatomy would not affect the outcome.

Additionally, six rabbits received quadruple fluorochrome labeling. The fluorochrome labels tetracycline (yellow), alizarin-complexone (red), calcein (green), and tetracycline (yellow) were subcutaneously administered at 1, 3, 5, and 7 weeks postoperatively, respectively. The treatment dose was 25 mg/kg body weight for all labels.

At 8 weeks postimplantation, euthanasia was performed with an overdose of Nembutal® (pentobarbital). The implants with surrounding cranial tissue were retrieved *en bloc* and prepared for light microscopy. In this study, the Dutch and the U. S. National Institutes of Health guidelines for the care and use of laboratory animals were observed.

8.2.5 Light microscopy (subjective and histomorphometry)

Implants for histology were fixed in 4 % phosphate-buffered formaldehyde solution (pH = 7.4), dehydrated in a graded series of alcohol, and embedded in methylmethacrylate. After polymerization, 10 µm transverse sections were made using a modified microtome technique.[21] These sections were stained with basic fuchsin and methylene blue for evaluation by light microscopy (Leica®).

In appropriate implants, two additional sections of 30 µm were made for fluorochrome labeling analysis. These sections were left unstained and examined with a fluorescence microscope (Leica®) equipped with an excitation filter of 470 –490 nm.
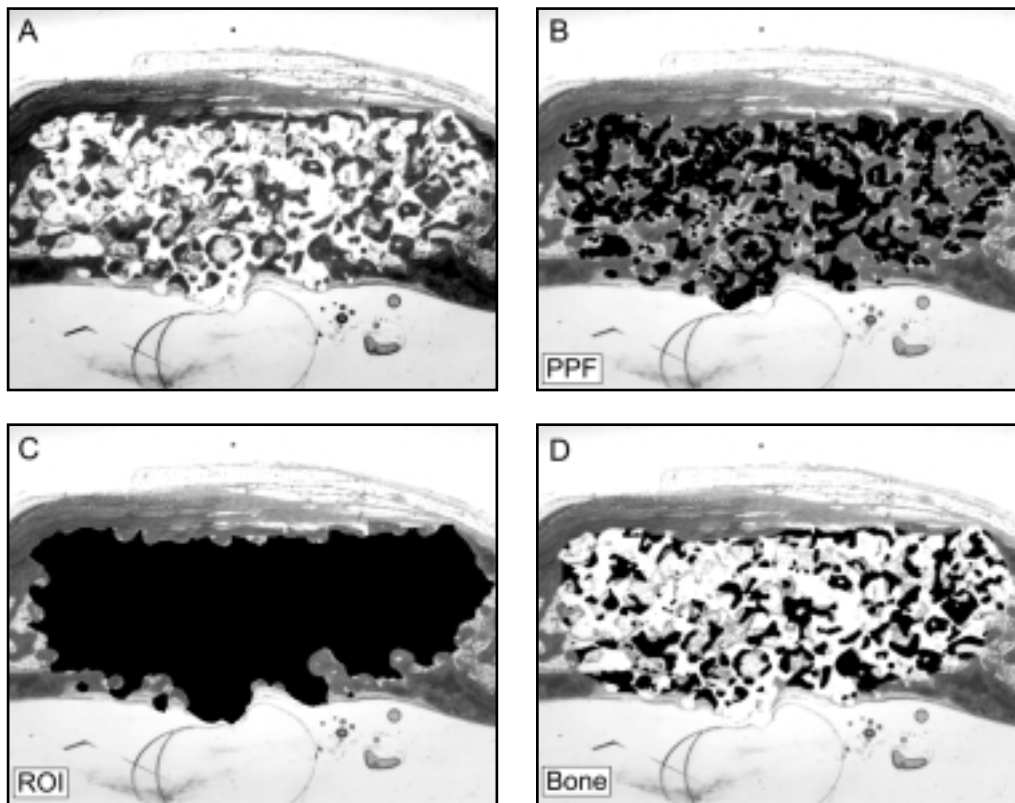
Figure 2.

Image analysis procedure. (**A**) Three histological sections per implant were digitalyzed at low magnification, allowing coverage of the entire PPF implant. (**B**) The computer detected and measured the area of the PPF. (**C**) The outline of the PPF area was then designated as the region of interest (ROI). (**D**) The computer detected and measured the area of bone within the ROI (bone surface area). From these areas, the analysis program calculated the pore area percentage, the bone area percentage and pore fill percentage.

Table 1.

The percent of bone formed in each of nine PPF scaffolds coated with TGF-β_1.

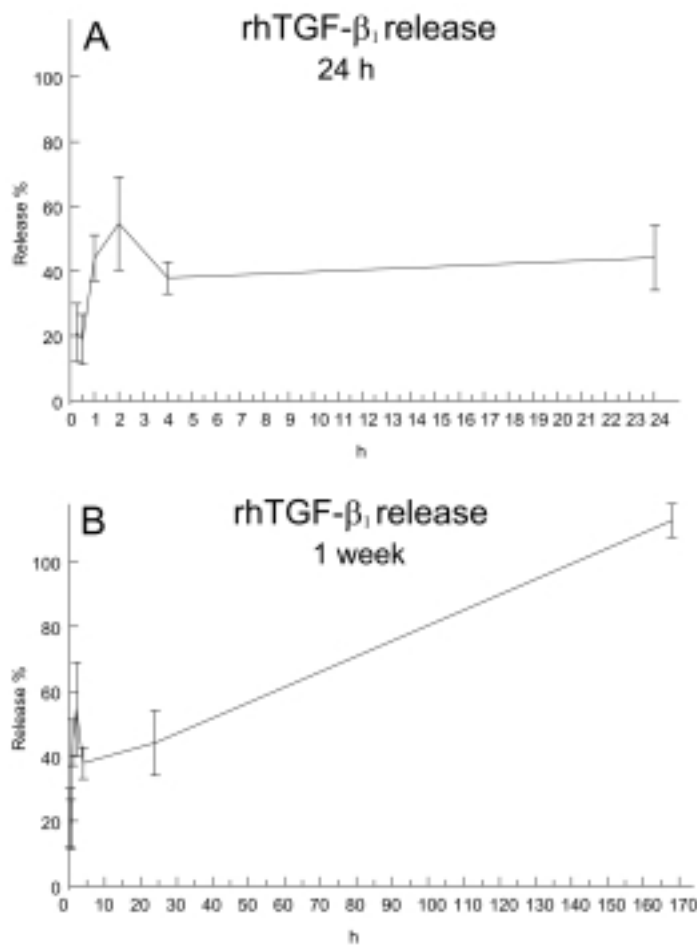| Implant number	Bone area %
1	0.9
2	16.6
3	5.7
4	4.2
5	6.3
6	12.9
7	24.3
8	10.8
9	19.5

Figure 3.

Graph showing the *in vitro* rhTGF-β_1 release.
(A) A burst release can be seen in which the majority of the rhTGF-β_1 was released by 2 h, **(B)** followed by a slow release up to 1 week [*data shown are mean +/- standard deviation (SD)*].

With the help of light- and fluorescence microscopy, the tissue response to the different implants was fully described. In addition, image analysis was performed on all sections to evaluate the quantity of newly formed bone. Specifically, three histological sections per implant were digitized at low magnification, allowing coverage of the entire PPF implant (**Figure 2A**). Using a Leica® Qwin Pro image analysis system, the computer detected the areas of the PPF implant and bone. The outline of the implant area was then designated as the region of interest (ROI). The image analysis program then measured the surface area of PPF (FSA) (**Figure 2B**), area of the ROI (**Figure 2C**), and *surface area of bone* (BSA) (**Figure 2D**). The analysis program then calculated the *percent of pore area* ([ROI - FSA]/ ROI), the *percent of bone area* (BSA/ROI), and *percent of pore fill* (BSA/ [ROI - FSA]).

Statistical Analysis
Statistical analysis was performed using a paired *t*-test. Nine repetitions were performed for all *in vivo* studied and all data are reported as means and standard deviations.

8.3 Results

8.3.1 *In vitro* TGF-β_1 release

The results of the TGF-β_1 release are depicted in **Figure 3**. A rapid release was observed during the first 2 h, during which almost 55 % of the total dose of TGF-β_1 was released. Following this initial peak, a decline in the level of TGF-β_1 occurred at 4 h. After 1 wk, the entire theoretical initial 2 µg dose was observed to have been released.

8.3.3 Experimental animal study

During the experiment all rabbits remained in good health and did not show any wound complications. At the end of the 8 wk study, all 36 implants were retrieved. At explantation, no inflammatory signs or adverse tissue reaction could be seen. For some of the PPF-TGF-β_1 implants, bone formation could already be observed macroscopically on the internal (dural) surface.

8.3.4 Light microscopy, subjective

Analysis of the sections via light microscopy revealed various levels of bone formation at 8 weeks post-implantation. For all implants, the defect edge was still visible. In all specimens, some inflammatory cells were seen.

In all non-TGF-β_1 coated implants (PPF-Pw, PPF-Gd, PPF-Fn), very limited bone growth inside the pores of the PPF scaffold could be observed (**Figure 4A,B**). Bone had grown from the edge of the former defect up to the PPF scaffold. An intervening fibrous capsule was present in between the newly formed bone and PPF scaffold. In addition, an organized fibrous capsule was present covering the top and bottom of the PPF. Inside the

PPF, some inflammatory cells, fibroblasts and small blood vessels were seen. Also, no signs of microfragmentation could be observed histologically. Subjective light microscopical analysis revealed no differences in histological appearance and bone in-growth between PPF-Gd, PPF-Fn and PPF-Pw implants.

On the other hand, in all PPF-TGF-β_1 implants bone formation had occurred. In five PPF-TGF-β_1 implants extensive bone formation had occurred (10%–25% of the original graft volume) (**Table 1**, **Figure 4E**). In these implants the bone had a trabecular appearance together with hemopoietic bone marrow-like tissue (**Figure 4F**). Bone was present throughout and surrounding the implant in close contact with the PPF pore surface without an intervening fibrous tissue layer. In some areas active bone formation could be observed with osteoblast-like cells and osteoid. Almost no PPF degradation was seen histologically. Occasionally multinucleated giant cells in contact with the PPF were observed. In the other four PPF-TGF-β_1 implants bone formation was limited (1%–6%) (**Table 1**, **Figure 4C**). The bone also had a trabecular appearance. Less hemopoietic bone marrow-like tissue was present (**Figure 4D**). In addition, some inflammatory cells were present. Where bone formation was not present within the scaffold, fibrous tissue ingrowth could be observed.

8.3.5 Fluorochrome labeling

The fluorochrome labels were clearly visible. In the non-TGF-β_1-coated implants, the accumulation sequence of the labels revealed that some initial bone formation had occurred starting at the wound edges up to the PPF scaffold (**Figure 5A**, **5B**). In the PPF-TGF-β_1 implants, bone formation was observed throughout the porous foam interior. Indeed, bone formation appeared to proceed from the interior of the pore towards the PPF scaffold (**Figure 5C**, **5D**).

8.3.6 Light microscopy, image analysis

The results of the histomorphometrical measurements show that the TGF-β_1-treated implants present an average bone surface area of 1.72 mm^2, whereas in the non-TGF-β_1-treated implants the average was 0.06–0.07 mm^2 (**Figure 6A**). Furthermore, bone filled approximately 11% of the defect area for the TGF-β_1-treated implants but less than 0.5% of the defect area for the non-TGF-β_1-treated implants (**Figure 6B**). Average pore fill percentage was approximately 16% for the TGF-β_1-treated implants and below 1% for the non-TGF-β_1-treated implants (**Figure 6C**). The pore area percentage of total scaffold volume was approximately 66% for the TGF-β_1-treated implants and 53 - 56% for the non-TGF-β_1-treated implants (**Figure 6D**).

Statistical evaluation, using a paired *t*-test, revealed significant differences between PPF-Gd and PPF-TGF-β_1 implants for bone surface area (P < 0.005), bone area percentage (P < 0.005), pore fill percentage (P < 0.005) and pore area percentage (P < 0.005) (**Figure 6**). No significant differences were observed between the PPF-Gd and PPF-Fn, and PPF-Gd and PPF-Pw implants for any parameter (**Figure 6**).

8.4   Discussion and conclusion

In our *in vitro* release study we found a burst effect during the first 2 h in which almost 55 % of the TGF-β_1 had been released. This initial burst release was followed by a slow completion of TGF-β_1 release by the end of week 1. Although this experiment does not provide data about the activity of the released TGF-β_1, our results suggest that the same release profile will occur *in situ*. The observed burst release of TGF-β_1 also corroborates previous work studying the growth factor release from titanium fiber mesh implants.[22] The initial phase of rapid protein loss is thought to be related to protein properties, especially solubility, rather than scaffold properties.[23,24] Furthermore, in the present study total

Figure 4.
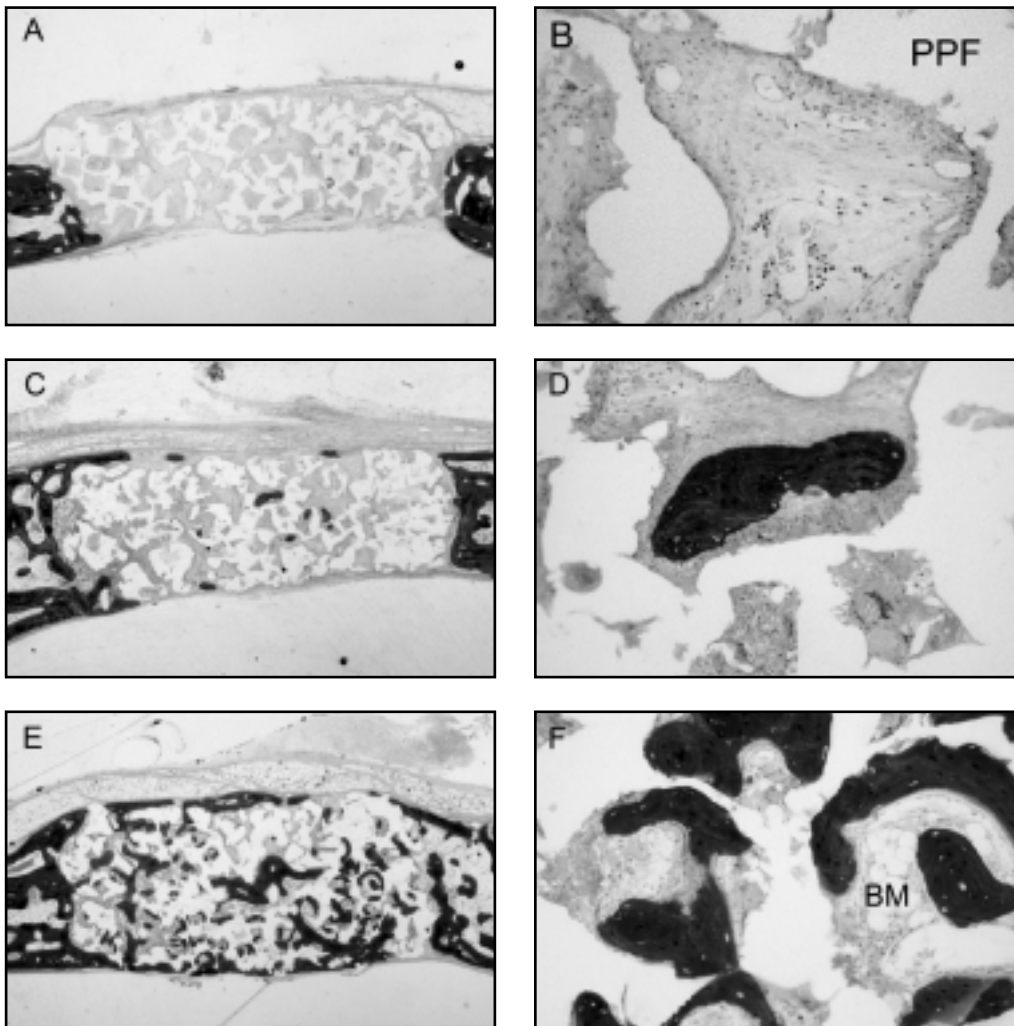
release was higher after 1 week than in our titanium mesh experiment. This may be attributable to the lower affinity of the PPF implants for TGF-β_1.[23] We also note that **Figure 3** shows a total release of approximately 112 +/- 5% (mean +/- SD), which is indicative of the error involved with the measurement.

We have previously demonstrated that the experimental design used is not a critical size defect model.[22] However, the purpose of this study was to evaluate the tissue response to TGF-β_1 adsorbed onto PPF scaffolds and non-TGF-β_1-treated PPF scaffolds. In view of this, our histological findings show again that, PPF is biocompatible with host bone.[25] There were slightly more inflammatory cells than are observed in the earlier titanium fiber mesh study.[22] but this is to be expected for a biodegradable material. However, histological

---

Figure 4.

(A) Undecalcified section of a non-coated porous PPF scaffold at 8 weeks post-implantation. Bone has grown up to the external edge of the PPF scaffold. Only very limited penetration of bone can be observed inside the PPF scaffold. PPF-Fn, PPF-Gd and PPF-Pw show a similar histological image (*orig. magn. 2.5x*).

(B) Undecalcified section of a non-coated porous PPF scaffold at higher magnification. Bone ingrowth is very limited. The porous spaces of the scaffold are filled with fibrous tissue and capillaries. The outside the PPF is surrounded by a small fibrous capsule. Some inflammatory cells (multi nucleated giant cells) are seen (*orig. magn. 20x*).

(C) Undecalcified section of a porous PPF scaffold coated with TGF-β_1. Only some bone is present throughout the porous PPF space (*orig. magn. 2.5x*).

(D) Undecalcified section of a porous PPF scaffold coated with TGF-β_1. Some bone formation is present. The formed bone has a trabecular appearance and is present in close contact with the PPF surface. Only some bone marrow-like tissue can be observed (*orig. magn. 2.5x*).

(E) Undecalcified section of a porous PPF scaffold coated with TGF-β_1. Bone is present throughout the porous PPF space. The bone has a trabecular appearance and is present in close contact with the PPF surface without an intervening fibrous tissue layer. In addition, hemopoietic bone marrow-like tissue (BM) appears to be present (*orig. magn. 20x*).

(F) Undecalcified section of a porous PPF scaffold coated with TGF-β_1. Again, the formed bone has a trabecular appearance and is present in close contact with the PPF surface without an intervening fibrous tissue layer. However, more bone marrow-like tissue (BM) can be observed compared with Figure 4D (*orig. magn. 20x*).
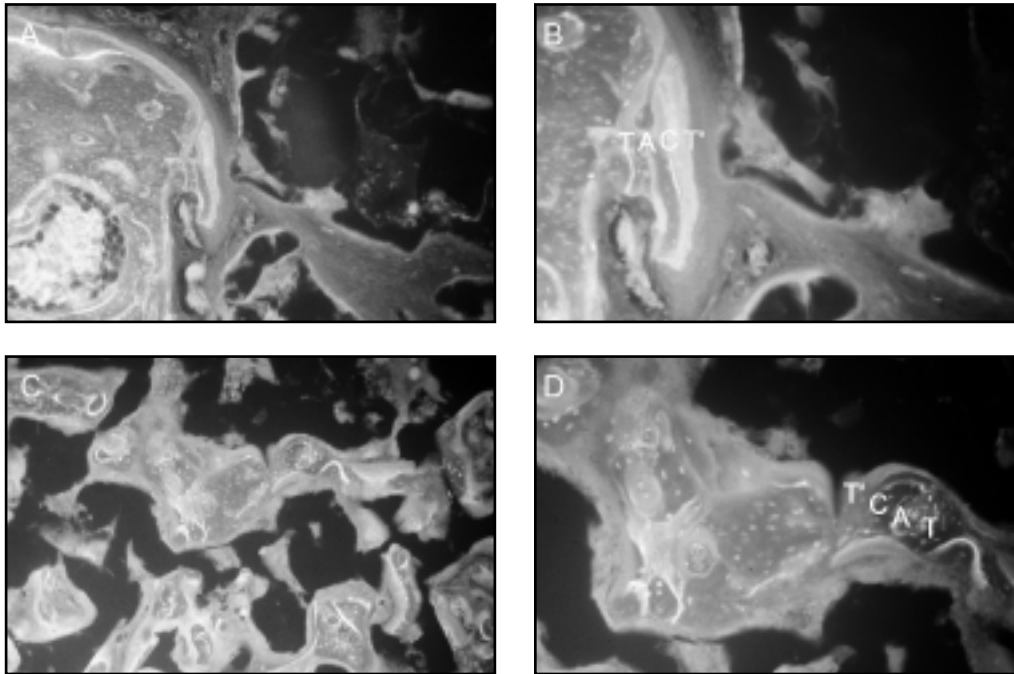
Figure 5.

(A)   Non-stained undecalcified section of a non-coated porous PPF scaffold viewed with a fluorescence microscope. Some initial bone bone guidance has occurred from the former defect edge up to the edge of the PPF scaffold. A similar result was observed in the PPF-Gd, PPF-Pw and PPF-Fn implants (*orig. magn. 10x*).

(B)   Non-stained undecalcified section of a of a non-coated porous PPF scaffold. In PPF-Gd, PPF-Pw and PPF-Fn implants, the accumulation sequence of the various labels, T = tetracylin (1 week), A = alizarin-complexon (3 weeks), C = calcein (5 weeks) and T' = tetracylin (7 weeks) label, indicates that some initial bone guidance has occurred, starting from the former defect edge up to the PPF scaffold edge (*orig. magn. 20x*).

(C)   Non-stained undecalcified section of a porous PPF scaffold coated with rhTGF-β_1. This section is viewed with a fluorescence microscope. We observe bone formation starting within the porous space (*orig. magn. 10x*).

(D)   Non-stained undecalcified section of a porous PPF scaffold coated with rhTGF-β_1. The accumulation sequence of the labels T = tetracylin (yellow, 1 week), A = alizarin-complexon (3 weeks), C = calcein (5 weeks) and T' = tetracylin (7 weeks) label (*see Figure 5 B*) indicates that bone formation has started in the center of the porous space and has grown towards the scaffold (*orig. magn. 20x*).
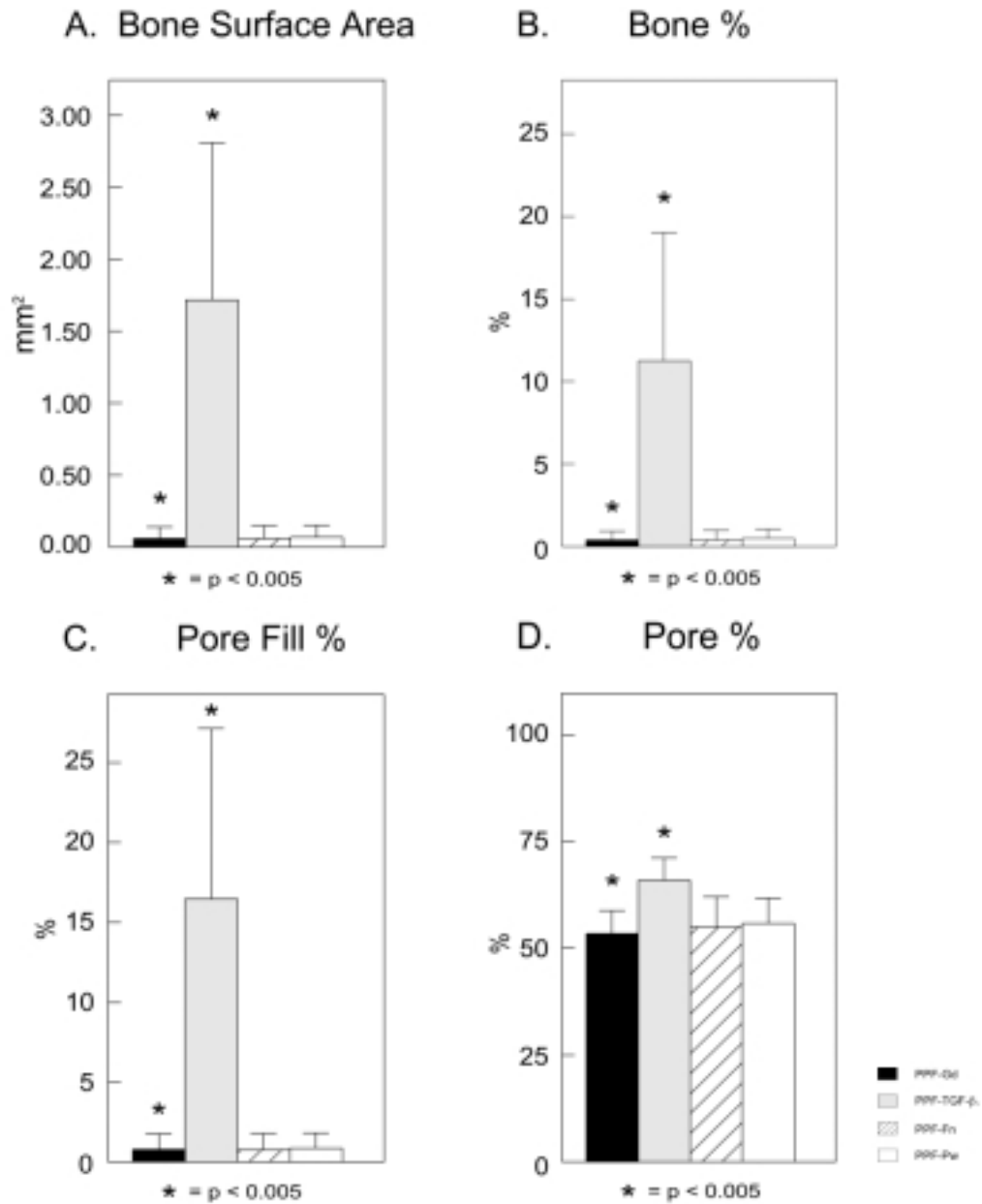
Figure 6.

Figure showing **(A)** the bone surface area, **(B)** bone area %, **(C)** pore fill % and **(D)** pore area %. In addition, the results of the paired *t*-test comparing PPF-Gd with the other implant types are shown. Significant differences between PPF-Gd and PPF-TGF-β_1 (⋆) are marked. No significant difference was found between PPF-Gd and the other non-coated implants for any parameter (p > 0. 05) (*data shown are mean +/- SD*).

observations found only a minimal sign of degradation. The polymer maintained its porous structure throughout the 8 week study. Chemically crosslinked PPF has been shown to degrade within days *in vivo* in a rat intramuscular site.[3] Furthermore, in a proximal tibial rat model, progressive replacement by bone had occurred by 5 weeks.[25] Both of these works, however, studied a PPF composite containing both a NaCl porogen and β-tricalcium phosphate. Consequently, full degradation characteristics of photocrosslinked PPF remain to be investigated over a longer time span.

The application of a fibronectin coating did not modify the tissue response to a PPF scaffold by 8 weeks. Though fibronectin has been proven to enhance osteoblast-like cell adhesion and *in vivo* bone formation by osteogenic cell-loaded scaffolds,[15] it does not further enhance the biological response in a porous PPF scaffold material. On the other hand, no adverse effects were observed. Therefore, in future experiments, we plan to investigate the osteogenic properties of fibronectin coated porous PPF scaffolds loaded with osteogenic cells.[26]

The bone stimulative effect of rhTGF-β_1 in combination with a porous carrier is in agreement with the results of many other studies.[22,27-44] The amount of bone formation within the scaffolds was variable. Five scaffolds with adsorbed TGF-β_1 showed significant amounts of bone, while four implants showed less. Comparison of the findings with our similarly designed titanium fiber mesh study[22] reveals that more bone occurred in the titanium fiber mesh with less inter-implant variation. In the present study average total bone surface area was 1.72 mm^2 per implant. In the titanium study the total bone surface area was approximately 2.74 mm^2 per implant. Two explanations can be given for these findings. First, coating difficulties caused by a relatively low affinity of TGF-β_1 for PPF could have resulted in a suboptimal amount of TGF-β_1 at the time of implantation. Although, the implants were treated with Gd to enhance adsorption, we know that a shadow effect exists, which prevents the Gd treatment to reach the surface of the inner pores. Second, a low affinity of TGF-β_1 for PPF can lead to insufficient retention of the TGF-β_1 after implantation. Unfortunately, no exact information is currently available about this phenomenon. For other osteoinductive growth factors, like BMPs, carrier-protein affinity has been more thoroughly studied.[23,24,45] The *in vivo* osteoinductive activity was found to be positively correlated with the amount of protein retained at the site. Higher retention yields a higher osteoinductive activity. Supposedly, if less growth factor is retained, a higher dose is needed for the same osteoinductive response. In view of this, due to coating difficulties or protein retention, the remaining dose on some of our implants might have been below the optimal osteoinductive level.[28,29,46,47]

Image analysis revealed a higher pore area percentage for the TGF-β_1 coated scaffolds (66 %) than for non-coated specimens (53–56 %). Several possible explanations can be given for this observation. A possible explanation is the reduced compression of the implanted PPF-TGF-β_1 foams (and thus reduced porosity decrease) because of the mechanical reinforcement of the foams due to increased bone formation. Another explanation is the reduced contraction of the implanted PPF-TGF-β_1 foams due to decreased fibrovascular tissue growth.[48] Alternatively, it may have occured due to the image analysis measuring technique which is based on color differences between the various structures. In general, the color difference between PPF and fibrous tissue is smaller than the difference between bone tissue and PPF. This may have resulted in a measurement error.

Further, fluorescent labeling revealed that in the TGF-β_1-coated scaffolds the process of bone formation had proceeded in a centrifugal manner, starting in the middle of the pores and growing towards the surface of the scaffold. We have also observed this type of bone formation in titanium scaffolds loaded with TGF-β_1, BMPs, or osteogenic cells.[22,49,50] Only for bioactive scaffold materials, so-called bonding osteogenesis, *i.e.* bone formation starting at the surface area and proceeding away from the surface, can occur.[51]

Despite the favorable effect of TGF-β_1 on bone healing, there is currently concern about the safety of this growth factor for use in humans.[52-58] One clinical trial has demonstrated that systemic administration of TGF-β_2 can lead to a reversible decline in renal function.[59] However, these observations do not prove a causal connection between local administration of low doses of TGF-β_1 and adverse effects. Nevertheless, it is important that a therapeutic index is established for TGF-β_1, allowing a rational approach for safe delivery and dosage of this growth factor in local therapeutic use.

Photocrosslinked PPF is biocompatible with host bone and shows minimal histological evidence of degradation during an 8 week experimental period. On the other hand, the osteoconductive properties of porous PPF are limited in the model used. Additionally, a fibronectin coating as applied in this study does not modify the bone response to these PPF scaffolds *in vivo*. TGF-β_1 did induce significant bone formation in these porous PPF scaffolds. These results indicate that porous PPF combined with an appropriate growth factor carrier is a good candidate for the creation of osteoinductive bone graft substitutes.

References

1. **Gresser JD, Hsu SH, Nagaoka H, Lyons CM, Nieratko DP, Wise DL, Barabino GA, Trantolo DJ.** Analysis of a vinyl pyrrolidone/poly(propylene fumarate) resorbable bone cement. J Biomed Mater Res 1995; 29:1241.
2. **Lewandrowski KU, Gresser JD, Wise DL, Trantol DJ.** Bioresorbable bone graft substitutes of different osteoconductivities: a histologic evaluation of osteointegration of poly(propylene glycol-co- fumaric acid)-based cement implants in rats. Biomaterials 2000; 21:757.
3. **Peter SJ, Miller ST, Zhu G, Yasko AW, Mikos AG.** *In vivo* degradation of a poly(propylene fumarate)/ beta-tricalcium phosphate injectable composite scaffold. J Biomed Mater Res 1998; 41:1.
4. **He S, Timmer MD, Yaszemski MJ, Yasko AW, Engel PS, Mikos AG.** Synthesis of biodegradable poly(propylene fumarate) networks with poly(propylene fumarate)-diacrylate macromers as crosslinking agents and characterization of their degradation products. Polymer 2001; 42:1251.
5. **Peter SJ, Suggs LJ, Yaszemski MJ, Engel PS, Mikos AG.** Synthesis of poly(propylene fumarate) by acylation of propylene glycol in the presence of a proton scavenger. J Biomater Sci Polym Ed 1999; 10:363.
6. **Peter SJ, Kim P, Yasko AW, Yaszemski MJ, Mikos AG.** Crosslinking characteristics of an injectable poly(propylene fumarate)/beta-tricalcium phosphate paste and mechanical properties of the crosslinked composite for use as a biodegradable bone cement. J Biomed Mater Res 1999; 44:314.
7. **Peter SJ, Yaszemski MJ, Suggs LJ, Payne RG, Langer R, Hayes WC, Unroe MR, Alemany LB, Engel PS, Mikos AG.** Characterization of partially saturated poly(propylene fumarate) for orthopaedic application. J Biomater Sci Polym Ed 1997; 8:893.
8. **Fisher JP, Dean D, Engel PS, Mikos AG.** Photoinitiated polymerization of biomaterials. Annu Rev Mater Res 2001; 31:171.
9. **Fisher JP, Holland TA, Dean D, Engel PS, Mikos AG.** Synthesis and properties of photocrosslinked poly(propylene fumarate) scaffolds. In press: J Biomat Sci Polym Ed 2001.
10. **Mikos AG, Lyman MD, Freed LE, Langer R.** Wetting of poly(L-lactic acid) and poly(DL-lactic-co-glycolic acid) foams for tissue culture. Biomaterials 1994; 15:55.
11. **Ayhan H, Gurhan I, Piskin E.** Attachment of 3T3 and MDBK cells onto poly(EGDMA/HEMA) based microbeads and their biologically modified forms. Artif Cells Blood Substit Immobil Biotechnol 2000; 28:155.
12. **Bhadriraju K, Hansen L K.** Hepatocyte adhesion, growth and differentiated function on RGD- containing proteins. Biomaterials 2000; 21:267.
13. **Bhatnagar RS, Qian JJ, Wedrychowska A, Sadeghi M, Wu YM, and Smith N.** Design of biomimetic habitats for tissue engineering with P-15, a synthetic peptide analogue of collagen. Tissue Eng 1999; 5:53.
14. **Dee KC, Rueger DC, Andersen TT, Bizios R.** Conditions which promote mineralization at the bone-implant interface: a model *in vitro* study. Biomaterials 1996; 17:209.
15. **Dennis JE, Caplan AI.** Porous ceramic vehicles for rat-marrow-derived (Rattus norvegicus) osteogenic cell delivery: effects of pre-treatment with fibronectin or laminin. J Oral Implantol 1993; 19:106.
16. **Ducheyne P, Qiu Q.** Bioactive ceramics: the effect of surface reactivity on bone formation and bone cell function. Biomaterials 1999; 20:2287.
17. **Healy KE, Rezania A, Stile RA.** Designing biomaterials to direct biological responses. Ann N Y Acad Sci 1999; 875:24.
18. **Karamuk E, Mayer J, Wintermantel E, Akaike, T.** Partially degradable film/fabric composites: textile scaffolds for liver cell culture. Artif Organs 1999; 23:881.
19. **Kornu R, Maloney W J, Kelly MA, Smith, RL.** Osteoblast adhesion to orthopaedic implant alloys: effects of cell adhesion molecules and diamond-like carbon coating. J Orthop Res 1996; 14:871.
20. **Schaffner P, Meyer J, Dard M, Nies B, Verrier S, Kessler H, Kantlehner M.** Induced tissue integration of bone implants by coating with bone selective RGD-peptides *in vitro* and *in vivo* studies. J Mater Sci Mater Med 1999; 10: 837.
21. **van der Lubbe HB, Klein CP, de Groot K.** A simple method for preparing thin (10 microM) histological sections of undecalcified plastic embedded bone with implants. Stain Technol 1988; 63:171.
22. **Vehof JWM, Haus MTU, de Ruijter JE, Spauwen, PHM, Jansen, JA.** Bone formation in Transforming Growth Factor beta-1-loaded titanium fiber mesh implants. In press: Clin Oral Impl Res, 2001.
23. **Uludag H, D'Augusta D, Palmer R, Timony G, Wozney J.** Characterization of rhBMP-2 pharmacokinetics implanted with biomaterial carriers in the rat ectopic model. J Biomed Mater Res 1999; 46:193.
24. **Uludag H, D'Augusta D, Golden J, Li J, Timony G, Riedel R, Wozney JM.** Implantation of recombinant human bone morphogenetic proteins with biomaterial carriers: A correlation between protein pharmacokinetics and osteoinduction in the rat ectopic model. J Biomed Mater Res 2000; 50:227.
25. **Yaszemski MJ, Payne RG, Hayes WC, Langer RS, Aufemorte TB, Mikos AG.** The ingrowth of new bone tissue and initial mechanical properties of a degrading polymeric composite scaffold. Tissue Eng 1995; 1:41.

26. **Dean D, Topham, NS, Rimnac C, Mikos AG., Goldberg DP, Jepsen K, Redfeldt R, Liu Q, Pennington D, Ratcheson R.** Osseointegration of preformed PMMA craniofacial prostheses coated with bone marrow impregnated Poly(DL-Lactic-co-Glycolic Acid)(PLGA)foam. Plast Reconstr Surg 1999; 104:705.

27. **Arnaud E, Morieux C, Wybier M, de Vernejoul MC.** Potentiation of Transforming Growth Factor (TGF-beta1) by natural coral and fibrin in a rabbit cranioplasty model. Calcif Tissue Int 1994; 54:493.

28. **Beck LS, Deguzman L, Lee WP, Xu Y, McFatridge LA, Gillett NA, Amento EP.** Rapid publication. TGF-beta1 induces bone closure of skull defects. J Bone Miner Res 1991; 6:1257.

29. **Beck LS, Amento EP, Xu Y, Deguzman L, Lee WP, Nguyen T, Gillett NA.** TGF-beta1 induces bone closure of skull defects: temporal dynamics of bone formation in defects exposed to rhTGF-beta1. J Bone Miner Res 1993; 8:753.

30. **Beck LS, Wong RL, DeGuzman L, Lee WP, Ongpipattanakul B, Nguyen TH.** Combination of bone marrow and TGF-beta1 augment the healing of critical-sized bone defects. J Pharm Sci 1998; 87:1379.

31. **Gombotz WR, Pankey SC, Bouchard LS, Phan DH, Puolakkainen PA.** Stimulation of bone healing by Transforming Growth Factor beta-1 released from polymeric or ceramic implants. J Appl Biomater 1994; 5:141.

32. **Lind M, Overgaard S, Nguyen T, Ongpipattanakul B, Bunger C, Soballe K.** Transforming Growth Factor beta stimulates bone ongrowth. Hydroxyapatite-coated implants studied in dogs. Acta Orthop Scand 1996; 67:611.

33. **Lind M, Overgaard S, Ongpipattanakul B, Nguyen T, Bunger C, Soballe K.** Transforming Growth Factor beta-1 stimulates bone ongrowth to weight- loaded tricalcium phosphate coated implants: an experimental study in dogs. J Bone Joint Surg Br 1996; 78:377.

34. **Lind M, Overgaard S, Soballe K, Nguyen T, Ongpipattanakul B, Bunger C.** Transforming Growth Factor beta-1 enhances bone healing to unloaded tricalcium phosphate coated implants: an experimental study in dogs. J Orthop Res 1996; 14:343.

35. **McKinney L, Hollinger JO.** A bone regeneration study: Transforming Growth Factor beta-1 and its delivery. J Craniofac Surg 1996 ; 7:36.

36. **Meikle MC, Papaioannou S, Ratledge TJ, Speight PM, Watt-Smith SR, Hill PA, Reynolds JJ.** Effect of poly DL-lactide--co-glycolide implants and xenogeneic bone matrix-derived growth factors on calvarial bone repair in the rabbit. Biomaterials 1994; 15:513.

37. **Moxham JP, Kibblewhite DJ, Bruce AG, Rigley T, Gillespy T 3rd, Lane J.** Transforming Growth Factor beta-1 in a guanidine-extracted demineralized bone matrix carrier rapidly closes a rabbit critical calvarial defect. J Otolaryngol 1996; 25:82.

38. **Moxham JP, Kibblewhite DJ, Dvorak M, Perey B, Tencer AF, Bruce AG, Strong DM.** TGF-beta1 forms functionally normal bone in a segmental sheep tibial diaphyseal defect. J Otolaryngol 1996; 25:388.

39. **Ongpipattanakul B, Nguyen T, Zioncheck TF, Wong R, Osaka G, DeGuzman L, Lee WP, Beck LS.** Development of tricalcium phosphate/amylopectin paste combined with recombinant human Transforming Growth Factor beta1 as a bone defect filler. J Biomed Mater Res 1997; 36:295.

40. **Ripamonti U, Bosch C, van den Heever B, Duneas N, Melsen B, Ebner R.** Limited chondro-osteogenesis by recombinant human Transforming Growth Factor beta-1 in calvarial defects of adult baboons (Papio ursinus). J Bone Miner Res 1996; 11:938.

41. **Sherris DA, Murakami CS, Larrabee WF Jr, Bruce AG.** Mandibular reconstruction with transforming growth factor-beta1. Laryngoscope 1998; 108:368.

42. **Sumner DR, Turner TM, Purchio AF, Gombotz WR, Urban RM, Galante JO.** Enhancement of bone ingrowth Transforming Growth Factor beta. J Bone Joint Surg Am 1995; 77:1135.

43. **Sun Y, Zhang W, Lu Y, Hu Y, Ma F, Cheng W.** Role of Transforming Growth Factor beta (TGF-beta) in repairing of bone defects. Chin Med Sci J 1996; 11:209.

44. **Zellin G, Beck S, Hardwick R, Linde A.** Opposite effects of recombinant human Transforming Growth Factor beta-1 on bone regeneration *in vivo*: effects of exclusion of periosteal cells by microporous membrane. Bone 1998; 22:613.

45. **Winn SR, Uludag H, Hollinger JO.** Sustained release emphasizing recombinant human bone morphogenetic protein-2. Adv Drug Del Rev 1998; 31:303.

46. **Blom E J, KleinNulend J, Yin L, Wenz R, Van Waas MAJ, Burger EH.** Transforming Growth Factor beta-1 in calcium phosphate cement stimulates osteotransductivity. In: Proceedings of the 6th World Congress Biomaterials, Kamuela, Hawaii, USA, 2000, abstract no 338.

47. **Heckman JD, Ehler W, Brooks BP, Aufdemorte, TB, Lohmann CH, Morgan T, Boyan BD.** Bone morphogenetic protein but not Transforming Growth Factor beta enhances bone formation in canine diaphyseal nonunions implanted with a biodegradable composite polymer. J Bone Joint Surg Am 1999; 81:1717.

48. **Goldstein AS, Zhu G, Morris GE, Meszlenyi RK, Mikos, AG.** Effect of osteoblastic culture conditions on the structure of Poly(DL-Lactic-co-Glycolic Acid) foam scaffolds. Tissue Eng 1999; 5: 421.

49. **Vehof JWM, Spauwen PHM, Jansen JA.** Bone formation in CaP-coated titanium fiber mesh. Biomaterials 2000; 21:2003.

50. **Vehof JWM, Mahmood J, Takita H, van 't Hof MA, Kuboki Y, Spauwen PHM, Jansen JA.** Ectopic bone formation in titanium mesh loaded with Bone Morphogenetic Protein and coated with calcium phosphate. Plast Reconstr Surg 2001; 108:434.

51. **Kuboki Y, Takita H, Kobayashi D, Tsuruga E, Inoue M, Murata M, Nagai N, Dohi Y, Ohgushi H.** BMP-induced osteogenesis on the surface of hydroxyapatite with geometrically feasible and nonfeasible structures: topology of osteogenesis. J Biomed Mater Res 1998; 39:190.
52. **Border WA, Noble NA.** Transforming Growth Factor beta in glomerular injury. Exp Nephrol 1994; 2:13.
53. **Border WA, Noble NA.** Transforming Growth Factor beta in tissue fibrosis. N Engl J Med 1994; 331:1286.
54. **Clouthier DE, Comerford SA, Hammer RE.** Hepatic fibrosis, glomerulosclerosis, and a lipodystrophy-like syndrome in PEPCK-TGF-beta1 transgenic mice. J Clin Invest 1997; 100:2697.
55. **Fausto N, Mead JE, Gruppuso PA, Castilla A, Jakowlew SB.** Effects of TGF-beta s in the liver: cell proliferation and fibrogenesis. Ciba Found Symp 1991; 157:165.
56. **Kelly F J, Anderson S, Thompson MM, Oyama TT, Kennefick TM, Corless CL, Roman RJ, Kurtzberg, L, Pratt BM, Ledbetter SR.** Acute and chronic renal effects of recombinant human TGF-beta2 in the rat. J Am Soc Nephrol 1999; 10:1264.
57. **Kopp JB, Factor VM, Mozes M, Nagy P, Sanderson N, Bottinger EP, Klotman PE, Thorgeirsson SS.** Transgenic mice with increased plasma levels of TGF-beta1 develop progressive renal disease. Lab Invest 1996; 74:991.
58. **Ledbetter S, Kurtzberg L, Doyle S, Pratt BM.** Renal fibrosis in mice treated with human recombinant transforming growth factor-beta2. Kidney Int 2000; 58:2367.
59. **Calabresi PA, Fields NS, Maloni HW, Hanham A, Carlino J, Moore J, Levin MC, Dhib-Jalbut S, Tranquill LR, Austin H, McFarland HF, and Racke MK.** Phase 1 trial of Transforming Growth Factor beta-2 in chronic progressive MS. Neurology 1998; 51:289.

Chapter 9

Summary, address to the aims, closing remarks and future perspectives

9.1 Summary and address to the aims

As a means to overcome the current clinical problems associated with the regeneration of bone defects, so-called tissue engineering techniques have been developed to create bone graft substitutes (BGSs). The current experimental approach consists of the use of a mostly synthetic porous scaffold or carrier to which osteogenic cells and/or growth factors are added. While extensive research has focussed on the ideal scaffold or carrier material, none of the carrier or scaffold materials that have been used so far meet all of the required demands with respect to clinical application. In view of this, we propose the use of titanium (Ti) fiber mesh as a candidate scaffold or carrier material. Titanium fiber mesh is biocompatible, easy to use during surgery and has excellent mechanical characteristics. An additional advantage is that the titanium mesh can be provided with a thin bioactive calcium phosphate (Ca-P) coating. Therefore, *in this thesis*, all of the investigations revolve around the potential use of titanium fiber mesh with or without a Ca-P coating as a carrier or scaffold material in the creation of BGSs. Consequently, a general introduction to the current knowledge on bone formation and the use of tissue engineering strategies is presented in **Chapter 1**. In the subsequent chapters, the aims as described in the scope of the thesis are addressed in a step-wise manner. Each subsequent chapter comprises a separate investigation.

Aims

1. What is the osteogenic expression in porous titanium fiber mesh loaded with rat bone marrow cells in vitro, and how is it influenced by cell seeding density and rhBMP-2 concentration?

In **chapter 2** titanium fiber mesh discs were seeded with two densities of cultured rat bone marrow (RBM) cells, i. e. a low density [3.54×10^4 cells/cm² = 10,000 cells per mesh] and a high density [3.54×10^5 cells/ cm² = 100,000 cells per mesh]. Cells were cultured for up to sixteen days, seven days of which the cells were in the presence of various concentrations of recombinant human Bone Morphogenetic Protein-2 (rhBMP-2) (0, 10, 100, and 1,000 ng/ml) in order to evaluate osteogenic expression. Scanning electron microscopy (SEM), light microscopy (LM), energy dispersive spectroscopy (EDS), DNA and calcium (Ca) content measurements, and X-ray diffraction (XRD) analysis were performed. SEM and EDS evaluation showed that a confluent layer of cells was present on top of the meshes together with collagen bundles and calcified globular accretions. Light microscopical evaluation showed a densely stained layer in the upper part of the mesh. SEM and Ca content measurement showed that calcification starts at eight days. In addition, it was demonstrated that DNA content peaked at eight days. LM, SEM, and Ca content evaluation revealed positive effects of increasing the cell seeding density, the rhBMP-2 concentration and the culture time on

mineralization. Increasing the cell seeding density also resulted in a positive effect on DNA content. No effects of rhBMP-2 concentration were seen on DNA content. Finally, XRD revealed that the deposited matrix contained a precipitate of a stable calcium phosphate phase. Therefore, we concluded that titanium fiber mesh sustains excellent osteogenic expression *in vitro*, increasing the cell seeding density has a positive effect on osteogenic expression in titanium mesh *in vitro*, and in high density specimens, rhBMP-2 concentrations of 100 ng/ml and 1,000 ng/ml, stimulate extracellular matrix calcification in a dose-responsive manner.

2. *What is the efficacy of a titanium fiber mesh loaded with cultured osteogenic cells on bone formation in an ectopic location, and what is the additional influence of the application of a thin Ca-P coating?*

Chapter 3 describes the investigation on the osteogenic activity of porous titanium fiber mesh and Ca-P-coated titanium fiber mesh loaded with cultured syngeneic osteogenic cells in a syngeneic rat ectopic assay model. In thirty syngeneic rats, Ca-P-coated and non-coated porous titanium implants were subcutaneously placed either without or loaded with cultured RBM cells. The rats were sacrificed at two, four, and eight weeks post-operative, and the implants were retrieved. Further, in the eight-week-group fluorochrome bone markers were injected at two, four, and six weeks. Histological analysis demonstrated that none of the Ca-P-coated and non-coated meshes alone supported bone formation at any time period. In RBM-loaded implants, bone formation started at two weeks. At four weeks, bone formation increased. However, at eight weeks bone formation was absent in the non-coated titanium implants, while it had remained in the Ca-P-coated titanium implants. Also, in Ca-P-coated implants more bone was formed than in non-coated samples. In general, osteogenesis was charac-terized by the occurrence of multiple spheres in the porosity of the mesh. The accumulation sequence of the fluorochrome markers showed that the newly formed bone was deposited in a centrifugal manner starting at the center of a pore. On the basis of our results, we concluded that the combination of Ti-mesh with rat bone marrow cells can indeed generate bone formation. In addition, a thin Ca-P coating can have a beneficial effect on the bone-generating properties of a scaffold material. Never-theless, the occurrence as well as the amount of new bone were very limited using the procedures described in this study.

3. *What is the effect of the cell seeding method in combination with prolonged in situ culturing on bone formation in titanium fiber mesh scaffolds in an ectopic location?*

In the investigation described in **chapter 3** we found that the occurrence as well as the amount of bone formation were very limited when osteogenic cells were seeded in Ti-fiber mesh scaffolds. We assumed that this was related to our culture and cell-loading technique that consisted of the use of the so-called droplet loading technique without prolonged culturing *in vitro*. Therefore, in the experiment described in **chapter 4** we examined the osteogenic activity of Ca-P-coated and non-coated porous Ti-fiber mesh loaded with cul-

tured syngeneic osteogenic cells after prolonged *in situ* culturing in a syngeneic rat ectopic assay model. RBM cells were loaded onto the CaP-coated and non-coated Ti-scaffolds using either a droplet or a suspension loading method. After loading, the RBM cells were cultured for eight days *in vitro*. Thereafter, implants were subcutaneously placed in thirty-nine syngeneic rats. The rats were sacrificed and the implants retrieved at two, four, and eight weeks post-operatively. Further, in the eight-week-group fluorochrome bone markers were injected at two, four, and six weeks. Histological analysis demonstrated that only the Ca-P-coated meshes supported bone formation. The amount of newly formed bone varied between single or multiple spheres to filling a significant part of the mesh porosity. In the newly formed bone, osteocytes embedded in a mineralized matrix could clearly be observed. On the other hand, in the non-coated Ti-implants abundant mineralization was present without a bone-like tissue organization. Calcium content analysis revealed that the cell-loading method did not influence the final amount of bone formation. In Ca-P-coated implants the accumulation sequence of the fluorochrome markers showed bonding osteogenesis. We conclude that the combination of Ti-mesh with RBM cells can indeed generate ectopic bone formation after prolonged *in vitro* culturing. The effect of prolonged culturing *in vitro* was different for the Ti-CaP and Ti implants: only Ca-P-coated implants supported bone formation. No effect of the loading method was observed on the final amount of bone. Finally, our results confirmed once again that a thin Ca-P coating can have an additional positive effect on the bone-generating properties of a scaffold material.

4. *Can titanium fiber mesh loaded with Bone Morphogenetic Proteins (BMPs) induce bone formation in an ectopic location, and can the osteoinductive effect of recombinant human BMP synergistically be enhanced by native bovine BMPs?*

In **chapter 5** we evaluated the osteoinductive properties of porous Ti-fiber mesh with or without a calcium phosphate (Ca-P)-coating and loaded with rhBMP-2 or rhBMP-2 and native bovine BMP [S-300 BMP cocktail (S-300)] in a rat ectopic assay model. One hundred and twelve Ca-P-coated and one hundred and twelve non-coated porous Ti-implants, either loaded with rhBMP-2 and S-300 or loaded with rhBMP-2 alone, were subcutaneously placed in fifty-six Wistar King rats. The rats were sacrificed at five, ten, twenty, and forty days post-operative and the implants retrieved. Histological analysis demonstrated that all growth factor and carrier combinations had induced ectopic cartilage and then bone formation at five and ten days, respectively. At twenty days, bone formation increased and was characterized by trabecular bone and bone marrow-like tissue. At forty days, more lamellar bone and hemopoietic bone marrow-like tissue were present. At both times more bone had been formed in the Ca-P-coated implants than in the non-coated samples. In addition, bone formation was higher in the rhBMP-2 and S-300-loaded specimens than in the rhBMP-2-only-loaded specimens. In rhBMP-2-only-loaded specimens bone formation was mainly localized inside the mesh material, while in specimens loaded with both rhBMP-2 and S-300 the bone was localized inside as well as surrounding the Ti-mesh. The histological findings were confirmed by calcium content and alkaline phospha-tase activity measurements. In addition, all specimens showed osteocalcin expression as early as five days. From these findings we deduced that the combination of Ti-mesh with BMPs can

158

indeed induce ectopic bone formation and that this bone formation seems to be similar to "*enchondral*" ossification, a thin Ca-P coating can have a beneficial ef-fect on the bone-inducing properties of a scaffold material, and rhBMP-2 and native BMP act synergistically in ectopic bone induction.

5. *What is the nature of the bone induction process in various BMP-loaded carrier materials?*

In **chapter 6** we studied the osteoinductive properties of porous Ti-fiber mesh with a calcium phosphate (Ca-P)-coating (Ti-CaP), insoluble bone matrix (IBM), fibrous glass membrane (FGM) and porous particles of hydroxyapatite (PPHAP), all loaded with rhBMP-2, using a rat ectopic assay model and short implantation periods. Twelve Ti-CaP, twelve IBM, twelve FGM and twelve PPHAP implants, all loaded with rhBMP-2 were subcutaneously placed in sixteen Wistar King rats. The rats were sacrificed at three, five, seven, and nine days post-operative, and the implants were retrieved. Histological analysis demonstrated that both IBM and Ti-CaP had induced ectopic cartilage and bone formation by five and seven days, respectively, while in PPHAP bone and cartilage formation were seen concurrently at seven days. At nine days, cartilage was seen together with trabecular bone in Ti-CaP, IBM, and PPHAP, while in FGM only cartilage was observed. We con-cluded that IBM, Ti-CaP, FGM, and PPHAP, when loaded with rhBMP-2, can indeed in-duce ectopic bone formation with a cartilaginous phase in a rat model at short implantation periods. Given the different nature of the carrier materials used these findings even suggest that an endochondral ossification-like process is always present in rhBMP-2 induced osteogenesis, even though the amount of cartilage may differ. We believe these differences are related to the vascular-inducing geometry.

6. *What is the bone formation-supporting efficacy of titanium fiber mesh as-received, provided with a thin calcium phosphate coating, or loaded with rhTGF-β_1 in an orthotopic site?*

In **Chapter 7** we evaluated the bone formation-supporting properties of porous tita-nium (Ti) fiber mesh with or without a calcium phosphate (Ca-P)-coating or loaded with recombinant human Transforming Growth Factor beta-1 (rhTGF-β_1) in a rabbit noncritical size cranial defect model. Nine Ca-P-coated and eighteen non-coated porous titanium implants, half of the latter loaded with rhTGF-β_1, were bilaterally placed in the cranium of eighteen New Zealand white rabbits. At eight weeks post-operative, the rabbits were eu-thanized and the skulls with the implants retrieved. Histological analysis demonstrated that in the TGF-β_1-loaded implants bone had been formed throughout the implant up to its center, whereas in the non-loaded implants only partial ingrowth of bone was observed. Bone formation had a trabecular appearance together with bone marrow-like tissue. No difference in ingrowth could be observed between the non-TGF-β_1-loaded, non-coated im-plants and the CaP-coated ones. All histological findings were confirmed by image analysis: 97% ingrowth was observed in the rhTGF-β_1-loaded implants, while only 57% and 54%

ingrowth was observed in the non-loaded Ca-P-coated and non-coated implants, respectively. Bone surface area and bone fill were significantly higher in the rhTGF-β_1-loaded implants (1.37 mm^2 and 36%, respectively) than in the non-loaded implants (0.57 mm^2 and 26%). No statistical difference was found for any parameter between the CaP-coated and non-coated implants. Quadruple fluorochrome labeling showed that in the Ti and Ti-CaP implants mainly bone guidance had occurred from the former defect edge, while in the Ti-TGF-β_1 implants bone formation had mainly started in the center of a pore and proceeded in a centrifugal manner. Based on these observations we concluded that the combination of Ti-mesh with TGF-β_1 can induce orthotopic bone formation, that Ti-fiber mesh has good osteoconductive properties, and that a thin Ca-P coating, as applied in this study, does not seem to further enhance the bone-conducting properties of a Ti-scaffold material.

7.   *What is the efficacy of porous PPF provided with rhTGF-β_1 on bone induction in an orthotopic site, and what is the effect of a fibronectin coating on the bone response to porous PPF?*

In **Chapter 8** we determined bone growth into pretreated poly(propylene fumarate) (PPF) scaffolds implanted into a sub-critical size, rabbit cranial defect. PPF scaffolds were first constructed using a photo-crosslinking/porogen leaching technique. These scaffolds were then either prewetted (PPF-Pw), treated with radio frequent (RF) glow-discharge (PPF-Gd), coated with fibronectin (PPF-Fn), or coated with rhTGF-β_1 (PPF-TGF-β_1). One of each scaffold type was subsequently placed into the cranium of nine New Zealand white rabbits. The rabbits were euthanized after eight weeks and the scaffolds were retrieved for histological analysis. Little or no bone formation was observed in implants without rhTGF-β_1 or in those with a fibronectin coating. No differences in bone formation were observed between the PPF scaffolds without rhTGF-β_1. The most bone formation was present in the PPF-TGF-β_1 implants; the newly formed bone had a trabecular appearance together with bone marrow-like tissue. However, bone formation showed a high inter-implant variation, from filling almost the entire porosity up to some bone formation because of the variable TGF-β_1 retention on the implants. These histological findings were confirmed by image analysis. Bone surface area, bone area percentage, pore fill percentage, and pore area percentage were significantly higher in the rhTGF-β_1-coated implants than in the non-coated implants. No statistical difference was seen between the PPF-Fn, PPF-Pw, or PPF-Gd scaffolds for these parameters. Quadruple fluorochrome labelling showed that in PPF-TGF-β_1 implants bone formation mainly started in the interior of a pore and proceeded towards the scaffold. In PPF-Gd, PPF-Pw and PPF-Fn implants, limited bone guidance had occurred from the former defect edge up to the PPF scaffold. We concluded that a PPF scaffold is bone biocompatible and, in the configuration utilized, shows minimal signs of degradation during the experimental period. TGF-β_1 can indeed adequately induce bone formation in porous PPF. These results indicate that PPF-TGF-β_1 scaffolds prepared by the photo-crosslinking/porogen leaching technique are good candidates for the creation of bone graft substitutes.

9.2 Closing remarks and future perspectives

The research conducted in this thesis provides evidence that the combination of Ti-mesh with osteogenic cells or osteoinductive factors like BMP and TGF-β can be used in the creation of bone graft substitutes.

This was demonstrated by the osteogenic expression *in vitro* and the deposition of bone-like tissue *in vivo*. *In vitro* we found that increasing the cell seeding density and rhBMP-2 concentration enhanced osteogenic expression. On the other hand, *in vivo* use of cell-based strategies in the creation of BGS, resulted in a limited amount of newly formed bone. Therefore, we investigated the efficacy of prolonged culturing *in vitro*. This effect appeared to be different for the Ca-P-coated and non-coated implants in which only the Ca-P-coated implants supported bone formation. Also, for these implants the amount of bone seemed to be slightly enhanced compared with the earlier study. Further experiments showed that the combination of Ti-mesh with BMPs can also effectively induce bone formation in ectopic locations. In addition, we showed that the combination of recombinant and partially purified native BMP act synergistically in ectopic bone induction. A comparison of the results of rhBMP-2 loaded and cell-loaded scaffolds, revealed that the rhBMP-2-loaded carrier yielded not only a greater quantity but also more reproducible bone formation in the rat ectopic assay model. The BMP-induced bone for-mation process also occurred with a cartilaginous phase present and therefore seemed similar to *"enchondral"* ossification. In addition, a comparative study between Ti-fiber mesh and various other carriers, some of which are known from previous studies to form bone through an endochondral ossification-like process (FGM, IBM) and one of which is known to induce direct ossification (PPHAP), showed the presence of a cartilaginous phase for all carriers. Considering the different nature of the carrier materials used, these findings even suggest that an endochondral ossification-like process is always present in rhBMP-2-induced osteogenesis, although the amount of cartilage does differ. The difference is believed to be related to the vascular-inducing geometry of the carriers. Carriers which show a higher vascular-inducing geometry lead to early osteogenesis and a early disappearance of cartilage, while a vascular-inhibiting geometry will lead to greater amounts of cartilage that remain for a longer time. Therefore, the terms *"bone-directing"* and *"cartilage-directing"* carrier might be appropriate for the former and the latter, respectively. This information, together with an increasing knowledge of the growth factor release profiles from different carriers, should allow a more rational approach towards carrier design and will also be beneficial in the final clinical application, where a carrier that yields high-quality bone within a short time period is highly desirable.

Further investigations showed that Ti-mesh loaded with TGF-β can stimulate bone defect healing. Our investigation of non-TGF-β-loaded titanium scaffolds revealed that the titanium fiber mesh itself has good osteoconductive properties. In addition to its application for the creation of bone graft substitutes, these investigations hold some promise for the use of titanium fiber mesh with or without growth factors in implant fixational use. Additional experiments with a newly developed porous poly(propylene fumarate) (PPF) scaffold demonstrated that this material was also bone-biocompatible and could adequately induce

bone formation when loaded with rhTGF-β_1. Nevertheless, when loaded with the same dose of rhTGF-β_1 as the Ti-carrier, PPF yielded less bone formation with a higher inter-implant variability. This was thought to be related to a lower retention of TGF-β on the PPF implants. In view of this, we have to notice that the choice of an appropriate material depends on the final application: degradation might be desirable in some situations while mechanical and structural properties are mandatory in others.

Despite the favorable effect of TGF-β on bone healing, it has to be emphasized that some concern exists with respect to the safety of this growth factor in human administration. However, no causal connection between local administration of low doses of TGF-β and adverse renal and hepatic effects have been proven. Still, it is important that a therapeutic index will be established for TGF-β, thereby allowing a rational approach for the safe delivery and dosage of this growth factor in local therapeutic use.

The application of a thin calcium phosphate coating has been shown to further stimulate the bone formation process for osteogenic cell- and BMP-2-loaded scaffolds. However, the coating technique-used might not be the optimal one for a porous scaffold, since it does not provide a bioactive surface throughout the scaffold. This was illustrated by the absence of bonding osteogenesis inside the CaP-coated scaffolds in cell-loaded and BMP- loaded scaffolds and the non-stimulative effect on the osteoconductive properties of the Ti-fiber mesh.

Consequently, future efforts should be directed towards approaches which provide a standardized and reproducible surface and improve the (biocompatibility and) functionality of the carrier material. Examples of such methodologies are sol-gel and biomimetic routes.

Our *in vitro* studies showed that the use of static culture methods resulted in the occurrence of osteogenic cells together with mineralized matrix in only the upper part of the mesh. After prolonged culturing *in vitro* and subsequent implantation, bone deposition was also observed in the upper mesh area. As a means of overcoming this problem, *in vitro* BGS culturing techniques should be directed towards dynamic seeding and culture methods like perfusion flow and rotating wall vessels (RWVs). Other investigators have proven that these methods are more beneficial in the generation of tissue-engineered bone-like tissue *in vitro*. In our group a perfusion system has also been used, which indeed did show an enhancement of osteogenic expression in titanium fiber mesh *in vitro*. Nevertheless the advantage of dynamic culture methods on *in vivo* bone formation remains to be investigated.

Moreover, we have to stress that the differentiation pathway of cells within the osteogenic lineage is still poorly understood. Increased knowledge in this area should enable a more rational approach towards tissue engineering of bone tissue. Cell selection that would enable the isolation of true osteo-progenitor cells or mesenchymal stem cells, for example through the development of specific cell markers or antibodies, would allow such an approach.

Although some of the intracellular signaling for BMPs through the Smad pathway, and the subsequent gene activation resulting in osteoblast differentiation, has now been elucidated the pathway used by BMPs in the activation of particular osteoblast genes remains to be investigated. Increased knowledge in this field will result in a rational basis in the development of clinical therapeutical strategies.

The favorable results that we obtained in rodents should be repeated in higher animals prior to a reliable transfer to the clinical situation. For example, in recent research, BMPs have been proven to be effective in clinical trials when used with a collagen carrier. However, the the response varies strongly between individuals. It has also to be emphasized that the BMP doses used are still unphysiologically high and that long-term efficacy and safety have to be awaited. Consequently, the combination of cells and growth factors and or the combination of different growth factors in an appropriate combination holds promise for the future. It might enable a decrease in the concentration of growth factors used and enhance the biological activity.

Another solution for the "*concentration*" problem of growth factors can perhaps be found by using a gene therapeutical approach in which cells within or outside the osteogenic lineage are genetically transfected *in vivo* or *in vitro* by different vectors such as retroviruses in order to overexpress growth factors. The safety of these methods concerning the fate of the transfected cells still needs further investigation.

Finally, the ultimate goal for large reconstructive surgical procedures will be the creation of a vascularized BGS using prefabrication techniques in which a vascular pedicle, for example muscle flap, is combined with an osteoinductive scaffold to form a preshaped-vascularized bone graft. Other researchers have proven that ceramic scaffolds loaded with BMPs placed in a muscle flap can be used to create a vascularized bone graft substitute and to regenerate a mandibular defect in minipigs. Again, the effectiveness of the combination of cell-based scaffolds and prefabrication remains to be proven in higher animals and humans.

Summary, address to the aims, closing remarks and future perspectives

Samenvatting, evaluatie van de doelstellingen, afsluitende opmerkingen en toekomstperspectief

9.3   Samenvatting en evaluatie van de doelstellingen

Om de huidige klinische problemen die optreden bij de behandeling van grote botdefecten te overwinnen, worden momenteel zogenaamde *tissue engineering* technieken ontwikkeld met als doel het vervaardigen van *bone graft substitutes* (BGSs) of bottransplantaat-vervangers. Hierbij wordt gebruik gemaakt van (meestal synthetische) poreuze drager-materialen, waaraan botvormende cellen en/of groeifactoren worden toegevoegd. De onderzoeksinspanningen hebben zich vooral toegespitst op het ontwikkelen van een ideaal dragermateriaal. Desondanks voldoet nog steeds geen van de nu beschikbare materialen aan alle gestelde klinische eisen. In dit verband stellen wij dan ook voor om het potentieel van titanium vezelgaas dragermateriaal te onderzoeken. Titanium vezelgaas is biocompati-bel, gemakkelijk te gebruiken bij operaties en bezit een zekere stevigheid, waardoor het met name veel geschikter lijkt voor toepassing bij de regeneratie van botweefsel dan alle tot nu toe geteste materialen. Een ander voordeel is dat titanium vezelgaas kan worden voorzien van een dunne bioactieve calciumfosfaat (Ca-P) coating. Het onderwerp van alle in dit proefschrift beschreven experimenten is dan ook het mogelijke gebruik van titanium vezelgaas met of zonder dunne Ca-P coating als dragermateriaal ter vervaardiging van BGSs. In **hoofdstuk 1** wordt een algemene inleiding gegeven over de huidige kennis op het gebied van botvorming en het gebruik van de diverse *tissue engineering* methoden. In de daarop volgende hoofdstukken worden de doelstellingen van dit *proefschrift* stapsgewijs uiteengezet. Elk hoofdstuk bevat een opzichzelfstaand onderzoek.

Doelstellingen

1. *Wat is de in vitro osteogene expressie van ratten beenmergcellen aangebracht in poreus titanium vezelgaas? Wat is verder de invloed van celdichtheid en rhBMP-2-concentra-tie op deze osteogene expressie?*

In **hoofdstuk 2** worden een zogenaamde lage dichtheid (3.54×10^4 cellen/cm^2 = 10.000 cellen per vezelgaas) en hoge dichtheid (3.54×10^5 cellen/cm^2 = 100.000 cellen per vezel-gaas) ratten beenmergcellen (RBM) aangebracht in titanium vezelgaas. Om de osteogene expressie te bepalen werden de cellen gedurende zestien dagen gekweekt, waarvan zeven dagen in aanwezigheid van diverse concentraties rhBMP-2 (0, 10, 100 en 1000 ng/ml).

Scanning electronen microscopie (SEM) en energie dispersieve spectrometrie (EDS) liet zien dat aan de bovenkant van het vezelgaas een confluente cellaag aanwezig was met verder collageen vezels en een neerslag van zogenaamde gecalcificeerde globuli. Licht microscopie (LM) bevestigde het osteogene karakter van deze laag. SEM en calcium-

bepalingen toonden aan dat het calcificatieproces van de cellen begon op dag acht. Verder bleek het DNA gehalte op die dag het hoogst te zijn. SEM, LM en calciumbepalingen lieten voorts een positief effect zien van het verhogen van de celdichtheid, de rhBMP-2 concentratie en de tijdsduur van de celkweek op de verkalking van de cellen in het vezelgaas. Het verhogen van de celdichtheid resulteerde tevens in een toename van het DNA-gehalte. Het variëren van de rhBMP-2 concentratie bleek geen effect op het DNA-gehalte te hebben. Ten slotte liet de XRD zien dat de gevormde matrix een neerslag bevatte van een stabiele calcium fosfaat fase. Hieruit concluderen we dat (1) titanium vezelgaas uitstekend de *in vitro* osteogene expressie van beenmerg cellen ondersteunt, (2) het verhogen van de celdichtheid een positief effect heeft op de *in vitro* osteogene expressie in titanium vezelgaas en (3) bij hoge celdichtheden rhBMP-2 concentraties van 100 ng/ml en 1000 ng/ml de calcificatie van de extracellulaire matrix stimuleren op een dosis afhankelijke wijze.

2. *Kan titanium vezelgaas geladen met gekweekte osteogene cellen, aanleiding geven tot botvorming in een ectopische locatie en wat is hierbij de additionele invloed van de toepassing van een dunne Ca-P coating?*

In **hoofdstuk 3** is de osteogene activiteit van poreus titanium vezelgaas, eventueel voorzien van een dunne Ca-P coating en geladen met ratten beenmergcellen onderzocht. Bij dertig genetisch identieke ratten werd poreus titanium vezelgaas met en zonder Ca-P coating en al dan niet geladen met gekweekte RBM-cellen, subcutaan geïmplanteerd. De ratten werden twee, vier of acht weken na het implanteren van de titaniumimplantaten opgeofferd, waarna histologisch onderzoek plaats vond van deze implantaten. Tevens dient hierbij opgemerkt te worden dat in de acht weken-groep na twee, vier en zes weken implantatie fluorochrome merkers geïnjecteerd werden in de ratten. Het histologisch onderzoek liet zien dat op geen enkel implantatietijdstip in geen enkel poreus titanium vezelgaas zonder RBM-cellen botvorming had plaatsgevonden. In titanium vezelgaas geladen met RBM-cellen vond wel botvorming plaats. De botvorming begon op twee weken en was na vier weken verder toegenomen. Echter na acht weken werd geen botvorming meer gezien in het niet Ca-P gecoate vezelgaas, terwijl nog wel botvorming aanwezig was in het titanium vezelgaas met een Ca-P coating. Ook was in het vezelgaas met een Ca-P coating meer bot gevormd dan in het vezelgaas zonder Ca-P coating. Over het algemeen werd de botvorming gekenmerkt door het optreden van meerdere bolvormige lokalisaties in de poriën van het titanium vezelgaas. De neerslagvolgorde van de fluorochrome merkers liet zien dat het bot was gevormd op centrifugale wijze en dat de botvorming was begonnen in het midden van een porie. Gebaseerd op deze resultaten concludeerden wij dat de combinatie van titanium vezelgaas met gekweekte RBM-cellen aanleiding kan geven tot botvorming op een ectopische lokatie. Daarnaast worden de botvormende eigenschappen van het titanium dragermateriaal verder bevorderd door het aanbrengen van een dunne Ca-P coating. Niettemin dient benadrukt te worden dat de hoeveelheid bot zeer beperkt was met de in deze studie gebruikte methoden.

3.   *Wat is het effect van de celzaai-techniek in combinatie met doorkweken in situ op ectopische botvorming in titanium vezelgaasdragers?*

In het onderzoek dat is beschreven in **hoofdstuk 3** bleek de hoeveelheid nieuw bot zeer beperkt te zijn in titanium vezelgaas geladen met osteogene cellen. We veronderstelden dat dit was gerelateerd aan onze kweek- en celzaai-techniek, die bestond uit een zogenaamde druppellaadtechniek zonder doorkweken *in vitro*. Daarom werden in het experiment zoals beschreven in **hoofdstuk 4** genetisch identieke osteogene cellen met behulp van een druppel- of een suspensiezaai-methode aangebracht in poreus titanium vezelgaas. Het vezelgaas was wederom al of niet van een Ca-P coating voorzien. Het titanium vezelgaas werd acht dagen in kweek gehouden na het aanbrengen van de beenmergcellen. Vervolgens werden de implantaten op dezelfde wijze en voor dezelfde implantatietijden, als beschreven in **hoofdstuk 3**, subcutaan aangebracht bij 39 genetisch identieke ratten. Wederom werden in de acht weken-groep fluorochrome merkers geïnjecteerd op twee, vier en zes weken. Histologisch onderzoek liet zien dat uitsluitend nieuw bot was gevormd in het titanium vezelgaas dat voorzien was van een Ca-P coating. De hoeveelheid gevormd bot varieerde van één of enkele bolvormige lokalisaties tot een hoeveelheid waarbij de porositeit voor een belangrijk deel werd gevuld. In het nieuw gevormde bot waren duidelijk osteocyten zichtbaar. Deze waren, ingebed in een gemineraliseerde matrix. In het titanium vezelgaas zonder Ca-P coating werd alleen een ruime hoeveelheid gemineraliseerde substantie waargenomen. Deze substantie vertoonde geen enkel teken van botweefsel organisatie. De calciumbepaling liet zien dat de celzaai-techniek niet van invloed was op de uiteindelijke hoeveelheid botvorming. In titanium vezelgaas met een Ca-P coating liet de neerslag volgorde van de fluorochrome merkers zien dat de botvorming begonnen was op het titanium vezelgaas oppervlak. Derhalve kan geconcludeerd worden dat de combinatie van titanium vezelgaas met RBM-cellen ectopische botvorming kan genereren na doorkweken *in vitro*. Het effect van het doorkweken *in vitro* verschilde voor titanium vezelgaas met en zonder Ca-P coating: botvorming was alleen aanwezig in dragers met een Ca-P coating. De celzaai-methode had geen enkele invloed op de uiteindelijke hoeveelheid bot. Tenslotte bevestigden onze resultaten dat een dunne Ca-P coating een additioneel positief effect kan hebben op de botvormende eigenschappen van een dragermateriaal.

4.   *Kan titanium vezelgaas dat voorzien is van botvorming stimulerende eiwitten, zogenaamde BMPs, botvorming induceren in een ectopische locatie en kan het osteo-inductieve effect van recombinant humane BMP synergistisch worden versterkt door bovine BMP?*

In **hoofdstuk 5** onderzochten wij de osteo-inductive eigenschappen van poreus titanium vezelgaas met of zonder dunne Ca-P coating en geladen met recombinant humane BMP-2 (rhBMP-2) of bovine BMP [S-300 BMP cocktail (S-300)]. Hiervoor werden 112 titanium vezelgaas dragers met een Ca-P coating en 112 zonder Ca-P coating, geladen met rhBMP-2 of rhBMP-2 + S-300. Deze implantaten werden vervolgens subcutaan aangebracht in 56 Wistar King ratten. De ratten werden na vijf, tien, twintig of veertig dagen

opgeofferd, waarbij de titanium implantaten werden verwijderd. Histologisch onderzoek liet zien dat alle groeifactor en drager combinaties na 5 en 10 dagen respectievelijk ectopische kraakbeen- en botvorming hadden geïnduceerd. Na 20 dagen nam de botvorming toe. De botvorming werd gekenmerkt door de aanwezigheid van trabeculair bot en beenmergachtig weefsel. Na 40 dagen was het bot meer lamellair van opbouw en was er meer beenmergachtig weefsel aanwezig. Na 20 en 40 dagen implantatie werd er ook duidelijk meer bot gezien in titanium vezelgaas met een Ca-P coating dan in titanium vezelgaas zonder Ca-P coating. Eveneens was er meer bot aanwezig in het vezelgaas geladen met de combinatie rhBMP-2 + S-300 dan in vezelgaas met alleen rhBMP-2. Verder was in titanium vezelgaas met rhBMP-2 de botvorming hoofdzakelijk gelokaliseerd binnen in het vezelgaas terwijl in het titanium vezelgaas met rhBMP-2 + S-300 botvorming zowel binnenin als aan de buitenkant van het titanium plaats vond. De histologische resultaten werden bevestigd door de calciumbepaling en alkalisch fosfatase-activiteit meting. Hieruit concludeerden we dat (1) de combinatie van titanium vezelgaas met BMPs ectopische botvorming kan induceren, (2) deze botvorming gekenmerkt lijkt te zijn door "*enchondrale ossificatie*", (3) een dunne Ca-P coating een positief effect heeft op de botinducerende eigenschappen van een dragermateriaal en (4) rhBMP-2 en S-300 hierbij synergistisch werken.

5. *Hoe verloopt het botvormingsproces onder invloed van BMP in verschillende drager-materialen?*

In **hoofdstuk 6** werden de osteo-inductieve eigenschappen van poreus titanium vezelgaas met een Ca-P coating (Ti-CaP), geïnactiveerde gedemineraliseerde bot matrix (IBM), glasvezel membraan (FGM) en poreuze hydroxyapatiet partikels (PPHAP) vergeleken. Al deze materialen werden geladen met rhBMP-2 en vervolgens voor 3, 5, 7 of 9 dagen subcutaan geïmplanteerd bij ratten. Histologisch onderzoek liet zien dat zowel IBM als Ti-CaP ectopische kraakbeen- en botvorming induceerden na respectievelijk 5 en 7 dagen. In PPHAP werd bot- en kraakbeenvorming waargenomen na 7 dagen implantatie. Na 9 dagen was er in Ti-CaP, IBM en PPHAP zowel kraakbeen als trabeculair bot aanwezig. In FGM daarentegen was op dit tijdsstip alleen kraakbeen te zien. Hieruit concludeerden wij dat in een rattenmodel zowel Ti-CaP, IBM, FGM als PPHAP geladen met rhBMP-2 reeds na korte tijd ectopische botvorming kunnen induceren. De botvorming ging altijd gepaard met kraakbeenvorming. De hoeveelheid kraakbeen kan hierbij echter verschillen. Wij veronderstellen dat deze verschillen samenhangen met de mate waarin bloedvatingroei in het dragermateriaal kan plaats vinden.

6. *Wat is de botvormingondersteunende activiteit van recombinant humane Trans-forming Growth Factor beta-1 (rhTGF-β1) aangebracht in titanium vezelgaas, in een orthotopische locatie?*

In **hoofdstuk 7** evalueerden we de botvormingondersteunende eigenschappen van poreus titanium (Ti) vezelgaas al of niet voorzien van een Ca-P coating (Ti-CaP) en geladen met rhTGF-β_1 (Ti-TGF-β_1) in een schedeldakdefect bij konijnen. Negen Ti-CaP, negen Ti en negen Ti-TGF-β_1 implantaten werden aangebracht in de schedels van achttien konijnen. Na acht weken werden de konijnen opgeofferd en werden de schedels met de implantaten verwijderd. Histologisch onderzoek liet zien dat in het vezelgaas met rhTGF-β_1 bot was ge-vormd door de gehele porositeit van het implantaat tot aan de kern. In de implantaten zonder rhTGF-β_1 vond slechts gedeeltelijke botingroei plaats. Het nieuw gevormde bot werd gekenmerkt door trabeculair bot met beenmergachtig weefsel. In de implantaten zonder rhTGF-β_1 werd geen verschil in botingroei gevonden tussen implantaten met en zonder Ca-P coating. Alle histologische bevindingen werden bevestigd door beeldanalyse; 97% ingroei werd gezien in de met rhTGF-β_1 geladen implantaten, terwijl de niet-geladen implantaten met of zonder Ca-P coating respectievelijk 57% en 54% ingroei lieten zien. Het totale botoppervlak in het vezelgaas (1,37 mm²) en de hoeveelheid bot als percentage van het totale vezelgaas oppervlak (36%) waren significant groter in de met rhTGF-β_1 geladen implantaten vergeleken met de niet-geladen implantaten (0,57 mm² en 26%). Er werden geen statistische verschillen gevonden tussen implantaten met of zonder Ca-P coating voor de bestudeerde parameters. Fluorochrome merkers lieten zien dat in de Ti en de Ti-CaP implantaten met name botgeleiding had plaatsgevonden vanuit de oorspronke-lijke rand van het botdefect. In de Ti-TGF-β_1 implantaten startte de botvorming in het mid-den van een porie en breidde zich vervolgens uit op centrifugale wijze. Op basis van deze bevindingen concluderen wij dat (**1**) de combinatie van titanium vezelgaas geladen met rhTGF-β_1 orthotopische botvorming kan induceren, (**2**) titanium vezelgaas goede osteo-conductieve eigenschappen bezit, en (**3**) een dunne Ca-P coating, zoals in deze studie werd toegepast, de botgeleidende eigenschappen van het Ti-dragermateriaal niet verder stimu-leert.

7. *Wat is het osteo-inductief vermogen van poreus poly(propyleen fumaraat) (PPF) voor-zien van rhTGF-β1 in een orthotopische locatie en wat is tevens het effect van het aan-brengen van een fibronectinecoating op het poreuze PPF op de uiteindelijke botrespons?*

In **hoofdstuk 8** bestudeerden we de botvormingondersteunende eigenschappen van voorbehandelde PPF-dragers aangebracht in een schedeldakdefect bij koijnen. Het poreuze PPF-dragermateriaal werd op vier verschillende manieren voorbehandeld: (**1**) voorbevoch-tigd met alcohol en water (PPF-Pw), (**2**) radiofrequent gloeien (PPF-Gd), (**3**) aanbrengen van een fibronectine coating (PPF-Fn) en (**4**) aanbrengen van een rhTGF-β_1 coating (PPF-TGF-β_1). Bij negen konijnen werd één specimen van elk type drager in de schedel aange-bracht. Na acht weken werden de konijnen opgeofferd en werden de implantaten histo-logisch bewerkt. Licht microscopisch onderzoek liet vervolgens zien dat in de implantaten zonder rhTGF-β_1 bijna geen bot was gevormd. Daarentegen werd wel bot gevormd in de

porositeit van de PPF-TGF-β_1 implantaten. Het nieuw gevormde bot had een trabeculaire structuur . Tussen de trabekels werd beenmergachtig weefsel gezien. Echter de botvorming in de PPF-TGF-β_1 implantaten vertoonde grote inter-individuele verschillen. De hoeveelheid botvorming varieerde van vrijwel volledige opvulling van de PPF-porositeit tot een zeer beperkte opvulling. Deze histologische bevindingen werden bevestigd door beeldanalyse, waarbij er kwantitatief telkens meer bot in de PPF-TGF-β_1 implantaten werd waargenomen in vergelijking met de andere voorbehandelingen. Fluorochrome merkers lieten zien dat in de PPF-TGF-β_1-implantaten de botvorming startte in het midden van een porie en zich vervolgens uitbreidde op centrifugale wijze in de richting van het oppervlak van de PPF. In PPF-Gd-, PPF-Pw- en PPF-Fn-implantaten was zichtbaar dat beperkte botgeleiding had plaatsgevonden vanuit de oorspronkelijke rand van het botdefect tot aan de PPF-drager. Op basis van deze bevindingen concludeerden we dat een PPF-dragermateriaal biocompatibel is met bot tijdens de experimentele periode. Daarnaast kan rhTGF-β_1 op adequate wijze botvorming induceren in poreus PPF. Deze resultaten geven aan dat een PPF-drager voorzien van rhTGF-β_1 zeer geschikt is voor het vervaardigen van BGSs.

9.4   Afsluitende opmerkingen en toekomstperspectief

Het onderzoek dat werd uitgevoerd in dit *proefschrift*, toont aan dat de combinatie van titanium vezelgaas met osteogene cellen of osteo-inductieve groeifactoren zoals BMP en TGF-β, gebruikt kan worden ter vervaardiging van bottransplantaten. Dit werd geïllustreerd door de ostegene expressie *in vitro* en de vorming van botachtig weefsel *in vivo*. *In vitro* vonden we dat het verhogen van de celdichtheid en de rhBMP-2 concentratie een positieve invloed had op de osteogene expressie. Het *in vivo* gebruik van *tissue engineering* strategieën waarbij cellen gebruikt worden voor het vervaardigen van BGSs, resulteerde in de vorming van een beperkte hoeveelheid nieuw bot. Daarom onderzochten we de werkzaamheid van doorkweken *in vitro*. Het effect van doorkweken bleek verschillend te zijn voor implantaten met en zonder Ca-P coating: alleen de eerstgenoemde groep bleek botvorming te ondersteunen. Voor de implantaten met een Ca-P coating leek de hoeveelheid nieuw bot enigszins te zijn toegenomen in vergelijking met de eerdere studie. Andere experimenten lieten daarnaast zien dat ook de combinatie van titanium vezelgaas met BMPs ectopische botvorming kan induceren. Bovendien hebben we laten zien dat de combinatie van recombinante humane BMP en (deels) gezuiverde bovine BMP hierbij synergistisch werkt. Wanneer de resultaten van het onderzoek –*waarin titanium met rhBMP-2 werd geladen*– worden vergeleken met het onderzoek –*waarin deze drager met cellen werd geladen*–, blijkt dat in de eerstgenoemde groep niet alleen meer bot gevormd wordt maar dat de botvorming eveneens op meer reproduceerbare wijze plaatsvindt. In het botvormingsproces dat door BMP wordt geïnduceerd is altijd een kraakbeenfase aanwezig. Een vergelijkende studie tussen titanium vezelgaas en andere dragers, twee waarvan eerder werd gevonden dat zij enchondrale botvorming induceerden (FGM, IBM) en één waarvan eerder was gevonden dat het directe botvorming induceerde (PPHAP), liet zien dat toch voor alle dragers een kraakbeenfase aanwezig was. Bovendien suggereren deze bevindingen dat bij rhBMP-2-geïnduceerde botvorming altijd een enchondrale botvormingachtig proces plaatsvindt ongeacht het gebruikte dragermateriaal. De hoeveelheid kraakbeen kan hierbij echter verschillen. Wij veronderstellen dat deze verschillen samenhangen met de mate waarin het dragermateriaal de ingroei van bloedvaten stimuleert. In dragers die vaatingroei stimuleren vindt vroege osteogenese plaats en verdwijnt het gevormde kraakbeen eerder. In dragers die de vaatingroei remmen wordt een grotere hoeveelheid kraakbeen gevormd die ook langer aanwezig blijft. Daarom zouden op deze twee groepen respectievelijk de termen "***bone-directing***" en "*cartilage directing*" van toepassing kunnen zijn. Deze informatie in combinatie met de toenemende kennis op het gebied van het afgiftepatroon van groeifactoren van verschillende dragers, zou een meer rationele benadering van het ontwikkelen van dragers mogelijk maken. Deze benadering is eveneens van belang bij de uiteindelijke klinische toepassing, waarbij een drager die bot induceert van een hoge kwaliteit binnen een korte tijdsperiode zeer wenselijk is.

Verder onderzoek liet zien dat titanium vezelgaas voorzien van rhTGF-β_1 eveneens de genezing van botdefecten kan stimuleren. Ons onderzoek van titanium vezelgaas zonder rhTGF-β_1 liet zien dat titanium vezelgaas zelf al over goede osteoconductieve eigenschappen bezit. In aanvulling op het gebruik van het titanium vezelgaas ter vervaardiging van

BGSs zijn deze resultaten veelbelovend voor de toepassing (met of zonder groeifactoren) van dit materiaal bij de fixatie van implantaten. Aanvullende experimenten met een nieuw ontwikkelde polymeer, poreus poly(propyleen fumaraat) (PPF) drager toonde aan dat dit materiaal biocompatibel was met bot en botvorming kon induceren wanneer het was voorzien van rhTGF-β_1. Echter wanneer dit materiaal werd voorzien van dezelfde hoeveelheid rhTGF-β_1 als de titanium drager resulteerde dit in minder botvorming waarbij ook nog eens een grotere variatie tussen de implantaten aanwezig was. Dit is mogelijk gerelateerd aan een lagere rhTGF-β_1 retentie in de PPF. Daarom is de keuze van een passend dragermateriaal afhankelijk van de uiteindelijke toepassing: afbreekbaarheid kan immers wenselijk zijn in bepaalde situaties, terwijl mechanische en structurele eigenschappen vereist zijn in andere situaties.

Ondanks het gunstige effect van TGF-β op botgenezing moet worden benadrukt dat enige bezorgdheid bestaat omtrent de veiligheid van deze groeifactor bij toediening aan mensen. Echter tot op heden is geen causaal verband aangetoond tussen lokale toediening van lage doses TGF-β en nadelige effecten op de nier of lever. Niettemin is het belangrijk dat een therapeutische index wordt bepaald voor TGF-β die een meer rationele benadering mogelijk maakt voor de veilige afgifte en dosering van deze groeifactor in lokale therapeutische toepassingen.

De toepassing van een dunne Ca-P coating op titanium vezelgaas heeft aangetoond dat dit de botvorming verder stimuleert, zowel voor dragers met osteogene cellen als dragers met BMP-2. Echter de gebruikte hoog vacuüm coating techniek zou wel eens niet de meest optimale kunnen zijn voor deze toepassing, omdat wij weten dat de coating niet door het hele materiaal heen dringt en het bioactieve oppervlak derhalve niet aanwezig is door het gehele dragermateriaal. Dit werd geïllustreerd door de wijze waarop de botvorming plaats vond in de dragers met een Ca-P coating. Tevens blijkt deze beperking van de gebruikte coating techniek uit het feit dat de osteoconductieve eigenschappen van titanium vezelgaas niet gestimuleerd werden.

Gelet op het voorgaande dient toekomstig onderzoek te zijn gericht op een aanpak die voorziet in het ontwikkelen van een gestandaardiseerde en reproduceerbare oppervlakte voorbehandelingstechniek, die de functionaliteit van een dragermateriaal kan verbeteren. Mogelijkheden zijn wellicht het gebruik van *sol-gel* en *biometische* coatings.

Onze *in vitro* studies lieten zien dat bij het gebruik van statische kweekmethoden cellen en gemineraliseerde matrix alleen gevonden worden bovenin het vezelgaas. Om dit probleem op te lossen moet meer gebruik gemaakt worden van dynamische zaai- en kweekmethoden zoals "*perfusion flow*" en "*rotating wall vessels*" (RVWs). Andere onderzoekers hebben reeds bewezen dat deze methoden nuttig kunnen zijn bij het vervaardigen van botachtig weefsel *in vitro*. In onze onderzoeksgroep hebben we reeds gebruik gemaakt van een "*perfusion flow*" systeem. Het gebruik van dit systeem liet inderdaad een toename zien van de osteogene expressie in titanium vezelgaas *in vitro*. Het voordeel van dynamische methoden op de botvorming *in vivo* moet echter nog worden onderzocht.

Daarnaast moeten we benadrukken dat het differentiatie proces van osteoblasten slechts voor een deel is opgehelderd. Een toename van de kennis op dit gebied zou een meer gerichte benadering mogelijk maken met betrekking tot *tissue engineering* van botweefsel. Celselectie van osteoprogenitor cellen of mesenchymale stamcellen door specifieke celmarkers of antilichamen zou in dit verband bijvoorbeeld een oplossing kunnen bieden.

Hoewel een deel van het intracellulaire communicatieproces voor BMPs via de zogenaamde *Smad* route en de daaropvolgende gen-activatie, die resulteert in osteoblast differentiatie, momenteel is opgehelderd, is de precieze route die BMPs gebruiken bij de activatie van specifieke osteoblastgenen nog niet onderzocht. Vergroting van de kennis op dit terrein is essentieel voor de uiteindelijke klinische therapeutische toepassing van BMP.

De positieve resultaten die werden gevonden in knaagdieren, dienen herhaald te worden in hogere dieren alvorens een betrouwbare extrapolatie mogelijk is naar de klinische situatie. In recent klinisch onderzoek bijvoorbeeld, is de werkzaamheid van BMPs met een collageen drager aangetoond bij het genezen van botdefecten. Echter de botvormingsrespons varieert sterk tussen individuen. Ook dient te worden benadrukt dat de gebruikte doses van BMP nog steeds onfysiologisch hoog zijn en dat de lange termijn effecten en veiligheid nog moeten worden afgewacht. Reden waarom de combinatie van cellen met groeifactoren of de combinatie van verschillende groeifactoren in de juiste verhouding veelbelovend voor de toekomst is. Dit zou een afname in de gebruikte concentratie van de groeifactor mogelijk maken en de biologische activiteit wellicht vergroten.

Een andere oplossing voor het "*concentratie*" probleem van groeifactoren is misschien gelegen in de toepassing van een gentherapeutische benadering. In deze benadering worden cellen, uit de osteoblasten reeks of daarbuiten, genetisch getransfecteerd *in vivo* of *in vitro*. Hierbij wordt gebruik gemaakt van verschillende vectoren zoals retro-virussen om groeifactoren tot (over)expressie te brengen. De veiligheid van deze methoden en de uiteindelijke afloop van de getransfecteerde cellen dient nader te worden onderzocht.

Tot slot is het ultieme doel voor grote reconstructieve chirurgische ingrepen het creëren van een gevasculariseerde BGS door gebruik te maken van préfabricage technieken. Hierbij wordt de aanwezigheid van een vaatvoorziening gecombineerd met een osteoinductieve drager (*door de drager bijvoorbeeld in een spierlap te plaatsen*), zodat op deze wijze een voorgevormd gevasculariseerd bottransplantaat kan worden vervaardigd. Andere onderzoekers hebben bij varkens (*minipigs*) reeds aangetoond dat wanneer keramische dragermaterialen voorzien van BMPs, in een spierlap worden geplaatst, dit resulteert in de vorming van een gevasculariseerd botransplantaat. Met deze transplantaten kunnen defecten in de mandibula worden genezen. Opnieuw dient de effectiviteit van préfabricage technieken in combinatie met dragers voorzien van botvormende cellen nog te worden bewezen in hogere diersoorten en mensen.

Dankwoord

Promoveren doe je niet alleen. Een groot aantal mensen zijn dan ook betrokken geweest bij de totstandkoming van dit proefschrift. Hierbij wil ik de volgende mensen bedanken voor hun bijdrage.

Prof. dr. J.A. Jansen, beste John, als promotor wil ik je bedanken voor de stimulerende en efficiënte samenwerking met hier en daar een relativerende noot. Je corrigeerde mijn artikelen steeds met een ongekende snelheid. Dit heeft er mede toe bijgedragen dat het proefschrift op zeven artikelen is gebaseerd. Verder heb ik veel van je geleerd over het bedrijven van wetenschap.

Prof. dr. P.H.M. Spauwen, als promotor en opleider, wil ik u bedanken voor het in mij gestelde vertrouwen. Daarbij denk ik ook aan de onzekere aanloopfase waarin een samenwerkingsverband en projectvoorstel nog niet bestonden. Tijdens de promotie waren onze besprekingen altijd zeer vruchtbaar en positief. Ook wil ik u bedanken voor de mogelijkheid tot klinische participatie in het Universitair Medisch Centrum (UMC) Nijmegen en later in het Canisius-Wilhelmina Ziekenhuis (CWZ). Dit vormde een welkome afwisseling op het "research gebeuren".

Drs. E.H.M. Hartman, beste Ed, als begeleider van mijn wetenschappelijke stage heb je me enthousiast gemaakt voor wetenschappelijk onderzoek. Nadat de samenwerking met de afdeling biomaterialen was gerealiseerd zijn we samen begonnen aan ons promotieavontuur. Daarmee is destijds de aanzet gegeven tot wat nu de "Engineered Bone onderzoeksgroep" is geworden. Daarnaast heb ik klinisch veel van je geleerd. Verder heb ik veel bewondering voor de wijze waarop je kliniek en promotieonderzoek weet te combineren.

Drs. D. Wijnberg, beste David, de klinische vrijdag in het CWZ was elke week weer een dag om naar uit te zien. Ik wil je bedanken voor hetgeen ik van je heb geleerd. Andere hoogtepunten waren M5-rijden en *one-minute free Hanos shopping*. Ook wil ik op deze plaats drs. J.F.M. van Tintelen en drs. J.H.M. Boode bedanken voor de prettige samenwerking in het CWZ.

Dr. Tony Mikos, (professor of Bioengineering, Rice University, Houston, Texas, USA), thank you for the nice way we cooperated in the writing of the PPF paper. Here, I would also like to thank John Fisher as a co-worker and friend for the cooperation in the PPF experiments and for the good time we had during your visits.

Dr. Yoshinori Kuboki (professor of Biochemistry, Hokkaido University, Sapporo, Japan), sensei I would like to thank you for your innovating ideas and my pleasant stays in Sapporo. You and your team were really amazing. Thanks to dr. Takita the experiments were performed with Japanese efficiency. Here, I also like to thank Javed Mahmood as a college and friend for the way we cooperated in the experiments. I would also like to thank your wife Trina for the great Indian curry. Further, I like to thank Masahiro, Jin, and all the members of the department for making me feel at home in Japan.

Prof. dr. M.A. van 't Hof, beste Martin, ik wil je bedanken voor je onmisbare hulp bij de statistische analyse van de data van de diverse experimenten.

Curriculum vitae

Johan Vehof werd op 18 maart 1970 geboren te Ambt-Delden. In 1988 behaalde hij het Atheneum-β diploma en begon met de studie geneeskunde aan de Katholieke Universiteit Nijmegen. Het doctoraal examen werd behaald in 1993. Aan het eind van de doctoraalfase en tijdens de co-schappen ging zijn interesse uit naar de plastische en reconstructieve chirurgie. Tijdens de co-schappen werd een keuze co-schap verricht op de afdeling *plastic and reconstructive surgery* van de *MAYO Clinic* in Rochester, Minnesota, de Verenigde Staten.

Gedurende de wetenschappelijke stage op de afdeling plastische en reconstructieve chirurgie van het Universitair Medisch Centrum (UMC) Nijmegen, met als onderwerp *tissue engineering* werd de eerste aanzet gegeven tot het promotieonderzoek door middel van het schrijven van een promotievoorstel. In april 1997 behaalde hij het artsexamen. In mei 1997 begon hij met het promotieproject "*engineered bone*" verbonden aan de afdeling biomaterialen (prof.dr. J.A. Jansen) en plastische en reconstructieve chirurgie (prof.dr. P.H.M. Spauwen) van het UMC Nijmegen en werd tevens aangenomen voor de opleiding plastische chirurgie (*opleider:* prof.dr. P.H.M. Spauwen).

Tijdens het onderzoek bracht hij in 1998 en 2000 een werkbezoek aan de afdeling biochemie van de Hokkaido universiteit in Sapporo, Japan (*hoofd:* prof.dr. Y. Kuboki). Dit resulteerde in twee publicaties (*zie hoofdstuk 5 en 6*). Eveneens werd nauw samengewerkt met de afdeling *bioengineering* van *Rice University* in Houston, Texas, de Verenigde Staten (*hoofd:* prof.dr. A.G. Mikos). Dit resulteerde eveneens in een publicatie (*zie hoofdstuk 8*).

In mei 2001 begon hij in het kader van de opleiding tot plastisch chirurg met de chirurgische vooropleiding in het Canisius-Wilhelmina Ziekenhuis te Nijmegen (*opleider:* dr. E.D.M. Bruggink).